

Therapeutic targets in neuroendocrine tumours

by

Virginia Kostoula

A thesis submitted to the University of London for the degree of
Doctor of Philosophy

March 2010

Department of Oncology
Royal Free and University College Medical School
University College London
91 Riding House Street, London W1W 7BS

*To my family, who believed in me
even in my darkest moments*

ABSTRACT

BACKGROUND: Neuroendocrine tumours (NETs) are fairly rare neoplasms that present many clinical challenges. The complexity, heterogeneity, and rarity of NETs have contributed to their limited therapeutic options. To improve the outcome from NETs, a better understanding of their biology is needed. Several receptor targets exist, against whom agents such as antibodies or tyrosine kinase inhibitors are being developed and tested in clinical trials. Several of these agents have been used in combination with chemotherapy or radiation with promising results. These receptors include the tyrosine kinases EGFR and C-KIT, and the somatostatin receptor SSTR2. However, their role in neuroendocrine tumour growth remains unclear.

METHODS: We investigated the anti-proliferative effect of EGFR inhibitor gefitinib, as single agent or in combination with widely used chemotherapeutic agents. The chemotherapeutic agents were also examined for their effect on EGFR activity. Cisplatin and radiation were studied for their effect in EGFR activity and localisation in combination with gefitinib and the anti-EGFR antibody cetuximab by immunoblotting and immunofluorescence, while the comet assay for quantitation of DNA damage was used to examine modulation of DNA repair by radiotherapy. The cytotoxic efficacy of agents against SSTR2 was also examined, while the expression of C-KIT was analysed in 95 NET patients by immunohistochemistry.

RESULTS: Gefitinib demonstrated anti-proliferative effect associated with induction of apoptosis but no cell cycle arrest. Cisplatin induced a transient activation of EGFR and nuclear translocation, which was mediated through the Ras/MAPK and PI-3K/Akt signalling cascades. Cisplatin and radiation-induced EGFR translocation was blocked by gefitinib and cetuximab, and this was associated with a delay in the repair of radiation-induced DNA strand breaks. Nuclear translocation was mediated by nuclear pore complex importins and exportins, and utilized the EGFR nuclear localisation sequence. C-KIT was identified in a number of NET patients. The drugs against SSTR2 had no effect on the growth of cells.

CONCLUSIONS: Targeting EGFR in combination with radiation may provide therapeutic potential in neuroendocrine tumours patients.

PUBLICATIONS

- Kostoula V, Khan K, Savage K, Stubbs M, Quaglia A, Dhillon AP, Hochhauser D, Caplin ME. Expression of c-kit (CD117) in neuroendocrine. tumours - A target for therapy?, *Oncol Reports*. 2005. Apr; 13 (4):643-7.

CONFERENCES

- **Oral Presentation - Best Abstracts Competition Basic Research 2nd Prize**
Kostoula V, Shah T, Caplin ME, Hochhauser D. Effect of cisplatin and ionizing radiation on EGFR signaling in neuroendocrine tumour cell lines, Third Annual ENETS Conference for the Diagnosis and Treatment of Neuroendocrine Tumor Disease, Prague, 22-24 March 2006
- V Kostoula, M E Caplin, T Shah, J A Hartley, D Hochhauser. Significance of nuclear EGFR in modulating the effects of ionising radiation and cisplatin on neuroendocrine tumour cell lines, NCRI Conference, International Convention Centre (ICC), Birmingham 8th-11th October 2006
- Kostoula V, Khan K, Savage K, Stubbs M, Quaglia A, Dhillon AP, Hochhauser D, Caplin ME. Expression of c-kit (CD117) in neuroendocrine tumours - A target for therapy?, UK NETwork/ENET Meeting on Neuroendocrine Tumours, London, 8–9 May 2003

ACKNOWLEDGEMENTS

I would like to thank my supervisor Prof. Martyn Caplin for all his help throughout my study, especially during the last months of my write-up for helping me with the final steps, organising my submission and my examination, and making my dream of submitting my thesis a reality.

I would also like to thank my post-graduate tutors Prof. Rachel Chambers and Prof. James Owen for their support and supervision in the last stages of my PhD. I would like to express my gratitude to Prof. Owen particularly, for encouraging me during the last few months and making sure that everything ran smoothly towards my submission.

My special thanks go to Dr. Minal Kotecha and Dr. Kostas Kiakos for their scientific help whenever I had problems with experiments but even more for being the best friends who are there whenever you need them. Getting through the difficult periods of this PhD would be impossible without them. I love you both very much.

Thank you also to Ali, Tahir, Giammy, Hemali, Boris, and Caroline for being very good friends and making me smile! Thank you to Giammy for the EGFR constructs and to Emily Eden from the Institute of Ophthalmology for the electron microscopy data.

Finally, I would like to thank my parents, Thanasis and Fani, my sister Katerina and her hubby Miltiades for believing in me, encouraging me to finish and telling me I am the best scientist in the world whenever I lost faith in myself. I could not have done this without you. You are the best family anyone could ever have!

THANK YOU,
Virginia

TABLE OF CONTENTS

ABSTRACT.....	3
PUBLICATIONS	4
ACKNOWLEDGEMENTS	5
TABLE OF CONTENTS.....	6
ABBREVIATIONS.....	12

CHAPTER 1 GENERAL INTRODUCTION

1.1	Cancer	18
1.1.1	Incidence and Mortality.....	18
1.2	Neuroendocrine tumours	19
1.2.1	Classification.....	19
1.2.2	Incidence and Mortality.....	21
1.2.3	NET markers.....	21
1.2.4	Diagnosis and Treatment of NETs.....	22
1.3	Protein Tyrosine Kinases (PTKs)	25
1.3.1	PTKs and Oncogenesis.....	25
1.3.2	EGFR (Epidermal Growth Factor Receptor).....	27
1.3.2.1	EGFR structure and function.....	27
1.3.2.2	EGFR signalling.....	29
1.3.2.3	EGFR (ErbB) family regulation and signalling specificity.....	31
1.3.2.4	EGFR and cancer.....	33
1.3.3	C-KIT.....	34
1.3.3.1	C-KIT structure and function.....	34
1.3.3.2	C-KIT signalling.....	35
1.3.3.3	C-KIT and Cancer.....	37
1.4	G Protein-Coupled Receptors (GPCRs)	39
1.4.1	GPCR Structure and Function.....	39
1.4.2	GPCR Signalling.....	40
1.4.3	GPCR regulation.....	41
1.4.4	GPCRs and Cancer.....	42
1.4.5	Somatostatin and Somatostatin Receptors	42
1.4.5.1	Structure and Function	43

1.4.5.2	Somatostatin Receptors and Cancer	44
---------	---	----

CHAPTER 2 TARGETING OF ENZYME AND RECEPTOR PATHWAYS: OVERVIEW AND IMPLICATIONS FOR THERAPY

2.1	Protein Tyrosine Kinases and Resistance to Genotoxic Therapies.....	47
2.2	Tyrosine Kinase Inhibitors.....	49
2.2.1	EGFR as a therapeutic target.....	50
2.2.1.1	Gefitinib (Iressa, ZD1839).....	52
2.2.1.2	Cetuximab (Erbix, IMC-C225).....	53
2.2.2	C-KIT inhibitor: Imatinib (STI571, Glivec, Gleevec).....	54
2.3	Resistance to Tyrosine Kinase Inhibitors.....	56
2.3.1	Resistance to EGFR inhibitors.....	56
2.3.2	Resistance to imatinib.....	57
2.4	Somatostatin analogue: Octreotide (Sandostatin, SMS201-995).....	59
2.4.1	Somatostatin Receptor-Mediated Imaging and Therapy.....	60
2.5	Chemotherapeutic Drugs for Anticancer Therapy.....	61
2.5.1	Cisplatin.....	63
2.5.2	Etoposide.....	64
2.5.3	Doxorubicin.....	65
2.5.4	Melphalan.....	66
2.5.5	Methotrexate.....	67
2.5.6	Paclitaxel.....	68
2.6	Ionising Radiation as Therapy in Cancer.....	69
2.7	Aims of this study.....	70

CHAPTER 3 MATERIALS AND METHODS

3.1	Chemical Reagents and Cytotoxic Drug Source.....	72
3.2	Experimental Cell Lines.....	73
3.2.1	Cell line culture – strengths and weaknesses.....	75
3.3	Tissue Culture.....	76
3.3.1	Maintenance of Cell Lines.....	76
3.3.2	Cell Count.....	77
3.3.3	Determination of Cell Doubling Time.....	77
3.3.4	Mycoplasma Testing.....	77

3.3.5	Storage and Retrieval of Cells in Liquid Nitrogen.....	78
3.4	Irradiation treatments.....	79
3.5	In Vitro Cytotoxicity Assay and Pharmacological Analysis.....	80
3.5.1	Sulphorhodamine B Growth Inhibition Assay.....	80
3.5.2	Isobologram Analysis.....	82
3.6	Single Cell Gel Electrophoresis (COMET) Assay.....	84
3.6.1	Methodology.....	84
3.6.2	Analysis.....	85
3.7	Detection of Apoptosis-Cell Death Detection ELISA.....	86
3.8	Protein Extraction.....	87
3.8.1	Cell Lysis for Whole Cell Extracts.....	87
3.8.2	Nuclear and Cytosolic Extraction.....	88
3.8.3	Measurement of Protein Concentration in cellular extracts.....	89
3.9	Immunoblotting.....	89
3.9.1	Electrophoresis.....	89
3.9.2	Protein Transfer and Immunoblotting.....	90
3.10	Densitometric Analysis.....	92
3.11	Immunofluorescent Staining.....	93
3.12	Transient Transfection Assay.....	94
3.13	Flow cytometry- FACS Analysis.....	95
3.14	Immunocytochemistry.....	97
3.15	Electron Microscopy.....	98

CHAPTER 4 INVESTIGATION OF COMBINATION TREATMENTS USING EGFR INHIBITORS WITH CHEMOTHERAPEUTIC AGENTS IN NET CELLS

4.1	Introduction.....	101
4.1.1	EGFR and Cancer.....	101
4.1.2	EGFR inhibition by gefitinib.....	101
4.1.3	Chemotherapy on EGFR activity.....	102
4.2	Results.....	103
4.2.1	Proliferation studies using gefitinib or chemotherapy as single agents	103
4.2.2	Combination treatments with gefitinib or chemotherapy.....	105

4.2.3	Gefitinib induces apoptosis in NET cell lines.....	117
4.2.4	Gefitinib does not induce cell cycle arrest in NET cell lines.....	118
4.2.5	Modulation of EGFR activity by chemotherapy drugs.....	123
4.2.6	Activation of EGFR signalling pathways by cisplatin.....	130
4.3	Discussion.....	131
4.3.1	Anti-proliferative effect by gefitinib and chemotherapy.....	132
4.3.2	Gefitinib induces apoptosis but no cell cycle arrest in neuroendocrine cells.....	134
4.3.3	Effect of chemotherapeutic agents on EGFR activity.....	135
4.3.4	Conclusions.....	136

CHAPTER 5 INVESTIGATION OF EFFECTS OF RADIATION AND EGFR INHIBITORS ON EGFR LOCALISATION IN NET CELLS

5.1	Introduction.....	139
5.1.1	Cisplatin and radiation-induced mechanisms of DNA repair.....	139
5.1.2	EGFR is linked to cisplatin- and radio-resistance.....	140
5.1.3	Nuclear EGFR.....	141
5.1.4	EGFR inhibition in DNA repair.....	142
5.2	Results.....	144
5.2.1	Proliferation studies with radiation and EGFR inhibitors.....	144
5.2.2	DNA repair modulation by EGFR inhibitors.....	147
5.2.3	Radiation induces EGFR phosphorylation and translocation to the nucleus.....	151
5.2.4	Gefitinib or Cetuximab inhibits radiation-induced EGFR nuclear translocation.....	155
5.2.4.1	Electron microscopy analysis.....	155
5.2.5	Cisplatin induces EGFR nuclear translocation.....	161
5.2.6	EGFR inhibition and DNA-PK _{CS} expression.....	163
5.3	Discussion.....	165
5.3.1	Anti-proliferative effect of EGFR inhibitors and radiation.....	165
5.3.2	Synergy between EGFR inhibitors and radiation in DNA repair.....	165
5.3.3	Radiation-induced nuclear EGFR translocation.....	166
5.3.4	Nuclear EGFR translocation is blocked by EGFR inhibitors.....	167

5.3.5	Effect of EGFR inhibitors on DNA-PK.....	167
5.3.6	Cisplatin-induced EGFR nuclear translocation.....	168
5.3.7	Conclusions.....	169

CHAPTER 6 CHARACTERISATION OF NUCLEAR EGFR IMPORT MECHANISM AND NUCLEAR TARGETS IN NET CELLS

6.1	Introduction.....	171
6.1.1	Nuclear EGFR function.....	171
6.1.2	Mechanisms of EGFR nuclear translocation.....	173
6.1.3	DNA repair protein targets of EGFR.....	175
6.2	Results.....	176
6.2.1	DNA repair modulation by WGA and leptomycin B.....	176
6.2.2	WGA and Leptomycin B effect on EGFR localisation.....	179
6.2.3	Transfection of wt and mutNLS EGFR.....	183
6.2.4	Nuclear targets of EGFR.....	186
6.3	Discussion.....	190
6.3.1	WGA and leptomycin B modulation of DNA repair and EGFR localisation.....	190
6.3.2	The role of the NLS sequence in EGFR.....	190
6.3.3	EGFR nuclear targets?.....	191
6.3.4	Conclusions.....	192

CHAPTER 7 INVESTIGATION OF C-KIT EXPRESSION IN NEUROENDOCRINE TUMOUR PATIENTS

7.1	Introduction.....	195
7.2	Results	196
7.2.1	Polyclonal antibody.....	198
7.2.2	Monoclonal antibody.....	201
7.2.3	Comparison of the two immunohistochemical studies.....	203
7.3	Discussion.....	207
7.3.1	C-KIT prognostic value in cancer.....	207
7.3.2	Comparison of monoclonal and polyclonal immunohistochemical studies.....	209
7.3.3	Comparison of this study with results from other groups.....	211

7.3.4	Imatinib as a therapeutic option for NET patients.....	211
7.3.5	Conclusions.....	213
CHAPTER 8	INVESTIGATION OF COMBINATION TREATMENTS USING OCTREOTIDE WITH CHEMOTHERAPEUTIC AGENTS IN NET CELLS	
8.1	Introduction	215
8.2	Results	216
8.2.1	SSTR expression in NETs.....	216
8.2.2	Proliferation studies using octreotide with chemotherapy.....	217
8.2.3	Octreotide effect on cell cycle of NET cell lines.....	224
8.3	Discussion.....	226
8.3.1	Proliferation studies.....	226
8.3.2	Drug treatments in serum-free media.....	226
8.3.3	Apoptosis and cell cycle analysis.....	227
8.3.4	Conclusions.....	227
CHAPTER 9	CONCLUSIONS AND FUTURE WORK.....	229
APPENDIX.....		240
REFERENCES.....		270

Abbreviations

¹³¹ I-MIBG	Iodine-131 labelled meta-iodobenzylguanidine
5-HT	5-hydroxytryptamine
ACTH	Adrenocorticotrophic hormone
ADCC	Antibody dependent cellular cytotoxicity
AML	Acute myelogenous leukaemia
APUD	Amine precursor uptake and decarboxylation
ATM	Ataxia-telangiectasia mutated
ATP	Adenosine triphosphate
ATR	Ataxia-telangiectasia and Rad3-related
b-FGF	Basic fibroblast growth factor
BSA	Bovine serum albumin
cAMP	Cyclic adenosine monophosphate
CCK-BR	Cholecystokinin-2 receptor
CDDP	Cisplatin or cis diaminedichloroplatinum
CDK2	Cyclin-dependent kinase 2
CML	Chronic myelogenous leukaemia
CSF-IR	Macrophage colony stimulating factor receptor
CT	Computerised tomography
DAG	Diacylglycerol
DFSP	Dermatofibrosarcoma protuberans
DHFR	Dihydrofolate reductase
DMSO	Dimethylsulphoxide
DNA	Deoxyribonucleic acid
DNA-PK	DNA protein kinase
DNA-PK _{CS}	DNA protein kinase catalytic subunit
DSB	Double strand break
DTPA	Diethylene-triamine-pentaacetic acid
DTT	Dithiothreitol
ECACC	European collection of cell cultures
ECL	Enterochromaffin-like
ECL	Enhanced chemoilluminescence
EDTA	Ethylenediaminesulphate tetra-acetic acid

EGFR	Epidermal growth factor receptor
ELISA	Enzyme-linked immunosorbent assay
ERK	Extracellular signal-regulated kinase
EtBr	Ethidium bromide
FACS	Fluorescent activated cell sorting
FAK	Focal adhesion kinase
FCS	Foetal calf serum
FDA	Food and Drug Administration
FITC	Fluorescein isothiocyanate
GABA	γ -Aminobutyric acid
GABP	GA-binding protein
GEP-NE	Gastro-entero-pancreatic neuroendocrine
GI	Gastrointestinal
GISTs	Gastrointestinal tumours
GPCRs	G protein-coupled receptors
GRKs	G protein-coupled receptor kinases
Gy	Gray (irradiation unit)
HAE	Hepatic artery embolization
HER1(c-erbB1)	Human epidermal growth factor receptor
HR	Homologous recombination
HRP	Horse radish peroxidase
ICC	Interstitial cells of Cajal
ICL	Interstrand cross-links
IGF-1	Insulin like growth factor
IGF-1R	Insulin like growth factor receptor-1
IMS	Industrial methylated spirit
i-NOS	Inducible nitric oxide synthase
IP3	Inositol triphosphate
JAK	Janus kinase
JNK	C-jun N-terminal kinase
kDa	kiloDaltons
MAPK	Mitogen-activated protein kinase
MRI	Magnetic resonance imaging
MTC	Medullary thyroid carcinoma

mRNA	Messenger RNA
NCAM	Neural cell adhesion molecule
NEDH	New England Deaconess Hospital
NET	Neuroendocrine tumours
NF- κ B	Nuclear factor- κ B
NHEJ	Non-homologous end joining
NLS	Nuclear localisation signal
NRGs	Neuregulins
NSCLC	Non small cell lung cancer
OD	Optical density
PBS	Phosphate buffered saline
PCNA	Proliferating cell nuclear antigen
PDGFR	Platelet derived growth factor receptor
PDGF- α	Platelet derived growth factor- α
PI	Propidium iodide
PI3K	Phosphatidylinositol-3 kinase
PIKK	Phosphatidylinositol-3 kinase-related kinases
PIP ₂	Phosphatidylinositol bisphosphate
PKB/Akt	Protein kinase B
PKC	Protein kinase C
PLC γ	Phospholipase C γ
PNETs	Pancreatic neuroendocrine tumours
PRRT	Peptide receptor radionuclide therapy
PTKs	Protein tyrosine kinases
RNA	Ribonucleic acid
ROS	Reactive oxygen species
RT	Room temperature
RTK	Receptor tyrosine kinase
SCCHN	Squamous cell carcinoma of the head and neck
SCF	Stem cell factor
SCID	Severe combined immunodeficient
SCLC	Small cell lung cancers
SDS	Sodium dodecylsulphate

SEER	Surveillance, Epidemiology and End Results
SH2	Src homology 2
SRB	Sulphorhodamine B
SRS	Somatostatin receptor scintigraphy
SSB	Single strand break
SST	Somatostatin
SSTRs	Somatostatin receptors
STAT	Signal transducer and activator of transcription
TBE	Tris-borate-EDTA
TBS	Tris buffered saline
TBS-T	Tris buffered saline Tween
TE	Tris-EDTA
TEMED	Tetramethylethylenediamine
TGF	Transforming growth factor
TKIs	Tyrosine kinase inhibitors
TSH	Thyroid-stimulating hormone
UV	Ultra violet
VEGF	Vascular endothelial growth factor
VIPomas	Vasoactive intestinal peptide tumours
WGA	Wheat germ agglutinin
WHO	World Health Organisation

CHAPTER 1

GENERAL INTRODUCTION

1.1 Cancer

Cancer is a disease involving dynamic changes in the human genome. The molecular basis of cancer involves mutations which produce oncogenes with dominant gain of function and tumour suppressor genes with recessive loss of function. Mutations vary from specific point mutations to alterations in whole chromosomes; these differences can affect the genes governing the normal regulatory mechanisms of cell growth and proliferation (Vogelstein & Kinzler, 1993). Uncontrolled cell proliferation or inefficient mechanisms of programmed cell death can result in tumour growth. There are well over 200 different forms of tumour subtypes arising in different organs.

As summarised by Hanahan & Weinberg, (2000), the vast majority of malignant tumours can be identified by six fundamental changes; self-sufficient growth signals, insensitivity to anti-growth signals, evading programmed cell death (apoptosis), limitless replicating potential (immortality), sustained angiogenesis and tissue invasion and metastasis. These characteristics can be acquired during the course of tumour development through a series of genetic changes culminating in the uncontrolled and eventual malignant transformation of a clonal cell population. This multi-step process initiating from a normal cell population, develops through a series of pre-cancerous lesions into a metastatic tumour.

Once transformed, a malignant tumour can become invasive and can spread into the surrounding tissue. In some cases cancerous cells migrate away from the primary tumour often via the lymphatic system. These micro-metastases can attach to new tissue elsewhere in the body and form secondary tumours (Hanahan & Weinberg, 2000).

1.1.1 Incidence and Mortality

Each year more than a quarter of a million people are newly diagnosed with cancer in the UK. Overall it is estimated that more than one in three people will develop some form of cancer during their lifetime. Of the different types of cancer, four types including breast, lung, large bowel (colorectal), and prostate account for over half of all new cases. Breast cancer is the most common cancer in the UK. The latest available mortality statistics for the United Kingdom (UK) are for 2004. In that year 153,397 people were registered as dying from a malignant neoplasm. Cancer is the cause of

approximately a quarter of all deaths in the UK of which over one fifth (22%) are caused by lung cancer. Colorectal cancer was the second most common cause of death from cancer (11%). Breast cancer is the third most common cause of death from cancer in all persons (8%).

1.2 Neuroendocrine tumours

Neuroendocrine tumours (NETs) constitute a heterogeneous group of tumours that derive predominantly from cells of the diffuse endocrine system of the gut and pancreas and can be found anywhere in the body (Rindi *et al.*, 1999). This system includes endocrine glands, such as the pituitary, the parathyroids and the adrenal medulla, as well as endocrine islets within glandular tissue (thyroid or pancreatic) and cells disseminated between exocrine cells, such as endocrine cells of the digestive and respiratory tracts (Arnold *et al.*, 1994; Kaltsas *et al.*, 2004). Neuroendocrine tumours were thought to rise from the so called APUD cells as they have the ability for Amine Precursor Uptake and Decarboxylation (Somogyi *et al.*, 2000). APUD cells are a group of unrelated endocrine cells found throughout the body with similar characteristics, which make a number of hormones with similar structures including serotonin (5-hydroxytryptamine, or 5-HT) and neurotensin. This idea has now been abandoned and the term neuroendocrine cell is defined by the cell's secretory products and cytoplasmic proteins, rather than its localisation or embryological derivation.

Neuroendocrine cells have distinctive characteristics presenting marker proteins and cell type-specific hormonal products. The cells have uniform nuclei with abundant granular or faintly stained cytoplasm and membrane-bound dense-core secretory granules in the cytoplasm. Neuroendocrine cells form small organs, distinct cell clusters within other tissues or a network of cells dispersed in thymus, thyroid, lung and gut. Consequently, common properties of NETs include ectopic hormone and bioamine release, the presence of tumour-associated antigens, and isozyme composition (Bombardieri *et al.*, 2001; Jensen, 2000).

1.2.1 Classification

NETs classification was traditionally based on site of origin and whether they are functioning (with a clinical syndrome) or non-functioning (without a clinical

syndrome). There are many types of neuroendocrine tumours including the medullary thyroid cancers, paragangliomas, pheochromocytomas, but the most common NETs are the gastro-entero-pancreatic neuroendocrine (GEP NE) tumours. GEP NE tumours are divided into: a) carcinoid tumours originating in the foregut (lung, thymus, stromal and proximal small bowel), midgut (ileum, caecum, proximal colon) or hindgut (distal colon, rectum), b) pancreatic neuroendocrine tumours (PNETs) or islet cell tumours, named after their main secretory product, including insulinomas, gastrinomas, VIPomas (vasoactive intestinal peptide tumours), and glucagonomas, and c) non-functioning tumours, which secrete peptides that do not cause any clinical syndrome (Solcia *et al.*, 1999). This old classification has been replaced by the new World Health Organisation (WHO) classification which divides NETs according to histomorphology, size and the presence of metastases into:

1. well-differentiated endocrine tumours
2. well-differentiated endocrine carcinomas
3. poorly differentiated endocrine carcinomas
4. mixed exocrine and endocrine carcinomas
5. tumour-like lesions

The old classification though, is still in use in clinical practise and in research papers (Jensen, 2000; Oberg, 2004) and for practical reasons is used in this study.

NETs occur most commonly in the digestive system. But they can also be found in other parts of the body. The commonest type of NET is the carcinoid tumour which accounts for 55% of GEP NE tumours. This cancer mainly arises from neuroendocrine cells of the appendix (38%), ileum (23%), rectum (13%), and bronchus (11.5%). But it can also grow in the pancreas, kidney, ovaries and testicles. 10% of carcinoids usually present with the so-called carcinoid syndrome characterised by flushing, diarrhoea, bronchoconstriction and right-sided heart disease due to excessive secretion of serotonin in the systemic circulation. The second type of NET is the group of pancreatic NETs (PNETs). According to data from the Surveillance, Epidemiology and End Results (SEER) registry on PNETs in the United States over the period from 1973-2000, the most common PNET is the non-functional type (90.8%). The next most common type of PNET is the gastrinoma (4.2%), a gastrin-releasing islet cell tumour of the pancreas (30-40%) or duodenum (60-70%) that is associated with peptic ulceration and the Zollinger-Ellison syndrome, which is caused by the over-production of gastrin,

followed by the insulinoma (presented with hypoglycaemic syndrome) (2.5%), an islet cell tumour that secretes excess insulin, the glucagonoma (1.6%) and the VIPoma (0.9%) (Jensen, 2000; Oberg, 2004; Halfdanarson *et al.*, 2008; Modlin *et al.*, 2008).

1.2.2 Incidence and Mortality

NETs are rare, mostly benign or slow growing tumours (although a proportion demonstrates aggressive tumour growth) with often differing phenotypes in their clinical behaviour (Mignon, 2000). Neuroendocrine tumours account for only 2% of all malignancies. In the last decades, the incidence of NETs has been rising. The incidence is approximately 5/100,000 with more female patients under the age of 50 and with metastases occurring in more than 80% of patients. According to the SEER registry on NETs in the United States over the period from 1973-2004, the primary sites of NETs differed considerably with sex and race. In total, 41% of NETs were foregut, 26% midgut and 19% hindgut, whilst the rest 13% had unknown primary site. Most neuroendocrine tumours are mainly sporadic, but association with the multiple endocrine neoplasia type 1 (MEN-1) syndrome and clustering within families is known. Survival is rated at 5-years according to stage: 93% in local disease, 74% in regional disease and 19% in metastatic disease. In metastatic disease, survival increased since 1992, when treatment with octreotide became largely available in the Netherlands (Taal, 2004; Yao *et al.*, 2008; Srirajaskanthan *et al.*, 2009).

1.2.3 NET markers

Most NETs produce and secrete a variety of cell type-specific peptide hormones and amines which cause clinical syndromes and are used as markers for the diagnosis of NET patients (Eriksson *et al.*, 2000). Diagnosis was historically based on silver stainings; the argyrophil staining by Grimelius, which is a general neuroendocrine marker, and the argentaffin staining by Masson, which demonstrates the serotonin content (Wilander *et al.*, 1989). In the absence of any symptoms diagnosis is based on detection of general NET markers, including the secretory granule proteins chromogranins A, B, and C, (of which chromogranin A is increased in 70-90% of all NETs), the synaptic vesicle membrane glycoprotein synaptophysin, the pancreatic polypeptide which is mainly increased in PNET patients, the cytosolic neuron-specific enolase, and the carcinoembryonic antigen (Lamberts *et al.*, 2001, Eriksson *et al.*, 2000). Specific neuroendocrine markers include insulin, gastrin, glucagon, vaso

intestinal polypeptide, urinary 5-hydroxyindoleacetic acid (5-HIAA), which is the main breakdown product of serotonin, and somatostatin (Tomassetti, 2001). The presence of somatostatin receptors has greatly aided the imaging of NETs.

1.2.4 Diagnosis and Treatment of NETs

The diagnosis of NETs is based on measurement of general or specific hormone and biochemical marker levels in the plasma, as well as the histological immunostaining including detection of the nuclear antigen Ki-67, which indicates the proliferative capacity of NETs. Localisation of these tumours is based on imaging tests such as ultrasound, computerised tomography (CT), magnetic resonance imaging (MRI), and somatostatin receptor scintigraphy (SRS or Octreoscan[®]). SRS is a very useful imaging modality as more than 80% of these tumour cells express somatostatin receptors, which will be discussed in more detail later.

Treatment options for NETs include the use of somatostatin analogues (which are used for the management of clinical symptoms caused by excessive hormone secretion), alpha interferons¹, chemotherapy, embolization, radionuclide receptor targeted therapy, new agents including e.g. tyrosine kinase inhibitors and mTOR inhibitors, and surgery (Jensen, 2000; Srirajaskanthan *et al.*, 2009; Desai *et al.*, 2009). The initial management of NETs is surgical excision of the tumour, if possible. This is the only form of treatment that cures NETs and is sufficient in the majority of benign tumours; however, the majority of GEP tumours are recurrent, malignant or disseminated tumours and thus require further treatment (Oberg *et al.*, 2004).

SST analogues and interferon-alpha (IFN- α) can achieve disease stabilization by symptomatic control in functional tumours and rarely shrinkage of tumour may occur, but in most cases, patients become refractory to therapy and additional treatment is required. Other options for therapy in these cases include systemic chemotherapy or radiotherapy (Oberg *et al.*, 2004; Srirajaskanthan *et al.*, 2009; Desai *et al.*, 2009).

¹ The mechanism of action for alpha interferon involves direct effects on the tumour cells by inhibiting the cell proliferation via cell cycle arrest at the G1/S phase. Furthermore, INF- α modulates the immune system by stimulating natural killer cells, macrophages and also presents anti-angiogenic effects.

Chemotherapy can temporarily produce response in patients with fast-growing poorly differentiated NETs, but many well-differentiated NETs are relatively chemoresistant (Oberg *et al.*, 2004). However, some types of NETs particularly those of foregut origin e.g. pancreatic NETs may be sensitive to chemotherapy and using a streptozocin based regimen may have a partial response rate of 30-50%, and similar responses have been demonstrated with a combination of cisplatin and etoposide. On the other hand, chemotherapy in patients with slow growing NETs such as midgut carcinoids has produced little response, and these tumours are mainly managed with somatostatin analogues, interferon therapy, and more recently radionuclide receptor therapy (Oberg, 2001; Srirajaskanthan *et al.*, 2009; Desai *et al.*, 2009). Chemotherapy has significant side effects including immunosuppression and myelosuppression and its use must be weighed against potential adverse effects (Kaltsas *et al.*, 2004).

Radionuclide therapy involves coupling a radioisotope to a peptide (e.g. somatostatin analogue), which will be internalised with the peptide-receptor complex through receptor uptake, and deliver a cytotoxic radiation dose to the tumour without damaging the surrounding healthy tissues (Krenning *et al.*, 1999). Aspects taken into consideration include the amount of radiolabelled ligand that can be concentrated inside tumour cells and the rates of internalization, degradation and recycling of the ligand-receptor complex (Wiseman & Kvols, 1995). Examples of radiolabelled molecules include the radionuclide labelled octreotide or octreotate (octreotide acid) with ^{111}In (Indium-111), ^{90}Y (Yttrium-90) or ^{177}Lu (Lutetium-177), as well as ^{131}I -MIBG (Iodine-131 labelled meta-iodobenzylguanidine).

Radionuclide labelled octreotide is generally used in neuroendocrine tumours, especially GEP NETs. Indium-111 was initially the most commonly used radioisotope, but has been replaced by Yttrium-90 and Lutetium-177. Therapy with ^{90}Y -octreotide caused stabilization of tumour growth and partial response in approximately 20% of NET patients (Waldherr *et al.*, 2002). ^{177}Lu -octreotate was used in 504 patients with gastroenteropancreatic tumours with complete response in 2% of patients, partial response in 28% and minor tumour response in 16%. The overall survival was extended by 40 to 72 months from time of diagnosis compared to previous controls (Kwekkeboom *et al.*, 2008). ^{131}I -MIBG has been used to treat patients with pheochromocytoma, neuroblastoma, carcinoid tumours, medullary thyroid carcinoma,

and paragangliomas. The tumour responses have been variable with the most encouraging results being in patients with pheochromocytoma (Wiseman & Kvols, 1995). The main side effect of radionuclide therapy is bone marrow suppression, which is usually seen after a number of treatment cycles.

NET metastases are often found in the liver. Liver resection is carried out especially when the tumour is isolated in one area of the organ, but is also considered when the metastasis is more extended in order to slow the progression of the disease. In total, liver resection is performed in approximately 10% of patients with a 5-year survival in 60-85% of the cases. Non-resectable liver metastases can also be treated with hepatic artery embolization (HAE), with a 5-year survival in more than 50% of patients (Srirajaskanthan *et al.*, 2009; Desai *et al.*, 2009). HAE is based on the observation that tumor cells get nearly all their nutrients from the hepatic artery, while the normal cells of the liver get about 75 percent of their nutrients (and about half of their oxygen) from the portal vein, and thus can survive with the hepatic artery effectively blocked (Pommier, 2003). HAE leads to tumour reduction by induction of ischaemia and therefore decrease of hormone secretion. Embolisation can be achieved with radionuclides or chemotherapeutic agents such as cisplatin and doxorubicin (Srirajaskanthan *et al.*, 2009; Desai *et al.*, 2009).

Based on the above, it is clear that neuroendocrine tumours present a heterogeneous group of tumours with different biological features and their treatment has been challenging to physicians worldwide. Forms of treatment should be individualised for each patient with consideration of the molecular biology and history of each tumour, especially in patients with well-differentiated slow-growing NETs, as such patients can have prolonged survival in the presence of extensive disease (Oberg *et al.*, 2004). Lately, treatment options for many types of tumours include targeting of specific growth factors and their receptors. A number of different traditional growth factors have been identified in neuroendocrine gut and pancreatic tumours such as IGF-1, PDGF- α , b-FGF, TGF- α , and the TGF- β family (Oberg, 1996), but the role of these growth factors and their receptors in NETs is still under investigation. The limited therapeutic options for NETs and the expression of growth factor receptors on the surface of NET cells provided the rationale for my study, which focuses on

identification of receptor proteins as potential therapeutic targets in neuroendocrine tumours. The receptors analyzed are members of two large receptor families; the protein tyrosine kinases (PTKs) and the G protein-coupled receptors (GPCRs). The protein tyrosine kinases investigated for their role in NET growth include the epidermal growth factor receptor (EGFR), which is expressed in a variety of cancer types, and C-KIT, which is mainly expressed by gastrointestinal stromal tumour cells. The GPCRs examined include the somatostatin receptors (SSTRs), which are well known markers of neuroendocrine differentiation. Analysis of the therapeutic potential of each receptor-target was mainly based on the efficacy of specific inhibitors, in the form of synthetic compounds or antibodies, which block the expression of each receptor-target. The receptors investigated as well as their respective inhibitors are analysed in detail in the following sections.

1.3 Protein Tyrosine Kinases (PTKs)

More than 20 years ago animal tumour viruses were found to encode for protein tyrosine kinases (Sawyers, 2002). PTKs play a fundamental role in multiple cellular mechanisms such as cell proliferation, differentiation, migration as well as apoptosis, all of which can lead to oncogenesis when deregulated. PTKs' function, which is literally the transfer of phosphate from ATP to tyrosine residues of target proteins needed for their activation or inactivation, is tightly controlled under physiological conditions (Skorski, 2002).

1.3.1 PTKs and Oncogenesis

Changes in more than 30 PTKs have been implicated in the development of neoplastic diseases (Blume-Jensen & Hunter, 2001). There are four general mechanisms by which tyrosine kinases become constitutively activated (figure 1). The first is as a result of chromosomal translocation. In this case, reciprocal chromosomal translocations generate fusion proteins, where the amino-terminal portion is responsible for oligomerisation, and this enables constitutive activation of the catalytic activity of the kinase domain located on the carboxy-terminal portion.

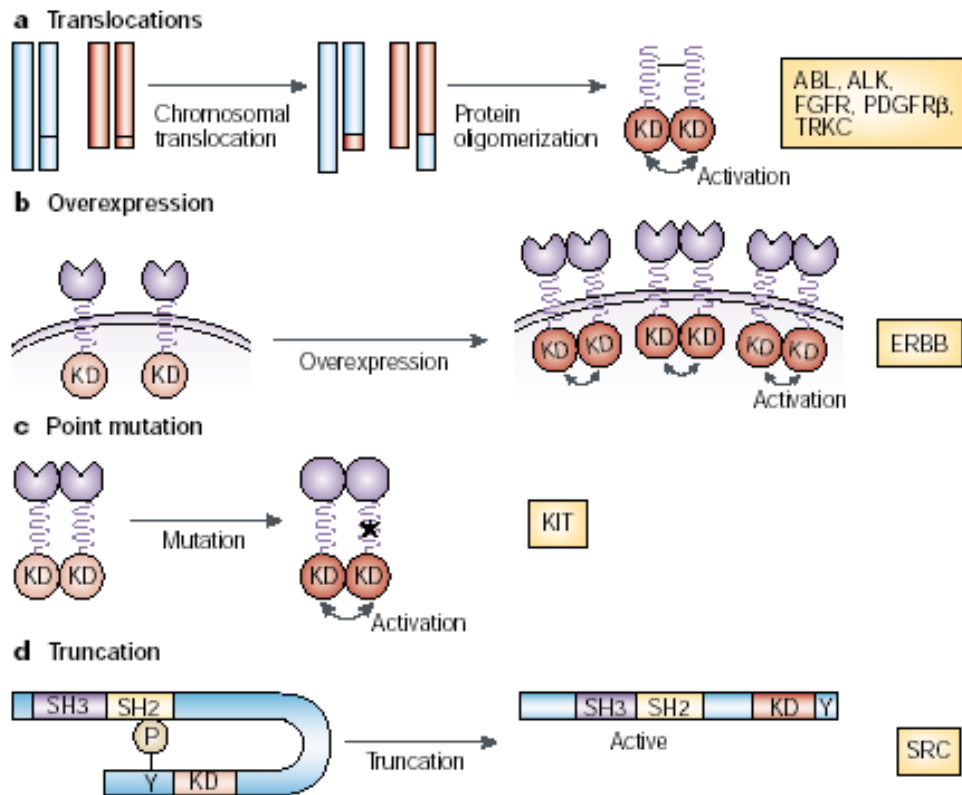


Figure 1: Genetic alterations leading to uncontrolled activation of PTKs in cancers
Source: T Skorski, Nature Reviews Cancer, 2002

The second mechanism is as a result of overexpression of the cell-membrane receptor tyrosine kinase which leads to spontaneous (or autocrine ligand-dependent) dimerisation and constitutive kinase activation. Third, point mutations in the juxtamembrane region of a receptor tyrosine kinase may cause constitutive ligand-independent dimerisation of the receptor and activation of its kinase activity. Finally, truncation of the carboxy-terminal portion may prevent phosphorylation of a tyrosine residue that is involved in protein folding and stabilize tyrosine kinase in its active conformation (Skorski, 2002). An overview of protein tyrosine kinases implicated in human cancer is shown in Table 1. The PTKs investigated in our study, EGFR and C-KIT, are analysed below.

Table 1: Oncogenic Tyrosine Kinases

OTK	Cancer type	Mechanism
ABL, ALK, FGFR, JAK2, PDGFR- β , TRKC	Acute and chronic leukaemias	Dysregulated by fusion with BCR, TEL or NPM causing oligomerisation and activation of the kinase by cross-phosphorylation
ERBB1-4, IGF1R, PDGFR- β , FGFR 1-4	Breast and ovarian carcinomas, lung cancer, glioblastomas, gastric and prostate carcinomas	Enhanced expression causes receptor dimerisation and activation of intrinsic kinase activity
Src, C-KIT	Gastrointestinal tumours, leukaemias, lung cancers, colon cancer	C-Terminal truncation or gain-of-function point mutations causing increased kinase activity

Adapted from Skorski T, Nature Reviews Cancer, 2002

1.3.2 EGFR (Epidermal Growth Factor Receptor)

Among the various families of growth factors known to contribute to the growth of tumour cells are the EGF-related peptides and their receptors. The EGFR family is another subset of the Receptor Tyrosine Kinase (RTK) super family. EGFR is also known as Human Epidermal Growth Factor Receptor (HER1) or c-erbB1 (Wells, 1999).

1.3.2.1 EGFR structure and function

The ErbB family or EGFR family consists of four structurally related RTKs: EGFR (ErbB1/HER1), ErbB2 (HER2/Neu in rodents), ErbB3 (HER3) and ErbB4 (HER4). Activation of the EGFR family is accomplished by a multitude of ligands creating a signal diversity that is critical to EGFR function (Holbro and Hynes, 2003). Three ligand groups have been identified so far (Yarden and Sliwkowski, 2001). Receptors and their ligands are illustrated in figure 2.

Members of the EGFR family contain an extracellular domain of approximately 620 amino acids involved in ligand binding and receptor dimerization, a single transmembrane spanning region, and a cytoplasmic tyrosine kinase domain in all receptors except for ErbB3 which lacks intrinsic kinase activity (Yarden, 2001). The extracellular region is made up of four subdomains, L1, CR1, L2 and CR2, where L

signifies a leucine rich repeat domain and CR a cysteine-rich region. These subdomains are also referred to in literature as domains I-IV respectively (Garrett, *et al.*, 2002; Ward *et al.*, 2007).

In EGFR, the intracellular domain is split into a short juxta-membrane domain, a tyrosine kinase domain and a long carboxyl tail with autophosphorylation sites (Wells, 1999). The tail also has three internalisation sites, for when ligand occupied EGFR is internalised and degraded. The ligands (secreted or membrane-bound glycoproteins) constitute a group of proteins with diverse function, which have an important role in early mammalian development (Salomon *et al.*, 1995). These include proteins such as EGF, TGF- α , amphiregulin, heparin-binding EGF-like growth factor, betacellulin, and epiregulin (Toyoda *et al.*, 1997; Wells, 1999). The related ErbB3 and ErbB4 receptors are activated by neuregulins (NRGs). ErbB2 has no known direct activating ligand, and may be in an activated state constitutively.

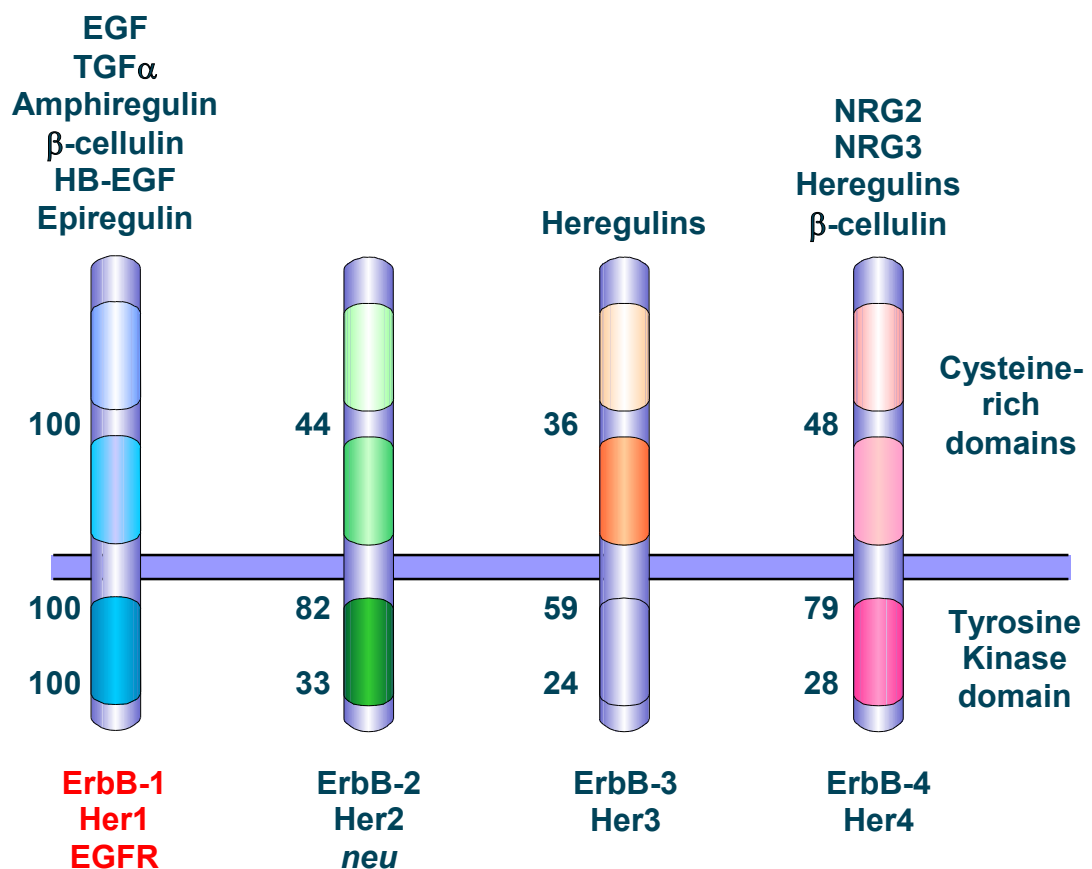


Figure 2: The EGFR family members
Adapted from PM Harari, Endocrine Related Cancer, 2004

Activation of the receptor results in the initiation of a diverse array of cellular pathways. In response to toxic environmental stimuli, such as ultraviolet irradiation, or to receptor occupation, receptors form homo- or heterodimers with other family members (Yarden, 2001; Harari, 2004). Ligand induced activation leads to activation of a number of signalling pathways which cease after endocytosis or receptor internalisation culminating in recycling or degradation of the receptor. EGFR is the only member of the family able to form a heterodimer with all other members of the EGFR family. ErbB2 does not have a ligand and may be in an activated state constitutively, but it is the preferred partner for the formation of a heterodimer. EGFR dimerisation leads to autophosphorylation of five tyrosine (Y) residues in the C-terminal domain of the receptor. These are Y992, Y1045, Y1068, Y1148 and Y1173. Each dimeric receptor complex will initiate a distinct signalling pathway by recruiting different Src homology 2 (SH2)-containing effector proteins. EGFR dimerization results in autophosphorylation of tyrosine residues in the cytoplasmic C-terminal tail of the receptor, initiating a downstream cascade of events, which produce an array of cellular responses including cell proliferation, differentiation, adhesion, migration, or apoptosis (Cohen, 2003; Wells, 1999).

1.3.2.2 EGFR signalling

The EGFR intracellular signal transduction pathways include the Ras/MAPK, the phosphatidylinositol-3 kinase (PI3K), the STAT pathway, and the phospholipase C γ (PLC γ) pathways (Carpenter, 2000; Grant *et al.*, 2002). Figure 3 shows a schematic diagram of the EGFR intracellular signalling cascades.

The best known pathway is the serine/threonine mitogen-activated protein kinase (MAPK) cascade (Schlessinger, 2004). Phosphorylated EGFR (ErbB1) is known to recruit the adaptor proteins Shc and Grb2, which act through the exchange factor Sos to activate Ras. This leads to the phosphorylation of the MAP kinase ERK1/2, which in turn induces the expression of selected transcription factors including Elk-1 and c-fos (Yarden & Sliwkowski, 2001). This pathway is associated with cell division and its abnormal activity may be involved in the uncontrolled cell proliferation occurring in tumours (Pal & Pegram, 2005).

Activation of the lipid kinase phosphatidylinositol-3 kinase (PI3K) leads to cell

division and survival. In this pathway, the Gab1 adaptor protein activates PI3K which initiates a positive feedback loop for Gab1 recruitment to the receptor. PI3K also phosphorylates AKT (PKB, protein kinase B) leading to an anti-apoptotic response through the transcription factor nuclear factor (NF)- κ B. This is also activated through PKC, a pathway associated with cell cycle progression (Prenzel *et al.*, 2001).

A third pathway is mediated by the cytoplasmic tyrosine kinase c-Src which is involved in a number of cellular processes, including mitogenic signalling (Hynes & Lane, 2005). Amongst the known c-Src substrates, the signal transducer and activator of transcription (STAT) family of transcription factors is known to be of particular importance in the proliferation and survival of cancer cells. In fact, activation of STAT3 initiates a TGF-induced autocrine growth of transformed epithelial cells (Yu & Jove, 2004).

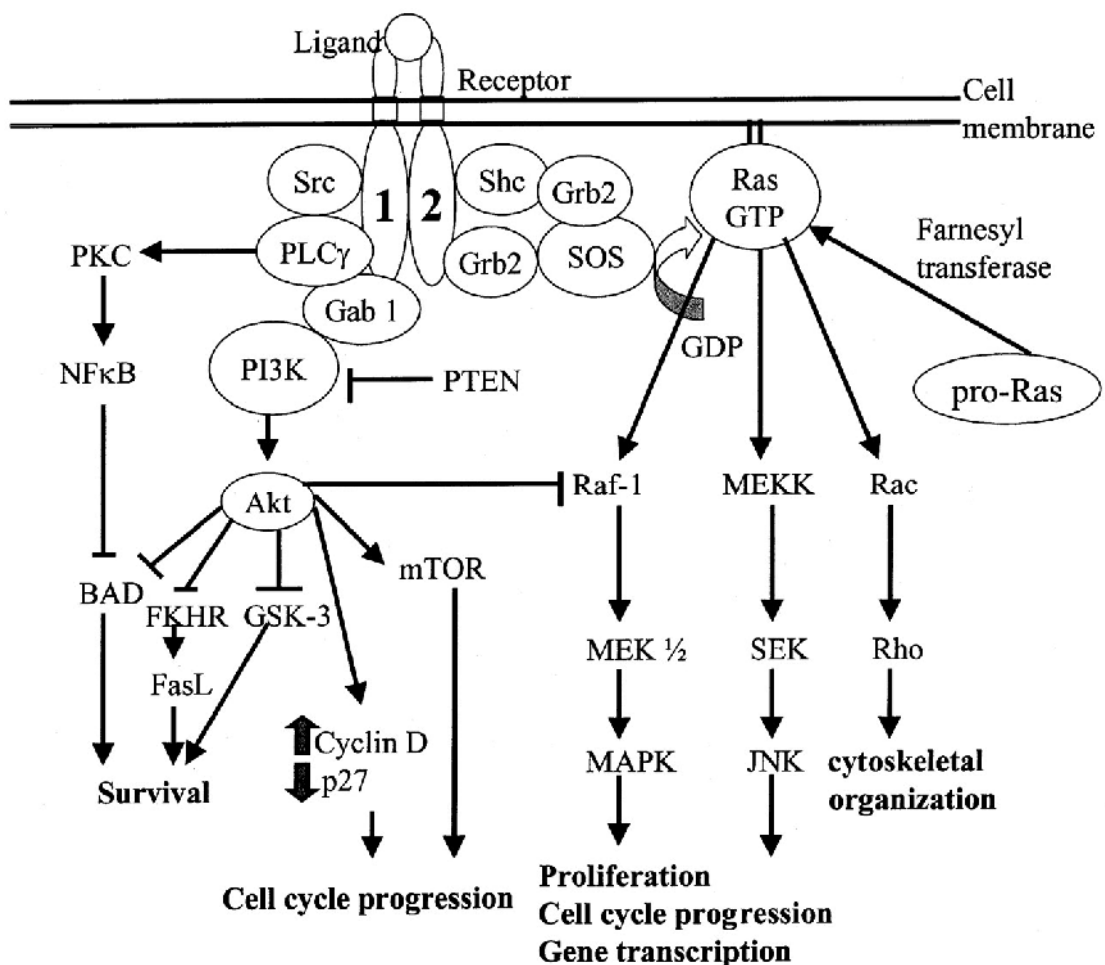


Figure 3: The EGFR signal transduction pathways
Source: G Atalay *et al.*, Annals of Oncology, 2003

Interestingly, ErbB mediated activation of STAT3 has also been implicated in the resistance of tumour cells to cytotoxic therapy (Masuda *et al.*, 2002). Furthermore, ErbB-induced activation of the phospholipase C γ (PLC γ) pathway has been linked to increased cell motility (Fedi *et al.*, 1994). The interaction of the erbB receptor family and the integrin signalling pathway is mediated by the focal adhesion kinase (FAK) and is important for tumour invasion and metastasis. Here, EGFR inactivates FAK, leading to the disturbance of cell–cell and cell–matrix interactions thus promoting cell motility and invasiveness (Lu *et al.*, 2001). EGFR also promotes angiogenesis. An example of this is the STAT3 regulated production of the angiogenic factor vascular endothelial growth factor (VEGF) (Niu *et al.*, 2002). Other proto-oncogenes activated include *fos*, *jun* and *myc* as well as a family of zinc-finger-containing transcription factors such as Sp1, Egr1 and Ets family members (e.g. GA-binding protein (GABP)) (Yarden, 2001).

1.3.2.3 EGFR (ErbB) family regulation and signalling specificity

The family of ErbB RTKs is involved in a wide variety of cellular processes such as proliferation, survival, angiogenesis and metastasis. ErbB RTKs activate multiple signalling pathways and different second messengers may mediate the same cellular response. In addition, the same ligand bound to the same receptor can activate multiple signalling pathways. The mechanism leading to the activation of a specific signalling pathway is complex and dependent on many parameters.

Activation of a specific pathway may occur in a tissue-specific or tumour-specific manner, as overexpression of individual ErbB types results in activation of specific groups of genes (Alaoui-Jamali *et al.*, 2003; Amin *et al.*, 2004). ErbB receptors upon activation form homo- or heterodimers in which different combinations of receptors activate distinct signalling pathways (Riese & Stern, 1998; Olayioye *et al.*, 1998). The specificity of the signalling cascade activated is also regulated by many other factors including: a) the ligand binding to the receptor (Amin *et al.*, 2004), b) the interaction with distinct substrates through different autophosphorylation sites of EGFR (Yarden & Sliwkowski, 2001), and c) the rate of endocytosis activated by ligand binding, which acts as a negative feedback leading to downregulation of the receptor (Bogdan & Klambt, 2001).

Ligand binding to a receptor can modulate its activity in many ways. Apart from the type of ligand, the concentration of ligand (or of the receptor itself) and the binding affinity of the ligand can modulate the potency and duration of signalling as well as the signalling pathway activated. Furthermore, it has been documented that the C-terminals of ligands (e.g. heparin binding-EGF), which result from cleavage of transmembrane ligand precursors, may translocate into the nucleus and regulate cell proliferation (Yotsumoto *et al.*, 2009).

The autophosphorylation sites in the kinase domain of EGFR serve as docking sites for various substrates which can be adaptor proteins or enzymes. EGFR autophosphorylated sites activate second messengers containing SH2 (Src homology domain 2) or PTB (phosphotyrosine binding) domains. On the other hand, EGFR can also be phosphorylated by other kinases such as PKC (protein kinase C), which regulates EGFR membrane distribution, or the JAK (Janus kinase) protein for the initiation of the JAK-STAT signalling pathway (Bogdan & Klambt, 2001; Yarden & Sliwkowski, 2001).

Phosphorylation and internalisation of EGFR leads to desensitization and downregulation of the receptor respectively. The mechanism of internalization employed also regulates EGFR signalling as trafficking via clathrin-coated pits (activated by EGF) leads to EGFR degradation within lysosomes, whereas internalization into early endosomes (activated by TGF- α) leads to receptor recycling. It is worth noting that EGFR actually remains active till its storage inside late endosomes (Bogdan & Klambt, 2001). The rate of receptor endocytosis may also influence the duration and potency of distinct signalling pathways (Baulida *et al.*, 2009).

Finally, the signalling pathway activated is also influenced by the cross-talk between EGFR and other membrane receptors including IGF-1R (insulin like growth factor receptor) and GPCRs (G-protein coupled receptors), which may activate EGFR directly via phosphorylation or indirectly by activating downstream members of EGFR signalling pathways (van der Veecken *et al.*, 2009; Bhola & Grandis, 2008).

1.3.2.4 EGFR and cancer

Excessive ErbB signalling is associated with the development of a wide variety of types of solid tumour. ErbB-1 and ErbB-2 are found in many human cancers and their excessive signalling may be critical factors in the development and malignancy of these tumours (Cho HS and Leahy DJ, 2002). EGFR activity has an important role in tumour development and progression by promoting cell proliferation, angiogenesis, metastasis, invasion, and inhibition of apoptosis. Enhanced activation of EGFR in cancer is either due to activating mutations, or overexpression and coexpression with its ligands which leads to constitutive autocrine stimulation of the receptor (Yarden Y, 2001).

Table 2: Tumour types with EGFR overexpression

Tumour Type	Percentage of Tumours
Bladder	31-48
Breast	14-91
Cervix/uterus	90
Colon	25-77
Oesophageal	43-89
Gastric	4-33
Glioma	40-63
Head and Neck	80-100
Ovarian	35-70
Pancreatic	30-89
Prostate	40-80
Renal cell	50-90
Non small-cell Lung	40-80

Source: PM Harari, Endocrine Related Cancer, 2004

EGFR and its receptors are involved in a large number of tumours, mainly epithelial malignancies such as bladder, brain, breast, prostate, ovary, gastrointestinal tract and brain cancers (Levitzki, 2003; Salomon *et al.*, 1995) (table 2). Overexpression of EGFR has also been identified in squamous cell carcinoma of the head and neck (SCCHN) and in non small cell lung cancer (NSCLC). In NSCLC, mutations are found in the intracellular portion of EGFR involving exons 17 to 21 (amino acids 712-979), and especially exon 19. Finally, mutations leading to EGFR overexpression have been associated with glioblastoma multiforme in which a more or less specific mutation of EGFR called EGFRvIII, where exons 2-7 (amino acids 6-273) are deleted, is often

found. Consequently, EGFR has been identified as a molecular target with high therapeutic potential in a variety of cancers. However EGFR overexpression alone does not predict response to anti-EGFR therapy (Bishop *et al.*, 2002).

1.3.3 C-KIT

C-KIT, the second receptor target studied, is a receptor tyrosine kinase (RTK) encoded by a 5-kb gene in chromosome 5 of mice and in chromosome 4q12 of humans. Initial characterisation was carried out on the viral oncogene *v-KIT*, a component of the Hardy-Zuckerman strain of feline sarcoma virus (HZ4-FeSV) (Besmer *et al.*, 1986). This viral gene was shown by cDNA cloning to be a truncated version of the cellular proto-oncogene *C-KIT*, the cleavage of which is thought to induce the activation of the oncogene (Yarden *et al.*, 1987; Qiu *et al.*, 1988).

1.3.3.1 C-KIT structure and function

Spontaneous mutations in murine loci *W* (white spotting) and *Sl* (steel locus) resulted in anaemia, lack of mast cells, pigmentation defects and infertility. These loci encode the C-KIT protein (Chabot *et al.*, 1988; Geissler *et al.*, 1988) and its ligand, stem cell factor (SCF, also known as mast cell growth factor, KIT ligand, steel factor) (Williams *et al.*, 1990; Zsebo *et al.*, 1990). The nature of the mutations between the two loci showed complementarity, suggesting the proteins encoded belonged to a receptor- ligand pair. The receptor was shown to be expressed in haematopoietic cells, melanocytes, and germ cells, whereas the ligand, which exists in either membrane-bound or soluble form, was produced by accessory environmental cells (e.g. bone marrow stromal cells or fibroblasts) that regulate the survival, proliferation, differentiation as well as the secretory function of the receptor-bearing cells (Galli *et al.*, 1994; Linnekin, 1999).

C-KIT belongs to the family of type III transmembrane receptor kinases that includes the platelet derived growth factor receptor (PDGFR) and the macrophage colony stimulating factor receptor (CSF-IR) (Besmer *et al.*, 1986; Yarden *et al.*, 1986). This family of receptors is a subset of the Protein Tyrosine Kinase (PTK) super family, comprising of transmembrane receptors with intrinsic protein tyrosine kinase activity. A schematic diagram of C-KIT is shown in figure 4.

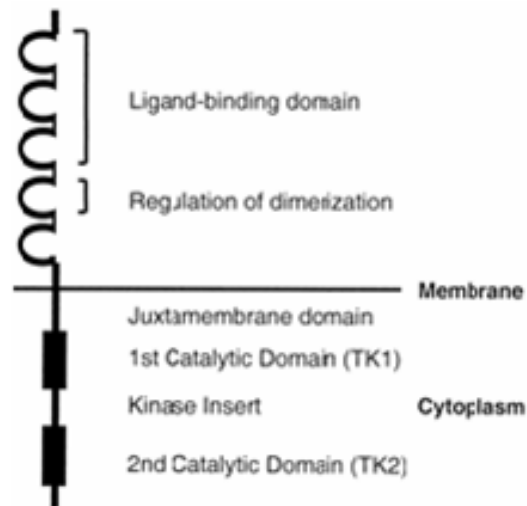


Figure 4: The structure of C-KIT
Source: MC Heinrich *et al.*, Journal of Clinical Oncology, 2002

The extracellular region of C-KIT contains five immunoglobulin domain repeats, three of which are involved in ligand binding. The binding of homodimerised ligand induces receptor dimerisation, activation of the receptor's intrinsic tyrosine kinase activity with subsequent autophosphorylation and activation of signal transduction pathways. The intracellular region of C-KIT contains two tyrosine kinase domains, TK1 and TK2, as well as a juxtamembrane domain which negatively regulates the TK1 and TK2 domains. The TK1 contains the ATP binding site while TK2 has possible autophosphorylation sites (Linnekin, 1999).

1.3.3.2 C-KIT signalling

Signalling downstream of C-KIT has been studied extensively using mast cells that express C-KIT endogenously as a model system. In cells whose survival depends on C-KIT signalling, apoptosis is inhibited through the PI3K/Akt pathway, while proliferation is promoted by the Ras/Erk, and the JAK/STAT pathways (Linnekin, 1999) as shown in figure 5.

1. The PI3-K pathway

C-KIT signalling through phosphatidylinositol-3 kinase (PI3K) induces a mitogenic response via activation of Akt and phosphorylation of Bad pro-apoptotic protein *in vivo* (Blume-Jensen *et al.*, 1998). C-KIT also induces resistance to apoptosis by upregulation of the anti-apoptotic protein Bcl-2 and Bcl-xL (Blume-Jensen *et al.*, 1998). PI3K binds tyrosine residue 721 of C-KIT via its p85 subunit. D816V, an activating mutation

present in acute myelogenous leukaemia (AML) and mastocytosis, is characterised by ligand- independent activation and transforming abilities and is associated with constitutive phosphorylation of tyrosine residues on PI3K. The significance of PI3K in the transforming ability of mutated D816V C-KIT was shown in immortalised murine progenitor cells transduced with the Y721F mutant D816V C-KIT, a mutant incapable of recruiting PI3K, where it was shown that tumourigenicity is PI3K-dependent (Chian *et al.*, 2001).

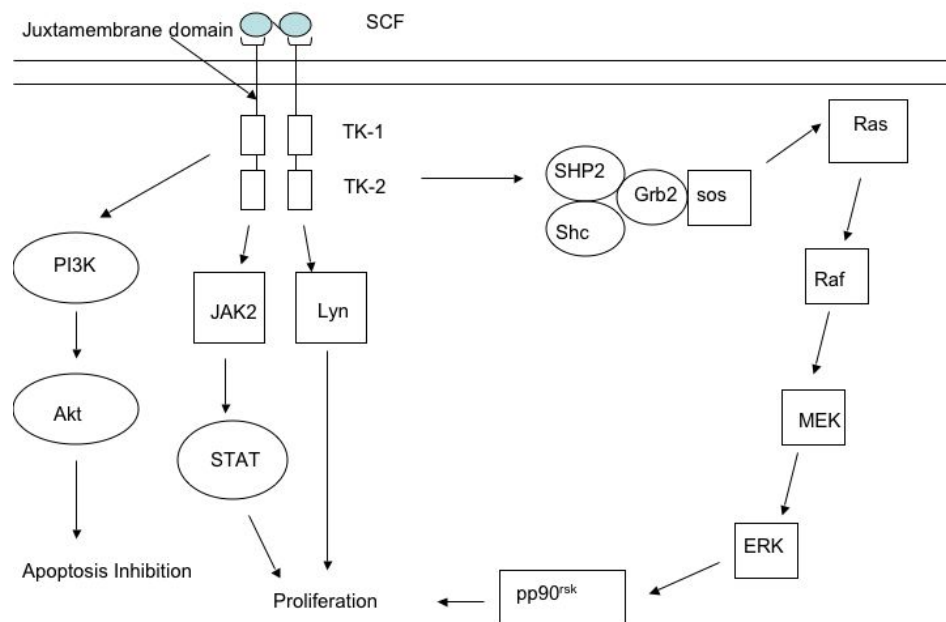


Figure 5: C-KIT signal transduction pathways

2. The Ras/Erk pathway

In a basic view of the Ras/Erk pathway, activated C-KIT recruits SH2-containing adapter proteins such as Grb2 to associate to its intracellular domain. Grb2 is bound in a complex with Sos, which then shifts to the plasma membrane and activates Ras. Activation of Ras is followed by phosphorylation of downstream kinases Mek and Erk. Erk kinases translocate to the nucleus and phosphorylate transcription factors such as c-Fos, which induce proliferation (Lennartsson *et al.*, 2005).

3. The JAK/STAT pathway

Ligand stimulation of C-KIT also leads to activation of the JAK (Janus kinase) protein tyrosine kinases. This is followed by phosphorylation and activation of the signal transducer and activators of transcription (STAT) proteins, which are transcription

factors containing DNA binding domains. Upon activation, STATs dimerise and translocate to the nucleus where they regulate the expression of genes promoting proliferation and survival (Linnekin, 1999; Lennartsson *et al.*, 2005).

1.3.3.3 *C-KIT and Cancer*

The association of C-KIT and its ligand SCF with defects in multiple cell lineages was followed by an extensive analysis and characterisation of its expression in human malignancies, shown in table 3. Normally C-KIT promotes the differentiation, survival and proliferation of tissues affected by *W* locus mutations such as erythropoietic cells, melanocytes, germ cells (Nocka *et al.*, 1989), tissue mast cells (Mayrhofer *et al.*, 1987), and bone marrow progenitor cells especially of the myeloid lineage (Ashman *et al.*, 1991; Escribano *et al.*, 1998). C-KIT immunoreactivity was more recently acknowledged in the well documented interstitial cells of Cajal (ICC), the pacemakers of the GI system (Torihashi *et al.*, 1995; Huizinga *et al.*, 1995).

The *C-KIT* oncogene has been associated with the aberrant proliferation of many tumours. Amplification or overexpression of *C-KIT* has been reported in AML (acute myeloblastic leukaemia) and in some cases of CML (chronic myelogenous leukaemia) (Kanakura *et al.*, 1993; Escribano *et al.*, 1998). Somatic activating mutations of *C-KIT* were also found in germ cell tumours (seminomas and dysgerminomas) (Ashman, 1999). Gain-of-function mutations of the receptor have been involved in the increased numbers of mast cells in mastocytosis, and in the malignant transformation of mast cells (Boissan *et al.*, 2000; Feger *et al.*, 2002; Tsujimura 1996). Activating mutations of *C-KIT* have been identified in many gastrointestinal tumours (Hirota *et al.*, 1998). These mutations lead to constitutive, ligand-independent phosphorylation of C-KIT, producing a growth and survival signal that is involved in the pathogenesis of the disease. In other cases though, which include small cell lung carcinoma and ovarian cancer the growth of the tumour was promoted by the paracrine or autocrine activation of the receptor by its ligand SCF and not by mutation (Parrott *et al.*, 2000; Krystal *et al.*, 1996).

Interestingly, gain of function mutations in the *C-KIT* gene occur at different sites in different neoplastic disorders, suggesting that the pathologic phenotype is determined both by the domain of mutation of the gene as well as the cell type in which the

mutation occurs. Exons 1-9 constitute the extracellular domain of the C-KIT protein. Mutations in this domain lead to ligand independent activation of the receptor and they have been identified in AML and GISTs. Exon 10 encodes the transmembrane domain with no mutations identified yet (Heinrich *et al.*, 2002; Lennartsson *et al.*, 2005).

Table 3: C-KIT expression in human malignancies

<i>Tumour Type</i>	<i>% Positive for KIT</i>	<i>% C-KIT Mutation</i>
Mastocytosis/mast cell leukaemia	100	>90
Gastrointestinal stromal tumour	100	>70
Sinonasal natural killer/T-cell lymphoma	NR	17
Seminoma/dysgerminoma	78-100	8.7
Thyroid carcinoma	100	NR
Small-cell lung carcinoma	91	NR
Malignant melanoma	0-90	NR
Adenoid cystic carcinoma	80-90	0
Ovarian carcinoma	71-87	NR
Acute myelogenous leukaemia	60-80	Rare
Anaplastic large-cell lymphoma (CD30 ⁺)	68	NR
Angiosarcoma	56	0
Endometrial carcinoma	44-100	NR
Paediatric T-cell ALL/lymphoma	43	NR
Breast carcinoma	Up To 81	NR
Prostate carcinoma	2	NR

Source: MC Heinrich *et al.*, Journal of Clinical Oncology, 2002

The juxtamembrane domain of the receptor, which is encoded by exon 11, serves as an antidimerisation domain and negatively regulates the two tyrosine kinase domains. Mutations in the juxtamembrane domain promote ligand independent dimerisation of the receptor and are found most commonly in GISTs. Exons 11-17 comprise the intracellular domains, with exons 13 and 17 encoding the tyrosine kinase domains. Mutations in exons 13 and 17 have been detected in systemic mastocytosis, GISTs and AML. Mutations in these domains affect the ATP binding ability of C-KIT and can yield gain of function or loss of function tyrosine kinase activity (Heinrich *et al.*, 2002; Lennartsson *et al.*, 2005).

The next group of receptors targeted includes the somatostatin receptors, which belong to the group of G protein coupled receptors.

1.4 G Protein-Coupled Receptors (GPCRs)

G protein-coupled receptors (GPCRs) are the largest family of transmembrane receptors with more than 800 members found in higher eukaryotes, including yeast, plants, and, especially, animals. This class of membrane proteins can respond to a wide range of agonists, including photon, odors, pheromones, amines, hormones, neurotransmitters and proteins, and vary in size from small molecules to peptides to large proteins. Their function is crucial, based on regulation of a wide range of molecular mechanisms including neurotransmission, endocrine and exocrine secretions, immune responses, cardiac and smooth muscle contraction, and blood pressure. GPCRs are involved in many diseases and represent the target of around half of all modern medicinal drugs (Dorsam & Gutkind, 2007).

1.4.1 GPCR Structure and Function

GPCRs are integral membrane proteins that possess seven membrane-spanning domains or transmembrane helices, therefore are also known as heptahelical receptors. The extracellular parts of the receptor may be glycosylated. These extracellular loops also contain two highly conserved cysteine residues which build disulfide bonds to stabilize the receptor structure. Some agonists bind to the extracellular loops of the receptor while others may penetrate into the transmembrane region (Pierce *et al.*, 2002).

The transduction of the signal through the membrane by the receptor is not completely understood. In its inactive state the receptor is bound to an inactive G protein, a heterotrimer of α , β and γ subunits. Ligand binding induces a change in the receptor conformation that mechanically activates the G protein, which detaches from the receptor (Dorsam & Gutkind, 2007).

It is believed that a receptor molecule exists in a conformational equilibrium between active and inactive biophysical states. The binding of ligands to the receptor may shift the equilibrium toward the active receptor state. If a receptor in an active state encounters a G protein, it may activate it. Some evidence suggests that receptors and G

proteins are actually pre-coupled. For example, binding of G proteins to receptors influences the receptor's affinity for ligands (Rubenstein & Lanzara, 1998).

1.4.2 GPCR Signalling

Inactive G proteins have GDP bound to the α subunit. Agonist-induced interaction between the GPCR and G protein causes the replacement of GDP for GTP in the α subunit and dissociation between α and $\beta\gamma$ subunits of the G protein. The separated α and $\beta\gamma$ subunits stimulate distinct downstream intracellular targets. The α subunits of G proteins are divided into four subfamilies: $G\alpha_s$, $G\alpha_i$, $G\alpha_q$ and $G\alpha_{12}$, and a single GPCR can couple to either one or more families of $G\alpha$ proteins. Each G protein activates several downstream effectors as shown in figure 6 (Neves *et al.*, 2002).

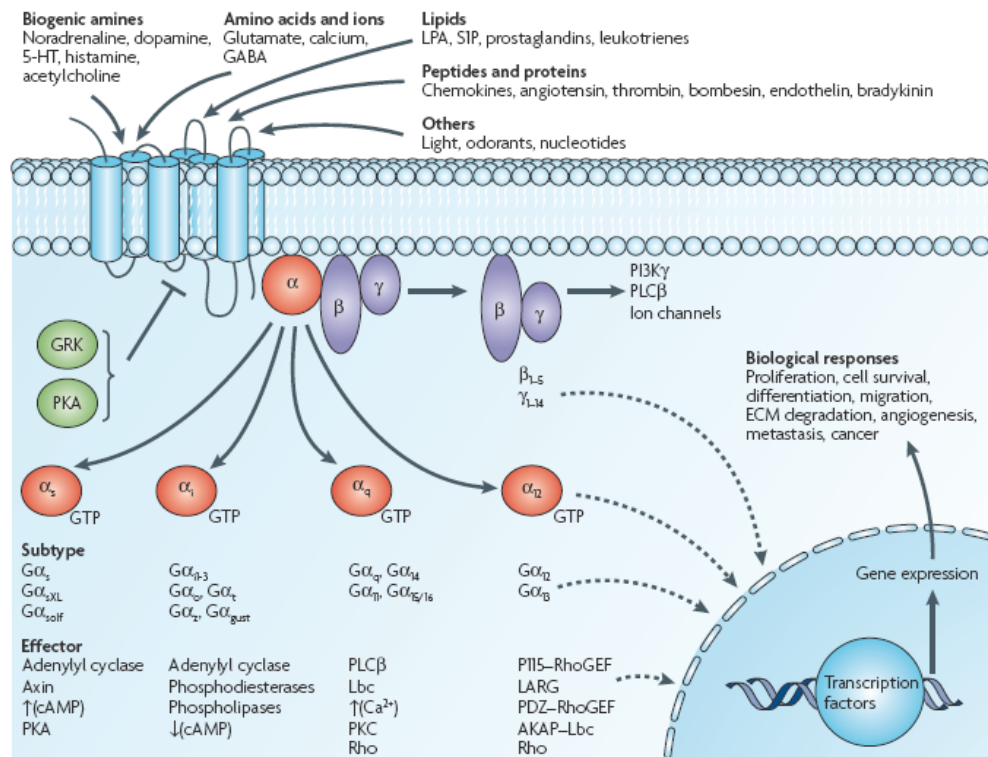


Figure 6: G protein-coupled receptor signalling

Source: RT Dorsam & JS Gutkind, Nature Cancer Reviews, 2007

Typically $G\alpha_s$ stimulates adenylyl cyclase and increases the levels of cyclic AMP (cAMP), whereas $G\alpha_i$ inhibits adenylyl cyclase and decreases cAMP levels and $G\alpha_q$ binds to and activates phospholipase C (PLC), which cleaves phosphatidylinositol bisphosphate (PIP₂) into diacylglycerol and inositol triphosphate (IP₃). The β and γ subunits function as a dimer to activate many signalling molecules, including

phospholipases, ion channels and lipid kinases. Besides the regulation of these classical second-messenger generating systems, G $\beta\gamma$ subunits and G α subunits such as G α_{12} and G α_q can also control the activity of key intracellular signal-transducing molecules, including small GTP-binding proteins of the Ras and Rho families and members of the mitogen-activated protein kinase (MAPK) family of serine-threonine kinases, including extracellular signal-regulated kinase (ERK), c-jun N-terminal kinase (JNK), p38 and ERK5, through an intricate network of signalling events that has yet to be fully elucidated (Pierce *et al.*, 2002; Marinissen & Gutkind, 2001).

1.4.3 GPCR regulation

GPCRs become downregulated after exposure to their ligand for a prolonged period of time. Two types of downregulation exist; the first one is homologous desensitization, in which the activated GPCR is downregulated by intracellular kinases and the heterologous desensitization, where an activated GPCR causes downregulation of a different GPCR. Downregulation is caused by phosphorylation in the cytoplasmic domain of the receptor by protein kinases. Phosphorylation is performed by c-AMP dependent kinases or by G protein-coupled receptor kinases (GRKs).

- Phosphorylation by cAMP-dependent protein kinases

Cyclic AMP-dependent protein kinases (i.e. protein kinase A) are activated by the signalling pathway initiated by ligand binding to GPCRs leading to activation of G proteins and consequently adenylate cyclase and cyclic AMP. In a feedback mechanism, these activated kinases phosphorylate the receptor. The longer the receptor remains active, the more kinases are activated, and thus more receptors are phosphorylated.

- Phosphorylation by GRKs

The G protein-coupled receptor kinases (GRKs) are protein kinases that phosphorylate only active GPCRs. Phosphorylation of the receptor results in translocation of the receptor, where the receptor is internalised into plasma membrane vesicles where it is dephosphorylated and then brought back to the surface (recycling). This mechanism is used to regulate long-term exposure, for example, to a hormone. The phosphorylated

receptor may also become connected to arrestin molecules that prevent it from binding to and activating G proteins for a short period of time.

(<http://en.wikipedia.org/wiki/GPCR> and references therein)

1.4.4 GPCRs and Cancer

The critical role of GPCRs in cancer progression is based on a number of experimental and clinical data. Constant GPCR stimulation by agonists produced and released from tumour or surrounding stromal cells leads to autocrine and paracrine activation and overexpression of the receptors in most tumour types (Heasley, 2001). Unregulated GPCR function has recently been correlated with the ability of malignant cells to proliferate independently, evade detection by the immune system, amplify their nutrient and oxygen supply, and spread to surrounding tissues and other organs (Castellone *et al.*, 2005; Dorsam & Gutkind, 2007). Activating mutations of G proteins and GPCRs were shown to promote the growth of some endocrine tumours, and constitutively active GPCR expression has been found in the genomes of human oncogenic DNA-viruses (Lyons *et al.*, 1990; Sodhi *et al.*, 2004). In colorectal cancer, GPCRs are also stimulated by prostaglandins, the products of enzymes cyclooxygenases 1 and 2 that cause inflammation, therefore providing a probable link between chronic inflammation and cancer (Brown & Dubois, 2005; Gupta & Dubois, 2001). Finally, GPCRs have a central role in tumour-induced angiogenesis, and tumour metastasis might involve the GPCR-guided migration of cancer cells to their target organs (Richard *et al.*, 2001).

Consequently, targeting GPCRs would be therapeutically valuable for patients with GPCRs-driven cancers. The receptors targeted in this study are the group of somatostatin receptors.

1.4.5 Somatostatin and Somatostatin Receptors

The group of GPCRs that have been targeted in this study includes the somatostatin receptors. Somatostatin was discovered and its hormonal function was defined more than 30 years ago. The wide range of anatomical distribution and actions of somatostatin and its receptors have motivated intense scientific and clinical interest. These receptors are strongly overexpressed in neuroendocrine tumours (NETs), therapy of which is the objective of our research, which will be discussed later in this chapter.

1.4.5.1 Structure and Function

Somatostatin (SST) is a cyclic disulphide-containing peptide hormone that was first discovered in the hypothalamus as an inhibitor of growth hormone (GH) secretion (Brazeau *et al.*, 1973). Somatostatin is a mixture of two peptides, one of 14 amino acids (SST-14), and the other of 28 (SST-28). They are produced throughout the central nervous system and in other peripheral organs such as the pancreas, gut, thyroid and adrenal glands, with a primary role in regulation of cell secretions (Patel, 1999). Both forms of somatostatin are generated by proteolytic cleavage of prosomatostatin, which itself is derived from preprosomatostatin (Patel, 1999). The relative amounts of SST-14 versus SST-28 secreted depend upon the tissue. For example, SST-14 is the predominant form produced in the nervous system and apparently the sole form secreted from pancreas, whereas the intestine secretes mostly SST-28. In addition to tissue-specific differences in secretion of SST-14 and SST-28, the two forms of this hormone can have different biological potencies. SST-28 is roughly ten-fold more potent in inhibition of growth hormone secretion, but less potent than SST-14 in inhibiting glucagon release (Tannenbaum *et al.*, 1982).

SST acts on various targets to produce a broad spectrum of biological effects. In the brain SST acts as a neurotransmitter and a regulator of paracrine and autocrine secretions (Epelbaum *et al.*, 1994). It also inhibits the basal and stimulated release of growth hormone and of the thyroid-stimulating hormone (TSH) (Patel & Srikant, 1986). Furthermore, it inhibits secretion of prolactin *in vitro* and diminishes elevated prolactin levels in acromegaly (Reichlin, 1983; Patel & Srikant, 1986).

SST is also secreted by cells in the pancreas and in the intestine, where it inhibits the secretion of a variety of other hormones. In pancreas, SST appears to act primarily in a paracrine manner to inhibit the secretion of both insulin and glucagon. It also has the effect in suppressing pancreatic exocrine secretions, by inhibiting cholecystokinin-stimulated enzyme secretion and secretin-stimulated bicarbonate secretion (Patel, 1999). SST is secreted by scattered cells in the GI epithelium, and by neurons in the enteric nervous system. In the GI tract, SST inhibits the release of virtually every gut hormone that has been tested, including gastrin, cholecystokinin, secretin and vasoactive intestinal peptide. In addition to the direct effects of inhibiting secretion of other GI hormones, SST has a variety of other inhibitory effects on the GI tract, which

may reflect its effects on other hormones, plus some additional direct effects. SST suppresses secretion of gastric acid and pepsin, lowers the rate of gastric emptying, and reduces smooth muscle contractions and blood flow within the intestine. Collectively, these activities seem to have the overall effect of decreasing the rate of nutrient absorption (Schubert, 2003; Patel *et al.*, 1995).

Five somatostatin receptors have been identified and characterized, all of which are members of the G protein-coupled receptor superfamily (Reisine & Bell, 1995). They are termed SSTR1-SSTR5 with SSTR2 receptor giving rise to two isoforms SSTR 2A and SSTR 2B through alternative splicing of the mRNA (Schindler *et al.*, 1998). These receptors are expressed in a variety of tissues including the brain, pituitary, pancreas and gastrointestinal tract (Patel, 1999). Each of the receptors activates distinct signalling mechanisms within cells, although all inhibit adenylyl cyclase (Benali *et al.*, 2000). Four of the five receptors do not differentiate SST-14 from SST-28. (Csaba & Dournaud, 2001)

1.4.5.2 Somatostatin Receptors and Cancer

A large variety of tumour cells exhibit SSTR expression and more than one isoform is usually present in each tumour. Most human tumours originating from SST target tissues such as gastroenteropancreatic, brain tumours, and pituitary tumours have their SSTRs conserved. SSTRs were first described in growth hormone producing adenomas and TSH-producing adenomas (Reubi *et al.*, 1992). Only half of endocrine inactive adenomas display somatostatin receptors. While brain tumours contain SSTRs, the receptor content varies with the tumour type. Medulloblastomas, oligodendrogliomas, and differentiated astrocytomas display somatostatin receptors. High grade glioblastomas lack SSTRs, whilst meningiomas express these receptors (Lamberts, 1991). A proportion of breast, prostate, colorectal and lung tumours also exhibit SSTRs on their surface (Reubi *et al.*, 1990). The expression of SSTRs and in particular of SSTR2 in high densities is found in 55-95% of NETs (Behr & Behe, 2002). Specifically, small cell lung cancer, medullary thyroid carcinomas and carcinoids contain a high density of homogeneously distributed SSTRs (Reubi *et al.*, 1990; Bousquet *et al.*, 2004).

SST has been implicated as having an anti-proliferative effect on a wide range of cell types. This may be an indirect effect, through suppression of secretion of growth factors and hormones vital for tumour growth or by blocking angiogenesis (Bousquet *et al.*, 2004). SST antineoplastic activity has also been shown *in vitro* against various cancer cell lines, in which cell cycle arrest or apoptosis is induced depending on the SSTR subtype as well as the target cell (Pollak & Schally, 1998). This anti-proliferative activity of SST led to the synthesis of analogues to the peptide that mimic the action of SST but can be more selective in their binding affinity to SSTR subtypes and more potent in their cytotoxic activity.

CHAPTER 2

TARGETING OF ENZYME AND RECEPTOR PATHWAYS: OVERVIEW AND IMPLICATIONS FOR THERAPY

The aim of my thesis is the study of enzyme and receptor pathways and this chapter provides an overview of the targets which I have explored.

2.1 Protein Tyrosine Kinases and Resistance to Genotoxic Therapies

PTKs can promote cancer through activation of the signalling pathways they control, which promote uncontrolled proliferation (independently of environmental survival factors such as growth factors), protection from apoptosis in the absence of external growth signals, inhibition of differentiation, and even supporting invasion and metastasis of cancer cells by deregulation of adhesion (Porter & Vaillancourt, 1998). In addition, it has recently been discovered that PTKs may also provide resistance to chemotherapy and radiotherapy, which could explain the failure of many anti-tumour treatments (Yu & Hung, 2000; Slupianek *et al.*, 2001). This was initially thought to be due to rapid detoxification, inactivation and efflux of drugs (El-Deiry, 1997). This was not proved to be the case, as these mechanisms arise late in the tumour development as a result of the selection of the tumour cells able to resist the genotoxins, whereas PTK-induced drug resistance is an early event in the transformation of cells which increases along with tumour progression and adds to its drug resistance (Masumoto *et al.*, 1999; Cambier *et al.*, 1998). PTK-transformed cells can accumulate additional genetic abnormalities, such as mutations or deletions of p53, p73, MSH2 or MLH1 which further increase genotoxic resistance (Strano *et al.*, 2001; Skorski, 2002). Resistance to genotoxic therapies can be induced by means of at least three mechanisms:

1. Enhanced DNA Repair

Cells transformed with the PTK can repair DNA lesions more rapidly than non-transformed cells. This was shown to be dependent on PTK activity (Majsterek *et al.*, 2002). The repair pathways activated by PTKs in cancer cells depend on the cytotoxic agent used and the types of DNA damage it causes (Skorski, 2002). Cells transformed by oncogenic fusion proteins such as the Bcr-Abl-like tyrosine kinases show upregulation of homologous recombination (HR) repair, responsible for DNA DSBs. This is through deregulated expression and phosphorylation of RAD51 (Slupianek *et al.*, 2002). Increased levels of RAD51 proteins have been observed in many tumours and correlate with drug resistance (Raderschall *et al.*, 2002; Vispe *et al.*, 1998). In contrast non-homologous end joining (NHEJ), which also repairs double strand breaks

(DSBs), appears to be downregulated in Bcr-Abl expressing cells (Deutsch *et al.*, 2001).

2. Checkpoint activation

Src PTK can dissociate cyclin-dependent kinase 2 (CDK2) from cyclin A in response to etoposide thus inducing S-phase arrest (Chen & Hitomi, 1999). In addition, Bcr-Abl-related PTKs induce pronounced G₂/M-checkpoint activation in response to various agents, including cisplatin (Raderschall *et al.*, 2002). The mechanism of G₂/M-checkpoint arrest in PTK-transformed cells is not known, but probably involves regulation of CDC2 phosphorylation (Slupianek *et al.*, 2002). It is thought that by prolonging the G₂/M phase, PTKs allow for HR to repair more DSBs and allow tumour cells to escape from the apoptotic pathway (Skorski, 2002).

3. Resistance to apoptosis

PTKs were shown to modulate the expression and post-translational modification of members of the BCL-2 family in order to protect cancer cells from apoptotic signals. Anti-apoptotic members such as Bcl-xL and Bcl-2 are stimulated, but proapoptotic members such as Bad and Bax are inhibited (Skorski, 2002). Bcr-Abl was shown to activate STAT5, a signal transducer and transcriptional activator responsible for Bcl_{XL} overexpression (Gesbert & Griffin, 2000). Additionally, Bcr-Abl also activates Akt which associates with Bad and keeps it away from the mitochondria. Akt can also stimulate the MDM2-dependent, ubiquitin-mediated degradation of p53 and subsequent downregulation of Bax and upregulation of Bcl-2 (Zhou *et al.*, 2001). C-KIT also induces resistance to apoptosis by upregulation of the Bcl-2 anti-apoptotic protein, and phosphorylation and inactivation of the pro-apoptotic Bad. As a result, cytochrome c release from mitochondria and consequent activation of caspase-3, events which are vital to induction of cell death by apoptosis, are inhibited (Carson *et al.*, 1994; Blume-Jensen *et al.*, 1998).

Resistance of cancer cells to chemotherapy or radiation due to overexpression of oncogenic protein tyrosine kinases has led to the selective targeting of these receptors as a new modality in the treatment of cancer patients.

2.2 Tyrosine Kinase Inhibitors

Approximately 200-300 PTKs are present in every cell. The ATP binding site is highly conserved within groups and this was initially a problem for the design of compounds with high specificity (Traxler *et al.*, 2001). The first drugs to be used against PTKs were broad-spectrum compounds such as herbimycin and sraurosporin which inhibited ATP binding at the active site of the enzyme targets. These drugs showed anti-proliferative activity against tumour cells expressing tyrosine kinases, but inactivation of multiple PTK targets was lethal and was considered less advantageous for clinical use than substrate based inhibitors (e.g. antibodies) (Sawyers, 2002).

Enormous progress in molecular, biochemical and cell biology technologies as well as advances in synthetic chemistry on natural products, crystallography and computerised molecular modelling have led to rational drug design of compounds with selective kinase inhibition (Traxler *et al.*, 2001, Sawyers, 2002). Screening for low molecular weight therapeutic agents against various cancers has become an important component of drug discovery. Recently, development of drugs such as imatinib (STI-571) which preferentially binds the inactive ATP binding site of the Abl protein preventing its activation, has led to a very important discovery: although the active binding site may be common among PTKs, in their inactive state proteins have a different conformation and therefore the binding site can be distinct allowing for selective drug targeting (Sawyers, 2002). Over the past few years, the number of receptors and in particular tyrosine kinases, being investigated as molecular targets in drug discovery has greatly increased. As a consequence, a growing number of compounds have been developed and used in clinical trials, as shown in table 4.

The extracellular domain of PTKs found in the plasma membrane is targeted with monoclonal antibodies that bind and inhibit activation of the receptor by its ligand. This may prevent receptor dimerisation, or promote receptor degradation. With the extracellular region of each receptor being unique, these agents are highly specific and do not cross react with other receptor tyrosine kinases. On the other hand, small molecule tyrosine kinase inhibitors target the intracellular ATP-binding region of the receptor and prevent its tyrosine kinase activity. These small molecule inhibitors have the advantage of being able to enter the cell, thus acting also against non-membrane

bound protein tyrosine kinases as well as receptors. The interaction with the target protein can be studied more easily using X-ray crystallography and computer modelling. As a result, their structure can be engineered in order to increase specificity as well as pharmacokinetic characteristics (Traxler *et al.*, 2001).

Table 4. Compounds targeted against tyrosine kinases

Drug	Company	Tyrosine kinase target
Monoclonal antibodies		
Herceptin	Genentech	Her-2/neu (ErbB-2)
MDX-H210	Medarex	Her-2/neu (ErbB-2)
2C4	Genentech	Her-2/neu (ErbB-2)
C225	Imclone	EGFR (ErbB-1)
MDX-447	Medarex	EGFR (ErbB-1)
Small molecule inhibitors		
STI-571	Novartis	Abl, c-kit, PDGFR
ZD1839	AstraZeneca	EGFR (ErbB-1)
OSI-774	OSI/Genentech	EGFR (ErbB-1)
PKI-166	Novartis	EGFR (ErbB-1); Her- 2/neu (ErbB-2)
PTK-787	Novartis/Schering	VEGFR (Flk-1/KDR)
SU5416	Sugen/Pharmacia	VEGFR (Flk-1/KDR)
SU6668	Sugen/Pharmacia	VEGFR (Flk-1/KDR), PDGFR, FGFR

Source: CL Sawyers, Current Opinion in Genetics and Development, 2002

Clinical studies conducted over the past decade have established several of these drugs as part of the standard treatment regimen for specific tumour types. These include imatinib (directed against Bcr-Abl and other kinases), trastuzumab (trade name Herceptin against HER2/ErbB2 receptor), and cetuximab (C225), erlotinib (OSI-774) and gefitinib (ZD1839), which are directed against the EGFR/ErbB1. Analysis of all the oncogenic tyrosine kinases and their inhibitors is beyond the scope of this discussion. However, the tyrosine kinases targeted and the inhibitors used in this study are outlined in detail below.

2.2.1 EGFR as a therapeutic target

Many types of EGFR inhibitors have been developed in the last decade, targeting different parts of the receptor protein structure or the synthesis of the protein itself. Of these, the most extensively studied drugs include monoclonal antibodies (table 5) binding the extracellular domain of the receptor such as cetuximab (Erbbitux; ImClone/BMS/Merck KGaA), or small molecule tyrosine kinase inhibitors (TKIs), that target the

intracellular (catalytic) tyrosine kinase domain of the receptor inhibiting downstream signalling effects, such as gefitinib (Iressa; AstraZeneca Pharmaceuticals) and erlotinib (Tarceva; ImClone Systems) (Harari, 2004).

Table 5. Monoclonal antibodies against EGFR

Agent	Type	Generic/Trade name	Institution
IMC-C225	Chimeric IgG1	Cetuximab/Erbitux	Imclone/BMS/Merck KGaA
ABX-EGF	Fully human IgG2	Panitumumab	Abgenix/Amgen
EMD72000	Humanized IgG1	Matuzumab	EMDpharms/Merck KGaA
MDX-447	Humanized bispecific: EGFR/FcR γ 1	HuMab-Mouse	Medarex/Merck KGaA
h-R3	Humanized	TheraCIM	YM biosciences/CIM
Mab 806	Anti-EGFR VIII	-	Ludwig Institute

Source: PM Harari, Endocrine Related Cancer, 2004

TKIs are synthetic, predominantly quinazoline derived molecules with low molecular weight and interact with the ATP binding domain of EGFR (Ciardiello *et al.*, 2000). A number of classes of TKI exist; reversible, irreversible, reversible dual ErbB1/2 TKIs and pan ErbB inhibitors (table 6) (El-Rayes and LoRusso, 2004). In July 2007 it was discovered that the blood clotting protein fibrinogen inhibits EGFR, thereby blocking re-growth of injured neuronal cells in the spine (Schachtrup *et al.*, 2007).

Table 6. EGFR tyrosine kinase inhibitors

Agent	Type	Generic/trade name	Institution
ZD1839	erbB1	Gefitinib/Iressa	AstraZeneca
OSI-774	erbB1	Erlotinib HC1/Tarceva	oSI/Genentech/Roche
CI-1033	Pan erbB1	Canertinib	Pfizer
EKB-569	erbB1/2	-	Wyeth Ayerst
GW2016	erbB1/2	-	GlaxoSmithKline
PKI-166	erbB1/2	-	Novartis

Source: PM Harari, Endocrine Related Cancer, 2004

2.2.1.1 Gefitinib (Iressa, ZD1839)

Gefitinib (figure 7) is an orally active, synthetic quinazoline-derived reversible EGFR inhibitor that interacts with the ATP-binding domain of EGFR, blocking its ligand-induced phosphorylation which leads to receptor activation (Ciardiello, 2000). Inhibition of EGFR by gefitinib has been shown both in cell lines and in xenograft models both as a single agent or in combination with a variety of chemotherapeutic agents, radiation therapy, or anti-sense oligonucleotides where additive or synergistic effects were identified (Ciardiello *et al.*, 2000; Ciardiello *et al.*, 2001a; Huang 2002; Friedmann *et al.*, 2004). The antiproliferative effect was shown to be due to cell cycle arrest or apoptosis. Inhibition of EGFR by gefitinib causes a reduction of the transcription factor, cFOS, mRNA which forms part of the AP1 complex, and a shift of cells from S phase into G0/G1 (Raben *et al.*, 2002). Gefitinib also causes reduction of VEGF, bFGF, and TGF- α , thereby inhibiting angiogenesis in a colon, breast, ovarian and gastric cells *in vitro* (Ciardiello *et al.*, 2000).

Gefitinib has shown antitumour activity and has been approved in many countries as a single treatment for refractive NSCLC (Harari, 2004). Research in gefitinib-sensitive patients with NSCLC showed that a mutation in the EGFR tyrosine kinase can facilitate efficacy of the drug. This mutation leads to activation of the anti-apoptotic Ras pathway which promotes cell proliferation. Malignant cell proliferation is inhibited by blocking of the Ras signal transduction pathway by gefitinib as well as other tyrosine kinase inhibitors (Lynch *et al.*, 2004; Paez *et al.*, 2004).

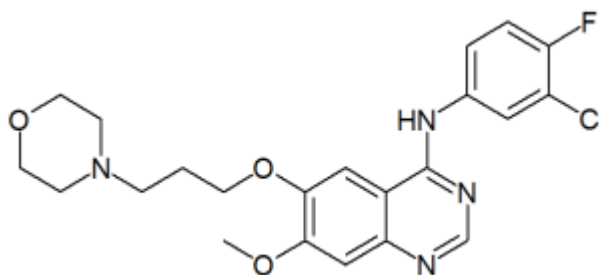


Figure 7: The chemical structure of gefitinib

Although the initial preclinical studies with gefitinib showed promising results a large study undertaken for the efficacy of gefitinib in patients with NSCLC failed to show improved survival in patients, and has been replaced in the United States by erlotinib,

which functions in a similar manner to gefitinib and has shown a survival benefit in the treatment of lung cancer in phase III trials (Shepherd *et al.*, 2005). Erlotinib has been approved by the FDA in November 2004 for the treatment of locally advanced or metastatic non-small cell lung cancer that has failed at least one prior chemotherapy regimen (Smith, 2005). In November 2005, the FDA approved the use of erlotinib in combination with gemcitabine for treatment of locally advanced, unresectable, or metastatic pancreatic cancer (Rocha-Lima *et al.*, 2007; Moore *et al.*, 2007).

2.2.1.2 Cetuximab (Erbix, IMC-C225)

The first and most extensively studied antibody against EGFR is cetuximab (Erbix; ImClone Systems, Inc). Cetuximab is a chimeric human/mouse mAb composed of the Fv (variable) regions of a precursor murine anti-EGFR antibody (mAb 225) with human IgG1 heavy and kappa light chain constant regions produced in mammalian (murine myeloma) cells. This recombinant antibody reduces the possibility of an anti-mouse immunological reaction in patients (Herbst and Shin 2002).

As other anti-EGFR antibodies, cetuximab operates by binding to the extracellular domain of EGFR, preventing ligand binding and activation of the receptor, and induces receptor internalisation and downregulation (Kim *et al.*, 2001). Studies in cell culture cells as well as xenograft models have also shown that cetuximab has an anti-angiogenic effect through inhibition of the vascular endothelial growth factor (VEGF), interleukin-8, and basic fibroblast growth factor (bFGF), resulting in growth inhibition of tumour cells (Perrotte *et al.*, 1999; Huang & Harari, 1999). Cetuximab has also been shown to mediate antibody dependent cellular cytotoxicity (ADCC) (Naramura *et al.*, 1993; Mendelsohn, 2001).

Studies of cetuximab in combination with various agents indicate dose-dependent additive or synergistic increase in growth inhibition. Several *in vitro* experiments and *in vivo* animal studies have also shown an enhancement of tumour response to radiation by cetuximab in human epidermoid, head and neck, and colon cancer xenografts (Saleh *et al.*, 1999; Milas *et al.*, 2000; Bianco *et al.*, 2000; Prewett *et al.*, 2002).

In 2004 cetuximab was approved by the Food and Drug Administration (FDA) to treat patients with advanced or metastatic colorectal cancer and is often given concurrently

with the chemotherapy drug irinotecan (Camptosar), a DNA topoisomerase I inhibitor, or alone for the treatment of irinotecan-resistant colorectal cancer (Harari, 2004). A large phase III randomised clinical trial showed that compared to radiation alone, combined treatment of cetuximab and radiation therapy increased the median survival and improved the duration of locoregional disease control in patients with head and neck cancer that has not spread to other parts of the body (Bonner *et al.*, 2006). Cetuximab was approved by the FDA in March 2006 for use in combination with radiation therapy for the treatment of locally or regionally advanced squamous cell carcinoma of the head and neck (SCCHN) or as a single agent for the treatment of patients with recurrent or metastatic SCCHN for whom prior platinum-based therapy has failed (Rocha-Lima *et al.*, 2007).

2.2.2 C-KIT inhibitor: Imatinib (STI571, Glivec, Gleevec)

Imatinib is an inhibitor against C-KIT, which has been extensively studied in literature. Imatinib (Glivec or STI571 by Novartis Pharmaceuticals) is a tyrosine kinase inhibitor that was initially developed to act against the fusion oncoprotein Bcr-Abl, a protein resulting from the Philadelphia chromosome translocation between chromosomes 9 and 22, which occurs in 95% of chronic myelogenous leukaemia (CML) patients. It suppresses CML primitive progenitors by decreasing their abnormal proliferation without increasing their apoptosis. Inhibition of Bcr-Abl by imatinib reinstates normal haematopoiesis. The drug also inhibits the tyrosine kinase activity of the normal Abl protein, C-KIT, and PDGFR (both α and β), (Holtz *et al.*, 2002; McGary *et al.*, 2002).

In vitro studies have shown that imatinib inhibits growth of cell lines expressing Bcr-Abl as well as primary cells (Druker *et al.*, 1996; Le Coutre *et al.*, 1999; Deininger *et al.*, 1997). Growth of cell lines transformed by Bcr-Abl, Tel-Abl, or Tel-PDGFR, where Tel is a putative transcription factor which like Bcr activates Abl and is required for the transforming function of the fusion protein, was inhibited by imatinib in the absence of exogenous growth factors (Carroll *et al.*, 1997). Imatinib also repressed SCF-mediated C-KIT activation and growth of the small cell lung cancer cell line H526. Growth reservation was accompanied by induction of apoptosis in media containing SCF as the only exogenous factor, but not in serum containing media where the effect of cell proliferation was cytostatic. Furthermore, imatinib efficiently blocked

SCF-mediated activation of C-KIT and of the MAP kinase and Akt, downstream target proteins involved in cellular proliferation and survival. The same effect was obtained by treatment with imatinib using the murine lymphoid Ba/F3 cell line transfected with various types of activating C-KIT mutant (Krystal *et al.*, 2000; Chen *et al.*, 2003).

Imatinib is a 2-phenylaminopyrimidine derivative (figure 8) that specifically inhibits activation of receptor tyrosine kinases by competitive binding to the ATP-binding site needed for autophosphorylation and stabilising the receptor in its inactive form (Gambacorti-Passerini *et al.*, 2003). Therefore, the drug can be effective in malignancies where the above tyrosine kinase receptors are the driving force for proliferation, and in mutations that do not affect the ATP-binding pocket conformation. Indeed, in the case of C-KIT, imatinib was shown to be effective against activating mutations in the juxtamembrane domain of the receptor (GISTs, mastocytosis) but not as effective against mutants in the tyrosine kinase domain (Chen *et al.*, 2003). The most notable example is the D816V mutant (exon 17), found in AML and mastocytosis, which results in constitutive activation of the receptor and resistance to imatinib due to increased affinity of this isoform to ATP or possibly due to conformational changes that inhibit binding of the drug (Heinrich *et al.*, 2002; Lennartsson *et al.*, 2005).

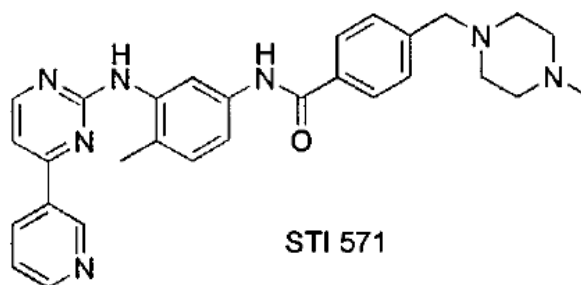


Figure 8: Chemical structure of imatinib

Addition of imatinib decreased the proliferation of GISTs and induced apoptosis in preclinical experiments (Demetri, 2001; Dematteo *et al.*, 2002). The drug is currently being used for the treatment of chronic-phase CML patients in whom interferon therapy has failed and for accelerated-phase and blast-crisis disease (Cohen *et al.*, 2005). Imatinib has also been approved for treatment of patients with unresectable and/or metastatic GISTs (Dagher *et al.*, 2002; Demetri *et al.*, 2002), with prolonged progression-free survival reported (Verweij *et al.*, 2004). Imatinib can induce high rates

of clinical response in patients with unresectable or metastatic dermatofibrosarcoma protuberans (DFSP; a tumor that forms under the top layer of skin). This has led to the approval of imatinib by the U.S. Food and Drug Administration for treating unresectable DFSP (McArthur, 2007).

One study demonstrated that imatinib was effective in patients with systemic mastocytosis, including those who had the D816V mutation (Droogendijk *et al.*, 2006). Imatinib is also increasingly being used in laboratory settings as an experimental agent to suppress PDGF by inhibiting its receptor PDGFR β . One of its effects is delaying atherosclerosis in mice with diabetes (Lassila *et al.*, 2004). Recent mouse animal studies at the Emory University in Atlanta have shown that imatinib and related drugs may be valuable in treating smallpox (Reeves *et al.*, 2005). Imatinib is also being used in the treatment of certain brain tumours including high grade glioblastoma.

2.3 Resistance to Tyrosine Kinase Inhibitors

Despite the promising preclinical data in various cell lines and animal models, as well as the initial responses of patients to single treatments using drugs against protein tyrosine kinases, the developing resistance of patients to these agents is a recognised problem. Mechanisms mediating resistance to TKI therapies include the presence of redundant tyrosine kinase receptors, increased angiogenesis, constitutive activation of downstream receptors, and development of specific mutations (Camp *et al.*, 2005).

2.3.1 Resistance to EGFR inhibitors

EGFR promotes survival and proliferation through downstream signalling pathways. Other tyrosine kinases also influence similar downstream pathways. An example of this is IGF-1R (Insulin like Growth Factor Receptor-1), a tyrosine kinase that activates the PI-3K/Akt downstream signalling pathway (Kulik *et al.*, 1997). IGF-1R over expression has been shown in EGFR inhibitor resistant cell lines (Chakravarti *et al.*, 2002). Activation of alternative tyrosine kinases such as IGF-1R allows tumour cells to bypass the EGFR pathway and develop resistance to EGFR targeting therapies.

EGFR mediated pathways promote tumour angiogenesis via VEGF upregulation. The EGFR ligands EGF and TGF α have been implicated in this process. Chronic

administration of monoclonal antibodies or TKIs to athymic mice bearing GEO colon cancer xenografts leads to development of resistant colon cancer cell lines showing a 5-10 fold increase in VEGF expression (Ciardiello *et al.*, 2003). These findings indicate increased expression of angiogenic mediators such as VEGF cause resistance against EGFR targeting therapies.

Constitutively active mediators of downstream signalling pathways cause resistance to EGFR targeting therapies in cancer. Downstream constitutive activation allows tumour cells to bypass the requirement for EGFR activation, decreasing the efficacy of EGFR inhibition (Camp *et al.*, 2005). Loss of PTEN phosphatase function commonly leads to downstream constitutive activation within the EGFR signalling pathway. PTEN is a PI-3K/Akt regulating tumour suppressor. Loss of PTEN causes over activation of the PI-3K/Akt pathway, promoting expression of the anti apoptotic genes Bcl-2 and Bclx (Marmor *et al.*, 2004). Akt has a major role in resistance to EGFR therapies and is implicated in resistance against both leading tyrosine kinase inhibitors gefitinib and erlotinib (Ramsay Camp *et al.*, 2005).

EGFR mutations such as the EGFRvIII mutation generate constitutively active EGFR. Compared to wild type EGFR this mutation is resistant to gefitinib (Learn *et al.*, 2004). Some EGFR activating mutations have been shown to confer sensitivity to EGFR targeting therapies such as gefitinib (Lynch *et al.*, 2004). Unfortunately these tumour cells have gone on to develop further mutations that confer resistance to gefitinib (Kobayashi *et al.*, 2005).

2.3.2 Resistance to imatinib

Resistance to imatinib is mainly due to mutations leading to constitutive phosphorylation and ligand-independent activation of C-KIT. The most prominent mutation associated with imatinib resistance is the D816V substitution, which is found in the activation loop of the kinase domain (exon 17) and has been implicated in the increased proliferation of cells in AML, germ cell tumours and mastocytosis (Kanakura *et al.*, 1993; Escribano *et al.*, 1998; Ashman, 1999; Boissan *et al.*, 2000; Feger *et al.*, 2002). Identification of such gain of function mutations in the cytoplasmic domain of C-KIT by Hirota and co-workers in 1998 helped identify C-KIT as a potential target in GISTs (Hirota *et al.*, 1998). In fact, C-KIT is now used for the diagnosis of GISTs and

for the differentiation between GISTs and other soft tissue sarcomas of the GI tract (Jiang *et al.*, 2008).

GIST-associated mutations have been identified in exons 9, 11, 13, and 17 of the receptor. The most common mutations are found in exon 11, which is the intracellular juxtamembrane domain of C-KIT, and they actually improve the response of patients to imatinib. However, mutations in exon 9, which is the extracellular juxtamembrane domain of C-KIT, are linked with decreased sensitivity to imatinib and shorter survival rates in patients (Heinrich *et al.*, 2006; Debiec-Rychter *et al.*, 2004).

Another implication in GISTs relates to the activation of other tyrosine kinases as an alternative route to signal transduction. Candidate proteins include the receptor tyrosine kinase AXL. Analysis of gene expression in imatinib resistant cell lines showed overexpression of AXL and not C-KIT compared to imatinib sensitive cells (Mahadevan *et al.*, 2007). Using the same cell models, it was also shown that the PI3-kinase pathway remains active in imatinib resistant cells probably through a different receptor and that inhibition of the PI3-K signalling alone promoted inhibition of cell growth (Bauer *et al.*, 2007).

By far the biggest setback in GISTs is the acquisition of secondary mutations in imatinib-treated patients (Braconi *et al.*, 2008; Jiang *et al.*, 2008). The most prevalent mutation in relapsing patients is the V654A substitution found in the kinase domain (exon 13), with the rest of the mutations occurring in exon 17, which corresponds to the second tyrosine kinase domain of the receptor. These mutations lead to conformational changes in the receptor which affect binding of imatinib (Heinrich *et al.*, 2006). To overcome this secondary resistance in GISTs, new tyrosine kinase inhibitors with multiple targets are being developed. Sunitinib is such an alternative to imatinib, targeting C-KIT, PDGFR, VEGFR, and FMS-related tyrosine kinase 3 receptor, and has shown efficacy in a number of relapsing patients (Braconi *et al.*, 2008; Jiang *et al.*, 2008).

Although most of our study has focused on protein tyrosine kinases and their inhibitors, we also examined the therapeutic potential of somatostatin receptors.

2.4 Somatostatin analogue: Octreotide (Sandostatin, SMS201-995)

Octreotide (Novartis, Basel, Switzerland) is an octapeptide synthetic analog of somatostatin (SST, figure 9) that possesses the same pharmacological properties as SST, except that it is cleared from the circulation at a much slower rate by being resistant to plasma degradation. The half life is 117 minutes as compared to approximately 3 minutes for SST, making it more suitable for therapeutic and imaging purposes (Degen & Beglinger, 1999). Octreotide, like SST, has been shown to inhibit exocrine and endocrine secretions of the digestive system, including gastrin, serotonin, growth hormone, insulin and glucagon. A number of signal transduction proteins are regulated by somatostatin and its analogues, and these include cyclic AMP, diacylglycerol (DAG), calcium and potassium channel proteins and tyrosine phosphatases (Oberg, 1996). Octreotide is used for the symptomatic control and inhibition of tumour growth in NET patients. It can also adjust the motility of the GI tract and biliary system and has been shown to induce apoptosis.

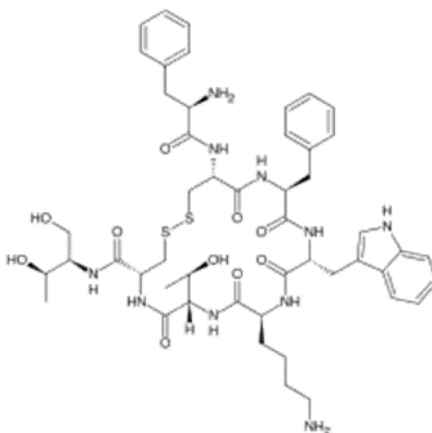


Figure 9: Chemical structure of octreotide

Octreotide binds SSTR2 and SSTR5 with high affinity, SSTR3 with low affinity, and has no affinity for SSTR1 and SSTR4 (Kulaksiz *et al.*, 2002). Two long acting SST analogues with similar efficacy to octreotide now in use in NETs include lanreotide (Ipsen, Paris, France) and octreotide-LAR (long-acting release), which are both administered monthly. SST analogues have shown anti-neoplastic activity in mammary, pancreatic, colorectal and lung cancers (Weckbecker *et al.*, 1993). Octreotide has also shown anti-proliferative effects *in vitro* against gastric and pancreatic adenocarcinoma cells (Hofsli *et al.* 2002, Wang *et al.*, 2003). It has been introduced for the treatment of

endocrine tumours of the gastrointestinal tract as it was shown to effectively control symptoms resulting from excessive hormone release in patients with carcinoid, Verner-Morrison and glucagonoma syndromes. In this way it improves the quality of life of patients whose tumours produce the above hormones. SST analogues may also have anti-tumour activity in a minority of carcinoid patients (Caplin, 1998). SST analogues have also been used for the treatment of insulinomas, as they inhibit insulin secretion (Bertherat *et al.*, 2003).

Octreotide is registered in most countries for the treatment of patients with carcinoid syndrome and also for glucagon and VIP producing tumours (Oberg, 2001). Long-term studies have shown that somatostatin analogues are safe and that the most important adverse effect is the development of gallstones. The antiproliferative potency of SST and its analogues *in vitro* and in experimental tumour models prompted a number of studies in patients with metastatic endocrine tumours that are generally unresponsive to conventional chemotherapeutic protocols. Stabilisation of tumour growth lasting for months to a few years was the most favourable result, occurring in 30 – 70% of patients (Behr *et al.*, 2002). In addition, a recent phase III PROMID study in patients with midgut carcinoid tumours using octreotide-LAR showed that time to progression was twice as long compared to placebo patients. These results indicate a possible anti-tumour effect by octreotide in well differentiated midgut NETs (Rinke *et al.*, 2009).

2.4.1 Somatostatin Receptor-Mediated Imaging and Therapy

The development of SST analogues such as octreotide has been very useful in the treatment of endocrine diseases and cancer. The molecular cloning of five distinct subtypes of SSTRs in the 1980s has led to the design and development of subtype-selective peptides and nonpeptide agonists and antagonists. The development of *in vivo* somatostatin receptor-mediated imaging known as somatostatin receptor scintigraphy (SRS or Octreoscan) is a valuable tool for the identification and localization of NETs and their metastases, and particularly GEP tumours, which mainly express SSTRs (Breeman *et al.*, 2001; Gibril & Jensen, 2004). This is based on visualisation of radiolabelled octreotide or lanreotide, binding to SSTRs. The next step was the exploitation of somatostatin analogues labelled with radionuclides emitting α or β particles, including Auger or conversion electrons, for neuroendocrine tumour

treatment, a technique called somatostatin receptor-targeted radiotherapy or peptide receptor radionuclide therapy (PRRT). These types of radionuclide labelled octreotide accumulate within tumour cells through receptor-peptide internalisation and are rapidly cleared from the blood due to their relatively small size (Reubi, 2004).

The radioisotopes used include ^{111}In (Indium-111), ^{90}Y (Yttrium-90) or ^{177}Lu (Lutetium-177). The peptide labelled with a radioisotope is covalently linked to a chelator, which stabilises the molecule. The chelator used for ^{111}In is diethylene-triamine-pentaacetic acid (DTPA) and 1,4,7,10-tetraazacyclododecane- $\text{N},\text{N}',\text{N}'',\text{N}'''$ -tetraacetic acid (DOTA) for ^{90}Y and ^{177}Lu . Octreotide labelled with ^{111}In is very effective in localising NETs (Kaltsas *et al.*, 2004), whilst ^{90}Y and ^{177}Lu are preferred for therapy (Srirajaskanthan *et al.*, 2009; Desai *et al.*, 2009).

Both ^{90}Y -octreotide and ^{177}Lu -octreotate have shown promising results in patients with GEP NETs (Kaltsas *et al.*, 2005). The use of $^{90}\text{Y}-(\text{DOTA})^0\text{-Tyr}^3\text{-octreotide}$ (^{90}Y -DOTATOC), resulted in 10–30% tumour response rates, and appears to be particularly effective in generally large tumours (Waldherr *et al.*, 2002). On the other hand, $^{177}\text{Lu}-(\text{DOTA})^0\text{-Tyr}^3\text{-octreotate}$ (^{177}Lu -DOTATATE) is better in small tumours. In a large study of more than 500 patients ^{177}Lu -DOTATATE produced 2% complete and 28% partial tumour response, with a survival benefit of several years (Kwekkeboom *et al.*, 2008). A combination of these drugs could therefore be beneficial in patients carrying both large and small tumours (Kaltsas *et al.*, 2005).

2.5 Chemotherapeutic Drugs for Anticancer Therapy

Cancer therapy is a major area of research and new treatments are actively being studied to target the leading cancers e.g. breast, lung, prostate and colon. Chemotherapy or radiotherapy is usually most effective against fast proliferating tumour cells. Neuroendocrine tumour cells are generally slow growing, so chemotherapy is therefore considered to be helpful in a minority of tumour patients. This has created the need for use of drugs with different mechanisms of action to treat patients, and the need to assess both single agent and combination therapies. One such consideration is the combination of growth factor inhibitors with chemotherapeutic agents.

In some uncommon tumours such as childhood cancers, lymphomas and teratomas, great progress has been made with the use of cytotoxic drugs. In other more common tumours such as lung and pancreatic carcinoma, the results have been less impressive, although modest improvements in survival have been obtained with chemotherapy and endocrine therapy in breast and colorectal cancer (De Vita *et al.*, 2005). Most anti-cancer agents serve to inhibit tumour cell growth and division although there is considerable potential for the development of agents which affect invasion, vascularisation and metastasis. Cytotoxic agents can reduce tumour cell growth and division by binding to DNA bases or impairing DNA synthesis to inhibit DNA replication, by damaging the mechanisms of cell division, or by blocking the pathways involved in cell growth. The main classes of chemotherapeutic agents are shown in figure 10.

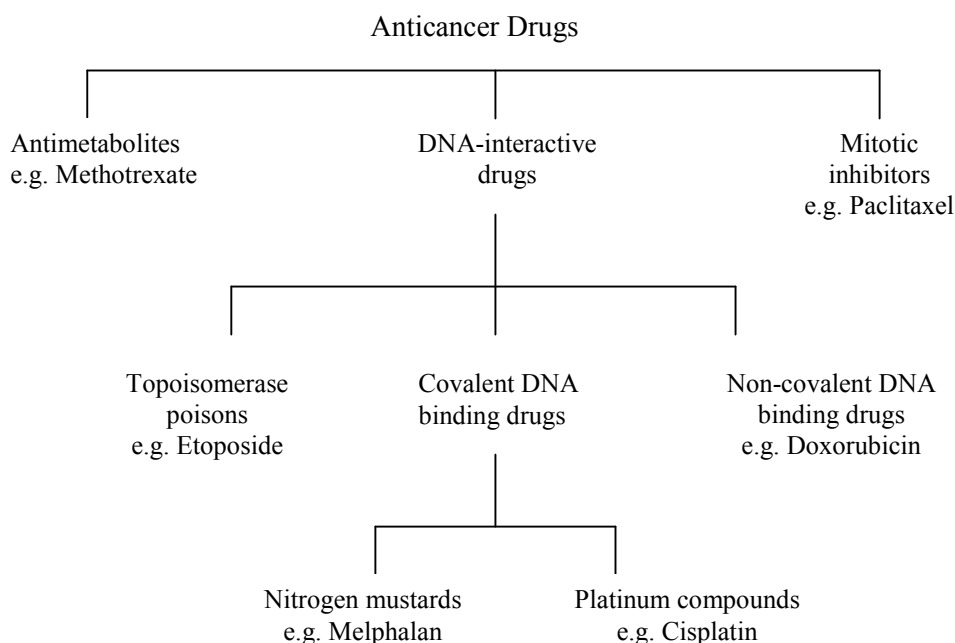


Figure 10: The different classes of anticancer drugs

To review all the chemotherapeutic agents is beyond the scope of this discussion. However, the agents used in this study are outlined in detail below. The merits of combination studies using growth factor inhibitors and chemotherapeutic agents will be discussed in detail and separately for each receptor target in the following chapters.

2.5.1 Cisplatin

Cisplatin or cis diaminedichloroplatinum (CDDP) is an inorganic compound with a planar configuration (figure 11) that kills cancer cells by binding to DNA and interfering with its repair mechanism, eventually leading to cell death by apoptosis. It exists in cis and trans conformations, of which only the cis isomer is cytotoxic. Cisplatin was discovered in a study by Barnett Rosenberg (1985) designed to study the possible effect of electric current on the growth of *Escherichia coli*. Inhibition of cell division but not cell growth leading to bacteria forming long filaments was identified and this was due to the electrolytic product of the platinum electrode. Cisplatin is clinically used for the treatment of a wide variety of tumours, including testicular, ovarian, oesophageal, head and neck, and lung cancer (Loehrer & Einhorn, 1984)

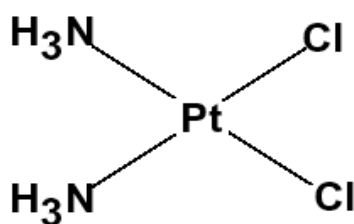


Figure 11: The chemical structure of cisplatin

The anticancer properties of cisplatin are similar to alkylating agents and commence with the substitution of one or both of its chloride ligands with hydroxyl groups after diffusion into the cell. This aquated complex of cisplatin is a reactive electrophilic agent that can form covalent bonds with nucleophilic species such as proteins, and nucleic acid bases of a DNA or an RNA strand (Reed *et al.*, 1999). DNA is the main target of cisplatin and this function is believed to mainly contribute to its cytotoxicity. Binding studies have shown a preference for nitrogen 7 (N⁷) on guanine.

As cisplatin is bifunctional, it can bind to DNA in several different ways. This results in the formation of inter- and intra-strand crosslinks, monoadducts, or DNA-protein crosslinks, which distort the shape of DNA, thus interfering with cellular transcription and replication (Trimmer *et al.*, 1999). The main adducts formed are shown in figure 12. The cisplatin-DNA complex attracts the HMG-1 (high mobility group-1) and other DNA repair proteins which become irreversibly bound and prevent effective repair.

Studies *in vitro* have shown cisplatin to react with DNA to form adducts of which 65% are 1,2-intrastrand d(GpG) crosslinks (between adjacent N⁷-guanine sites), 25% are 1,2-intrastrand d(ApG) crosslinks (between adjacent N⁷-guanine and N⁷-adenine sites), with the remaining 10% of adducts in the form of other intrastrand crosslinks, interstrand crosslinks, monofunctional adducts and DNA-protein crosslinks (Fichtinger-Schepman *et al.*, 1985; Dronkert & Kanaar, 2001). Cisplatin is not cell phase specific.

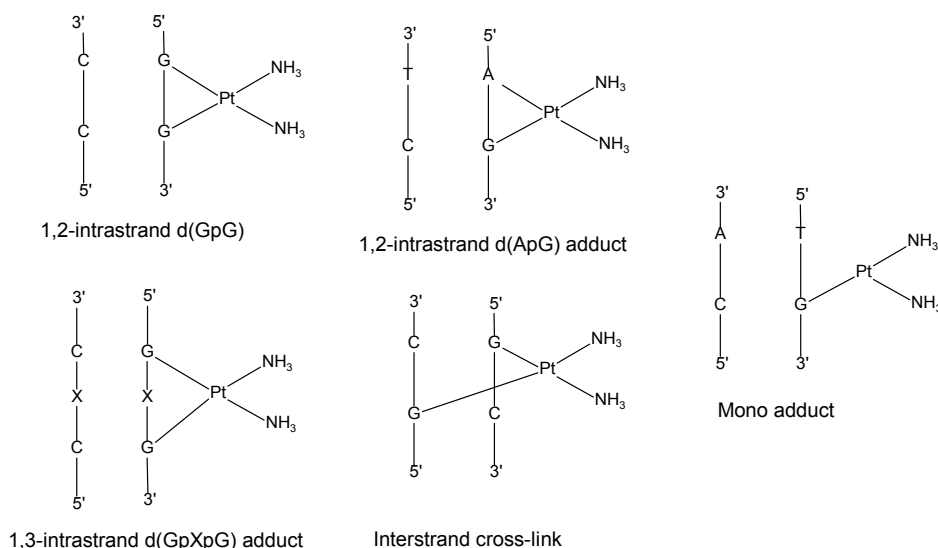


Figure 12: Types of DNA adducts formed by cisplatin

2.5.2 Etoposide

Etoposide (VP-16) is a semisynthetic derivative of podophyllotoxin, a toxin found in the *Podophyllum peltatum* plant (figure 13). It is used for the treatment of lung cancer, testicular cancer, lymphoma, non-lymphocytic leukaemia, and is often given in combination with other drugs. It belongs in the group of chemotherapeutic agents that inhibit chromatin function by inhibiting topoisomerase II. DNA inside cells is extensively twisted (supercoiled) to fit inside the nucleus. Topoisomerase II enzymes are multisubunit proteins that permit selected regions of DNA to untangle to allow replication and transcription to occur. Untangling involves transient breakage of DNA, allowing for change of topology by passing an intact helix through the double-stranded break, and then resealing the breaks.

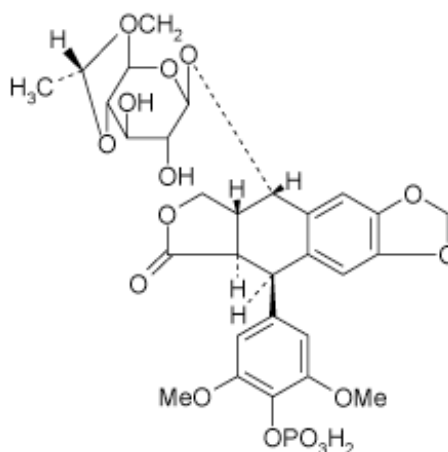


Figure 13: Chemical structure of etoposide

The mechanism of action of etoposide is in stabilizing the topoisomerase II-DNA complex and preventing it from making a topological change. When the replication fork encounters the DNA-topoisomerase complex it converts the transient break into an irreversible double strand break which is lethal to cells in S and G2 phases of the cell cycle. Permanent DNA double strand breaks then trigger apoptotic cell death (Hande, 1998).

2.5.3 Doxorubicin

Doxorubicin is an anthracycline antibiotic produced by the fungus *Streptomyces peucetius* (figure 14). Anthracyclines are intercalating drugs which have planar regions allowing them to stack between paired DNA bases forming tight (non-covalent) drug-DNA interactions. They include doxorubicin (adriamycin) and daunorubicin and have a planar ring system attached to an amino sugar.

The drug interacts with DNA by intercalation. The quinone ring is metabolised producing reactive oxygen species (ROS) which subsequently lead to free radical cleavage of DNA. This results in partial unwinding of DNA, impaired DNA and RNA synthesis and single strand breaks in DNA. It is also non-phase specific (Zhong *et al.*, 2001). It is therefore plausible that these multiple mechanisms which also have downstream effects on cell-cycle checkpoints have a clinical advantage over an agent with a single mechanism of action (Hurley, 2002). It has wide clinical activity for a variety of solid tumours (breast, ovarian and lung cancer) and leukaemia.

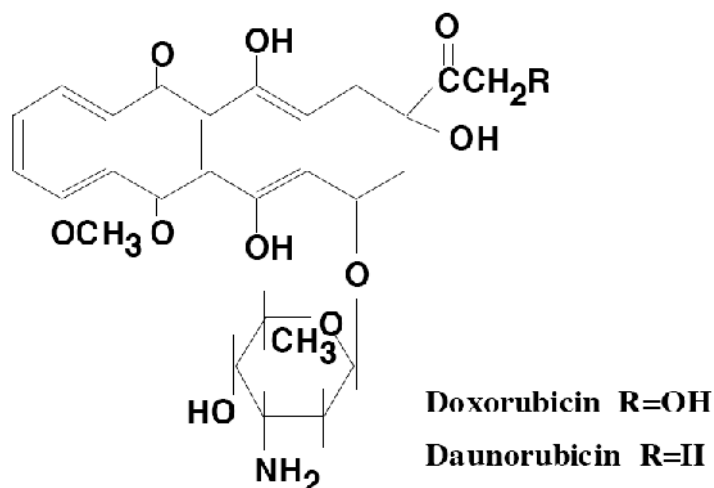


Figure 14: Chemical structure of anthracyclines

Doxorubicin shows an enhanced selectivity for cancer cells over normal cells. Intercalation prevents the progression of topoisomerase II and induces protein-associated strand breaks by stabilising the topoisomerase II – DNA complex after the enzyme has broken the DNA for replication. Preventing the DNA double helix from unwinding stops the process of replication (Fornari *et al.*, 1994; Tewey *et al.*, 1984). Given that these processes require protein binding to DNA, the selectivity of agents that target these processes might be dependent on the level of the associated target protein (for example, topoisomerase I or II), so cells with elevated levels of topoisomerase would be more sensitive to doxorubicin, and this is the basis for enhanced cancer-cell selectivity (Henderson & Hurley, 1995).

2.5.4 Melphalan

Melphalan is a chemotherapy drug that belongs to the class of nitrogen mustard alkylating agents. This includes mechlorethamine; a derivative of war gas sulphur mustard that was originally used in the 1940's to treat lymphomas. Melphalan is the phenylalanine derivative of mechlorethamine (figure 15) and it is used for the treatment of multiple myeloma, malignant melanoma and carcinoma of the ovary and breast.

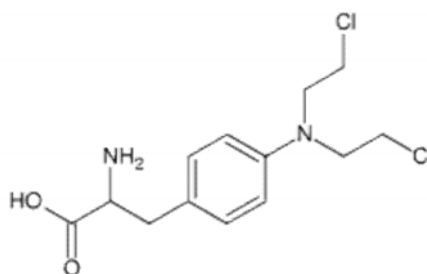


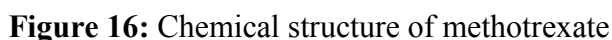
Figure 15: Chemical structure of melphalan

The mechanism of action involves the loss of chloride ions in water resulting in a carbonium ion that interacts with nucleophilic sites on DNA bases forming mono and bi-adducts depending on the ionisation of one or both chloride groups. In addition to N⁷-guanine adducts, melphalan also forms a large amount of adenine adducts with properties consistent with the alkylation at the N³ position (Povirk & Shuker, 1994). It should be noted that the N⁷-guanine atom faces into the major groove of the DNA structure while the N³-adenine atom faces into the minor groove. Thus, the melphalan-induced adduct exerts much greater pressure on DNA conformation than mechlorethamine.

2.5.5 *Methotrexate*

Methotrexate is an antimetabolite drug used in the treatment of cancer and autoimmune diseases. Antimetabolites are structurally related to naturally occurring compounds i.e. vitamins, amino acids or nucleotides. These drugs interfere with the production of nucleic acids by inhibiting specific enzymes needed for nucleoside triphosphate synthesis or by substituting for normal purine or pyrimidine bases. They are usually cell cycle dependent. Their action results in a decrease in DNA or RNA synthesis, thereby interfering with cell growth and proliferation (Pratt *et al.*, 1994).

Methotrexate (figure 16), an analogue of the vitamin folic acid, is an indirect inhibitor of thymidine nucleotide production. It does this by competitively and reversibly inhibiting dihydrofolate reductase (DHFR), a key enzyme in the biosynthesis of purines and the conversion of dUMP to dTMP. Methotrexate acts specifically during DNA and RNA synthesis, and thus it is cytotoxic during the S-phase of the cell cycle. Logically, it therefore has a greater toxic effect on rapidly dividing cells such as cancerous cells (Johnston *et al.*, 2005).



Paclitaxel is a highly complex organic compound isolated from the bark of Pacific yew tree *Taxus Brevifolia*. It is one of the most active anticancer drugs effective against carcinomas of breast, head and neck and is also used in combination with cisplatin in ovarian and lung carcinomas. It belongs to the group of microtubule inhibitor drugs which work by disrupting the equilibrium between polymerised and free tubulin dimers (Pratt *et al.*, 1994).

The chemical structure of compound 10 is a complex polycyclic molecule. It features a central polycyclic core with several stereocenters indicated by wedged and dashed bonds. The molecule includes a benzamide group (a benzene ring attached to a carbonyl group, which is further attached to an NH group) and a hydroxyl group (OH). There are also several ester and ether linkages, and a phenyl group (a benzene ring) is attached to the structure. The overall structure is highly complex and represents a significant synthetic challenge.

68

2.6 Ionising Radiation as Therapy in Cancer

Tyrosine kinase inhibitors were also used in this study in combination with x-rays (called radiation in the context of this study). X-rays is a type of ionising radiation. Ionising radiation in general refers to the energy transfer by a subatomic particle (alpha, beta, or neutron) or by a short-wavelength electromagnetic wave (high-frequency ultraviolet, X-ray, or gamma ray) which causes the detachment of electrons from atoms or molecules (DNA in living tissue) and therefore ionises them.

The degree of biological damage depends on the ionisation potency and the energy of the particle or electromagnetic wave. Alpha particles are heavily ionising and may cause 20 times more biological damage compared to x-rays, but they have little energy and a low range; they are only harmful when ingested and cannot penetrate the skin. Beta particles are less ionising than alpha and can penetrate a few millimeters into the tissue. Gamma rays are very energetic and penetrate tissue easily. X-rays are less energetic than gamma rays. Soft x-rays (0.12-12KeV) cannot penetrate matter. Hard x-rays (12-120KeV) can penetrate tissue easily and are largely used in diagnostic radiography (http://en.wikipedia.org/wiki/Ionising_radiation and references therein).

Ionising radiation is used for the treatment of malignant tumours (called radiation therapy or radiotherapy). In clinical practice radiotherapy can be used alone, or as an adjuvant treatment in combination with surgery, chemotherapy, or hormone therapy, depending on the type, size and locality of the tumour. In cases where cure is not feasible it can be used as a palliative treatment for the control of the disease and the associated symptoms. Radiation damages the DNA mainly by the formation of highly toxic free radicals, particularly hydroxyl radicals, by ionisation of the water molecules. These radicals damage the DNA structure. The most common result of ionising radiation is the formation of double strand breaks, which can be lethal to the cell. Another effect is the production and accumulation of mutations in cancer cells, which do not repair DNA as efficiently as healthy cells. These inherited mutations will finally lead to apoptosis of cancer cells.

2.7 *Aims of this study*

This study examines novel putative targets in neuroendocrine tumours. Combinations of growth factor inhibitors with chemotherapy and radiotherapy were undertaken in order to determine the best treatment options for therapy. This was examined using various techniques to assess the impact on the putative targets in NETs. The mechanism of interaction between the different agents used was also analysed with the intention to understand the biology of neuroendocrine tumour cells and the reason behind the lack of efficacy of previous treatment protocols in patients with NETs.

- In chapter 4 we combined chemotherapy and the EGFR inhibitor gefitinib with the intention to identify possible synergies. This was followed by examination of the effect of chemotherapeutic agents on EGFR activity. The chemotherapeutic drugs used were cisplatin, etoposide, paclitaxel and methotrexate. We identified activation of EGFR by cisplatin. This was further investigated by analysis of EGFR localisation in response to cisplatin.
- In chapter 5 we examined the effect of radiation in combination with EGFR inhibitors on cellular proliferation, EGFR activity and EGFR cellular localisation. Activation and concurrent nuclear translocation of EGFR by radiation was followed by investigation for a possible synergistic effect between EGFR inhibitors and radiation on DNA repair. The DNA repair mechanism impaired was investigated using the key DNA repair enzyme DNA-PK_{CS}.
- In chapter 6 we investigated the mechanism of EGFR translocation to the nucleus using nuclear import/ export inhibitors and analysed the possible role of the putative nuclear localisation sequence of EGFR in the translocation of the receptor into the nucleus. Finally, we tried to identify nuclear targets of EGFR using the nuclear proteins i-NOS (inducible nitric oxide synthase), Rad-51 and DNA-PK_{CS}.
- In chapter 7 we aimed to immunohistochemically identify C-KIT in NET patients.
- In chapter 8 we analysed the effect of the somatostatin receptor 2 inhibitor octreotide in combination with chemotherapeutic agents on cell growth of NET cell lines.

CHAPTER 3

MATERIALS AND METHODS

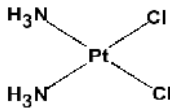
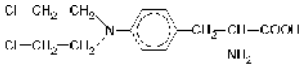
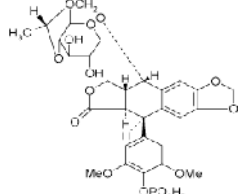
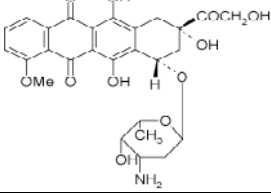
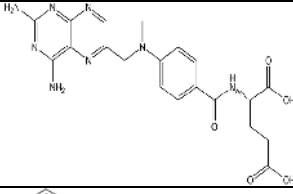
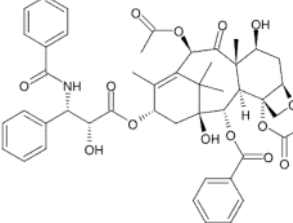
MATERIALS AND METHODS

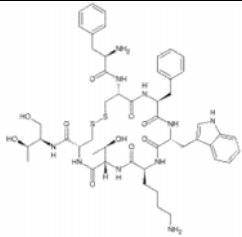
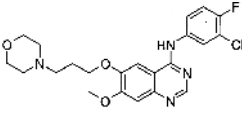
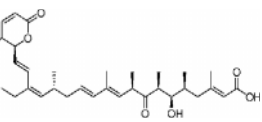
3.1 Chemical Reagents and Cytotoxic Drug Source

All reagents and disposables were obtained from Sigma Chemical Co., Poole, UK or VWR International Ltd., Poole, UK unless otherwise stated.

Cytotoxic drugs (Table 7) were prepared as stocks in advance, or as fresh prior to individual experiments depending on stability and activity in solution as well as experimental parameters. The concentration ranges used for experiments were modified based on previous personal communications on the cytotoxicity of individual agents where necessary.

Table 7: Cytotoxic drugs used in this study

Drug	Chemical Structure	Stock Solution	Solvent	Supplier
Cisplatin		3.3mM	Injection (Sterile Concentrate)	DBL, Warwick, UK
Melphalan		Fresh	Ethanol + 1% conc. HCl	Sigma, UK
Etoposide		Fresh	DMSO	Sigma, UK
Doxorubicin		1mM	H ₂ O	Sigma, UK
Methotrexate		10mM	1M NaOH + PBS	Sigma, UK
Paclitaxel (Taxol)		1mM	DMSO	Sigma, UK

Drug	Chemical Structure	Stock Solution	Solvent	Supplier
Octreotide		500µg/ml (~491µM)	Injection vial (Sterile Concentrate)	Novartis
Gefitinib (Iressa™, ZD1839)		10mM	DMSO	AstraZeneca
Cetuximab (Erbix, IMC-C225)	-	2mg/ml	H ₂ O ¹ (Sterile concentrate)	ImClone Systems, Inc
Wheat Germ Agglutinin	-	5mg/ml	PBS	Sigma, UK
Leptomycin B1		5µg/ml	Methanol: H ₂ O 7:3 (Sterile Concentrate)	Sigma, UK

3.2 Experimental Cell Lines

The cell lines used are outlined in table 8. CRI G1 (rat islet tumour), NCI-H727 (human bronchial carcinoid), RIN-5F (rat islet tumour), and SHP-77 (human SCLC) were obtained from ECACC. HCT-116 (human colon carcinoma), and BON-1 (human pancreatic endocrine cell line) were kindly provided by Prof. Watson (Cancer Studies Unit, Nottingham, UK).

NCI-H727 cell line was derived from non small cell carcinoma cells taken from the lung of a 65 year old female, which expresses p53 mRNA (Takahashi *et al.*, 1989). SHP-77 cell line was derived from a non encapsulated primary tumour of the lung of a 54 year old male with a modal chromosome number of 54 before and after

¹ Cetuximab is supplied at a concentration of 2mg/ml and is formulated in a preservative-free solution containing 8.48 mg/ml sodium chloride, 1.88 mg/ml sodium phosphate dibasic heptahydrate, 0.42 mg/ml sodium phosphate monobasic monohydrate and water.

transplantation in nude mice. SHP-77 cell line displays the biochemical properties of classical SCLC shown by the presence of dense core secretory granules and the expression of neuroendocrine markers such as NCAM (neural cell adhesion molecule) and L-dopa decarboxylase (Fisher & Paulson, 1978). CRI-G1 cell line originated from a NEDH (New England Deaconess Hospital) rat transplantable islet cell tumour, which secretes insulin and glucagon (Carrington *et al.*, 1986). RIN-5F cell line is a secondary clone of the rat islet tumour cell line RIN-m (ECACC catalogue no. 95071701), which expresses L-dopa decarboxylase, secretes insulin, and displays secretory granules (Chick *et al.*, 1977). BON-1 cell line is a human carcinoid-derived pancreatic tumour with a modal chromosome number of 57, which expresses somatostatin receptors and synthesizes serotonin and chromogranin A (Evers *et al.*, 1991; Lopez *et al.*, 2010). Finally, HCT-116 cell line was one of three strains isolated from a human with colonic carcinoma and is highly tumourigenic in nude mice (Brattain *et al.*, 1981).

Table 8: Cell lines used in this study

Cell Line	Origin	Culture Conditions	Supplier
NCI-H727	Human Bronchial Carcinoid-Adult Female	RPMI 1640	ECACC
CRI-G1	Rat islet tumour	DMEM	ECACC
RIN-5F	Rat islet tumour	RPMI 1640	ECACC
SHP-77	Human Small Cell Lung Cancer- Adult Male	RPMI 1640	ECACC
BON-1	Human pancreatic endocrine tumour	DMEM:F12K (50:50)	Cancer Studies Unit, Nottingham, UK
HCT-116	Human Colon Carcinoma- Adult Male	RPMI 1640	Cancer Studies Unit, Nottingham, UK

Cell lines were maintained in Dulbecco's Minimal Essential Medium (DMEM) (for CRI G1), RPMI 1640 (for NCI-H727, RIN-5F, HCT-116 and SHP-77 cell lines), or 50:50 DMEM: F-12K (F-12 Ham, Kaighn's Modification Nutrient Mixture) for BON-1 cells. All tissue culture media were supplied by Autogen Bioclear, Calne, UK apart from the F-12K media which were supplied by Sigma Chemical Co., Poole, UK. All media were supplemented with 10% foetal calf serum (FCS) (which was previously

heat-inactivated for 30 minutes at 57°C for SHP-77 cells), and 1% glutamine. The growth medium described for the routine propagation of exponentially growing cell lines is referred to as complete growth medium throughout.

3.2.1 Cell line culture – strengths and weaknesses

Cell lines used in research are immortalised cells which can proliferate indefinitely. Tumour-derived cell lines (like the ones used in this study) are immortalised spontaneously by random mutations in genes promoting senescence. Normal cells can also be used to establish cancer cell lines but these need to be immortalised artificially by the introduction (via a plasmid or a virus) of foreign genes which block senescence. The transduced genes usually inhibit aging of cells by the induction of oncogenes or the inhibition of tumour suppressor genes. Immortalisation is commonly induced by the transduction of normal cells with viral genes such as the gene for large T protein of the simian virus (SV40), which inactivates tumour suppressor genes p53 and Retinoblastoma (Rb) (Yeager & Reddel, 1999). Other transduced genes include the E6 and E7 genes of human papillomavirus (HPV), which also inhibit p53 and Rb and partially activate telomerase, or the entire genome of the Epstein-Barr virus (EBV) (Katakura *et al.*, 1998). The artificial induction of the telomerase gene, which stabilises DNA by maintaining the ends of chromosomes (telomeres), is also used for the artificial immortalization of cells. This is carried out using hTETR (human telomerase reverse transcriptase) expression vectors. The hTETR immortalised cell lines though are not cancerous as they retain ‘normal cell’ characteristics (Yeager & Reddel, 1999).

Culturing of cell lines has greatly advanced medicine as it is used for drug testing as well as the production of therapeutic biological compounds including proteins, hormones or vaccines on a large scale. Cell lines offer a controlled environment (pH, temperature, oxygen, carbon dioxide, etc.) in which a single homogeneous population of cells can be observed and analysed. In this way, an unlimited number of carefully characterized cells with a desired phenotype can be used in a multitude of applications. This is in contrast with organs or *in vivo* models where the function of a number of different cell types needs to be analysed, making the interpretation of results more complex. Also, the use of cell lines for drug testing is time- and cost-effective compared to *in vivo* models, and is carried out without the manipulation of animals, which may raise serious ethical issues.

On the other hand, cross-contamination of cell lines by other cell types (e.g. HeLa cell line) has been identified in 15-20% of studies which invalidates any results obtained in these cases. To this end, major cell line repositories such as ATCC (American Type Culture Collection) and ECACC (European Collection of Cell Cultures) authenticate all cell lines submitted by HLA typing and DNA fingerprinting using short tandem repeats (STR) (Cabrera *et al.*, 2006).

Tumour-derived cell lines are also genetically unstable and may present inconsistent phenotypes over time due to accumulated mutations, leading to changes in morphology, functions or range of genes expressed. Similarly, artificially immortalized cell lines may show loss of the differentiated characteristics of normal cells they are derived from as well as loss of normal cell cycle check-points (Yeager & Reddel, 1999). Genetic instability of cell lines is difficult to overcome and the recently developed hTETR immortalised cell lines may avoid unwanted genetic changes when studying normal cell biology. In our study we examined putative targets in neuroendocrine tumours and therefore made use of relevant tumour-derived cell lines.

It is a well known fact that differences in response have been observed between *in vitro* drug testing and clinical trials in patients making the use of cell lines somewhat controversial. These differences are generally due to the external environment of cells in each case. Cancer cells *in vitro* are cultured in an isolated and externally controlled environment whereas cancer cells in a patient's organ receive a multitude of signals from other cell types in the vicinity and from the entire human body. The acquisition of mutations associated with the genetic instability of cancer cell lines may also contribute to the differences seen. *In vitro* drug testing is therefore an initial step in the drug screening process and should be validated when possible by *in vivo* models before testing in humans.

3.3 Tissue Culture

3.3.1 Maintenance of Cell Lines

All cell lines were grown in 75cm² (T75) flasks and maintained at 37°C with 5% CO₂ in dry incubators (Forma Scientific, UK). All procedures were carried out in Class II MDH biological safety cabinet (Intermed MDH, UK) using aseptic techniques.

Exponentially growing cells were maintained at a cell concentration according to the European Collection of Cell Cultures (ECACC), Salisbury, UK.

Cells were routinely passaged at 80-90% confluence (biweekly). To this end, cells were washed with 10ml of 0.01M phosphate buffered saline (PBS) to remove serum. To detach the cells from the flask 5ml of 1X Trypsin/EDTA (Autogen Bioclear, Calne, UK) was then added for 5 minutes at 37°C. 5ml of complete growth medium was then added to inactivate the trypsin and the cell suspension was pelleted by centrifugation at 1,500rpm for 5 minutes at room temperature. Cells were then resuspended in complete growth medium and re-plated at an appropriate passage ratio for the cell line. The passage number was increased by one. Cells were discarded after approximately 25 passages and fresh cells were taken from the initial passage number used.

3.3.2 Cell Count

Trypsinised cells were resuspended in 10ml of complete growth medium and counted using a haemocytometer. To this end, 20µl of cell suspension was mixed with 20µl trypan blue (Sigma, UK) to exclude dead cells and the cell number was determined for each of five separate 1mm² fields. The average was multiplied by 2x10⁴ to give the number of cells per ml of suspension.

3.3.3 Determination of Cell Doubling Time

Cells were seeded out at an initial total cell number of 1x10⁵ cells per 25cm² (T25) flask containing 10ml of complete growth medium with an individual flask for every time-point. Cells were trypsinised, centrifuged, resuspended and counted using a haemocytometer as described above and the subsequent concentration used to determine the total cell count per flask. Further samples were taken every 24 hours until confluence. The doubling time of each cell line was calculated by reading off the exponential portion of the growth curve derived by plotting number of hours against total number of cells counted.

3.3.4 Mycoplasma Testing

Cell cultures were routinely tested for *Mycoplasma* contamination every 6 months. A total number of 5x10⁴ cells for each cell line were seeded onto a sterile coverslip placed in a flat bottom Falcon tube. Cells were allowed to adhere to the coverslips for 24 hours

at 37°C with 5% CO₂. Previously, the cell lines to be *Mycoplasma* tested had been set up such that the cells reached confluency concurrently with the set-up of the *Mycoplasma* test. Thus, from a flask containing a confluent cell population to be tested, 500µl of the supernatant growth medium was removed and transferred to the *Mycoplasma* testing tube. The cell-free supernatant must not contain additives such as hydrocortisone, cholera toxin or antibiotics that might interfere with *Mycoplasma* growth. The cells were incubated until they reached confluence. The medium was removed and the cells washed once with 0.01M PBS. The cells were then fixed in absolute methanol for 5 minutes and subsequently washed twice with 0.01M PBS and stained with 5µg/ml of Hoechst 33258 dissolved in 0.01M PBS for 10 minutes. Following two more washes with 0.01M PBS, the coverslips were carefully removed from the *Mycoplasma* testing tube, placed cell surface upwards on a glass microscope slide and covered with a coverslip. Analysis was performed under a fluorescent microscope using a x40 objective and ultra-violet (UV) illumination. Control cells showed intense blue-white staining of the nuclei only. *Mycoplasma* infected cells would have been covered in a fine lawn of speckles all over.

3.3.5 Storage and Retrieval of Cells in Liquid Nitrogen

Frozen cell stocks in liquid nitrogen were routinely prepared. Cells were grown in a 175cm² (T175) flask to semi-confluency. They were trypsinised and resuspended in media with 20% FCS containing 10% dimethylsulphoxide (DMSO). 1ml aliquots were frozen slowly in cryotubes in a styrofoam box at -80°C overnight before the cryotubes were transferred to a liquid nitrogen tank the next day. Each cryotube contained cells at a 10X higher concentration compared to the concentration at which they were grown.

Cells were recovered from liquid nitrogen by thawing rapidly in a 37°C water bath before being transferred into a T25 flask containing 10ml of growth medium supplemented with 20% FCS. Each cryotube was wiped off with paper towel sprayed with 70% industrial methylated spirit (IMS) to prevent accidental contamination of cell lines through bacteria and other cells stuck to the outer wall of the cryotube. Cells were split after 24 hours to remove any DMSO present in the media.

3.4 Irradiation treatments

X-radiation is traditionally known to induce DNA damage in the form of double DNA strand breaks. In our study x-radiation was also used to analyse possible changes in EGFR and DNA-PKcs activity and location within the cell. In radiotherapy, ionising radiation potency refers to the measurement of charge deposited in the tissue (unit is coulomb/kg), which is called the exposure. However, for living tissue the measurement of energy deposited is more relevant (unit is Gray or Gy, 1 Gy being the amount of radiation required to deposit 1 Joule of energy in 1 kg of matter) and this is called the absorbed dose. The doses used in cancer patients typically range between 20 and 80 Gy depending on the tumour type.

It is worth noting that an equal amount of absorbed dose (e.g. 1Gy) by different types of ionizing radiation (alpha or beta particles, gamma rays and x-rays) can cause different amounts of damage. To measure the biological damage the equivalent dose is implemented, which is measured in Sievert (Sv). Sievert is the absorbed dose multiplied by the quality factor, which depends on the radiation type. The quality factor for alpha particles is 20 while for gamma rays or x-rays is 1. The ionizing radiation chosen for use in this study is x-radiation as it has a low quality factor. X-ray radiation in our study is measured in Gy and refers to the absorbed dose (or simply dose) of radiation of neuroendocrine tumour cells (http://en.wikipedia.org/wiki/Ionising_radiation and references therein).

For irradiation treatments, cells were placed on ice and irradiated using the General Electric X-Ray source (250 Kv Newton victor). The x-ray machine was set up and calibrated by an independent nuclear physicist at the Middlesex Hospital to a dose rate of 2.35g/min; 212KV/12.5mA. The amount of absorbed dose is dependent on the exposure, distance from x-ray source, and the use of appropriate filter.

- Cells used in immunofluorescence, electron microscopy, or immunoblotting for EGFR or DNA-PKcs (in either whole lysates, or cytoplasmic and nuclear extracts) including transiently transfected cells, were used for analysis of EGFR/ DNA-PKcs activity and cellular localisation. Radiation dose was 4 Gy for all cells, except NCI-H727 cells which were radiated at 30Gy.

- Cells used in COMET analysis including transiently transfected cells were used to measure the amount of DNA damage and rate of repair. Radiation dose was 15 Gy for all cells, except NCI-H727 cells which were radiated at 30Gy.

For these studies cells were treated with either one or two drugs followed by irradiation.

- Single drug treatments include gefitinib or cetuximab at a fixed concentration for a period of 3 hours followed by irradiation at the appropriate dose.
- In double drug treatments gefitinib is added first for 3 hours with a second drug (wheat germ agglutinin or leptomycin B1) added in the last 30 minutes followed by irradiation.
- Irradiated cells are immediately transferred to a 37⁰C incubator for suitable intervals: a) 0-20 minutes for immunoblotting and immunofluorescence to analyse EGFR activity and cellular localisation, and b) 0-120 minutes to measure the amount of DNA damage and rate of repair.

3.5 *In vitro* Cytotoxicity Assay and Pharmacological Analysis

3.5.1 *Sulphorhodamine B Growth Inhibition Assay*

Cytotoxicity of drugs alone or in combination was determined using the Sulphorhodamine B (SRB) assay in 96-well microtitre plates. As described previously by Skehan *et al.*, (1990), they developed a rapid, sensitive, and inexpensive method for measuring the cellular protein content of adherent and suspension cultures based on the binding of the SRB purple dye to cellular protein. They showed the SRB assay to produce results linear with the number of cells and with values for cellular protein measured by both the Lowry and Bradford assays at densities ranging from sparse sub-confluence to multilayered supra-confluence. The signal-to-noise ratio at 564 nm is favourable and the resolution is 1000-2000 cells/well. In addition, they showed that the sensitivity of the SRB assay compared favourably with sensitivities of several fluorescence assays and was superior to those of both the Lowry and Bradford assays and to those of 20 other visible dyes. The SRB assay provides a colorimetric end point that is non-destructive, indefinitely stable, and visible to the naked eye. It provides a sensitive measure of drug-induced cytotoxicity, is useful in quantitating clonogenicity, and is well suited to high-volume, automated drug screening. SRB fluoresces strongly

with laser excitation at 488 nm and can be measured quantitatively at the single-cell level by static fluorescence cytometry (Skehan *et al.*, 1990; Voigt, 2005).

The optimal cell concentrations were determined from the previously calculated doubling times in order to achieve a final cell concentration ideal for accurate optical density (OD) measurement. Cells were plated in 96-well flat-bottomed microtitre plates, each well containing 100µl cell solution (4×10^3 or 15×10^3 cells/well depending on cell doubling time). Prior to drug treatment, cells were allowed to adhere at 37°C with 5% CO₂ for 24 hours.

Following drug treatment, media was carefully removed and the cells subsequently fixed with 100µl of 10% trichloroacetic acid solution for 20-30 minutes at 4°C. The fixed cells were washed three times with tap water and any remaining water flicked out of the wells. 100µl SRB stain (0.4% in 1% acetic acid) was then added to each well to allow visualisation of cellular proteins and incubated at room temperature for 20-30 minutes. Any excess SRB was removed by washing 4-5 times with 1% acetic acid. Plates were air-dried overnight. Finally the dye was dissolved in 100µl 10mM Tris/1mM EDTA for 10 minutes on a plate shaker. Plates were read at an absorbance of 540nm on a Tecan Microplate reader and analysed using computer spreadsheet (Microsoft Excel).

Growth inhibition was expressed as a percent proliferation of control and was calculated using the following equation:

$$\frac{\text{OD (treated)}}{\text{OD (control)}} \times 100 = \text{Proliferation (\%)}$$

The data shown represents the averages of three different experiments, each performed in triplicate and includes related standard deviations as calculated. The IC₅₀ is defined as the drug concentration needed to produce a 50% growth inhibition. The dose-response curves obtained for each treatment were used to calculate their respective IC₅₀ values.

Single Agent Treatments

For single-agent studies, drugs were added at a range of concentrations to triplicate wells. Incubations performed were continuous (24, 48, or 72 hours followed by 2 days

drug-free medium). All drugs were diluted in complete growth medium and 100µl of the relevant concentration added to the appropriate wells. One solvent control lane was included in each experiment. The concentration range for each drug was optimised if necessary following analysis of results from the first experiments. Following the 24, 48, or 72 hour incubation with the drug, the drug solution was removed and replaced with 200µl drug free complete growth medium. Plates were incubated at 37°C with 5% CO₂.

Dual Agent Treatments

For combination studies, drugs were added simultaneously for 72 hours followed by 2 days in drug-free growth medium, or sequentially by delivering drug A for 24 hours, then the drug B for 48 hours, followed by 2 days in drug-free growth medium.

For acute drug exposure, cells were incubated for 2 hours with drug A followed by 72 hours with drug B followed by 2 days drug-free-medium. Control wells were treated in the same way with aspiration at each period respectively. Again, plates were incubated at 37°C with 5% CO₂.

For determination of synergy, one of the drugs was added at a fixed sub-toxic concentration (e.g. producing 10% or 20% inhibition of proliferation) to a range of concentrations for the other drug.

Combination studies with radiotherapy

Radiation doses used in proliferation studies were 4 Gy for all cells except NCI-H727 cells which were radiated at 30 Gy. These doses were chosen for their 50% inhibition of proliferation.

In combinations treatments, cells were radiated on day 1 at the appropriate dose, followed by treatment with a drug at a range of concentrations. The reverse order with drug treatment preceding radiation was also performed. Treatments were followed by 2 days in drug-free growth medium.

3.5.2 Isobologram Analysis

Isobologram analysis can be applied in order to assess whether a combination dose of any two given drugs behave in a synergistic or additive fashion. The methodology applied has been previously described by Tallarida, (2001). Briefly, a particular effect

level is selected, in our case 50% of the maximal inhibition of proliferation (IC_{50}) and doses of each drug alone that give this effect are plotted as axial points in a Cartesian plot. This is illustrated in figure 18 where Drug A (x-axis) has an IC_{50} of 20(μ M) and Drug B (y-axis) has an IC_{50} of 100(μ M). The straight line connecting the IC_{50} s of drugs A and B is called the additivity line and defines the locus of all dose pairs (or isoboles) that will produce 50% of maximal inhibition of proliferation in a simply additive combination. This includes either one drug alone (points 0,100 and 20,0). This line of additivity allows a comparison with the IC_{50} obtained when the two drugs are added together experimentally. Thus, the IC_{50} for two drugs added together lying well above this line have a sub-additive or antagonistic effect (illustrated by the letter R). If the IC_{50} for two drugs added lie on or close to the line they are said to have an additive effect (illustrated by the letter P). And if they exist well below the line a super-additive or synergistic effect is achieved (illustrated by the letter Q).

In our combination studies one of the two drugs e.g. drug A is added at a fixed dose, while drug B is titrated. In this case the IC_{50} for the two drugs added together is defined by values x = fixed dose for drug A and y = IC_{50} for the two drugs.

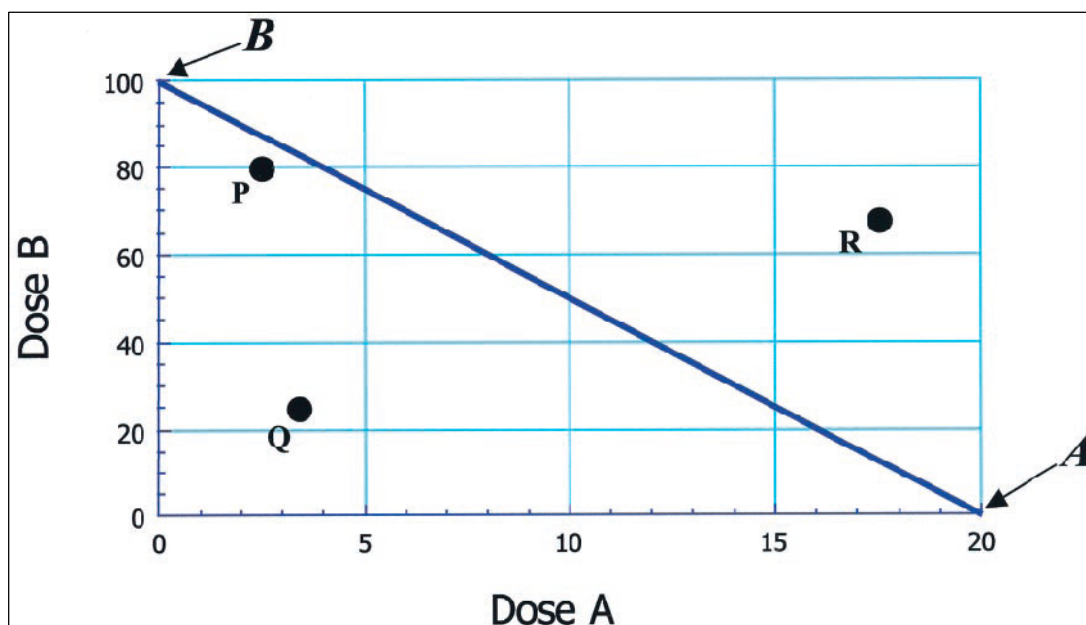


Figure 18: Illustrated isobologram for some particular effect.

Source: Tallarida RJ, J Pharmacol Exp Ther (2001)

It is important to note, that the isobologram graph does not allow for absolute statistical precision. For example, the so-called grey areas such as ‘on or close to the line’ do not provide the conclusive ideal distinctions and so these values would be subject to further pharmacological tests such as regression analysis. To continue with these tests is beyond the aims of this study and the isobologram test provides the necessary pharmacological analysis required.

3.6 *Single Cell Gel Electrophoresis (COMET) Assay*

The drug-induced DNA damage in the form of strand breaks and subsequent repair was assessed using the single-cell gel electrophoresis (comet) assay as described previously (Spanswick *et al.*, 1999; Olive, 2002). The comet assay was originally developed as a method for the detection and visualisation of DNA damage within individual cells and is used extensively for the assessment of strand breaks in a range of applications.

3.6.1 *Methodology*

Exponentially growing cells were seeded at 2.5×10^4 cells/ml (5×10^4 cells/well) in six well plates (NuncTM, VWR) and incubated for 24h at 37°C in 5% CO₂. To examine the extent of DNA damage and subsequent rate of repair, ideal doses of irradiation were chosen for each cell line. To this end, cells were treated with a range of irradiation doses to determine a suitable schedule. Cells were treated with drugs at a fixed concentration (one drug alone for 3 hours or drug A for 3 hours with drug B added in the last 30 minutes). Cells were then irradiated at a specific dose and then immediately transferred to a 37°C incubator for suitable intervals to measure the amount of DNA damage and rate of repair.

All procedures were carried out on ice and in subdued lighting. Cells were embedded in 1% Type VII agarose and placed on precoated microscope slides with 1% Type 1-A agarose, and lysed for 1 hour in lysis buffer (100mM disodium EDTA, 2.5 M NaCl, 10mM Tris-HCl, pH 10.5) containing 1% Triton X-100 (added immediately before analysis). Following this, they were washed every 15 minutes in distilled water for 1 hour. Slides were then incubated in alkali buffer (50mM NaOH, 1mM disodium EDTA, pH 12.5) for 45 minutes, followed by electrophoresis in the same buffer for 25 minutes at 18 V (0.6 V/cm), 250 mA. The slides were finally rinsed in neutralising buffer (0.5 M

Tris-HCl, pH 7.5) followed by saline. After drying, the slides were stained with propidium iodide (2.5µg/mL) for 15 minutes and then rinsed in distilled water.

3.6.2 Analysis

Images were visualised with the use of a NIKON inverted microscope with a high-pressure mercury light source (NIKON UK Limited, Kingston Upon Thames, UK), 510 to 560 nm excitation filter, and 590 nm barrier filter at x20 magnification.

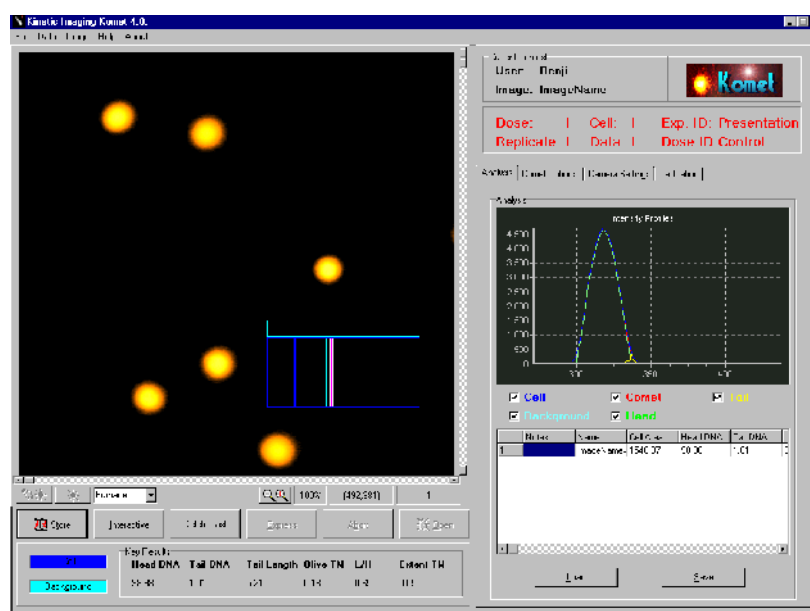


Figure 19: Sample screen display of comets (with no tails) as seen using the Komet Analysis Software.

Images were captured by using an on-line charge-couple device (CCD) camera and analysed with Komet Analysis software (Figure 19) (Kinetic Imaging, Liverpool, UK). For each duplicate slide 25 cells were analysed. DNA damage and subsequent repair was measured by the increase in the tail moment (measured in µMetres), a function of the amount of DNA in the tail and the length of the tail (Spanswick *et al.*, 1999). Analysis was then achieved using a computer spreadsheet (Microsoft Excel). The data shown is a representation of three independent experiments, and include related standard error bars as calculated. As can be seen in Figure 20, irradiating cells induces strand breaks, which produce a tail moment dependent on the x-ray dose.

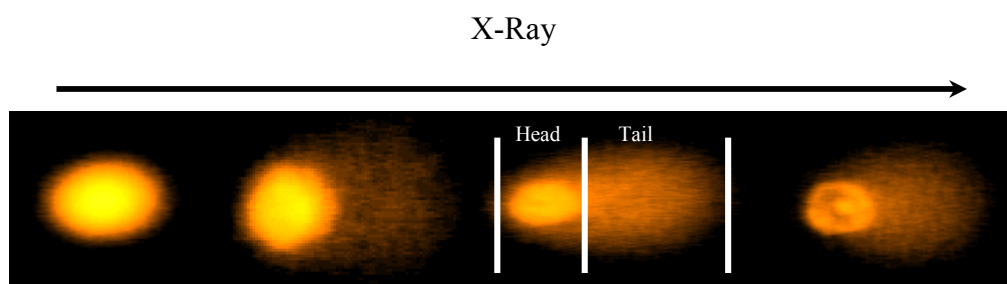


Figure 20: Illustration of DNA tail as a result of irradiation.

The selection of fields for analysis in the comet assay was carried out visually. Obviously, an effort was made to select representative fields and in two experiments analysis was performed by Mrs. Janet Hartley, Department of Oncology, UCL, but nevertheless analysis is subject to bias.

3.7 Detection of Apoptosis - Cell Death Detection ELISA

To address whether inhibition of EGFR leads to the induction of apoptosis, the ELISA Cell Death Detection Assay was performed. This is a photometric enzyme-immunoassay (Figure 21) for the qualitative and quantitative *in vitro* determination of cytoplasmic histone-associated DNA fragments (mono- and oligonucleosomes) after induction of apoptosis. Apoptosis is characterised by membrane blebbing (zeiosis), condensation of cytoplasm and the activation of an endogenous endonuclease and specific proteases. The endogenous endonuclease is Ca^{2+} and Mg^{2+} dependent and cleaves DNA at the most accessible internucleosomal linker region generating mono- and oligonucleosomes. In contrast, the DNA of nucleosomes is tightly complexed with the core histones H2A, H2B, H3 and H4 and therefore is protected from cleavage by the endonuclease. The DNA fragments yielded are discrete multiples of an 180 bp subunit which is detected as a 'DNA ladder' on agarose gels after extraction and separation of the fragmented DNA. The enrichment with mono- and oligonucleosomes in the cytoplasm of apoptotic cells is due to the fact that DNA degradation occurs several hours before plasma membrane breakdown.

DNA and histones are targeted using mouse monoclonal antibodies provided. The anti-histone antibody is conjugated to biotin in order to bind the streptavidin-coated well of the microplate. The anti-DNA antibody is bound to horse radish peroxidase (HRP) which is determined photometrically using ABTS as a substrate.

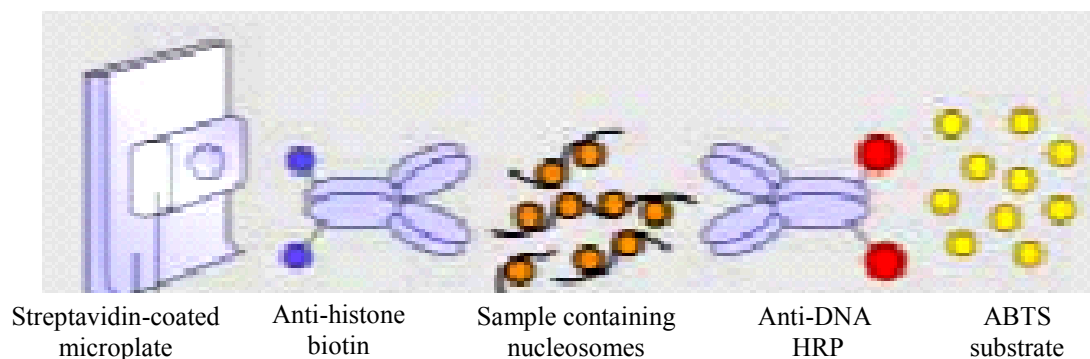


Figure 21: Apoptosis Detection ELISA Assay.

Source: Cell death detection ELISA^{PLUS} assay, Roche

The experiment was performed according to the instructions of the Cell Death Detection ELISA^{PLUS} assay from Roche. Cells were plated (at 15×10^3 or 4×10^3 cells/well depending on cell doubling time) in a total volume of 100 μ l in flat 96-well plates and left overnight at 37°C. Drug was added for a period of 72 hours. The plates were then centrifuged at 200 x g for 10 minutes and the supernatant removed. The cell pellets were resuspended in 200 μ l of Lysis buffer (provided) and left for 30 minutes at room temperature. Cell lysates were centrifuged at 200 x g for 10 minutes. 20 μ l of each supernatant was transferred to a streptavidin-coated microplate. 80 μ l of immunoreagent containing anti-histone-biotin and anti-DNA-HRP in incubation buffer was added per well. The microplate was then covered in an adhesive foil and incubated on a shaker at 300rpm for 2 hours at room temperature. The solution was removed and unbound components were removed by rinsing each well three times in incubation buffer. 100 μ l of ABTS solution was then pipetted into each well and incubated at room temperature till colour development was sufficient for photometric analysis (approximately 10-20 minutes). Plates were read at an absorbance of 405nm against ABTS solution as a blank (reference wavelength approx. 490nm) on a Tecan Microplate reader and analysed using computer spreadsheet (Microsoft Excel).

3.8 Protein Extraction

3.8.1 Cell Lysis for Whole Cell Extracts

Cells cultured and treated in 75cm² (T75) flasks were washed twice in PBS at room temperature, drained well and placed in ice. To lyse the cells, 100 μ l RIPA buffer (1%

deoxycholic acid, 1% Triton X-100, 0.1% SDS, 250 mM NaCl, 50 mM Tris pH 7.5, 100 µg/ml AEBSF, 17µg/ml aprotinin, 1µg/ml leupeptin, 1µg/ml pepstatin, 5µM fenvalerate, 5µM potassium bisperoxo (1,10-phenanthroline) oxovanadate (V) (BpVphen) and 1µM okadaic acid) was added to each flask for 10 minutes with occasional rocking. Cells were then scraped into a 1.5ml Eppendorf tube using a cell scraper (VWR International Ltd.) and centrifuged at 13,000rpm for 10 minutes at 4°C. The supernatant (containing total cell protein) was then carefully transferred to a fresh tube and the pellet discarded. This is the total cell lysate and can be stored at -80°C.

3.8.2 Nuclear and Cytosolic Extraction

To separate out nuclear and cytosolic components of total cell lysates, the TransFactor[®] Extraction Kit (Clontech Laboratories, UK) was used according to the manufacturer's instructions. Briefly, all steps were performed at 4°C unless otherwise specified. Reagents were pre-cooled to 4°C, and not used until fully defrosted. Cells were collected and transferred to an Eppendorf tube centrifuged at 13,000rpm for 10 minutes at 4°C and the supernatant discarded. The pellet was then washed twice in PBS and the pellet size estimated. Lysis buffer was prepared as follows: 150ml 10x Pre-lysis Buffer (Hypotonic) (100mM HEPES pH 7.9, 15mM MgCl₂, 100mM KCl), 15ml 0.1M DTT, 15ml Protease Inhibitor Cocktail (Aprotinin, Pepstatin A, Bestatin, trans-Epoxy succinyl-L-leucylamido (4-guanidino) butane, and 4-(2-aminoethyl) benzenesulfonyl fluoride hydrochloride in DMSO) and 1.32ml ddH₂O. Cells were resuspended in a volume of lysis buffer equal to five times the cell pellet volume and incubated on ice for 15 minutes. Following centrifugation at 13,000rpm for 10 minutes at 4°C, the supernatant was carefully removed and the pellet resuspended in a volume of lysis buffer equal to twice the cell pellet volume. Suspension was then slowly drawn into a syringe through a narrow-gauge (No. 27) needle and then ejected with a single rapid stroke. This was repeated ten times and centrifuged at 13,000rpm for 10 minutes at 4°C. The supernatant was then transferred to a fresh Eppendorf tube and is the cytosolic fraction. This can be snap-frozen and stored at -70°C.

Extraction Buffer was prepared as follows: 147ml Pre-extraction Buffer (20mM HEPES pH 7.9, 1.5mM MgCl₂, 0.42M NaCl, 0.2mM EDTA, 25% (v/v) glycerol), 1.5ml 0.1M DTT and 1.5ml Protease Inhibitor Cocktail. The crude nuclear pellet was resuspended in a volume of Extraction Buffer equal to two-thirds of the cell pellet volume. To

disrupt the nuclei, the suspension was then syringed as before and placed on a shaker at low speed for 30 min at 4°C. The nuclear suspension was then centrifuged at 13,000rpm for 10 minutes at 4°C. The supernatant or nuclear fraction was transferred to a fresh Eppendorf tube and can be snap-frozen and stored at -80°C.

3.8.3 Measurement of Protein Concentration in cellular extracts

To determine the protein concentration of a particular cell lysate (whole cell or cytoplasmic and nuclear extracts), the Biorad Protein Assay kit was used. Briefly, 2µl of each lysate is added to 18µl H₂O in 1.5ml Eppendorf tubes. In a separate Eppendorf, 20µl *Reagent S* is mixed with 1ml *Reagent A*. 100µl of this is added to each 20µl lysate sample and mixed well with a short spin. 800µl *Reagent B* is then added to each and incubated at room temperature for 15 minutes. The optical density (O.D.) for each sample is then read on a spectrophotometer (Beam PU 8600 Series UV/Vis Single, Philips®) at 750nm and the protein concentration determined using the following formula: $\text{O.D.} \times 25 = [\text{ }]/\mu\text{l}$ (i.e. µg/µl)

3.9 Immunoblotting

3.9.1 Electrophoresis

Protein concentrations of total cell lysates were determined using the protein assay outlined in Section 2.8. For each sample the required volume containing 30-50µg of protein was transferred to a fresh Eppendorf tube. Loading (Laemmli) buffer (4% SDS, 10% β-Mercaptoethanol, 20% glycerol, 0.02% bromophenol-blue and 100mM Tris HCl (pH 6.8)) was then added to each lysate before heating at 95°C for 4 minutes to denature the proteins. Samples are then centrifuged at 13,000rpm for 10 minutes at 4°C and the pellet discarded.

The NuPAGE® Electrophoresis System (Invitrogen, UK) was used. For analysis of proteins with a molecular weight of between 120 and 410 KDa, lysates and immunoprecipitates were loaded onto NuPAGE® Novex 3-8% Gradient Tris-Acetate Pre-Cast Gels which were placed in the XCell SureLock™ Mini-Cell (two gels per cell) and included an appropriate marker (Kaleidoscope pre-stained standards, BioRad, Hemel-Hempstead, UK) or a positive protein control (A431+EGF cell lysate; BD Biosciences, UK). Upper (200ml) and lower (600ml) buffer chambers were then filled

with 1x NuPAGE[®] Tris-Acetate SDS Running Buffer (diluted from a 20x stock: 50mM Tricine, 50mM Tris base, 0.1% SDS, pH 8.24) and Mini-Cells were run at 150V constant at 4°C for approximately 1h 30min (Expected 40-55 mA/gel at start; 25-40 mA/gel at end).

For analysis of proteins with a molecular weight of between 10 and 180 KDa lysates and immunoprecipitates were loaded onto NuPAGE[®] Novex 4-12% Gradient Bis-Tris Pre-Cast Gels and placed in Mini-Cells as above. Upper (200ml) and lower (600ml) buffer chambers were then filled with 1x NuPAGE[®] MOPS SDS Running Buffer (diluted from a 20x stock: 50mM MOPS, 50mM Tris base, 0.1% SDS, pH 7.7) and Mini-Cells were run at 200V constant at 4°C for approximately 50min (Expected 100-125 mA/gel at start; 60-80 mA/gel at end).

3.9.2 Protein Transfer and Immunoblotting

Proteins were electrically transferred to Immobilon[™] polyvinylidenedifluoride (PVDF) membranes (Millipore, UK). These extremely hydrophobic membranes will not wet in aqueous solution and so were prepared as follows: blots were immersed in 100% methanol for three seconds and then placed in H₂O for 2 minutes to elute the methanol. To equilibrate, membranes were then soaked in protein transfer buffer (diluted from a 10x stock: 3% TrisBase, 14.4% glycine and 20% methanol). Gels and prepared membranes were then placed into the X-Cell II[™] Blot Module (Novex[®]) as illustrated in Figure 22.

Transfer was achieved at 40V for 2h using the XCell *SureLock*[™] Mini-Cell (two blots per cell) and filled with protein transfer buffer as described in the NuPAGE Novex[®] protocol. Membranes were then blocked in 3% casein blocking buffer [(3% skimmed milk powder (Marvel, UK) in TBS-Tween (TBS-T) (20mM TrisBase, 0.15M NaCl pH 7.5 in Elga H₂O with 0.1% Tween-20)] for at least 1 hour on a shaker at 4°C.

Membranes being probed for phosphorylated proteins were blocked in 5% Bovine Serum Albumin (BSA) in TBS-T. This is due to the fact that milk contains a number of phosphorylated proteins which interfere with a phosphotyrosine antibody's ability to bind specific proteins of interest. Blots were then probed with primary antibody against proteins of interest for at least 2h on a roller at room temperature. Antibodies used in

this study are detailed in Table 9. All were diluted in a 1:1 mix of either Milk-TBS-T or BSA-TBS-T and TBS as necessary. Following this, membranes were washed three times for 5 minutes in TBS-T followed by three more washes for 5 minutes with TBS. Membranes were then probed with an appropriate horseradish peroxidase conjugated secondary antibody for at least 1h and washed as before.

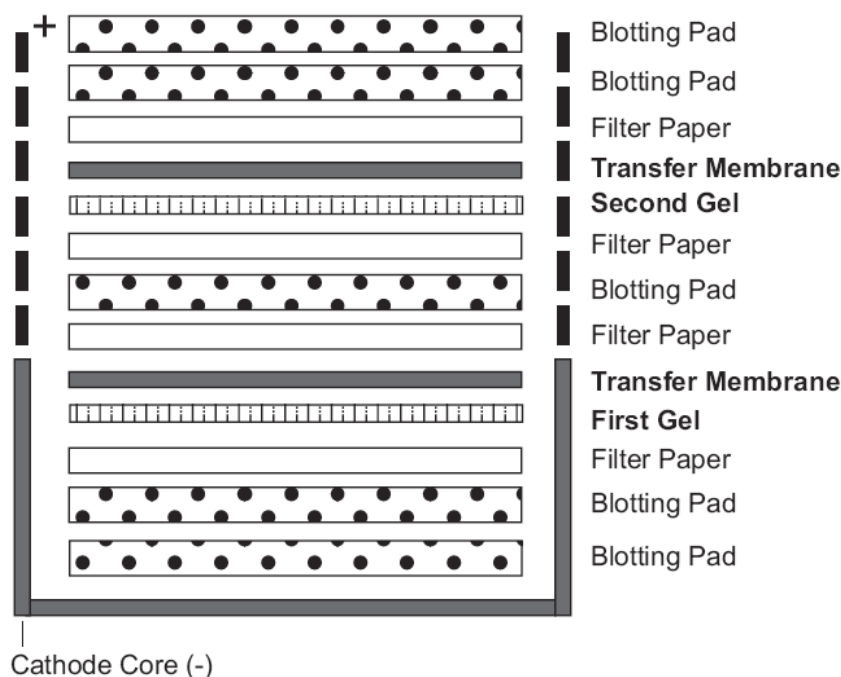


Figure 22: Gel/Membrane sandwich for 2 gels.
Source: NuPAGE[®] Technical Guide, Invitrogen, UK

Immunocomplexes were visualised using the enhanced chemiluminescence (ECL) system (Amersham Pharmacia, Little Chalfont, UK) by incubating the membranes in the ECL system solution for 1 minute before wrapping the moist blots in cling film and exposing the blots to Kodak X-OMAT[™]LS film for varying exposure times (two seconds to 24h) (Sambrook *et al.*, 1989).

In order to remove or 'strip' pre-bound antibody, membranes were rehydrated in TBS for 5 minutes and placed in a hybridiser (Techne, UK) with 100ml of stripping buffer (100mM β -Mercaptoethanol, 2% SDS, 62.5mM Tris-HCl, pH 6.7) and left for 30 minutes at 50°C. Membranes were then washed twice in TBS-T for ten minutes each, blocked and reprobed as described above.

Table 9: Primary and secondary antibodies used in this study.

Primary Antibodies					
Antibody	Description	Supplier	Antibody	Description	Supplier
C-KIT 145KDa	Rabbit, Polyclonal	DAKO, UK	EGFR 170KDa	Mouse, Monoclonal	Santa Cruz, USA
C-KIT 145KDa	Mouse, Monoclonal	Novocastra, UK	EGFR 170KDa	Rabbit, Polyclonal	Abcam, UK
C-KIT 145KDa	Rabbit, Polyclonal	Santa Cruz, USA	P-EGFR (PY20) 175KDa	Mouse, Monoclonal	BD Biosciences, UK
SSTR-1 60KDa	Rabbit, Monoclonal	Gramsch Laboratories, Germany	P-EGFR (Tyr-1068) 175KDa	Rabbit, Polyclonal	Cell Signaling Technology, USA
SSTR-2A 80KDa	Rabbit, Monoclonal	Gramsch Laboratories, Germany	iNOS 130KDa	Rabbit, Polyclonal	BD Biosciences, UK
SSTR-3 45,80KDa	Rabbit, Monoclonal	Gramsch Laboratories, Germany	Rad51 37KDa	Rabbit, Polyclonal	Santa Cruz, USA
SSTR-5 65KDa	Rabbit, Monoclonal	Gramsch Laboratories, Germany	P-AKT (Ser-473) 70KDa	Rabbit, Polyclonal	Abcam, UK
DNA-PK _{CS} 460KDa	Mouse, Monoclonal	Sigma, UK	P-MAPK 43KDa	Rabbit, Polyclonal	Abcam, UK
α -Tubulin 170KDa	Mouse, Monoclonal	Sigma, UK	Lamin B1 67KDa	Mouse Monoclonal	Abcam, UK

Secondary Antibodies			
Antibody	Supplier	Antibody	Supplier
HRP-Conjugated Goat Anti-Mouse	BD Biosciences, UK	FITC-Conjugated Goat Anti-Mouse	Abcam, UK
HRP-Conjugated Goat Anti-Rabbit	Abcam, UK	Biotinylated goat anti- mouse/rabbit antibody	DAKO

3.10 Densitometric Analysis

To mathematically compare the intensity of particular bands produced by immunoblotting, densitometric analysis was used. Briefly, blots were placed in the imaging densitometer (Imaging Densitometer GS-670 BioRad, UK) and the bands of interest selected. Intensity was then measured by computer and the background

subtracted. Data is represented as a percentage of control band intensity. The screen-grab shown in Figure 23 illustrates the methodology. In this case V5 serves as a background, V1 is the control and bands V2-4 represent different drug treatments.

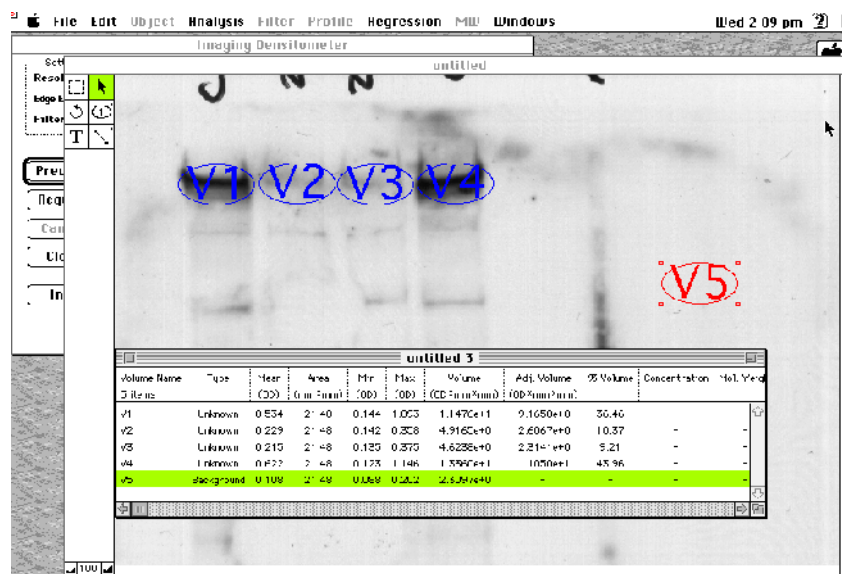


Figure 23: Sample screen display of densitometric analysis as seen using the BioRad Imaging Densitometer Software.

3.11 Immunofluorescent Staining

Exponentially growing cells were seeded at 2×10^4 cells per well on rectangular glass slides with 8 chambers (NuncloTM, VWR) and incubated for 24h at 37°C in 5% CO₂. Cells were then treated as required, the media subsequently removed and the cells washed twice with cold PBS. Cells were then fixed using 500µl/well of 50% methanol / 50% acetone mix at 4°C for 8 minutes. Following this the slides were then washed twice with cold PBS and permeabilized using 500µl/well of 0.5% TritonX-100 in PBS. Slides were then blocked in 3% casein blocking buffer [(3% skimmed milk powder (Marvel, UK) in TBS-Tween (TBS-T) (20mM TrisBase, 0.15M NaCl pH 7.5 in Elga H₂O with 0.1% Tween-20)] overnight at 4°C.

Slides were then washed 3 times in cold PBS following which the cells were incubated with anti-EGFR (1:50 dilution) or anti-DNA-PK_{CS} antibody (1:100 dilution) for 1 hour. Slides were then washed 3 times with washing buffer (0.1% TritonX-100 in PBS) and then incubated for 1 hour at room temperature with FITC-labelled secondary antibody: Alexa fluoro[®] 488 goat anti-mouse IgG (green) (1:1000 dilution). Nuclear

counterstaining was performed using 2µg/ml propidium iodide (red) for 3 minutes followed by destaining with distilled water for 20 minutes. Slides were mounted using *VectaMount*TM AQ mounting medium (Vector Laboratories) and covered with coverslips before being viewed and photographed using a confocal microscope.

3.12 Transient Transfection Assay

Wild-type EGFR and a selected nuclear localisation sequence (NLS) - mutant EGFR construct were transiently transfected into RIN-5F and CRI-G1 cells using the GeneJuice[®] transfection reagent (Novagen[®] EMD Biosciences Darmstadt, Germany). Exponentially growing cells were seeded at 1×10^4 cells per well on rectangular glass slides in 8 well plates (NuncTM, VWR) or 1×10^5 cells in six well plates (NuncTM, VWR) and incubated for 24 or 48h at 37°C in 5% CO₂ prior to transfection. The optimum amount of Genejuice[®] reagent recommended for successful transfection of 1µg of DNA is 3µl. This was added to eppendorf tubes containing 100µl of serum free medium and allowed to incubate at room temperature for 5 minutes. Following this 1µg DNA was added to each tube and incubated at room temperature for 15 minutes after which the entire mixture was added slowly over the surface of the appropriate well. Cells were then incubated for 24 or 48h allowing both cell recovery and transfection to take place. The plasmid DNA used was the pUSEamp vector (Upstate Cell Signaling Solutions, NY, USA) and its map is illustrated in Figure 24 with the key sites highlighted.

The different EGFR constructs were kindly provided by Gianmaria Liccardi, Oncology Department, UCL. There were two constructs made using the pUSEamp vector and encoded wild-type EGFR and the NLS EGFR mutant. The NLS sequence in the juxtamembrane domain of EGFR is RRRHIVRKRTLRR (Hsu SC & Hung MC, 2007), which was changed into AAAHIVAKATLAA. In addition to using untransfected cells as a control, cells transfected with the parental pUSEamp vector were also studied. Transiently transfected cells at 48 hours were chosen for further experiments. After 24 hour incubation with the plasmid, cells were washed with complete media and incubated for a further 24 hours before treatment. Cells were then treated with gefitinib, irradiation or both, at appropriate concentrations and doses, based on previous studies with the cell lines, and used for immunofluorescence and COMET analysis.

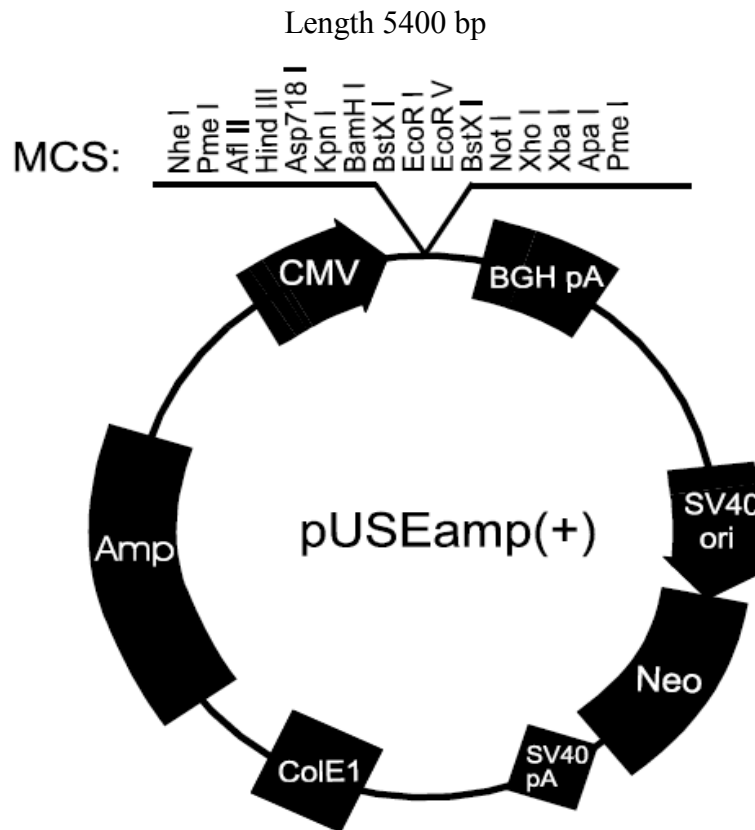


Figure 24: Map of the pUSEamp vector used for expressing various EGFR constructs.

Source: Upstate Cell Signaling Solutions

http://search.cosmobio.co.jp/cosmo_search_p/search_gate2/docs/UBI_/21147.20040204.pdf

3.13 Flow cytometry- FACS Analysis

This procedure utilizes ethanol to fix the cells and permeabilize the membrane, which allows the dye (Propidium Iodide) to enter the cells. Propidium Iodide (PI) is a DNA-binding fluorochrome that intercalates in the double-helix. Ribonuclease-A is used to eliminate the staining of double-stranded RNA. This procedure uses DNA staining for analysis of the cell cycle.

Collection and fixation

Exponentially growing cells were seeded at 2.5×10^4 cells/ml (5×10^4 cells/well) in six well plates (NuncTM, VWR) and incubated for 24h at 37°C in 5% CO₂. Cells were drug treated for 24 or 72 hours, the media subsequently removed and the cells washed with PBS. 1ml of trypsin was added per well for approximately 2 minutes followed by addition of 1ml of complete media. The cells were collected in 15ml sterile falcon tubes and centrifuged for 5 minutes at 1500rpm. The pellets were resuspended in 1ml of ice-cold 0.02% sodium azide –PBS per sample. Cells were fixed by addition of 7ml of 70%

ethanol to each sample. For proper fixation and to prevent cell aggregation, gentle vortexing was employed while fixing. The cells were wrapped in silver foil and left to fix for one hour at 4°C. The cells can be left in this stage at 4°C for up to 3 days before being stained.

Staining DNA for Cell Cycle Analysis

The fixed cells were centrifuged as above and washed in 7ml ice-cold 0.02% sodium azide –PBS then centrifuged again. Each pellet is then resuspended in 50µl propidium iodide, 9µl DNase-free RNase A, and 941 µl 0.02% sodium azide –PBS to make a total of 1ml per pellet. Cells were gently mixed and left at 4°C or on ice (covered with silver foil to protect from light) for a minimum of 30 minutes. The cells were analysed on a FACSCalibur cytometer (Becton Dickinson, UK).

Figure 25 below shows an example of a graph derived using flow cytometry for cell cycle analysis. The y-axis demonstrates the number of cells whereas the x axis shows the intensity of fluorescence designated as FL2-H. 'FL2-H' denotes DNA content by propidium iodide staining. Cells at the beginning of the FL2-H axis (below 140), denotes cells with sub-G1 DNA content, indicative of apoptosis. The cells under normal growth conditions form two populations designated by the bars M1 and M2, which are shown by the two peaks. Cells in G1/S phase of the cell cycle are represented by the first peak, whereas the second peak represents cells in the G2/M phase of the cell cycle. Note that the peaks are respectively at 200 and 400. The intensity in the second peak is double which signifies the presence of duplicated DNA in the cells of the G2/M phase.

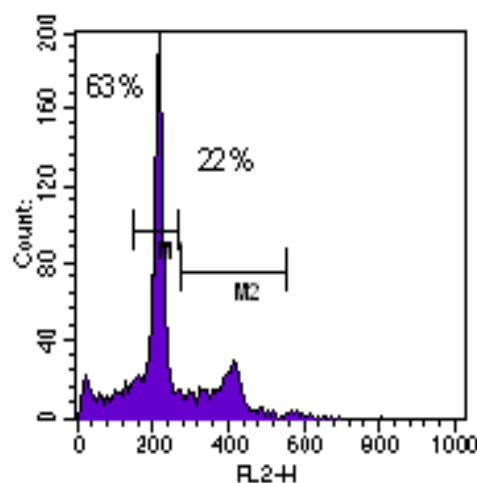


Figure 25: DNA analysis of cells by flow cytometry on a FACSCalibur cytometer.

3.14 Immunohistochemistry

Patient Sections

Tissue from 85 consecutive unselected patients at the Royal Free Hospital with neuroendocrine tumours in various organs including liver, pancreas, small bowel, lung and brain and normal control tissues for each patient whenever possible were assessed. Tissue samples were fixed in formalin and embedded in paraffin. Sections were cut 3 μ m thick and placed on a water bath at 45°C before being positioned on top of microscope slides. GIST sections were used as positive control. The presence of mast cells in tissue samples was also used as an internal positive control. Negative controls included omission of the primary antibody.

Immunohistochemistry

Tissue sections were dewaxed in xylene (Chemicon, UK) for 10 min, dehydrated in 100% alcohol and then rinsed in distilled water for 5 min. All sections were incubated in 3% hydrogen peroxide for 10 min to inhibit endogenous peroxidase enzyme activity. For exposure and detection of the C-KIT protein with both antibodies, the slides were microwaved in prewarmed 0.01 M citrate buffer for 5 min and washed in distilled water to cool the slides down. From this point onwards, the slides must be kept wet at all times to facilitate staining. The sections are circled with a hydrophobic pen to prevent drying of the slides.

Slides are incubated in tris-buffered saline (TBS) for 5 minutes to equilibrate. Non-specific binding of the antibody to Fc fragments in the tissue was blocked by incubating the sections in 10% normal goat serum (DAKO, UK) in TBS for 15 min. The serum is tipped off and approximately 100 μ l of anti-human C-KIT antibody (dilution 1:50 in TBS) was added to each section for 1 hour. Negative control studies for each tissue section were performed without primary antibody. Binding was detected using biotinylated goat anti-mouse/rabbit antibody (DAKO) at a dilution of 1:200 in TBS for 30 minutes at room temperature, followed by 30 min with streptavidin-biotin/ horse radish peroxidase mix (DAKO, 1:200 in TBS each). Sections were washed in TBS for 5 min then visualised using diaminobenzidine tetrahydrochloride (DAB; Vector laboratories), a chromagen- substrate for HRP, by incubating the slides at room temperature for 10 min. Sections were counterstained in Carrazi's haematoxylin (which

stains nuclei blue), dipped in acid alcohol and blueing solution, dehydrated in alcohol and xylene and mounted in DPX, a xylene-based adhesive.

Scoring of immunohistochemistry

All sections were scored independently by myself and two independent histopathologists. Intensity of staining was made in comparison to the GISTs tumour samples, which were used as positive control. Immunostaining was scored as follows: strong 3; moderate 2; weak 1; no staining 0.

3.15 Electron Microscopy

Cells were left to reach 80-90% confluence in 75cm² (T75) flasks. Cells were then treated with gefitinib for 3 hours prior to irradiation at 4Gy. Control unirradiated samples were also used.

Fixing and embedding:

Cells were fixed in 4% PFA/0.1% gluteraldehyde in 0.1M Phosphate buffer for 2 hours at RT, and washed in 20mM glycine at RT. Cells were then scraped in 1% gelatin and collected into 1.5ml eppendorf tubes, followed by spinning horizontally at 1500rpm for 1 min. Supernatant was removed and the pellet was resuspended in 12% gelatin at 37°C and left to infuse for a few minutes at 37°C. The cells were then centrifuged horizontally at 5000rpm for 1 min, the supernatant was removed and the tubes were placed on ice for 15 minutes. The ends of the tubes were cut off and the pellet was sliced in half into PBS in ice. The pellet was cut into blocks (block faces should be approx 0.6 -0.4 x 0.3-0.4 mm) and infused with 2.3M sucrose overnight at 4°C on rotation. Blocks were mounted onto pins (Agar) and stored in liquid nitrogen. 70nm sections were cut at -120°C, picking the sections up in 2% methyl cellulose/ 2.3M sucrose (1 / 1) onto formvar/carbon-coated copper grids. Sections were then stored at 4°C.

Staining:

Grids were placed on 2% gelatin in phosphate buffer and incubated at 37°C for 20 minutes and rinsed in PBS + 0.1% glycine 5 times for 1min. Sections were then blocked in PBS +1% BSA/0.1% BSA-c for 5min, followed by incubation in primary sheep anti-

EGFR antibody (Fitzgerald, 1:250 in 1% BSA) overnight at 4°C. Sections were then washed in PBS 4 times for 2 minutes each and incubated in secondary anti-goat IgG coupled to 15nm colloidal gold particles (1:40 in 1% BSA) for 45 minutes at RT. Sections were rinsed in PBS 3 times for 5 seconds each, and washed as before in PBS 4 times for 2 minutes each. Sections were stabilised with 1% gluteraldehyde in PBS for 5-30 minutes at RT, and washed in water 10 times for 1 minute. Cells were then stained in methyl cellulose / uranyl acetate (9 / 1) on ice in the dark for 5 minutes and after excess methyl cellulose / uranyl acetate was drained off on filter paper, sections were allowed to air dry for 10 minutes (or left overnight) at RT.

Location of EGFR was analysed by viewing samples on a JEOL 1010 Transmission Electron Microscope, and gathering images with a Gatan OriusSC100B CCD camera. Staining of samples and viewing of images was performed by Emily Eden, UCL Institute of Ophthalmology, London, UK.

CHAPTER 4

INVESTIGATION OF COMBINATION TREATMENTS USING EGFR INHIBITORS WITH CHEMOTHERAPEUTIC AGENTS IN NET CELLS

4.1 Introduction

4.1.1 EGFR and Cancer

Epidermal growth factor receptor (EGFR) is expressed in many cancers and is associated with poor prognosis. EGFR activation pathways have been well characterised using tumour cell lines and are known to involve EGFR activation through autophosphorylation (Rusch *et al.*, 1996; Hirono *et al.*, 1995). Phosphorylation of downstream signalling molecules, such as ERK1/2 (extra-cellular signal regulated kinase 1 & 2), and PKB/Akt (protein kinase B), leads to enhanced tumour cell survival and proliferation (Yarden, 2001).

EGFR is frequently expressed in neuroendocrine tumours (Wang *et al.*, 1997; Nilsson *et al.*, 1995; Rusch *et al.*, 1996). A potential implication of EGFR in progression of gastrointestinal carcinoids and PNETs was shown by the presence of activated EGFR in these cells (Papouchado *et al.*, 2005; Wulbrand *et al.*, 1998; Peghini *et al.*, 2002). Co-expression of EGFR and TGF- α was shown in midgut and hindgut carcinoids, phaeochromocytomas and MTCs suggesting an autocrine mechanism for tumour-growth regulation (Nilsson *et al.*, 1995). EGFR expression or overexpression was shown to affect tumour growth and progression of NETs (Wulbrand *et al.*, 1998; Peghini *et al.*, 2002).

Recent data suggests that there is no direct correlation between the results of EGFR immunostaining and the response to anti-EGFR therapy (Dei Tos & Ellis, 2005). However, a study by Shah *et al.* found EGFR in >90% of NET tumour patients. They demonstrated expression of EGFR in 96% of tumour samples, while 63% were positive for activated EGFR. The subsequent activation of intracellular signalling pathways was demonstrated by the immunostaining for p-Akt and p-MAPK in NET tissue samples. Importantly, the histological score for the activation of Akt and MAPK correlated with the histological score for activated EGFR. These data provide a rationale for considering EGFR inhibitors in the treatment of NETs (Shah *et al.*, 2006).

4.1.2 EGFR inhibition by gefitinib

Gefitinib (Iressa or ZD1839) is a specific tyrosine kinase inhibitor of EGFR used for the treatment of non-small cell lung cancer as well as for other solid tumours (Schiller,

2003; Herbst, 2002; Blackledge & Averbuch, 2004). Antineoplastic activity has been shown in a variety of human cancers including prostate, breast, ovarian, colon and lung cancer cells. Gefitinib has been shown to induce apoptosis and cell cycle arrest in a variety of tumour cells including neuroendocrine gastrointestinal tumour cells (Hopfner *et al.*, 2003). EGFR targeting in NET cell lines by gefitinib has been investigated by Hopfner and co-workers. They showed that inhibition of EGFR tyrosine kinase promoted growth suspension by apoptosis and cell cycle arrest in NE gastrointestinal tumour cells (Hopfner *et al.*, 2003). Inhibition of EGFR by gefitinib as a single agent has been shown both in cell lines and in xenograft models. Combination treatments with a variety of chemotherapeutic agents (including cisplatin, carboplatin, paclitaxel, etoposide and doxorubicin) or anti-sense oligonucleotides, demonstrated synergistic effects in inhibition of proliferation, induction of apoptosis, and antitumor activity *in vitro* and *in vivo* (Ciardiello, 2000; Ciardiello, 2001; Sirotnak *et al.*, 2000). Similarly, combination of gefitinib with radiation showed increased inhibition of proliferation and had pro-apoptotic effects *in vitro*, while in human tumour xenografts there was increased tumour growth delay (Huang *et al.*, 2002; Bianco *et al.*, 2002).

4.1.3 Chemotherapy on EGFR activity

Cisplatin has been shown to induce diverse cellular responses including the activation of the JNK and p38 MAPK cascades as well as members of the ERK subfamily of MAPKs (Benhar *et al.*, 2001). It has been shown that cisplatin-induced ERK activation is significantly elevated in transformed cells, such as NIH3T3 cells that overexpress EGFR (Benhar *et al.*, 2001). These findings led to further investigations confirming that apart from cisplatin, other drugs such as doxorubicin, and camptothecin, which is a topoisomerase I inhibitor, but not paclitaxel, induced activation of EGFR in NIH-3T3 human fibroblast and U87MG human glioma transformed cells lines that overexpress EGFR (Benhar *et al.*, 2002). EGFR activation by cisplatin was also shown in MCF-7 breast cancer cell line (Friedmann, 2004).

Aims

In the first part of this study we analysed the potential therapeutic value of EGFR in NETs by proliferation studies. The cell lines used included the NCI-H727 human bronchial carcinoid, the SHP-77 human small cell lung cancer (with neuroendocrine features), and the CRI-G1 and RIN-5F rat islet tumour cells. Experiments were also

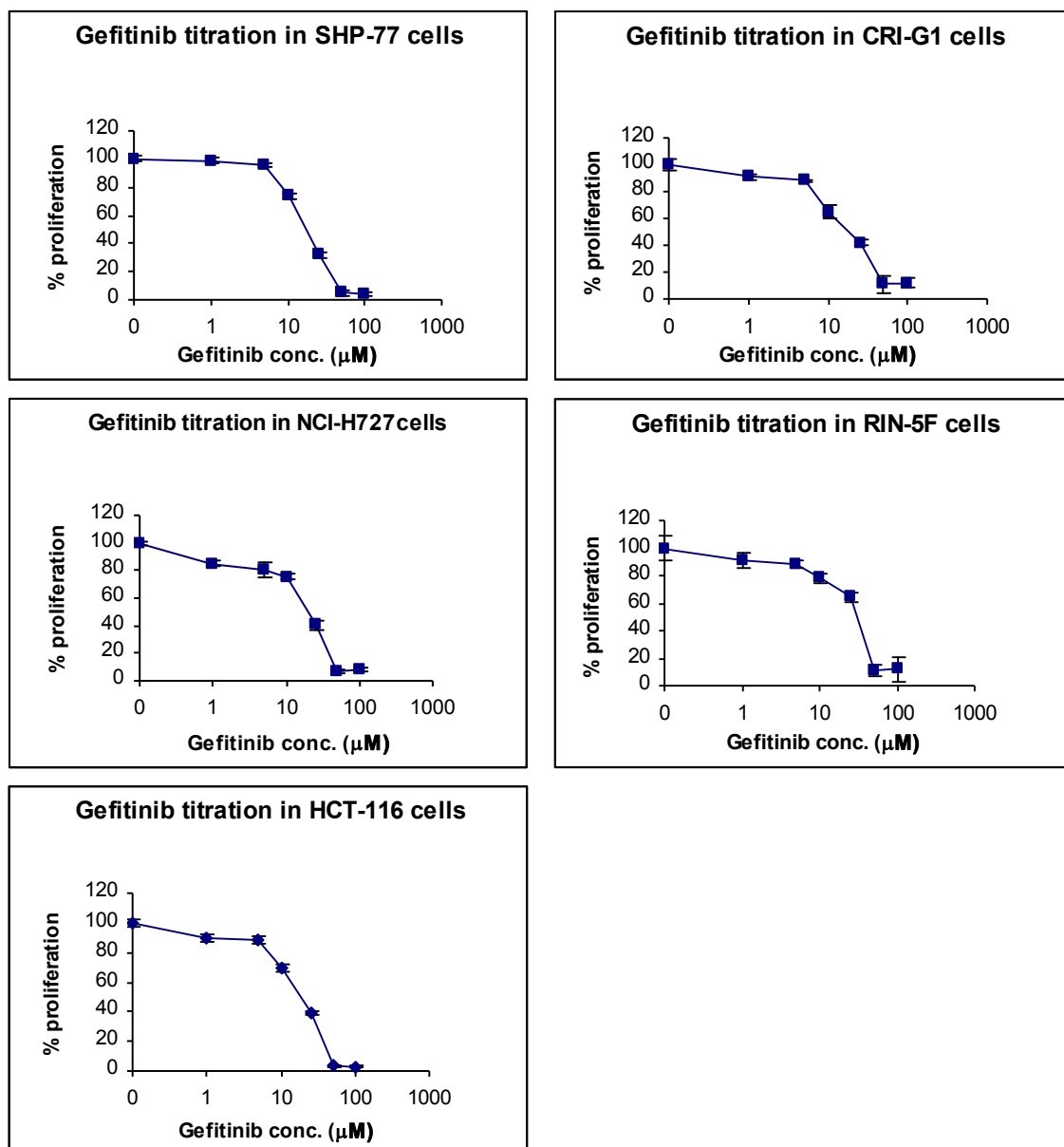
performed in the HCT-116 colon cancer cell line, which expresses EGFR at levels comparable to neuroendocrine cell lines. Initially, we assessed the potentially anti-proliferative effect of gefitinib alone, or in combination with the widely used chemotherapeutic drugs cisplatin, etoposide, paclitaxel and methotrexate. The effect of gefitinib in NET cell lines was analysed further for cell cycle arrest or apoptosis. In the second part of this study, based on the effect of chemotherapy on EGFR activation reported in the literature, we also investigated the effect of cisplatin, etoposide, paclitaxel, and methotrexate on EGFR activity in order to analyse to a greater extent the mechanism of interaction between gefitinib and chemotherapeutic agents.

4.2 Results

4.2.1 Proliferation studies using gefitinib or chemotherapy as single agents

Cytotoxicity of drugs was determined by the Sulphorhodamine B (SRB) proliferation assay. Initially, single agent treatments were carried out on all cell lines to obtain suitable dose ranges for different exposure times. Single agent administration included addition of drugs for 24, 48, or 72 hours followed by 2 days incubation in drug-free media. Gefitinib as a single agent added for a period of 72 hours was cytotoxic to all cells tested and had a dose response effect (figure 26), demonstrating 50% growth inhibition at the high doses of 18-20 μ M in 4/5 cell lines and in RIN-5F cells at 32 μ M (IC_{50} s shown in table within figure 26). The IC_{50} s for the 48 hour treatments were very similar, while the IC_{50} s for the 24 hour treatment were much lower (data not shown).

Anti-cancer drugs also decreased tumour cell proliferation as single agents in a dose-dependent fashion in all cell lines. IC_{50} s are shown in table 10 for the standard 72 hour treatment. The drugs were also administered as single agents for 24 and 48 hours with lower cytotoxic abilities (data not shown). Paclitaxel was the most effective drug with IC_{50} s below 0.05 μ M, followed by methotrexate with IC_{50} s of approx. 0.2-25 μ M. Etoposide and cisplatin give slightly higher IC_{50} s to methotrexate, but are nevertheless effective in inhibiting proliferation of neuroendocrine cells.



IC ₅₀ s of gefitinib in NET cells (μM)					
	SHP-77	CRI-G1	NCI-H727	RIN-5F	HCT-116
Gefitinib	20.3 ± 1.42	19.2 ± 1.78	21.1 ± 1.86	32.3 ± 0.95	18.6 ± 2.16

Figure 26: SHP-77, GRI-G1, NCI-H727, RIN-5F and HCT-116 cells were incubated with gefitinib for 3 days at the indicated concentrations followed by 2 days incubation in drug-free media. Proliferation was calculated as a % of control untreated cells. IC₅₀s values shown represent means of 3 independent experiments, each done in triplicate, with standard deviation.

Table 10 : IC₅₀s of chemotherapeutic agents in NET cells (μM)

	SHP-77	CRI-G1	NCI-H727	RIN-5F	HCT-116
Cisplatin	9 ± 1.12	2.41 ± 0.34	10 ± 1.22	0.48 ± 0.029	12.7 ± 1.32
Etoposide	1.64 ± 0.32	1.3 ± 0.23	6.8 ± 0.86	0.5 ± 0.057	1.3 ± 0.46
Methotrexate	0.43 ± 0.062	0.75 ± 0.078	1.8 ± 0.38	2.6 ± 0.47	0.22 ± 0.051
Paclitaxel	0.033 ± 0.037	0.042 ± 0.036	0.047 ± 0.051	0.031 ± 0.029	0.033 ± 0.028

Note: IC₅₀s of treatments with drugs for a period of 3 days followed by 2 days in complete media. The values represent means of 3 independent experiments, each done in triplicate, with standard deviation.

4.2.2 Combination treatments with gefitinib or chemotherapy

As mentioned in section 1.2.4, chemotherapy has shown temporary efficacy in managing NETs of foregut origin, including pancreatic, but is of limited benefit in mid-gut and hindgut carcinoid tumours. Therefore, the aim for combining two different therapies such as chemotherapy and EGFR inhibitors in this study was to find the conditions that sensitise cells to chemotherapy. The second aim was to use lower drug concentrations than the ones used in single treatments. As a result, for combination treatments, the subtoxic and clinically relevant concentration of 10μM gefitinib, which causes up to 20% inhibition of proliferation in all cell lines, was added to a range of concentrations for chemotherapy. Cells were treated with anticancer drugs with a variety of mechanisms of action, including the DNA crosslinking compound cisplatin, the topoisomerase II poison etoposide, the mitotic inhibitor paclitaxel, and the antimetabolite methotrexate, in order to identify possible synergisms in neuroendocrine tumours.

Administered schedules included:

- Simultaneous addition gefitinib with cisplatin, etoposide, methotrexate or paclitaxel, for a period of 72 hours
- Incubation with gefitinib for 24 hours followed by chemotherapy drugs for 48 hours
- Incubation with chemotherapy drugs for 24 hours followed by gefitinib for 48 hours

- Cytotoxic drugs were added at 0-100 μ M for cisplatin, methotrexate and etoposide, and paclitaxel at 0-10 μ M.
- Drug incubations were followed by 2 days incubation in drug-free media before analysis

Cytotoxicity of drugs was determined by the Sulphorhodamine B (SRB) proliferation assay. The isobologram analysis was used to determine inhibitory, additive or synergistic effects between the two drugs used in combination. The IC₅₀s of each of the two agents combined are at the ends of the x and y axis respectively, and are connected by a straight line called 'additivity line'. This line is the locus of all dose pairs that, based on these potencies, should give the same effect for these two drugs added together. Any point of combined IC₅₀ found well below the line denotes positive synergy, while all points found well above denote negative synergy.

The graphs and the IC₅₀ values shown only include cases with synergistic or additive effect by dual treatment. The rest of the combination treatments are shown in the appendix 1A-1E for each cell line.

Etoposide

Etoposide displayed synergy with gefitinib when both drugs were added simultaneously for 72 hours in 2/5 cell lines, leading to increased cytotoxicity of 20-50% (figures 27-30). Etoposide with gefitinib combined gave an IC₅₀ of 0.3 μ M in SHP-77 and 0.32 μ M in CRI-G1 cells, 0.5 μ M in HCT-116 and 1 μ M in NCI-H727 cells respectively (table 11). The synergies were identified in CRI-G1 and SHP-77 cells, where at value 0.5 μ M of etoposide, simultaneous addition of gefitinib increased the anti-proliferative effect by 50% (figures 27-28). In NCI-H727 and HCT-116 cells (figures 29-30) simultaneous treatment with both agents increased inhibition of proliferation by 37% and 40% respectively at value 0.5 μ M of etoposide and displayed an additive effect.

In NCI-H727 and CRI-G1 cells (but not in SHP-77 and HCT-116 cells) synergies were identified when cells were treated with gefitinib for 24 hours followed by incubation with etoposide for 48hours (figures 28-29), indicating that weakening of EGFR signalling before etoposide administration may be of therapeutic value. The rest of the

combinations analysed, shown in the appendix 1A-1E, did not increase the cytotoxic effect of etoposide.

Table 11: IC₅₀s (μM)

	SHP-77	CRI-G1	NCI-H727	HCT-116
Gefitinib 72h	20.3 ± 1.42	19.2 ± 1.78	21.1 ± 1.86	18.6 ± 2.16
Etoposide 72h	1.64 ± 0.32	1.5 ± 0.23	6.8 ± 0.86	1.9 ± 0.36
Etoposide and gefitinib for 72h	0.3 ± 0.052	0.32 ± 0.044	1 ± 0.21	0.5 ± 0.067
Gefitinib 24h, then etoposide 48h		0.32 ± 0.047	1.7 ± 0.46	

Note: IC₅₀s of treatments with drugs in single or dual treatments for a period of 3 days followed by 2 days in complete media. The values represent means of 3 independent experiments, each done in triplicate, with standard deviation.

The isobologram graphs in figures 30-33 indicate the synergistic or additive effects of etoposide and gefitinib. The IC₅₀ values for etoposide and gefitinib as single agents are at the ends of the x and y axis respectively, and are connected the 'additivity line'. This line is the locus of all dose pairs that, based on these potencies, should give the same effect for these two drugs added together. As can be seen in the figures 30-31, the IC₅₀s of simultaneous addition of etoposide with 10μM gefitinib for 72hours in SHP-77 and CRI-G1 cells lie well below this line and therefore indicate a superadditive or synergistic effect. Points well below the additivity line are also found when gefitinib is added for 24hours followed by etoposide for 48 hours in NCI-H727 and CRI-G1 cells. In fact, in GRI-G1 cells the point is the same for both types of double treatments.

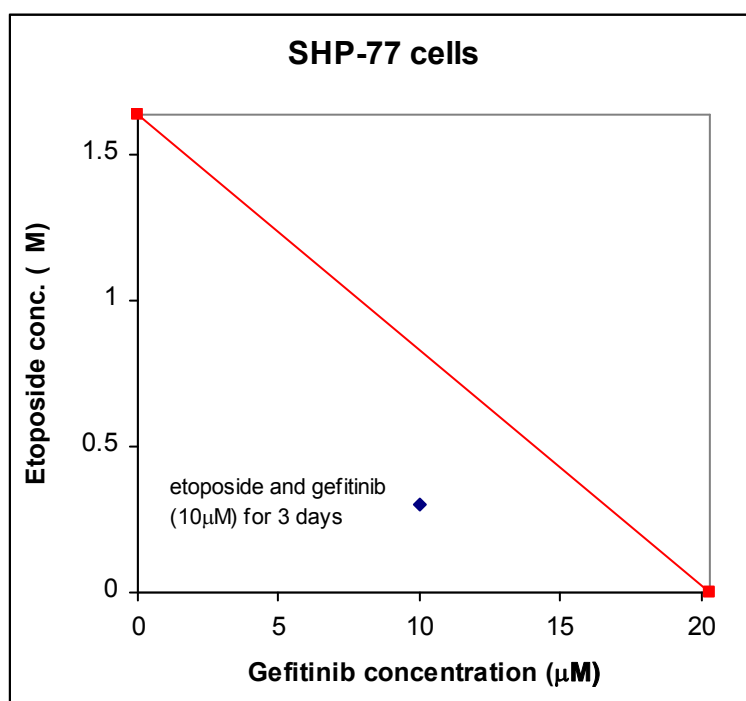
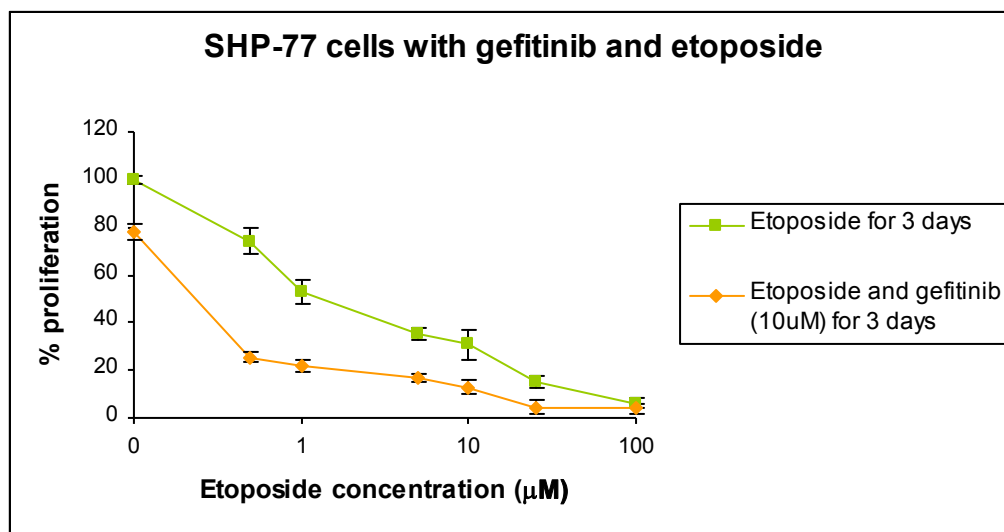


Figure 27: Etoposide and gefitinib combination treatment in SHP-77 cells.

Top graph: Growth inhibition SRB assay. Cells were treated with etoposide at the indicated concentrations alone, or simultaneously with gefitinib (10μM) for 72 hours, followed by 48 hours in drug free medium. Proliferation was calculated as a % of control untreated cells. Data represents the averages of three different experiments, each performed in triplicate; *bars*, SD.

Bottom graph: Isobologram analysis. Red line is additivity line connecting the IC₅₀s (■) of the two drugs. Points well below the line demonstrate synergistic effect, while points close to the line demonstrate an additive effect. Combined treatment IC₅₀ (◆) of etoposide and gefitinib together.

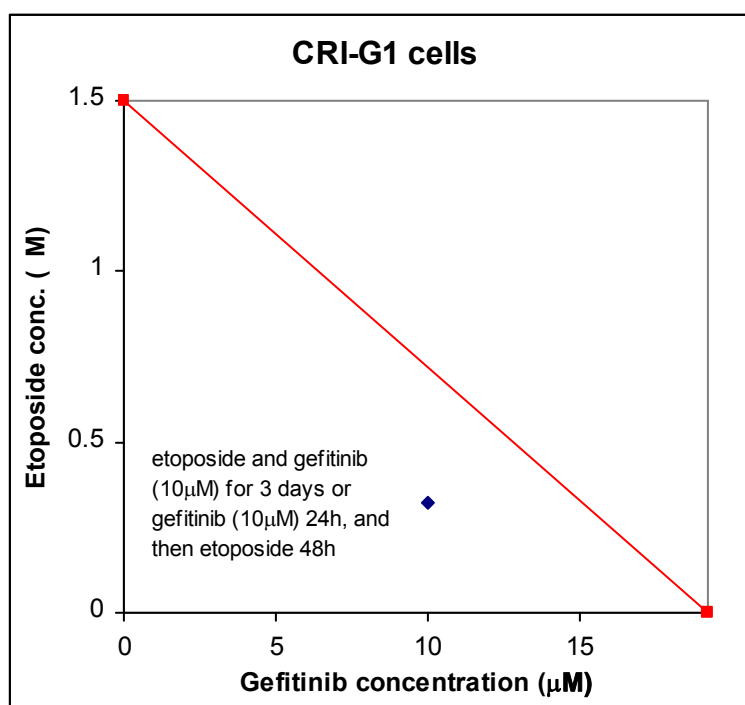
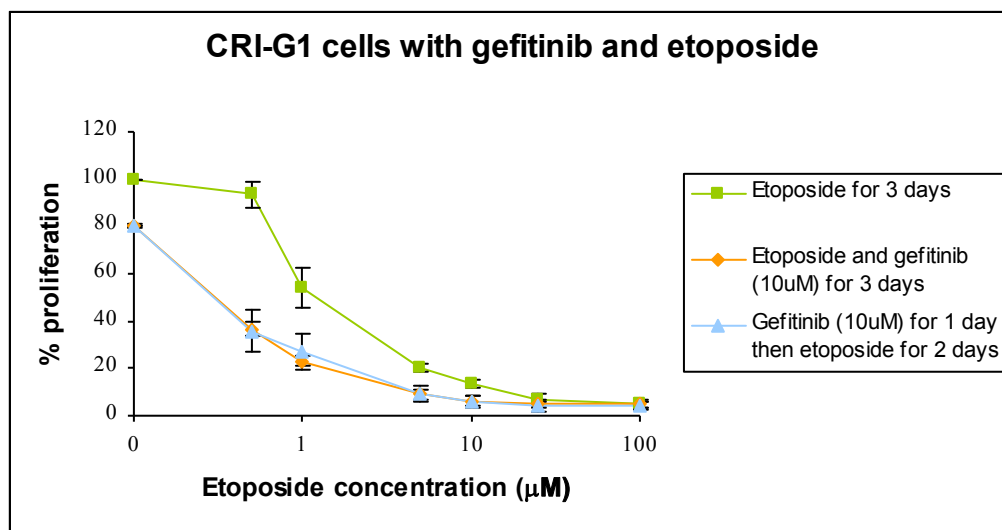


Figure 28: Etoposide and gefitinib combination treatment in CRI-G1 cells.

Top graph: Growth inhibition SRB assay. Cells were treated with etoposide at the indicated concentrations alone, simultaneously with gefitinib (10μM) for 72 hours, or with gefitinib first and then etoposide, followed by 48 hours in drug free medium. Proliferation was calculated as a % of control untreated cells. Data represents the averages of three different experiments, each performed in triplicate; *bars*, SD.

Bottom graph: Isobologram analysis. Red line is additivity line connecting the IC₅₀s (■) of the two drugs. Points well below the line demonstrate synergistic effect, while points close to the line demonstrate an additive effect. Combined treatment IC₅₀s (◆) of etoposide and gefitinib together.

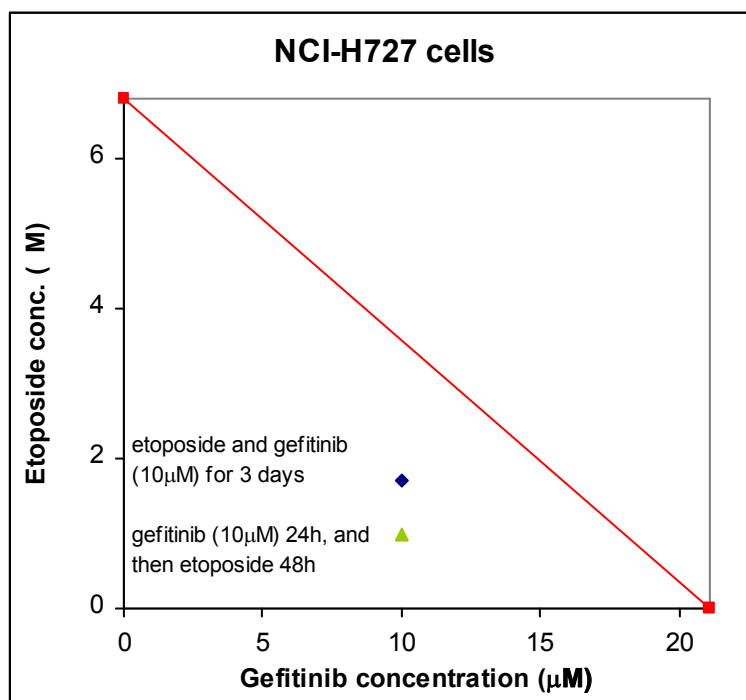
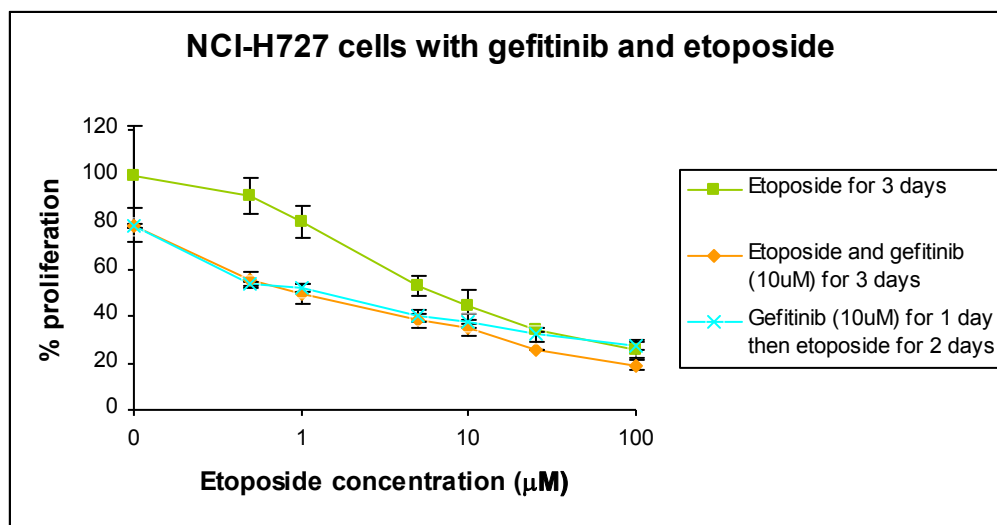


Figure 29: Etoposide and gefitinib combination treatment in NCI-H727 cells.

Top graph: Growth inhibition SRB assay. Cells were treated with etoposide at the indicated concentrations alone, simultaneously with gefitinib (10μM) for 72 hours, or with gefitinib first and then etoposide, followed by 48 hours in drug free medium. Proliferation was calculated as a % of control untreated cells. Data represents the averages of three different experiments, each performed in triplicate; *bars*, SD.

Bottom graph: Isobologram analysis. Red line is additivity line connecting the IC₅₀s (■) of the two drugs. Points well below the line demonstrate synergistic effect, while points close to the line demonstrate an additive effect. Combined treatment IC₅₀s (◆), (▲) of etoposide and gefitinib together.

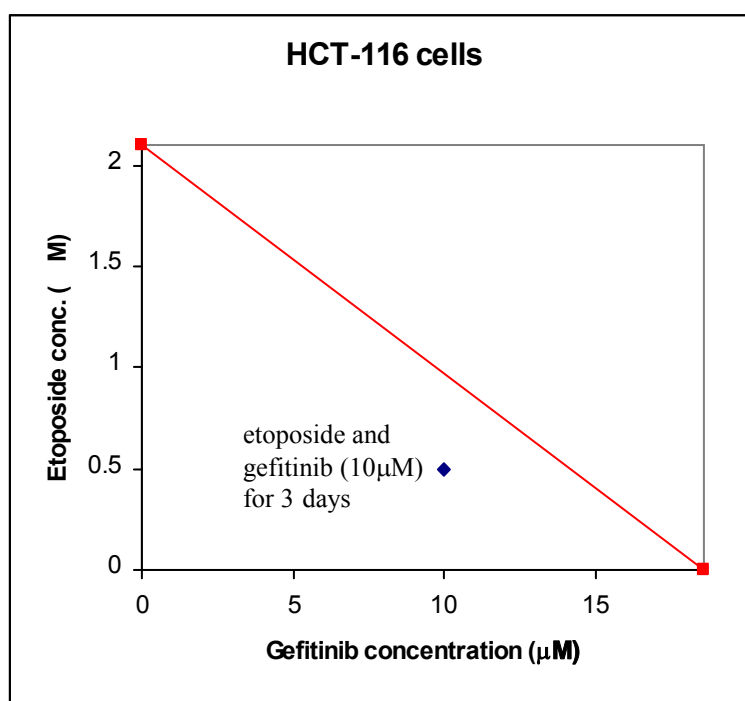
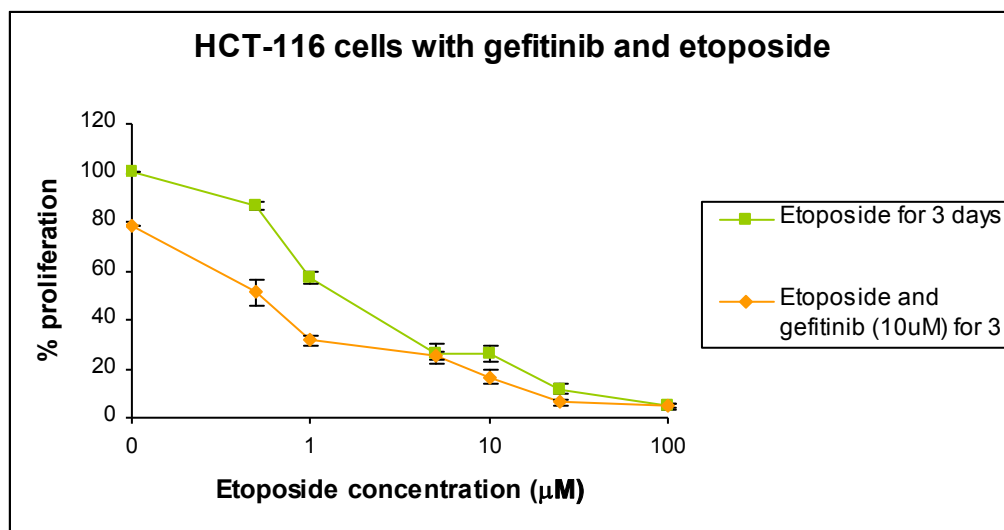


Figure 30: Etoposide and gefitinib combination treatment in HCT-116 cells.

Top graph: Growth inhibition SRB assay. Cells were treated with etoposide at the indicated concentrations alone, or simultaneously with gefitinib (10 μM) for 72 hours, followed by 48 hours in drug free medium. Proliferation was calculated as a % of control untreated cells. Data represents the averages of three different experiments, each performed in triplicate; *bars*, SD.

Bottom graph: Isobologram analysis. Red line is additivity line connecting the IC₅₀s (■) of the two drugs. Points well below the line demonstrate synergistic effect, while points close to the line demonstrate an additive effect. Combined treatment IC₅₀ (◆) of etoposide and gefitinib together.

Cisplatin

Cisplatin showed synergy when combined with gefitinib in NCI-H727 cells (figure 31). Treatment with cisplatin and gefitinib concurrently for 72 hours or with gefitinib for 24 hours followed by cisplatin for 48 hours resulted in a 40% increased anti-proliferative effect at values 0.5 and 1 μ M of cisplatin. When NCI-H727 cells were treated with cisplatin alone the IC₅₀ was 10 μ M. Addition of gefitinib simultaneously or before cisplatin gave IC₅₀s of 1 μ M and 2.2 μ M respectively (table 12).

Also, in HCT-116 cells (figure 32), increased inhibition of proliferation was identified when cisplatin treatment preceded gefitinib, with a joint IC₅₀ of 6.3 μ M compared to 12.7 μ M of cisplatin alone (table 13). Isobologram analysis demonstrated this combination to result in an additive effect, but no synergy. No synergistic or additive effects were identified in any other cell line with cisplatin and gefitinib combinations (data shown in the appendix 1A-1E).

Table 12: IC₅₀s (μ M)

NCI-H727	
Gefitinib 72h	21.1 \pm 1.86
Cisplatin 72h	10 \pm 1.22
Cisplatin and gefitinib for 72h	1 \pm 0.23
Gefitinib 24h, then cisplatin 48h	2.2 \pm 0.30

Table 13: IC₅₀s (μ M)

HCT-116	
Gefitinib 72h	18.6 \pm 2.16
Cisplatin 72h	12.7 \pm 1.32
Cisplatin 24h, then gefitinib 48h	6.3 \pm 0.75

Note: IC₅₀s of treatments with drugs in single or dual treatments for a period of 3 days followed by 2 days in complete media. The values represent means of 3 independent experiments, each done in triplicate, with standard deviation.

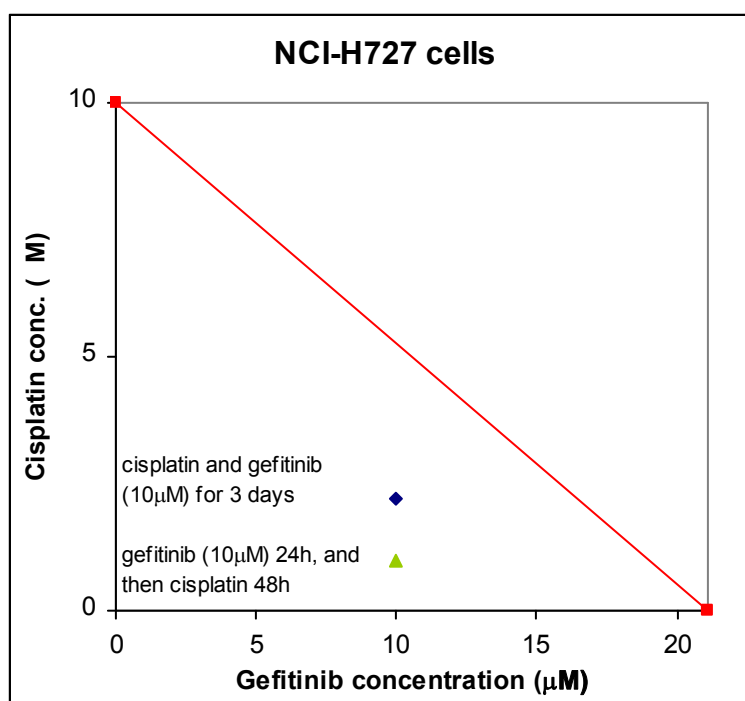
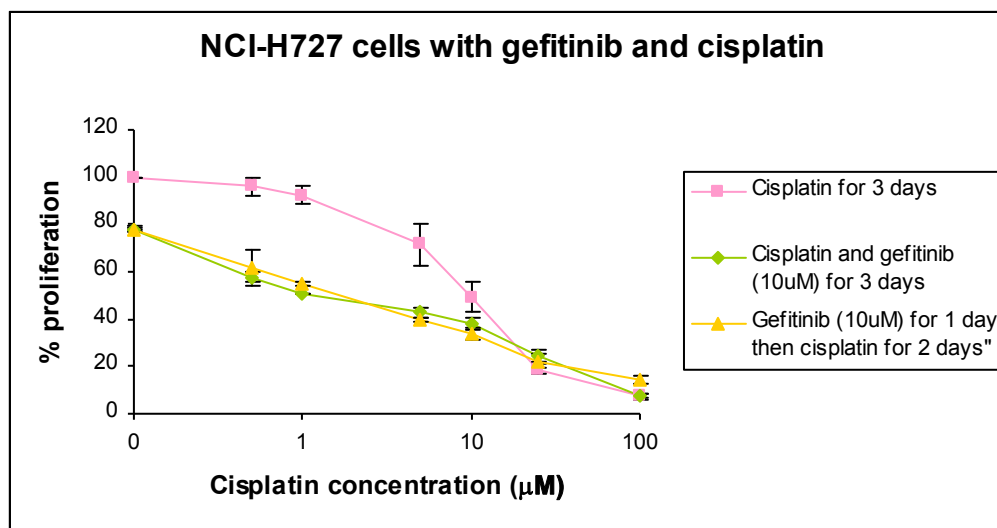


Figure 31: Cisplatin and gefitinib combination treatment in NCI-H727 cells.

Top graph: Growth inhibition SRB assay. Cells were treated with cisplatin at the indicated concentrations alone, simultaneously with gefitinib (10 μM) for 72 hours, or with gefitinib first and then cisplatin, followed by 48 hours in drug free medium. Proliferation was calculated as a % of control untreated cells. Data represents the averages of three different experiments, each performed in triplicate; bars, SD.

Bottom graph: Isobologram analysis. Red line is additivity line connecting the IC₅₀s (■) of the two drugs. Points well below the line demonstrate synergistic effect, while points close to the line demonstrate an additive effect. Combined treatment IC₅₀s (◆), (▲) of cisplatin and gefitinib together.

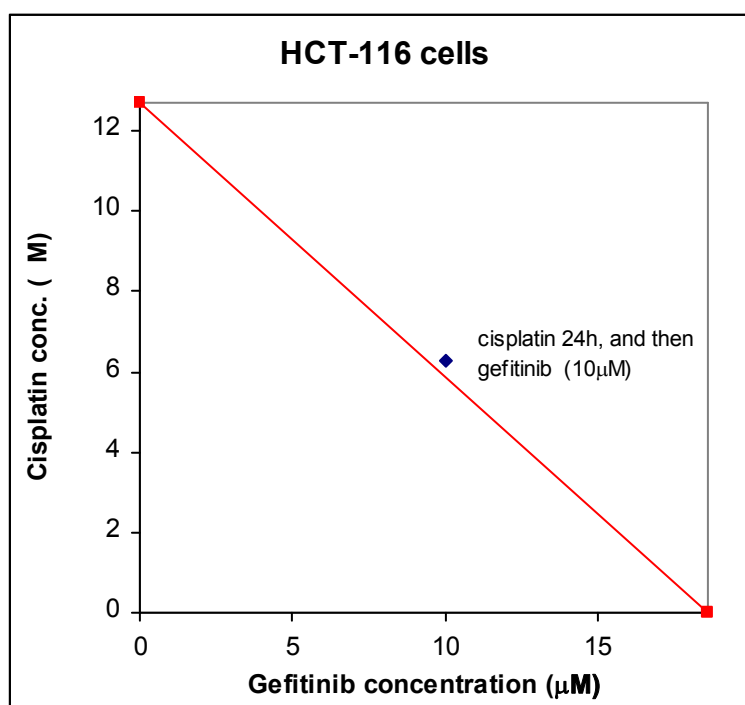
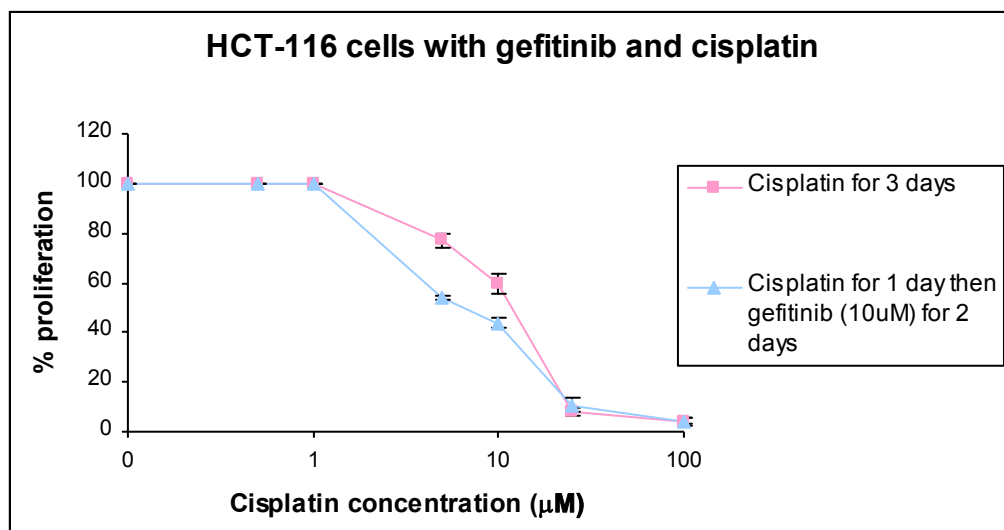


Figure 32: Cisplatin and gefitinib combination treatment in HCT-116 cells.

Top graph: Growth inhibition SRB assay. Cells were treated with cisplatin at the indicated concentrations alone, or with cisplatin first and then gefitinib (10μM), followed by 48 hours in drug free medium. Proliferation was calculated as a % of control untreated cells. Data represents the averages of three different experiments, each performed in triplicate; bars, SD.

Bottom graph: Isobologram analysis. Red line is additivity line connecting the IC₅₀s (■) of the two drugs. Points well below the line demonstrate synergistic effect, while points close to the line demonstrate an additive effect. Combined treatment IC₅₀ (◆) of cisplatin and gefitinib together.

Paclitaxel

Paclitaxel's effect on tumour cell growth was increased in NCI-H727 cells when gefitinib and paclitaxel were added together, or when paclitaxel was added first for 24 hours and gefitinib was added second for 48 hours (figure 33). In both combination treatments inhibition of proliferation was increased by 20% at values 0.05 and 1 μ M of paclitaxel. Joint treatments gave IC₅₀ values of 0.03 for the simultaneous addition of drugs, and 0.031 μ M when paclitaxel administration preceded gefitinib, compared to the IC₅₀ of 0.047 μ M of paclitaxel alone (table 14) demonstrating to an additive effect for this combination. NCI-H727 was the only cell line where the combined treatment of gefitinib and paclitaxel had an increased effect in inhibition of proliferation. No effect was seen in the rest of the cell lines used.

Table 14: IC₅₀s (μ M)

NCI-H727	
Gefitinib 72h	21.1 \pm 1.86
Paclitaxel 72h	0.047 \pm 0.051
Paclitaxel and gefitinib for 72h	0.03 \pm 0.004
Paclitaxel 24h, then gefitinib 48h	0.031 \pm 0.003

Note: IC₅₀s of treatments with drugs in single or dual treatments for a period of 3 days followed by 2 days in complete media. The values represent means of 3 independent experiments, each done in triplicate, with standard deviation.

Methotrexate

Methotrexate showed no synergy with gefitinib in any of the cells tested and in any of the administered schedules. Gefitinib had no effect in the anti-proliferative effect of methotrexate as a single agent.

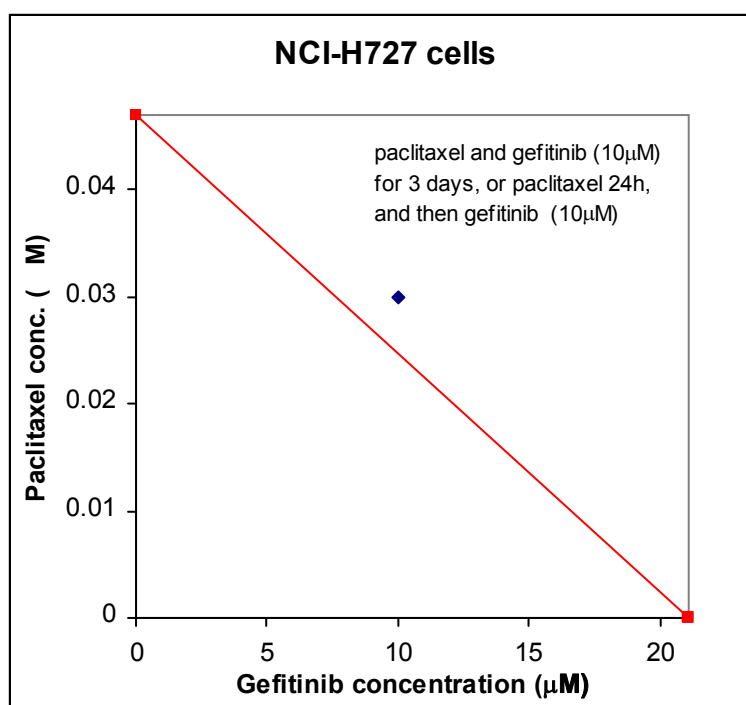
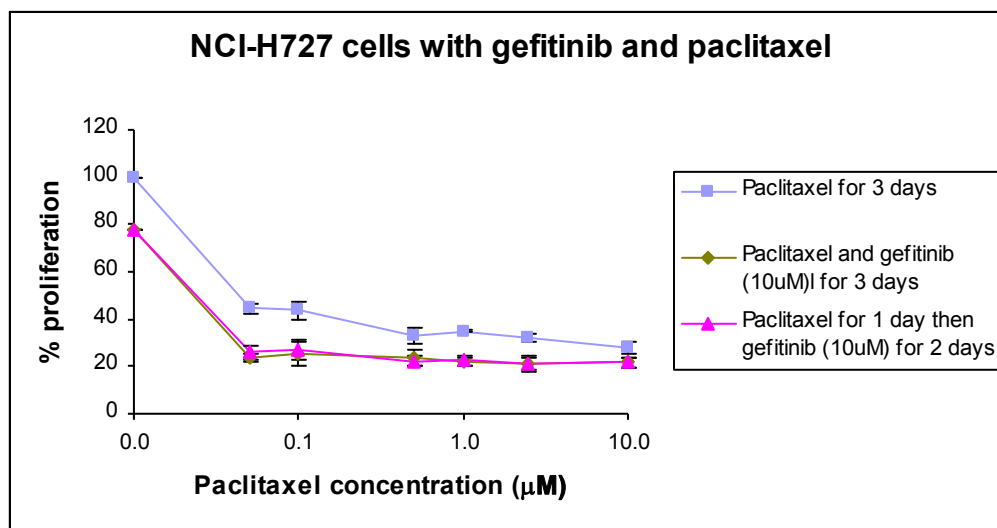


Figure 33: Paclitaxel and gefitinib combination treatment in NCI-H727 cells.

Top graph: Growth inhibition SRB assay. Cells were treated with paclitaxel at the indicated concentrations alone, simultaneously with gefitinib (10μM) for 72 hours, or with paclitaxel first and then gefitinib, followed by 48 hours in drug free medium. Proliferation was calculated as a % of control untreated cells. Data represents the averages of three different experiments, each performed in triplicate; *bars*, SD.

Bottom graph: Isobologram analysis. Red line is additivity line connecting the IC₅₀s (■) of the two drugs. Points well below the line demonstrate synergistic effect, while points close to the line demonstrate an additive effect. Combined treatment IC₅₀s (◆) of paclitaxel and gefitinib together.

4.2.3 Gefitinib induces apoptosis in NET cell lines

To investigate whether the antineoplastic effect of gefitinib in neuroendocrine tumour cells is associated with the induction of programmed cell death, we investigated the presence of mono- and oligonucleosomes in the cytoplasmic fraction of cell lysates, which indicates apoptosis. Apoptosis is primarily characterised by DNA fragmentation, a phenomenon that is followed several hours later by plasma membrane degradation and this results in the enrichment of the cytoplasm with mono- and oligonucleosomes (for details on apoptosis see section 3.7). Mono- and oligonucleosomes were identified using the ELISA cell death detection assay (figure 21), which is a quantitative sandwich-enzyme immunoassay using a biotin-conjugated antibody against histone and an anti-DNA antibody bound to horse radish peroxidase (HRP), which is determined photometrically.

Cells were treated with 0-50 μ M gefitinib for 72 hours as in the proliferation experiments. As shown in figure 34, at the highest concentration of gefitinib DNA fragmentation was mostly present in RIN-5F cells, followed by NCI-H727 and then SHP-77 cells. It is worth noting that the results of apoptosis come in concordance with the proliferation studies. Apoptosis is detected at the high concentrations of 25-50 μ M that correlate to the IC₅₀s found in the growth inhibition assay (table 15 below taken from section 4.2.1). In contrast, CRI-G1 cells showed no DNA fragmentation after 72 hours incubation with gefitinib. Since CRI-G1 cells are the most responsive to gefitinib (IC₅₀ of 19.2 μ M), a possible explanation would be that CRI-G1 cells undergo apoptosis more readily than the rest of the cells and by 72 hours they are completely degraded.

Table 15: IC₅₀s of gefitinib in NET cells (μ M)

	SHP-77	CRI-G1	NCI-H727	RIN-5F
Gefitinib 72h	20.3 \pm 1.42	19.2 \pm 1.78	21.1 \pm 1.86	32.3 \pm 0.95

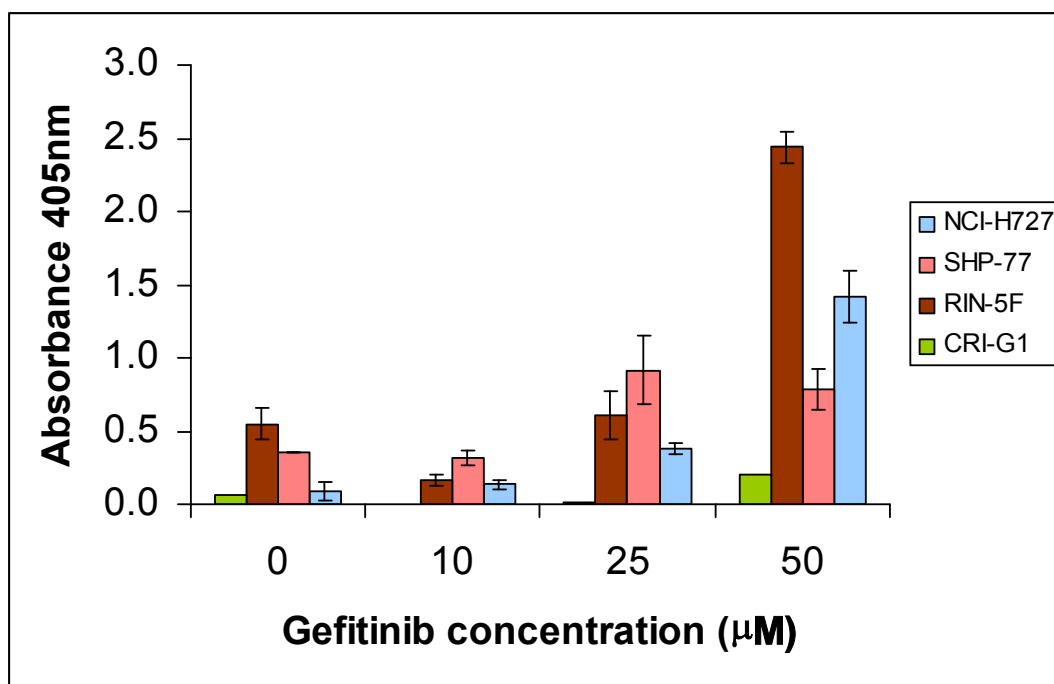


Figure 34: Cells were incubated with 0-50μM gefitinib for 72 hours. Absorbance of 0.5 or higher indicates the presence of mono- and oligonucleosomes. Columns represent averages of three independent experiments, each done in triplicate; bars, SD.

4.2.4 Gefitinib does not induce cell cycle arrest in NET cell lines

To further examine the inhibition of neuroendocrine tumour growth by gefitinib, we assessed gefitinib for its ability to induce cell-cycle arrest using flow-cytometric cell cycle analysis. Cells were treated with gefitinib at 0-50μM for 72 hours. Propidium iodide staining of DNA was used to determine the cell cycle status of cells. For more detailed information please refer to section 3.13 (p.90-92). All experiments were repeated 3 times and representative graphs are shown in figures 35-38.

No effect on the cell cycle of cells was seen in any of the cell lines used with cells treated with 10μM gefitinib for 72 hours demonstrating the same percentages of cells in G1 or G2/M phase of the cell cycle as in the control untreated cells (upper left graph in each page). At the highest concentration of 50μM, gefitinib induced apoptosis in RIN-5F, NCI-H727, SHP-77 and CRI-G1 cells, represented as a movement of cells to the beginning of the FL2-H axis (fluorescence axis, denotes DNA content by propidium iodide staining), which indicates apoptosis. The effect was more prominent in CRI-G1 cells that undergo programmed cell death even at 25μM gefitinib. This agrees with the

results obtained from the study of apoptosis in section 4.2.3, where CRI-G1 cells are completely degraded at 50 μ M gefitinib.

CRI-G1

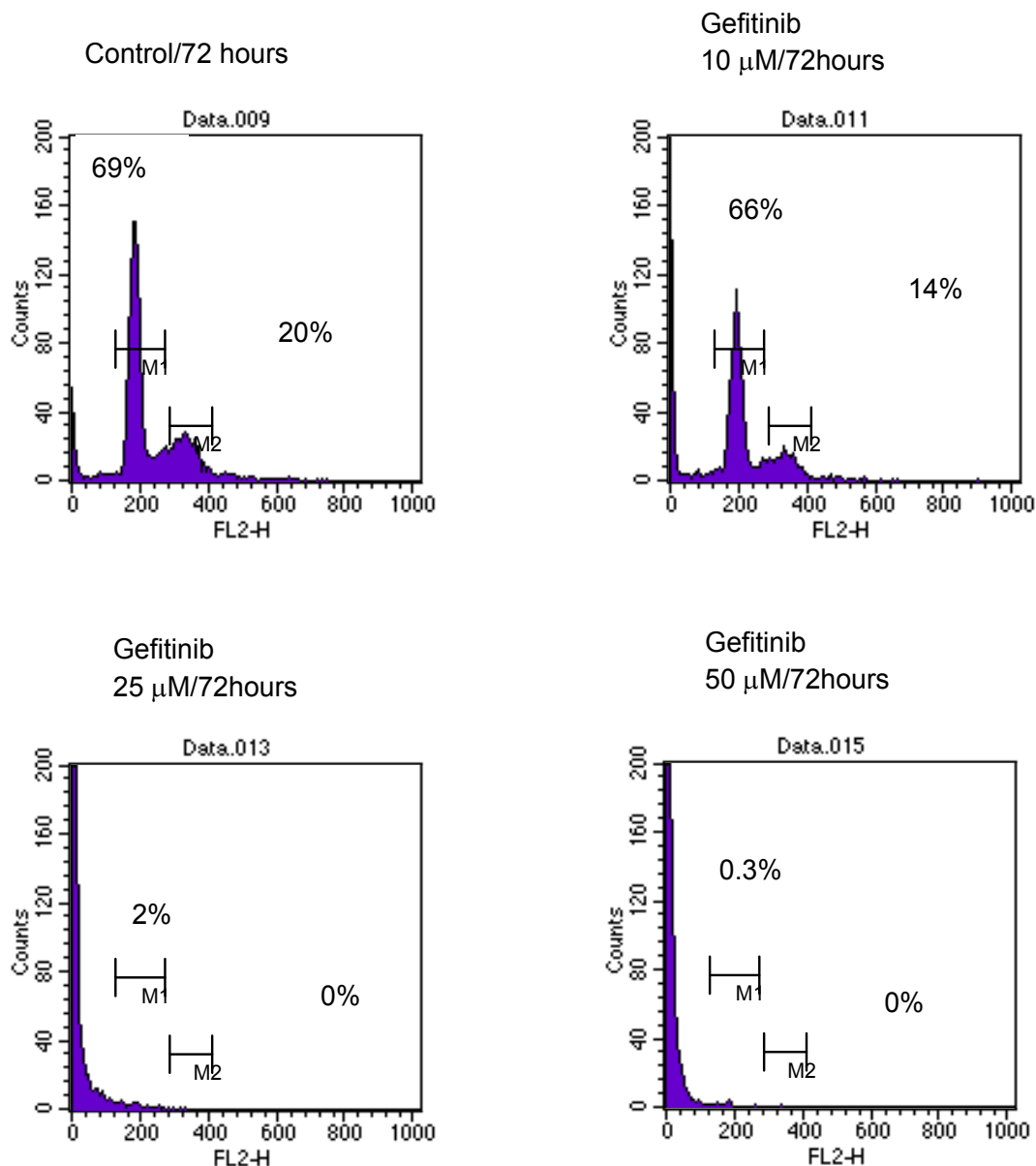


Figure 35: CRI-G1 cells were treated with gefitinib at 0-50 μ M for 72 hours. 'FL2-H' denotes DNA content by propidium iodide staining, while 'counts' denotes cell number. Bars M1 and M2 indicate populations of cells at phases G1 and G2/M of the cell cycle respectively. Cells at the beginning of the FL2-H axis (below 140), denotes cells with sub-G1 DNA content, indicative of apoptosis.

RIN-5F

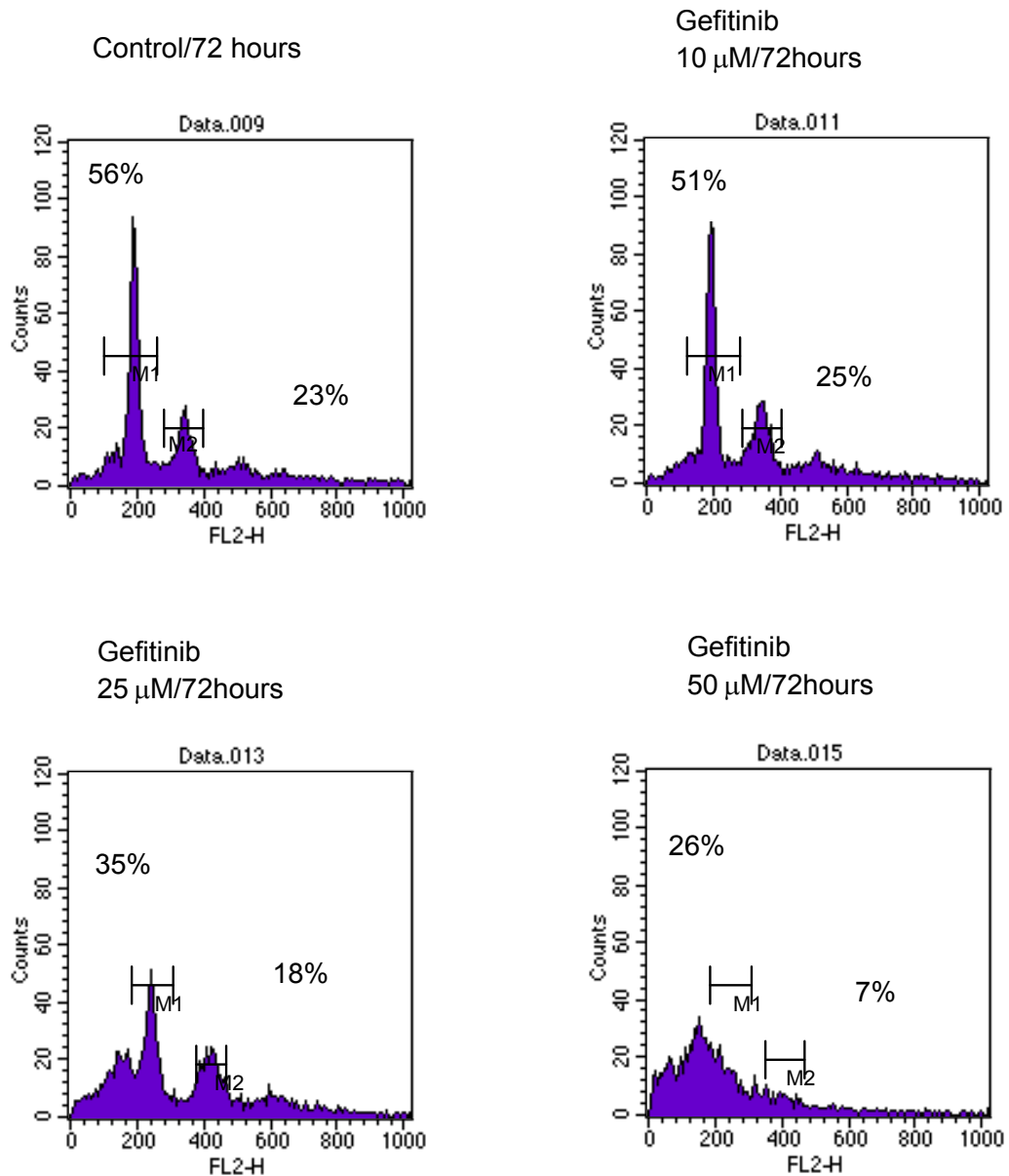


Figure 36: RIN-5F cells were treated with gefitinib at 0-50 μ M for 72 hours. 'FL2-H' denotes DNA content by propidium iodide staining, while 'counts' denotes cell number. Bars M1 and M2 indicate populations of cells at phases G1 and G2/M of the cell cycle respectively. Cells at the beginning of the FL2-H axis (below 140), denotes cells with sub-G1 DNA content, indicative of apoptosis.

NCI-H727

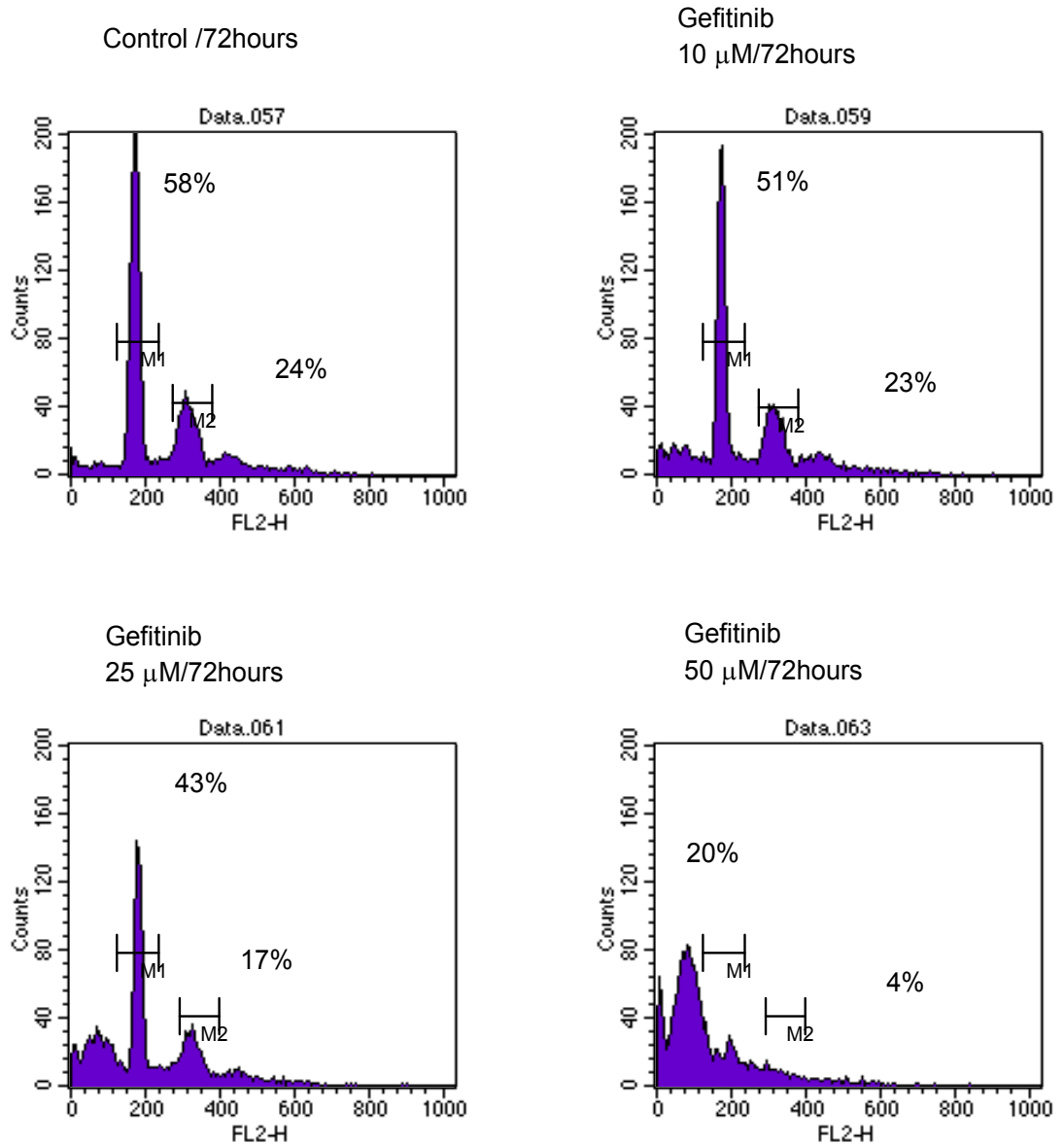


Figure 37: NCI-H727 cells were treated with gefitinib at 0-50 μM for 72 hours. 'FL2-H' denotes DNA content by propidium iodide staining, while 'counts' denotes cell number. Bars M1 and M2 indicate populations of cells at phases G1 and G2/M of the cell cycle respectively. Cells at the beginning of the FL2-H axis (below 140), denotes cells with sub-G1 DNA content, indicative of apoptosis.

SHP-77

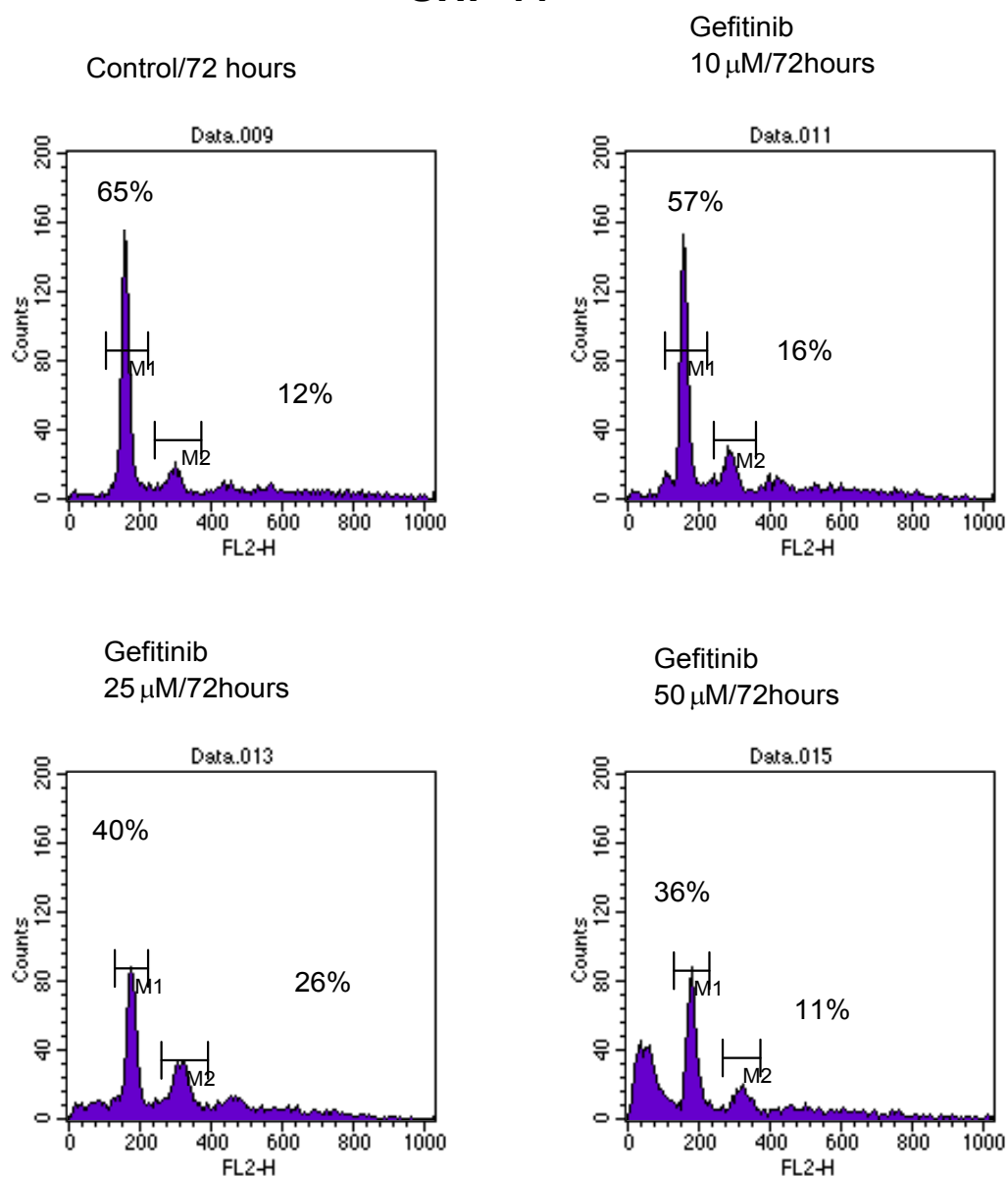


Figure 38: SHP-77 cells were treated with gefitinib at 0-50μM for 72 hours. ‘FL2-H’ denotes DNA content by propidium iodide staining, while ‘counts’ denotes cell number. Bars M1 and M2 indicate populations of cells at phases G1 and G2/M of the cell cycle respectively. Cells at the beginning of the FL2-H axis (below 140), denotes cells with sub-G1 DNA content, indicative of apoptosis.

4.2.5 Modulation of EGFR activity by chemotherapy drugs

DNA damaging agents such as cisplatin, camptothecin and doxorubicin have been proposed to activate EGFR in NIH-3T3 human fibroblast and U87MG human glioma transformed cells lines that overexpress EGFR (Benhar M *et al*, 2002). EGFR activation by cisplatin was also shown in MCF-7 breast cancer cell line (Friedmann B *et al*, 2004). To investigate whether a similar effect was seen in NET cell lines, two different experiments were set up:

- A. Cisplatin, etoposide, methotrexate and paclitaxel were administered to NCI-H727, CRI-G1, SHP-77 and RIN-5F cells at the cytotoxic concentration of 100 μ M for cisplatin, etoposide, and methotrexate or at 10 μ M paclitaxel for 0-24 hours. This experiment would assess the effect of drugs (at a specific concentration) with time on EGFR activity (time-course analysis).
- B. Cisplatin, etoposide, and methotrexate were administered at 0-100 μ M, and paclitaxel at 0-10 μ M for 24 hours to see whether different dosages at the same time duration have diverse effects on EGFR phosphorylation (dose-response analysis).

All experiments were repeated at least 3 times with representative blots shown for each experiment. Results are shown for cisplatin and etoposide with the effects of paclitaxel and methotrexate added in appendix 1F-1I. For immunoblots of phosphorylated EGFR, the A431 cells that overexpress EGFR were used as positive control (figure 39). The amounts of phosphorylated EGFR were calculated by densitometry analysis of the bands. The figure below shows basal expression of phosphorylated EGFR in all cell lines tested.

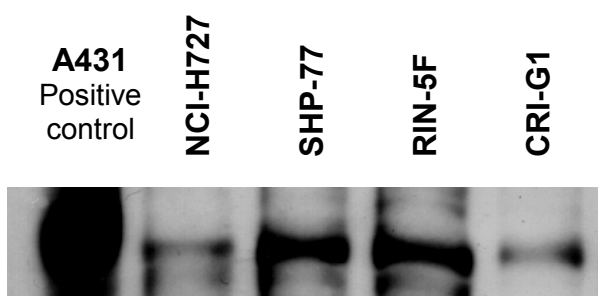


Figure 39: Whole cell lysates of A431 cells (positive control), NCI-H727 human bronchial carcinoid, SHP-77 human small cell lung cancer, CRI-G1 and RIN-5F rat islet tumour cells untreated, were immunoblotted for phosphorylated EGFR (PY20, 170kDa). A-tubulin bands (50kDa) were used as loading control.

A. Time-course analysis

Cisplatin

Cisplatin at 100 μ M induced activation of EGFR in all cell lines, as shown in the western blots in figure 40. This activation is transient lasting up to 3 hours in NCI-H727, SHP-77, and RIN-5F cells, or 6 hours in CRI-G1 cells. At 12 hours phosphorylated EGFR levels are decreased and are less than in the control samples showing a downregulation of the receptor which is also evident at 24 hours (blots shown in figure 42). The blots were stripped and immunoblotted for EGFR showing similar results (data not shown).

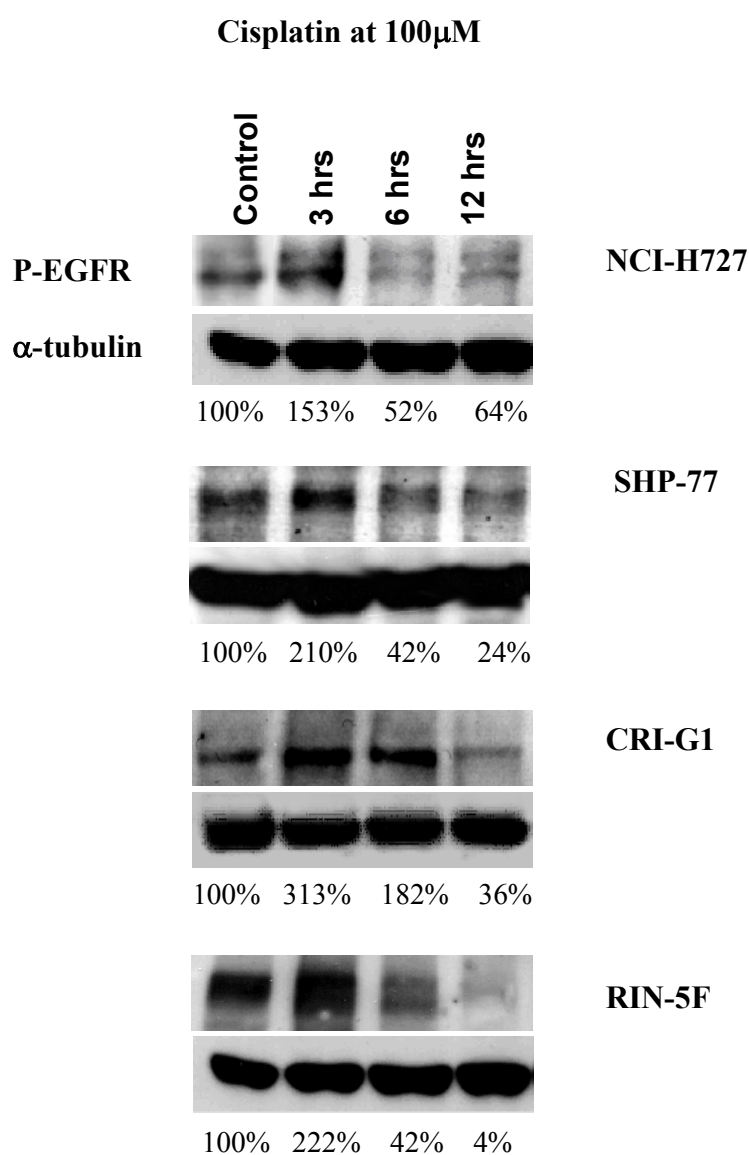


Figure 40: Tyrosine phosphorylation of EGFR in NET cell lines determined by immunoblotting for PY20 (170kDa). Cells were treated with cisplatin at 100 μ M for 3, 6 or 12 hours. α -tubulin bands (50kDa) were used as loading control. Amounts of P-EGFR in percentages were determined by densitometry analysis.

Etoposide

Etoposide treatment at 100 μ M upregulated EGFR at 3 hours in NCI-H727 and CRI-G1 cells but had no effect in the other cells (figure 41). In RIN-5F cells a transient downregulation is seen up to 6 hours but is probably due to less amount of lysate being loaded as shown by the α -tubulin control. In all cells the receptor activity is equal to control levels by 12 hours.

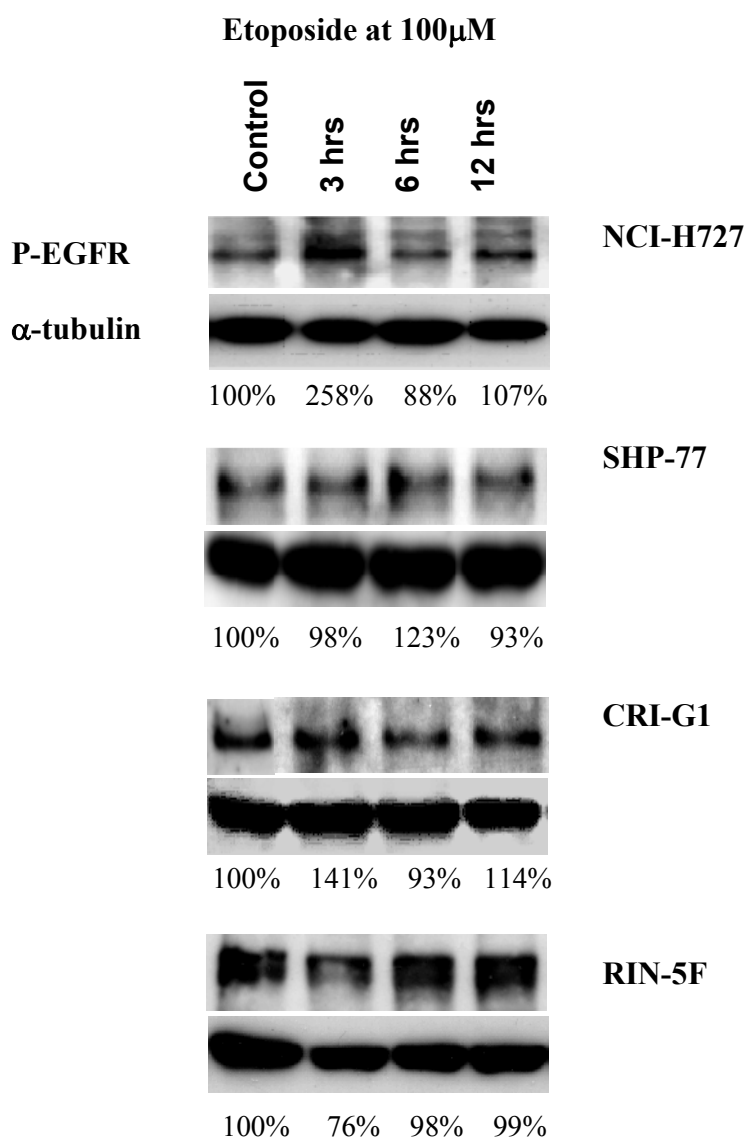


Figure 41: Tyrosine phosphorylation of EGFR in NET cell lines determined by immunoblotting for PY20 (170kDa). Cells were treated with etoposide at 100 μ M for 3, 6 or 12 hours. α -tubulin bands (50kDa) were used as loading control. Amounts of P-EGFR in percentages were determined by densitometry analysis.

Methotrexate

Interestingly, as seen in appendix 1F, methotrexate induced downregulation of EGFR in all NET cell lines. By 3 hours, EGFR activation is at lower levels than in control untreated cells. EGFR downregulation persists at 6, 12 and 24 hours (appendix 1H), and almost abolishes any EGFR activity. Methotrexate is the only chemotherapeutic agent that induced downregulation of EGFR in all cell lines.

Paclitaxel

Paclitaxel also induces downregulation of EGFR in NCI-H727, CRI-G1 and SHP-77 cells, (appendix 1G) showing that paclitaxel shuts down EGFR as part of its mechanism of cell growth inhibition. This downregulation is continued at 24 hours post treatment (appendix 1I). In RIN-5F cells paclitaxel treatment at 10 μ M shows a very small activation of EGFR at 6 hours but downregulation of the receptor there after.

B. Dose-effect analysis

Cisplatin

Treating cells for 24 hours with increasing amounts of cisplatin (figure 42) decreased the amounts of activated EGFR in all NET cell lines tested in a dose-dependent fashion. This downregulation agrees with the results from the time course analysis, where activation of EGFR by toxic amounts of cisplatin lasts for 3 hours and EGFR activation is decreased thereafter. In RIN-5F cells the effect of cisplatin is most dramatic, with almost complete shut-down of the receptor even at 10 μ M. The downregulation is also strong in SHP-77 cells. In NCI-H727 cells only the highest dose blocked EGFR activity completely, while the two highest doses had the same effect in CRIG1 cells.

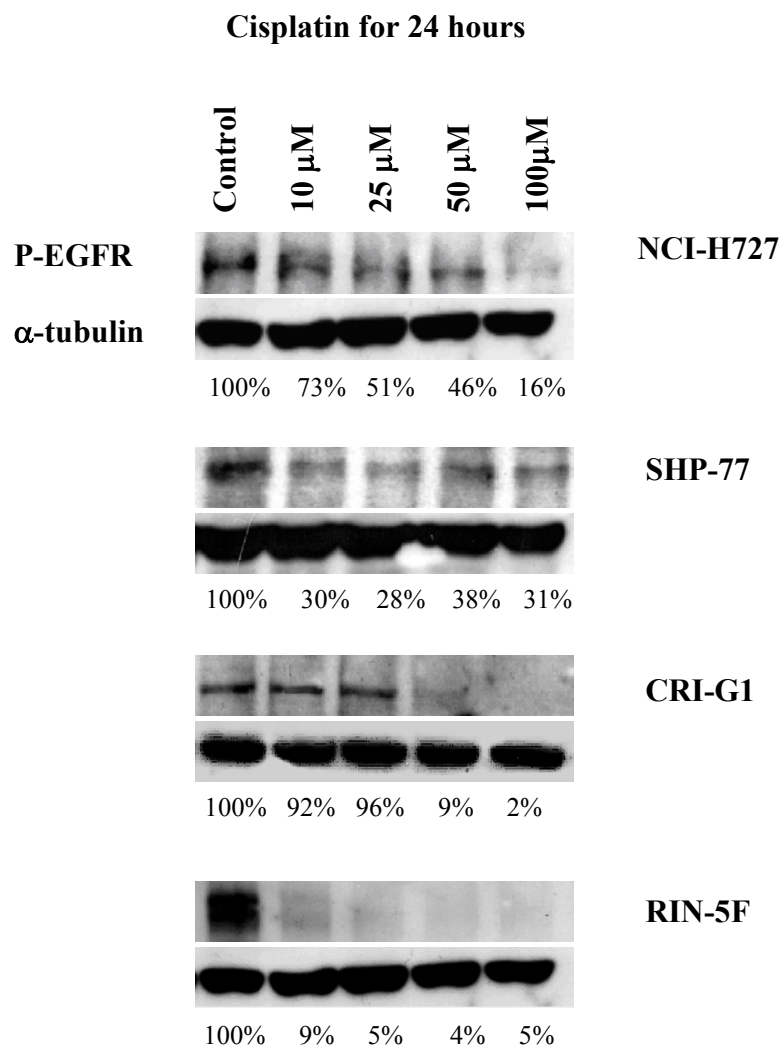


Figure 42: Tyrosine phosphorylation of EGFR in NET cell lines determined by immunoblotting for PY20 (170kDa). Cells were treated with cisplatin at 0, 10, 25, 50 or 100 μ M for 24 hours. Bottom panel shows α -tubulin bands (50kDa) as loading control. Amounts of P-EGFR in percentages were determined by densitometry analysis.

Etoposide

Increasing the dosage of etoposide led to downregulation of EGFR in CRI-G1 and RIN-5F cells (figure 43). In NCI-H727 cells the levels of P-EGFR remained relatively unaffected, while in SHP-77 cells EGFR activity was slightly decreased. As mentioned previously, etoposide induced activation of EGFR up to 3 hours in NCI-H727 and CRIG1 cells, but at 12 hours the receptor was back to normal levels. This is in accordance to these results where in NCI-H727 cells the receptor activity is slightly decreased, while the downregulation in CRIG1 cells is more evident.

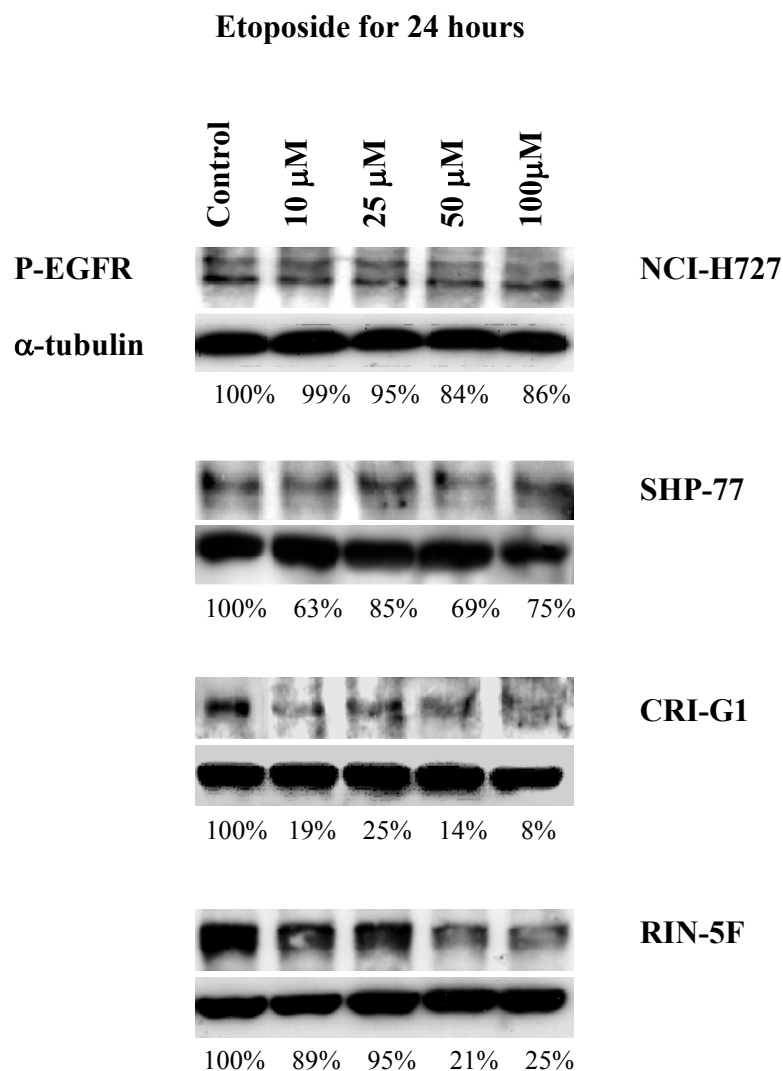


Figure 43: Tyrosine phosphorylation of EGFR in NET cell lines determined by immunoblotting for PY20 (170kDa). Cells were treated with etoposide at 0, 10, 25, 50 or 100 μ M for 24 hours. Bottom panel shows α -tubulin bands (50kDa) as loading control. Amounts of P-EGFR in percentages were determined by densitometry analysis.

Methotrexate

At 24 hours of methotrexate treatment (appendix 1H), as in the time course experiment (appendix 1F), EGFR is downregulated in all neuroendocrine cell lines. The effect of methotrexate on EGFR is dose-dependent with highest inhibition of EGFR activation at the highest concentrations.

Paclitaxel

Increase of paclitaxel concentration induces receptor downregulation in all cell lines tested (appendix 11), which agrees with the results obtained from the time-course experiment. Like methotrexate, the effect of the paclitaxel is dose-dependent and agrees with the results obtained from the time-course experiment. The effect is most evident in CRI-G1 cells in both time-course and dose response analyses. The effects on EGFR activity by chemotherapeutic drugs are summarised in table 16.

Table 16

A: Time-course effect (0-24hours of 100 μ M) of chemotherapy drugs on activity of EGFR in NET cell lines

	Cisplatin	Etoposide	Methotrexate	Paclitaxel
RIN-5F	Upregulation up to 3 hours	No effect	Downregulation	Upregulation up to 6 hours
NCI-H727	Upregulation up to 3 hours	Upregulation up to 3 hours	Downregulation	Downregulation
CRI-G1	Upregulation up to 6 hours	Upregulation up to 3 hours	Downregulation	Downregulation
SHP-77	Upregulation up to 3 hours	No effect	Downregulation	Downregulation

B: Dose response effect (0-100 μ M for 24hours) of chemotherapy drugs on activity of EGFR in NET cell lines

	Cisplatin	Etoposide	Methotrexate	Paclitaxel
RIN-5F	Downregulation	Downregulation	Downregulation	Downregulation
NCI-H727	Downregulation	No effect	Downregulation	Downregulation
CRI-G1	Downregulation	Downregulation	Downregulation	Downregulation
SHP-77	Downregulation	No effect	Downregulation	Downregulation

4.2.6 Activation of EGFR signalling pathways by cisplatin

Cisplatin is the only chemotherapeutic agent that induces activation of the receptor in all neuroendocrine cell lines in our study. Activation of the EGFR pathway traditionally results in downstream signalling pathways including the lipid kinase phosphatidylinositol (PI) 3-kinase (involving PKB/Akt) and the serine/threonine kinase (Ras/MAPK) pathways. Based on this and in the correlation between phosphorylated EGFR and phosphorylated PKB/Akt and MAPK also found recently in NET tissue samples by immunostaining (Shah *et al.*, 2006), we decided to further investigate the upregulation of EGFR by cisplatin.

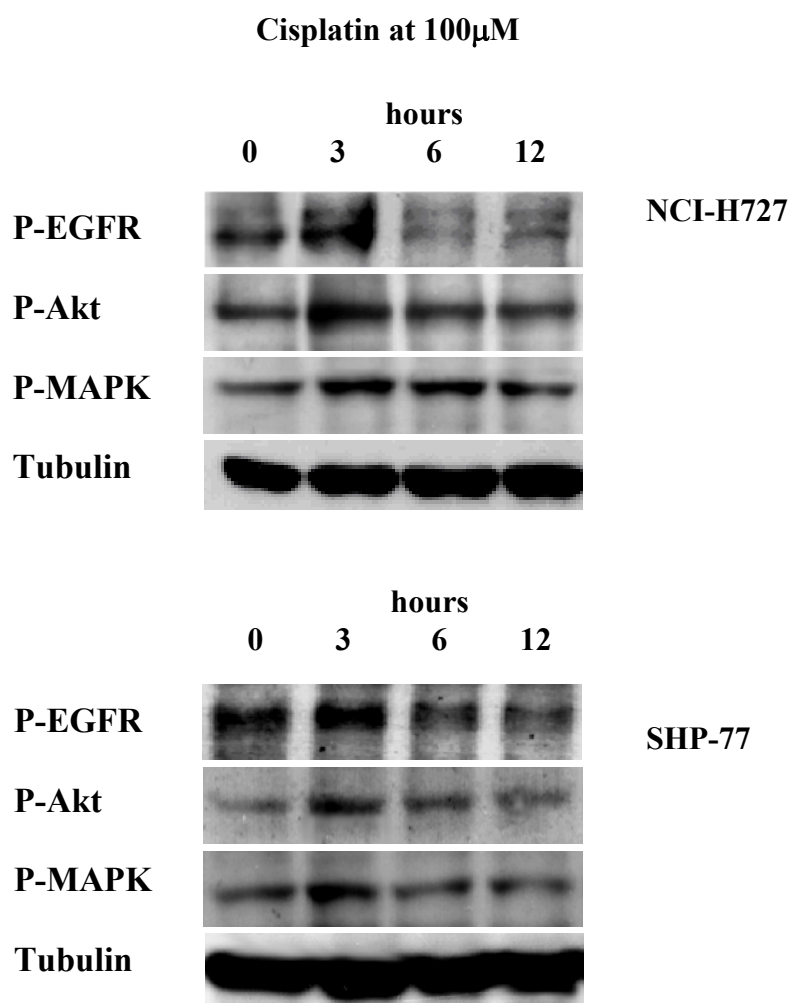


Figure 44: Blots for phosphorylated EGFR in NCI-H727 and SHP-77 cell lines were stripped of antibody and re-blotted for P-Akt and P-MARK. A-tubulin bands (50kDa) were used as loading control.

Cisplatin was analysed for its effect in PKB/Akt and MAPK signalling pathways, by immunoblotting for p-Akt and p-MAPK. Our results (figures 44-45) show that activation of EGFR by cisplatin leads to activation of the PI-3K and Ras/ MAPK signalling pathways in a fashion that follows EGFR activation. Therefore Akt and MAPK are activated up to 3 hours post-treatment in NCI-H727, SHP-77, and RIN-5F cells and up to 6 hours in CRI-G1 cells, followed by downregulation there after.

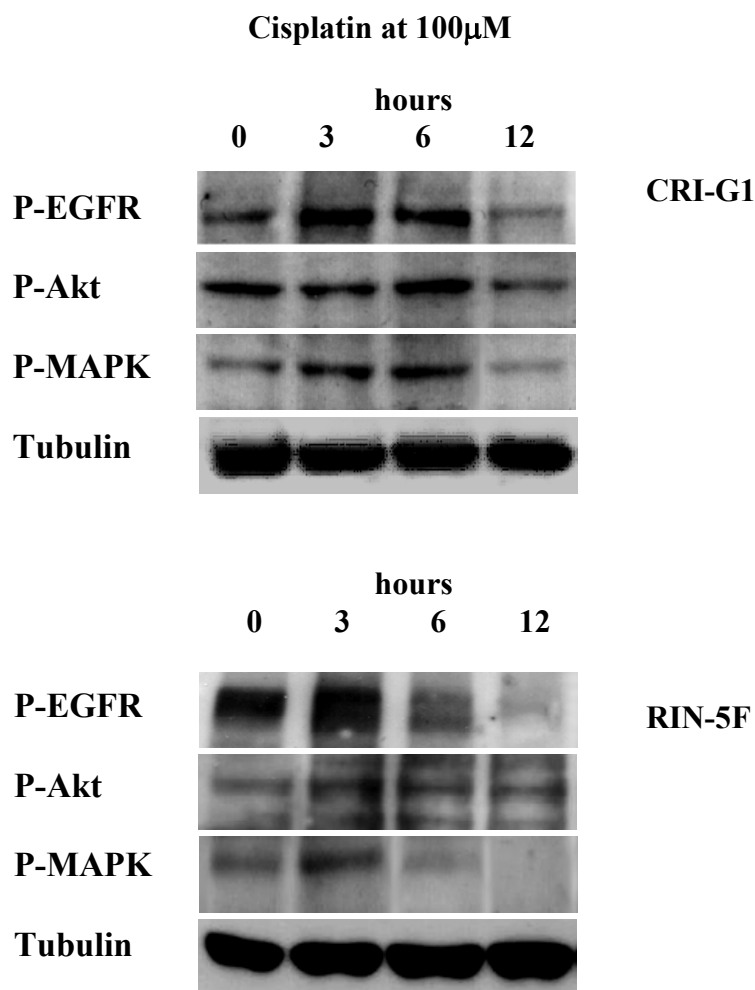


Figure 45: Blots for phosphorylated EGFR in CRI-G1 and RIN-5F cell lines were stripped of antibody and re-blotting for P-Akt and P-MARK. A-tubulin bands (50kDa) were used as loading control.

4.3 Discussion

EGFR aberrant expression is implicated in a variety of human tumours. Blockade therefore of EGFR signalling pathways represents a promising strategy for anti-cancer therapy. Gefitinib, a reversible tyrosine kinase inhibitor of EGFR has shown anti-proliferative activity in non-small cell lung cancer *in vivo*, and is now approved for

clinical use (Harari, 2004). Gefitinib alone or in combination with other anti-cancer therapies, such as chemotherapy drugs and radiation therapy has demonstrated efficacy against tumour growth in a variety of cancer cell lines and in xenograft models (Ciardiello *et al.*, 2000; Ciardiello *et al.*, 2001b; Huang, 2002; Magne, *et al.*, 2002; Sirotnak, *et al.*, 2000).

4.3.1 Anti-proliferative effect by gefitinib and chemotherapy

In this study, gefitinib demonstrated an antineoplastic effect on a panel of neuroendocrine tumour cell lines; two rat islet tumour cell lines CRI-G1 and RIN-5F, the NCI-H727 human lung carcinoid cell line and the SHP-77 human SCLC cell line. The colorectal cancer cell line HCT-116, expressing moderate levels of constitutively active EGFR (Cunningham *et al.*, 2006), was also tested. Gefitinib was used both as a single agent and in combination with the commonly used anti-cancer drugs cisplatin, etoposide, methotrexate and paclitaxel. Gefitinib showed a dose-response cytotoxic effect in all cell lines, with an IC_{50} of 19-32 μ M in neuroendocrine tumour cells and of 18.6 μ M in the colon cancer cells. These concentrations are considerably higher than the ones used in previous *in vitro* studies as well as to the clinical dose of gefitinib used in patients (Ciardiello *et al.*, 2000). Neuroendocrine cells are therefore resistant to doses which are clinically relevant. A possible explanation would be that the cell lines used by others had high EGFR levels and therefore increased sensitivity to gefitinib. Neuroendocrine cells and HCT-116 colon cancer cells have moderate levels of EGFR expression and are relatively resistant to gefitinib. Also, the cell lines in this study are generally slow growing and cytotoxic effects are less evident than in fast growing cells. Finally, the SRB proliferation assay used in our study measures inhibition of proliferation and is therefore largely dependent on cell growth rate, and could not be compared with clonogenic assays which measure colonies after a period of 2 weeks including 6 days of daily replenished drug treatment as performed by other groups.

On the other hand, in a study by McKillop *et al.*, it was shown that the concentration of gefitinib in tumour tissue of breast cancer patients was 16.7 μ M, which is much higher than the routinely measured plasma concentration of gefitinib (McKillop *et al.*, 2005). This value is more agreeable to the values obtained in our study. Moreover, it must be noted that although the IC_{50} of gefitinib required for EGFR inhibition is 20nM, the

concentration needed for tumour growth inhibition in a variety of cell lines is much higher reaching 20 μ M, and varies considerably between different cell types (Moasser *et al.*, 2006). The reason for such a higher concentration may rely on the fact that more than one signalling cascades may be involved in tumour growth inhibition.

Gefitinib demonstrated synergy with etoposide in CRI-G1 and SHP-77 cell lines when the two drugs were added simultaneously, or when gefitinib preceded etoposide in CRI-G1 and NCI-H727 cells. Gefitinib also displayed synergy with cisplatin in NCI-H727 cells either when the two drugs were added simultaneously or when gefitinib preceded cisplatin. This is in agreement with studies on the schedule-dependence of gefitinib and chemotherapy or radiation, where simultaneous addition or pre-treatment with gefitinib produced increased tumour growth inhibition ((Magné *et al.*, 2002). Clinical as well as *in vitro* studies have previously shown optimal therapeutic effect when chemotherapy preceded gefitinib which was not shown in this study. The reason for such differences probably relies on the cell type as well as the dosages, schedules (gefitinib added daily vs. added once only) and methods used for measurement of tumour growth (Ciardiello *et al.*, 2000; Sirotnak *et al.*, 2000). Nevertheless, gefitinib can increase the efficacy of various cytotoxic agents with different mechanisms of action. This co-operation may not therefore be dependent at the original site of action of each drug but may be downstream of all drugs' pathways, at the level of growth control signalling. This ability of gefitinib to affect the cytotoxicity of various chemotherapeutic agents is shared by monoclonal antibodies against EGFR, which were shown to potentiate the effects of cisplatin or doxorubicin (Baselga *et al.*, 1993; Fan *et al.*, 1993) and by antisense oligonucleotides targeting EGFR that showed co-operation with cisplatin, doxorubicin, paclitaxel and topotecan (Ciardiello *et al.*, 2001a).

Paclitaxel displayed an additive effect with gefitinib in NCI-H727 cells only. Methotrexate on the other hand, did not synergise or show any additive effect with gefitinib in any of the cell lines tested, indicating that the mechanism employed by methotrexate to kill NET cells is probably independent of the EGFR pathway inhibited by gefitinib. To our knowledge, no synergy between methotrexate and gefitinib has been demonstrated so far in the literature, confirming that the pathways of the two drugs may be independent of each other. No synergy or additive effect with any of the

drugs tested was evident in RIN-5F cells, indicating that EGFR signalling blockade by gefitinib utilizes a route that does not engage with chemotherapeutic agents at any point of their cytotoxic pathway.

The same principle applies for all combinations of gefitinib with all four cytotoxic agents not leading to an additive or synergistic inhibition of proliferation. The anti-proliferative effect of gefitinib administered with an anti-cancer drug was different for each cell line. The chemotherapeutic drugs used in our study have well-characterised and specific mechanisms of DNA damage and ultimately of inhibition of cell growth. The reason for a synergy seen between an anti-cancer drug and gefitinib in one cell line but not in another cell line is therefore purely cancer cell type-dependent. Even if the pathways used by both drugs are the same at the initiation stage where the drug makes its contact with the cell, proteins downstream their pathways are regulated in different ways from one cell type to another and probably even more so from one type of cancer cell to another.

4.3.2 Gefitinib induces apoptosis but no cell cycle arrest in neuroendocrine cells

Gefitinib has demonstrated tumour cell growth inhibition both by arresting cells in the G1/G0 phase of the cell cycle and by inducing apoptosis in a variety of human cultured cells (Ciardiello *et al.*, 2000; Hopfner *et al.*, 2003). Hopfner M and co-workers also postulated that fast growing cells mainly arrested in G1/G0 phase but slow-growing cells mainly underwent apoptosis when treated with gefitinib (Hopfner *et al.*, 2003). Based on this, the NET cells used in our study, which are generally slow growing, would be expected to mainly undergo apoptosis. Using the same dosage with Hopfner's published data this phenomenon was demonstrated in all four cell lines. As mentioned before, CRI-G1 cells show no DNA fragmentation probably because by 72 hours they are degraded due to apoptotic cell death. Apoptosis is induced at really high concentrations of gefitinib, which are not specific to EGFR, indicating that other tyrosine kinase signalling mechanisms may be involved in the gefitinib-induced apoptosis of neuroendocrine cells. Experiments examining the induction of apoptosis by gefitinib will be carried out with shorter exposures and concentrations up to 10 μ M of the drug to these cells. In addition, cell cycle studies showed no cell cycle arrest of NET cells at 72 hours treatment with gefitinib, but induction of apoptosis in all cell lines,

which would agree with our results and the results exhibited from by Hopfner and his co-workers (Hopfner *et al.*, 2003).

Protein tyrosine kinases have been shown to modulate the expression and post-translational modification of members of the BCL-2 family in order to protect cancer cells from apoptotic signals. Anti-apoptotic members such as Bcl-xL and Bcl-2 are stimulated, but proapoptotic members such as Bad and Bax are inhibited (Skorski, 2002). Stimulation of apoptosis by gefitinib has therefore been attributed to inhibition of anti-apoptotic proteins and induction of pro-apoptotic ones. In a study by Magné *et al.* gefitinib induced upregulation of the pro-apoptotic protein Bax and downregulation of the anti-apoptotic protein Bcl-2 (Magné *et al.*, 2003). Induction of apoptosis by gefitinib has been proposed to be a general mechanism in sensitising cancer cells to chemotherapeutic agents. In our study, gefitinib was shown to induce apoptosis but this did not result in synergy with all cytotoxic drugs used, therefore apoptosis alone cannot account for the presence of absence of synergy.

4.3.3 Effect of chemotherapeutic agents on EGFR activity

Analysis of the effect of chemotherapeutic drugs on EGFR activity showed activation of EGFR after 3 or 6 hours of cisplatin treatment in all the NET cell lines, after 3 hours of incubation with etoposide in CRI-G1 and NCI-H727 cell lines, and after 6 hours of incubation with paclitaxel in RIN-5F cell line. Activation of EGFR was due to increased expression and phosphorylation of the receptor. Increased levels of phosphorylated EGFR in response to cytotoxic drug treatment have also been shown by other groups in cell lines that express functional EGF receptors (Benhar *et al.*, 2002; Friedmann *et al.*, 2004). This phenomenon is probably a shock response of the cell to counteract the cytotoxic effect of the anti-cancer agent. The mechanism involved in upregulation of EGFR by cisplatin was analysed further for downstream signalling pathways involved. Activation of EGFR by cisplatin was found to be mediated through the Ras/MAPK and PI-3K/Akt signalling cascades. These signalling cascades have been implicated in a variety of processes including proliferation, angiogenesis and metastasis of cancer cells (Carpenter G, 2000; Grant S *et al.*, 2002). Therefore highly toxic amounts of cisplatin induce EGFR-dependent survival pathways in neuroendocrine tumour cells. The anti-proliferative effect of gefitinib has been suggested to involve inhibition of PI-3K/Akt, and this could in part explain the lack of synergy between cisplatin and gefitinib in $\frac{3}{4}$

neuroendocrine cells in our study (She *et al.*, 2003; Janmaat *et al.*, 2003).

It is worth noting is that activation of EGFR in the NET cells used is always transient and not evident in samples treated with the same drug for 6 or 12 hours. In fact by 12 or 24 hours EGFR is downregulated in all cells. This phenomenon indicates that this shock response lasts up to 3 hours (or up to 6 hours in CRI-G1 cells treated with cisplatin), after which EGFR signalling is paused along with induction of cell death. Benhar M showed prolonged EGFR activation for up to 24 hours in transformed NIH3T3 cells that overexpress EGFR, and this could be because these cells are more drug-resistant than the ones used in our study (Benhar *et al.*, 2002). Indeed, high levels of EGFR expression have been found in drug-resistant cell lines (Wosikowski *et al.*, 1997) and EGFR inhibition can sensitise cells to chemotherapeutic agents. For example, inhibition of EGFR activation by gefitinib in MCF-7 breast cancer cells led to inhibition of repair of etoposide-induced DNA damage for more than 24 hours, compared to 4 hours for complete DNA repair after removal of etoposide. Similar results were obtained with the repair of cisplatin-induced interstrand cross-links, showing that EGFR activation is needed for drug-resistance (Friedmann *et al.*, 2004).

Finally, the cytotoxic drugs formed two groups depending on their effect on EGFR phosphorylation, with methotrexate and paclitaxel mainly causing downregulation of the receptor, and cisplatin and etoposide mainly causing upregulation of EGFR in a time-dependent fashion. Methotrexate and paclitaxel are known to induce DNA damage indirectly by inhibiting DNA synthesis and arresting cells in metaphase respectively, whereas cisplatin and etoposide promote direct DNA damage in the form of interstrand cross-links and double DNA strand breaks respectively. This separation indicates that direct forms of DNA damage such as the mechanisms employed by cisplatin and etoposide are more toxic to cells and may thus produce the acute response of EGFR activation, which would explain the fact that this activation is only seen transiently up to 3 hours post-treatment, but not there after.

4.3.4 Conclusions

This study has shown that sensitivity to chemotherapeutic agents can be enhanced significantly by inhibition of growth factor pathways such as the EGFR signalling pathway. In contrast to the preclinical data from other groups and ours, a number of large phase III

clinical trials in patients with either locally advanced solid tumours or stage IV NSCLC failed to show any benefit for combined treatment of gefitinib or erlotinib (EGFR tyrosine kinase inhibitor similar to gefitinib) with cisplatin, carboplatin, gemcitabine or paclitaxel (Giaccone *et al.*, 2004; Herbst *et al.*, 2004; Gatzemeier *et al.*, 2007; Smith, 2005). The upregulation of phosphorylated receptor following treatment with chemotherapeutic agents shown by us and other groups (Benhar *et al.*, 2002) could explain the failure of combination treatments in clinical trials. Therefore, the investigation of the appropriate agents to be used in combination, the concentrations the drugs should be added at, and the optimal scheduling of administration, is vital for the development of suitable therapies in cancer patients. Furthermore, investigation of the mechanism of interaction between two drugs with different modes of action may help unravel why certain combinations of drug treatments are more efficient in promoting cell death than others in human cancer cells, which may help in the future drug development techniques.

In this study so far, etoposide or cisplatin along with inhibition of EGFR tyrosine kinase activity by gefitinib have shown promising results, which could help identify a novel therapeutic modality in neuroendocrine tumour patients. Further advances in EGFR targeted anti-tumour therapy may follow the full characterisation of EGFR mutations, including the commonly occurring EGFRvIII deletion mutation, which can determine tumour behaviour as well as response to anti-EGFR therapy. In particular, a number of mutations have been discovered, occurring at the region encoding for the ATP binding site of EGFR, which result in enhanced EGFR activation as well as a higher susceptibility to TKIs (Lynch *et al.*, 2004; Paez *et al.*, 2004). These mutations however, have been shown not to occur in neuroendocrine tumours (Gilbert *et al.*, 2005), whereas the role of EGFRvIII in neuroendocrine tumours has not yet been determined. Whether specific mutations affect response to a chemotherapeutic agent is still unclear. Although gefitinib has not shown clinical benefit with the addition of chemotherapy, cetuximab antibody has shown superadditive effects in chemotherapy-refractory colon cancer (Cunningham *et al.*, 2004). Cetuximab has been reported to induce sensitisation to chemotherapy through DNA repair mechanisms, which will be discussed in detail in the next chapter. On the other hand, small molecule inhibitors of Akt and MAPK are also currently under development. The demonstration of activated Akt in a majority of NET samples and activated MAPK in virtually all the NET tissue samples (Shah *et al.*, 2006) signals a promising future for the role of Akt and MAPK inhibitors in the treatment of NET patients.

CHAPTER 5

INVESTIGATION OF EFFECTS OF RADIATION AND EGFR INHIBITORS ON EGFR LOCALISATION IN NET CELLS

5.1 Introduction

5.1.1 Cisplatin- and radiation-induced mechanisms of DNA repair

Cisplatin is a widely used chemotherapeutic agent that damages DNA by the formation of cisplatin-DNA adducts. These adducts are recognised by a number of cellular proteins, including the DNA damage-recognition factors XPC, hHR23b, MSH2, MSH6 and the high-mobility group protein HMG1 (Wang & Lippard, 2005). Cisplatin-DNA adducts are subject to repair by several pathways, including nucleotide excision repair, mismatch repair and homologous recombination. Cisplatin treatment has also been linked to activation of other repair factors including the DNA-dependent protein kinase (DNA-PK), a serine/threonine kinase that consists of a 350-kDa catalytic subunit (DNA-PK_{CS}) and a heterodimeric regulatory complex Ku70/80. DNA-PK is a member of phosphatidylinositol (PI) 3-kinase superfamily which includes ATM (Ataxia-telangiectasia mutated) and ATR (Ataxia-telangiectasia and Rad3-related) (Reeves *et al.*, 1997). DNA-PK is widely known for its participation in the repair of double strand DNA breaks by the non-homologous end joining (NHEJ) repair pathway. Double strand DNA breaks can be introduced by external sources such as ionizing radiation, by chemotherapeutic drugs such as topoisomerase poisons and by normal biological processes such as V(D)J recombination. DNA-PK has been implicated in both NHEJ repair pathway and in V(D)J recombination, as mutations in DNA-PK_{CS} cause both x-ray sensitivity and defective V(D)J recombination (Khanna & Jackson, 2001).

The role of DNA-PK in signalling pathways following DNA damage has been studied extensively. It has been shown that the Ku70/80 heterodimer can bind to DNA ends at double-strand breaks and to DNA fragments with cisplatin-DNA adducts (Turchi *et al.*, 1999). DNA-PK_{CS} is autophosphorylated following exposure to radiation (Ding *et al.*, 2003; Lou *et al.*, 2004). This modifies its binding with Ku and has been implicated in the phosphorylation of a wide range of DNA damage/checkpoint proteins (Block *et al.*, 2004). MDC1, which is generally associated with the regulation of both intra S-phase and G₂/M phase checkpoints, directly binds to DNA-PK via repeat regions and augments these early auto-phosphorylation events (Lou *et al.*, 2004). DNA-PK has also been implicated in the phosphorylation of a number of other substrates including c-ABL, p53, replication factor A and H2AX but as yet there have been no links to function (Collis *et al.*, 2005). Furthermore, DNA-PK activity has also been shown to be

regulated by a number of proteins. One such example is the oncogenic tyrosine kinase c-ABL which phosphorylates DNA-PK thus modulating DNA-PK/Ku/DNA interactions (Kharbanda *et al.*, 1997).

5.1.2 EGFR is linked to cisplatin- and radio-resistance

Oncogene-transformed cells *in vitro* are characterised by sensitivity to stress stimuli such as chemotherapy or radiation. In contrast, cells from advanced tumours often lose this sensitivity and become resistant to stress-induced apoptosis. To investigate the mechanism of resistance, the effect of cisplatin was analysed by Benhar *et al.* who postulated that transformed mouse embryonic fibroblast NIH-3T3 cells overexpressing EGFR (DHER14 cells) displayed enhanced sensitivity to cisplatin-induced apoptosis compared to parental cells. Cisplatin-induced apoptosis was mediated by the induction of stress kinases including the c-Jun N-terminal kinase (JNK) and the p38 MAPK, and the associated increased production of reactive oxygen species (ROS). Sensitisation of EGFR-overexpressing cells to cisplatin through JNK and p38 MAPK was independent to the overexpressed EGFR (Benhar *et al.*, 2001). In HT29 colon cancer cells, which derive from a well-differentiated human tumour, these stress kinases are suppressed indicating that downregulation of JNK and p38 MAPKs may be involved in the chemoresistance displayed by advanced tumour cells.

On the other hand, cisplatin also induced the activation of downstream effector proteins ERK1,2 in DHER14 cells and U87MG human glioma transformed cells lines that overexpress EGFR, and this was found to be mediated by EGFR. The same effect was produced by other chemotherapeutic agents including doxorubicin and camptothecin, but not by paclitaxel. In this case though, EGFR activation by cisplatin promoted cell survival as inhibition of EGFR phosphorylation enhanced the sensitivity of cells to cisplatin (Benhar *et al.*, 2002). Similar results were obtained using the MCF-7 breast cancer cells, with cisplatin-induced EGFR activation. In these cells inhibition of EGFR by gefitinib significantly delayed the repair of cisplatin-induced interstrand cross-links, enhancing sensitivity of cells to cisplatin (Friedmann *et al.*, 2004). As a result, EGFR upregulation can be associated to the resistance to DNA-damaging agents.

EGFR has also been linked to radiotherapy resistance. EGFR blockade by cetuximab, a humanised anti-EGFR antibody, led to increased radiosensitivity of cells and radiation-

induced apoptosis (Huang & Harari, 2000). Several *in vitro* and *in vivo* experiments with human glioblastoma and head and neck squamous cell cancer xenografts have also shown an enhancement of tumour response to radiation by cetuximab (Huang *et al.*, 1999; Eller *et al.*, 2005). The increased sensitivity to radiotherapy induced by cetuximab may be due to a number of factors including accumulation of cancer cells in the more radiosensitive cell cycle phases (G1, G2/M), inhibition of radiation-induced DNA repair mechanisms, and reduction of VEGF which is important for tumour angiogenesis (Huang & Harari, 2000; Ciardiello & Tortora, 2001). The association of EGFR to radioresistance was recently proven clinically. A phase III trial in squamous cell carcinoma of the head and neck (SCCHN) showed that the addition of cetuximab to radiotherapy improved survival rates and enhanced local control as compared with radiation alone (Bonner *et al.*, 2006).

Sensitisation to radiotherapy can also be obtained by blocking the signal transduction downstream of EGFR. Using antisense oligonucleotides to raf-1, or the specific MEK1/2 inhibitor PD98059 in irradiated human monocytic leukaemia cells (U937/pREP4) caused a reduced proliferation and increased apoptosis as compared to single agent treatments (Pirollo *et al.*, 1997; Cartee *et al.*, 2000).

5.1.3 Nuclear EGFR

Further investigation of the radio- or chemoresistance association with EGFR overexpression was carried out by Dittmann *et al.* using the A549 human bronchial carcinoma cells. They showed that cisplatin, hydrogen peroxide, and ionising radiation induced EGFR phosphorylation (in a ligand-independent manner) and translocation to the nucleus along with proteins Ku70/80, involved in regulation of DNA-PK_{CS} activity. Subsequently, complex formation between EGFR and DNA-PK_{CS} was detected in the nucleus, which was associated with an increase in DNA-PK_{CS} activity (Dittmann *et al.*, 2005a; Dittmann *et al.*, 2005b). Therefore, in mammalian cells one consequence of EGFR activation by irradiation is its internalisation and nuclear translocation, concomitant with nuclear translocation of DNA-PK subunits present in lipid rafts (Lucero *et al.*, 2003) or cytoplasm. These data suggest modulation of DNA repair by EGFR possibly via direct activation of DNA-PK_{CS} under stress conditions.

After exposure to irradiation multiple signalling pathways are activated including EGFR activation and increased signalling through the Ras/MAPK pathway (Dent *et al.*, 2003). Thus exposure to irradiation triggers intracellular signalling cascades that overlap with pathways initiated by ligand binding to EGFR.

5.1.4 EGFR inhibition in DNA repair

It has been demonstrated that cetuximab but not ligand (EGF, TGF- α) treatment triggers a specific physical interaction between EGFR and DNA-PK_{CS} or its regulatory heterodimeric complex Ku70/80 in a variety of cell types both *in vitro* and *in vivo* (Bandyopadhyay *et al.*, 1998). Furthermore, it has been shown that the cetuximab-induced EGFR/DNA-PK_{CS} association was accompanied by a redistribution of DNA-PK_{CS} from the nucleus to the cytosol, and this caused a decrease in the activity of nuclear DNA-PK by about 70% with a concomitant increase in the activity of cytoplasmic DNA-PK (Bandyopadhyay *et al.*, 1998; Huang & Harari, 2000). In agreement to these studies, Dittmann *et al.* showed that cetuximab was able to block radiation-induced EGFR import to the nucleus and activation of DNA-PK. Incubation with cetuximab for 1 hour prior to irradiation caused the formation of a complex between EGFR and DNA-PK in the cytoplasm within 10 minutes after irradiation. This resulted in inhibition of radiation-induced DNA damage repair and sensitization of cells to radiation (Dittmann *et al.*, 2005a; Dittmann *et al.*, 2005b).

Similar results to cetuximab on EGFR have also been obtained with gefitinib. Friedmann *et al.* observed that gefitinib inhibited the repair of DNA damage following cisplatin and etoposide treatment in cell lines with different EGFR expression levels. Immunoprecipitation experiments showed an association between EGFR and DNA-PK_{CS}, which was increased following gefitinib treatment (Friedmann *et al.*, 2004). Further investigation of the effects of gefitinib on the functional activity of DNA-PK_{CS} and the interaction between EGFR and DNA-PK_{CS} showed that gefitinib reduced DNA-PK_{CS} activity in cells expressing high or moderate levels of EGFR. Furthermore, gefitinib-induced EGFR/ DNA-PK_{CS} association was accompanied by a redistribution of DNA-PK_{CS} from the nucleus to the cytosol (Friedmann *et al.*, 2006). Figure 46 summarises the events reported in all the above studies in association to EGFR. Based on the above, molecular blockade of EGFR signalling may influence the ability of tumour cells to repair DNA lesions effectively after irradiation or cytotoxic damage.

Aims

The results shown in chapter 4 indicate that synergy between gefitinib and chemotherapeutic agents in neuroendocrine tumours is possible but appropriate scheduling of treatments is needed to overcome the upregulation of EGFR signalling caused by chemotherapeutic agents leading to chemoresistance. Furthermore, targeted radiotherapy is a major modality of treatment for NET patients with moderate results in foregut NETs but has no effect in midgut or hindgut NETs. Based on the reported clinical failure of gefitinib in combination with chemotherapy, and the success of cetuximab in radiosensitising patients with head and neck squamous cell carcinoma, we decided to investigate any interaction between radiation treatment and EGFR inhibition by gefitinib and cetuximab which could be exploited clinically, and to study the underlying mechanisms. To investigate their interaction, radiation in combination with EGFR inhibitors were assessed for their collective effect in cell proliferation, EGFR expression and EGFR localization within the cell.

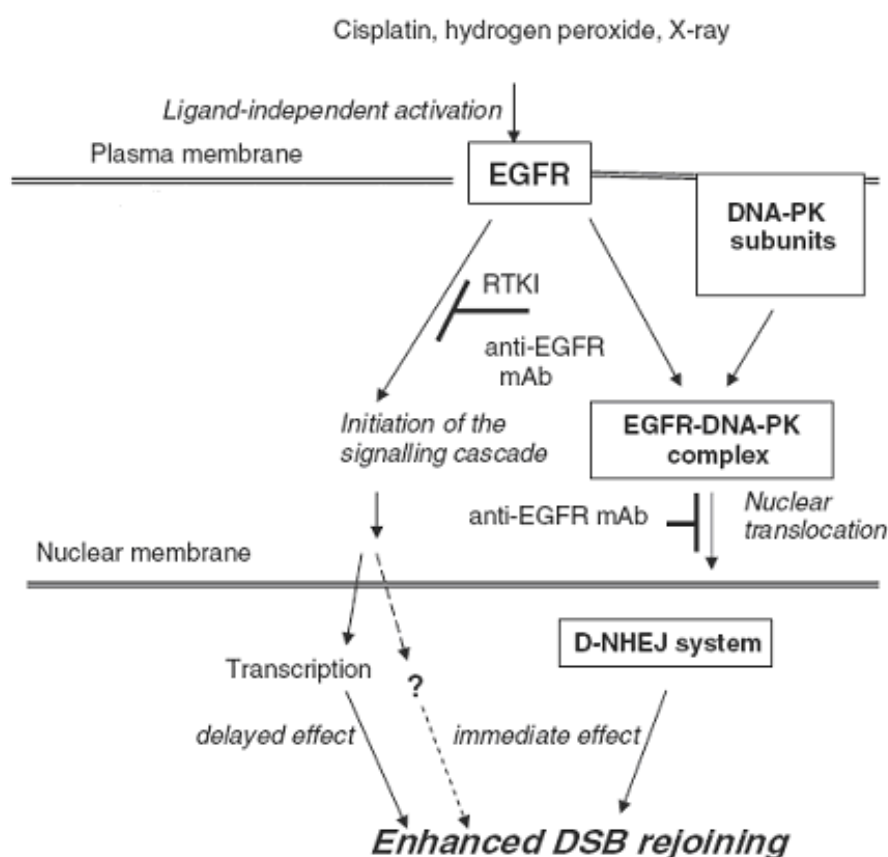


Figure 46: EGFR pathway in response to radiation or cisplatin-induced DNA damage. (D-NHEJ: DNAPK-dependent NHEJ; RTKI: receptor tyrosine kinase inhibitors)

Adapted from I Szumiel, Cellular Signalling, 2006

5.2 Results

5.2.1 Proliferation studies with radiation and EGFR inhibitors

Radiotherapy and EGFR inhibitors (gefitinib and cetuximab) were combined in this study in order to identify possible synergisms in neuroendocrine tumours. In proliferation experiments the irradiation dose of 4Gy was used in CRI-G1, RIN-5F and SHP-77 cells and 30Gy for NCI-H727 cells. These doses cause approximately 30% inhibition of proliferation as measured by SRB proliferation assays (data not shown).

Administered schedules included:

- Incubation with gefitinib or cetuximab on day1, followed by irradiation on day 2.
- Irradiation on day 1, followed by gefitinib or cetuximab on day 2 (for 24 hours).
 - Drugs were added at 0-25 μ M for gefitinib, and at 0-60nM for cetuximab.
 - Treatments were followed by 2 days incubation in drug-free media before analysis.

Growth inhibition was determined by the Sulphorhodamine B (SRB) proliferation assay. Graphs are shown for CRI-G1 and RIN-5F cells only, with results for the other cell lines added in the appendix 2A-2B.

As seen in figure 47, gefitinib as a single agent in CRI-G1 cells caused 16% and 60% inhibition of growth at 10 μ M and 25 μ M respectively, while the doses for cetuximab (30nM and 60nM) caused 13% and 25% inhibition of proliferation. Irradiation at 4Gy in CRI-G1 cells combined with gefitinib resulted in increased inhibition of proliferation by 47% at 10 μ M and 19% at 25 μ M gefitinib. A similar result was obtained in the combined treatment of radiation and cetuximab, with an increase in inhibition of growth by 49% at 30nM cetuximab, which stays at 45% with 60nM. Therefore, radiation effects on proliferation are increased by EGFR inhibition.

In RIN-5F cells (figure 48) gefitinib caused 22% and 35% inhibition of growth at 10 μ M and 25 μ M respectively, while cetuximab at 30nM and 60nM caused 20% and 23% inhibition of proliferation. Combination treatments between radiation and EGFR inhibitors led to a lesser increase in inhibition of proliferation by 18% and 22% with gefitinib or by 22% and 20% with cetuximab. No differences were observed between the two different sequences of administration as shown in figures 47-48.

The combination treatments of radiation with gefitinib in CRI-G1 and RIN-5F cells were examined for synergistic or additive effect by isobologram analysis as shown in figure 49. Even though isobologram analysis is used to study combinations of two drugs rather than combinations of drugs with radiotherapy, we used them as a basis for analysing our results. In RIN-5F cells the point of combination appears very close to the additivity line, indicating an additive effect, while CRI-G1 cells show the point of combination below the additivity line, and therefore demonstrate synergy of gefitinib with radiation.

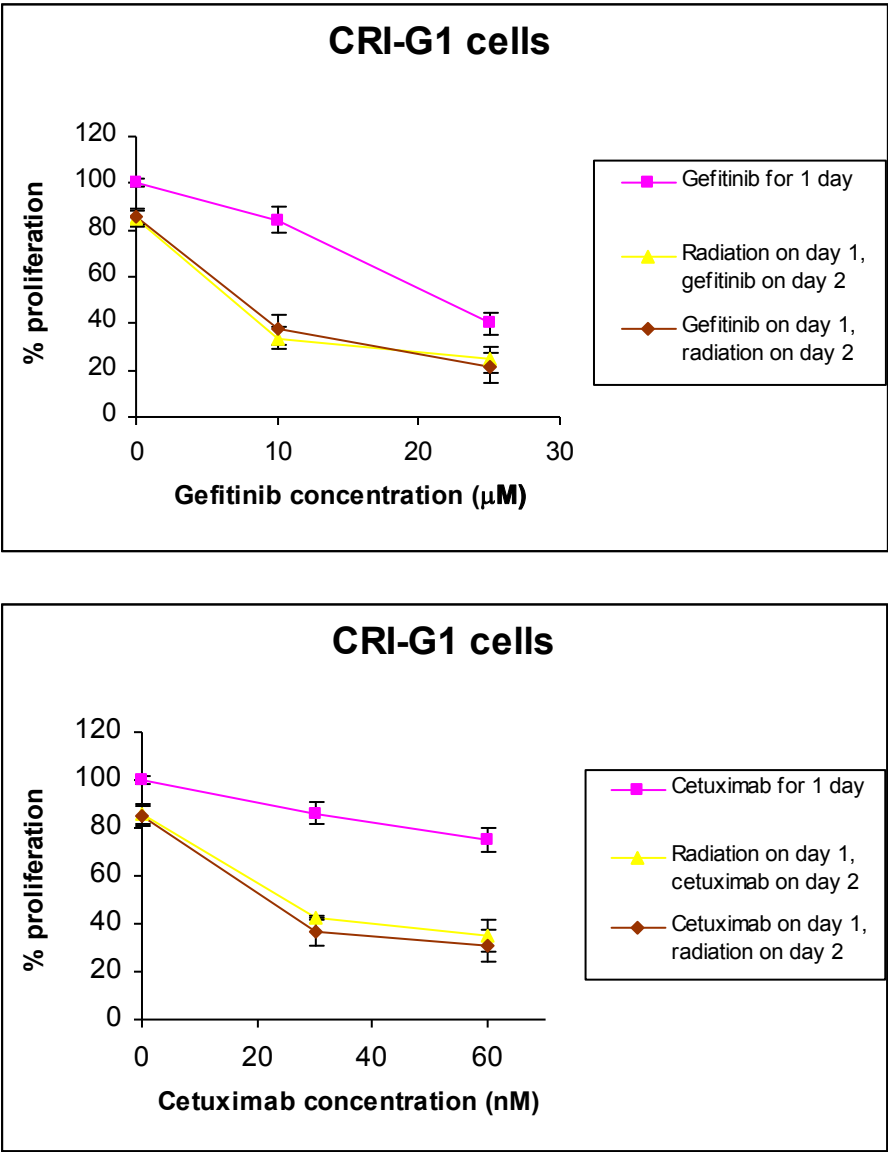


Figure 47: Growth inhibition SRB assay. CRI-G1 cells were treated with radiation at 4Gy on day 1 and gefitinib or cetuximab at the indicated concentrations on day 2, or in reverse order, followed by 48 hours in drug free medium. Proliferation was calculated as a % of control untreated cells. Data represents the averages of three different experiments, each performed in triplicate; bars, SD.

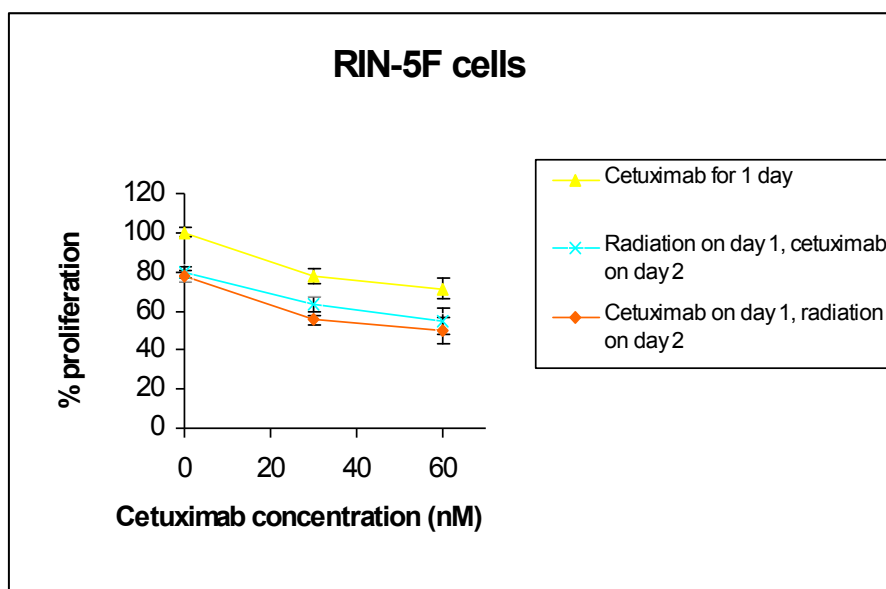
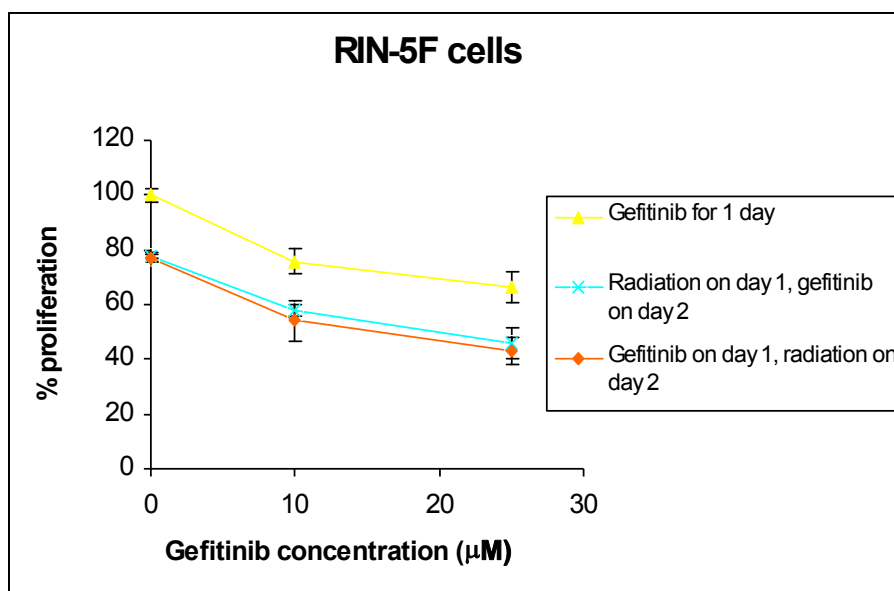


Figure 48: Growth inhibition SRB assay. RIN-5F cells were treated with radiation at 4Gy on day 1 and gefitinib or cetuximab at the indicated concentrations on day 2, or in reverse order, followed by 48 hours in drug free medium. Proliferation was calculated as a % of control untreated cells. Data represents the averages of three different experiments, each performed in triplicate; *bars*, SD.

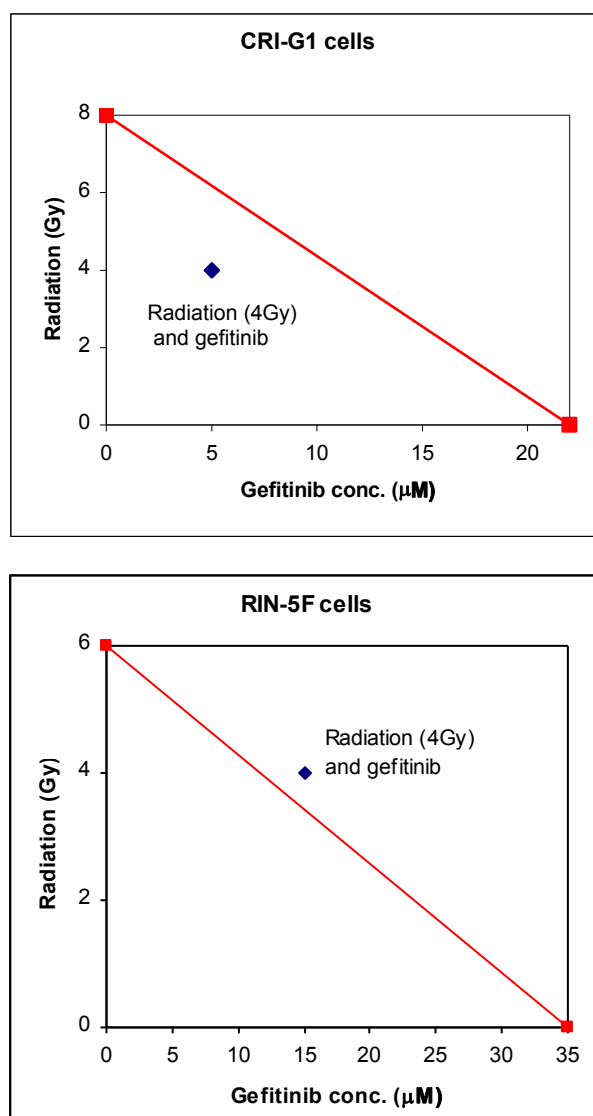


Figure 49: Isobologram analysis for combination treatment of radiation and gefitinib in CRI-G1 and RIN-5F cells. Cells were treated with radiation (4Gy) on day 1, followed by gefitinib on day 2 or in reverse order, followed by 48 hours in drug free medium. Red line is additivity line connecting the IC₅₀s (♦) of the two drugs. Combined treatment IC₅₀s (◆) of radiation and gefitinib together.

5.2.2 DNA repair modulation by EGFR inhibitors

To further investigate the interaction between radiotherapy and EGFR inhibitors, we analysed their effect on DNA repair using the Single Cell Gel Electrophoresis (COMET) Assay. The comet assay allows for detection and visualisation of DNA damage within individual cells. As an example, figure 50 shows screen images of individual CRI-G1 cells after irradiation treatment alone. Irradiation produces DNA strand breaks causing the DNA to migrate further on an agarose gel than undamaged DNA. This forms a tail moment which is a function of the amount of DNA in the tail

and the length of the tail (measured in μ meters). Within 10 minutes after irradiation treatment, the strand breaks start to be repaired as measured by a shortened tail moment (bottom left-hand panel). After 80 minutes, almost complete repair is achieved with very low detectable tail moment (bottom right-hand panel). For analysis, the average tail moment of 50 individual cells is calculated from two independent slides and plotted for each time point.

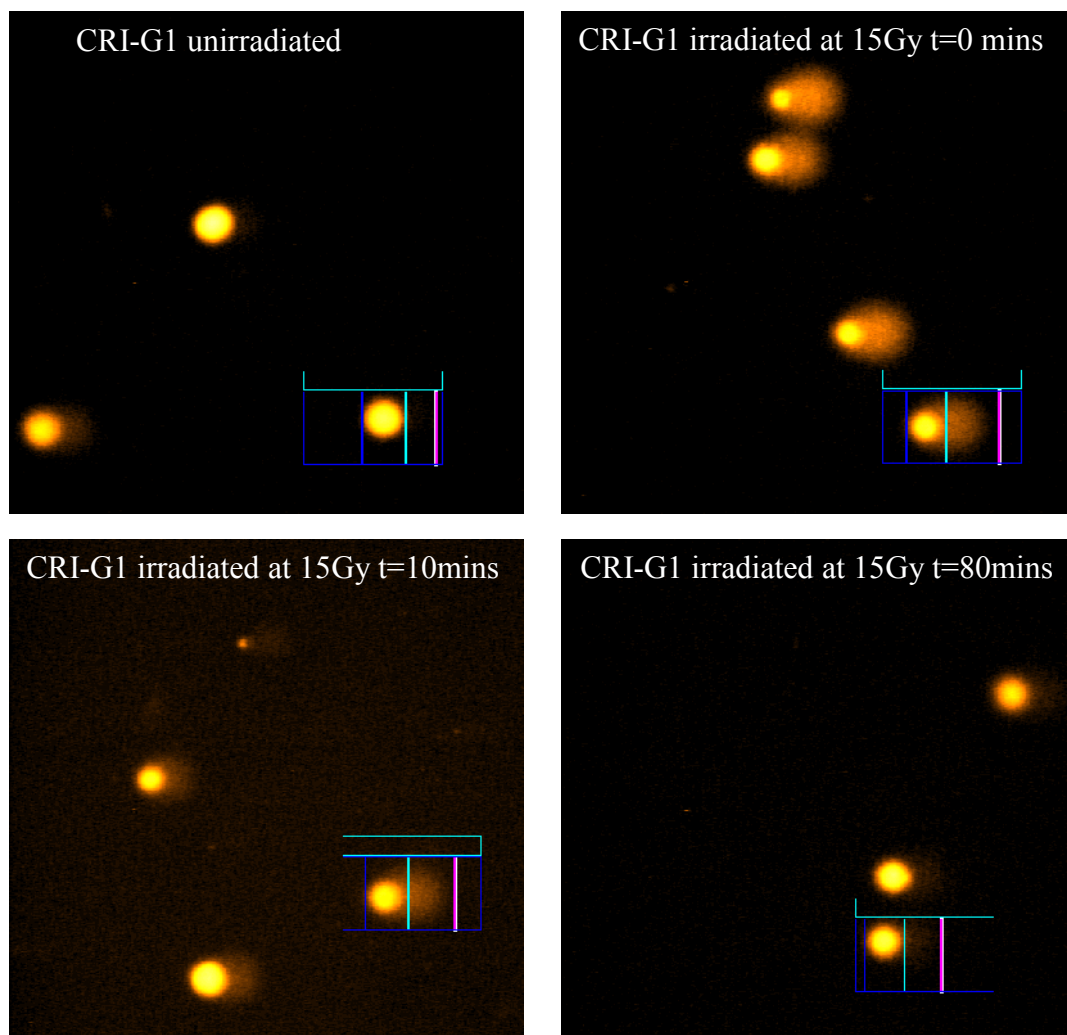


Figure 50: Sample screen display of comet images for irradiation (15Gy) induced damage and repair after 10 and 80 minutes in CRI-G1 cells. Images were viewed using an inverted fluorescence microscope and analysed using the Komet Analysis Software.

Radiation-induced DNA damage in the form of double DNA strand breaks is repaired within approximately 2 hours (figures 47-48). As a result, for our combined studies, treatment with EGFR inhibitors preceded radiation treatment. Gefitinib and cetuximab were added (at the low doses of 10 μ M and 30nM respectively, causing no more than 10% growth inhibition at 3 hours) for 3 hours followed by irradiation treatment in order

to assess the effect of acute drug treatment in DNA repair. Furthermore, for accurate analysis of DNA repair kinetics, significant DNA damage must be induced. The radiation dose of 15Gy produces an adequate amount of DNA damage (producing a tail moment of approximately 16 in the CRI-G1 cell line and 13 in the RIN-5F cell line), which is needed for accurate analysis of DNA repair kinetics. This dose was used for all cells except for NCI-H727 cells which were radiated at 30Gy. The doses were calculated following a titration of radiation treatments in all cell lines (data not shown).

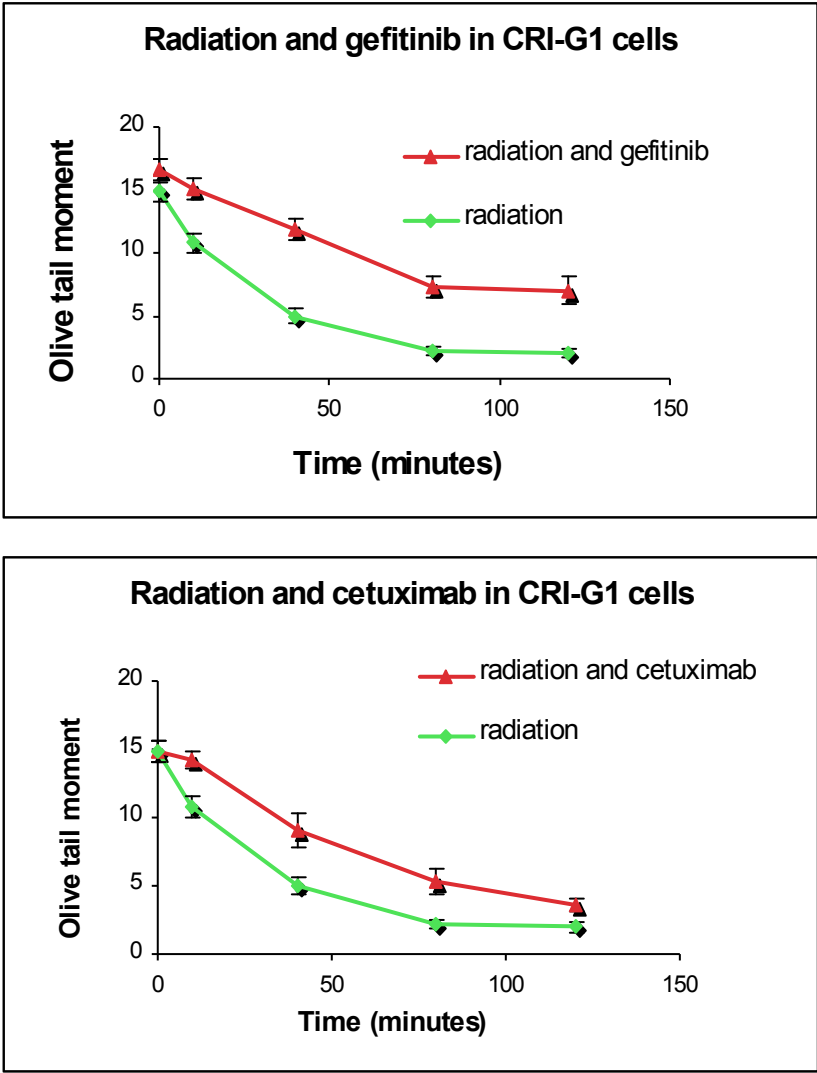


Figure 51: Measurement of irradiation-induced DNA strand breaks and their repair in CRI-G1 cells. Strand break formation quantitated as tail moment, plotted against time after irradiation. Cells were treated with gefitinib at 10 μ M or cetuximab at 30nM for 3 hours, drug was removed, and then cells were irradiated at 15 Gy and incubated for up to 120 minutes at 37°C. Data represents the averages of three different experiments, each performed in triplicate; bars, SD.

As shown in figures 51 and 52, following treatment with radiation alone the repair of strand breaks is complete at 120 minutes in both cell lines. The repair of strand breaks starts almost immediately with a 28% decrease in tail moment at 10 minutes post-treatment and 67% repair at 40 minutes post radiation in CRI-G1 cells. A similar result is seen in RIN-5F cells which exhibit a 27% and a 62% decrease in tail moment at 10 and 40 minutes after radiation treatment respectively. Incubation of cells with 10 μ M gefitinib for 3 hours before radiation resulted in delayed repair of strand breaks in the CRI-G1 cell line (figure 51) by 42% at 40 minutes post radiation and 31% at 120 minutes post radiation.

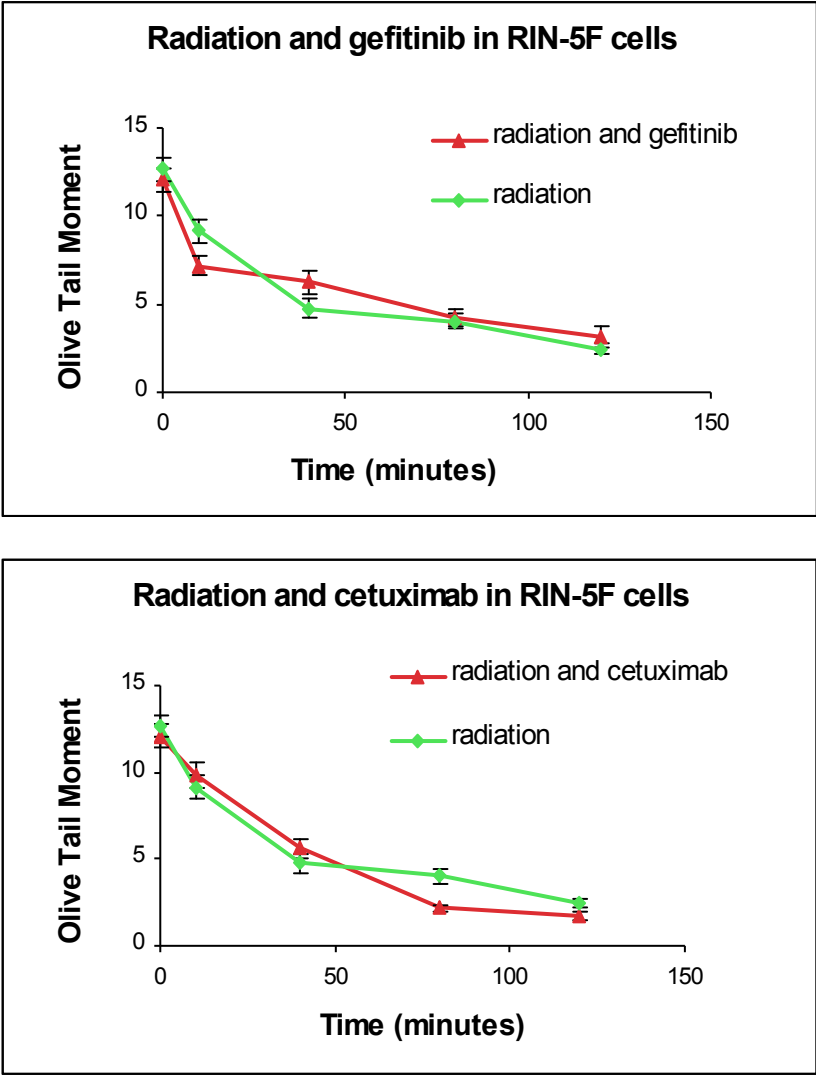


Figure 52: Measurement of irradiation-induced DNA strand breaks and their repair in RIN-5F cells. Strand break formation quantitated as tail moment, plotted against time after irradiation. Cells were treated with gefitinib at 10 μ M or cetuximab at 30nM for 3 hours, drug was removed, and then cells were irradiated at 15 Gy and incubated for up to 120 minutes at 37°C. Data represents the averages of three different experiments, each performed in triplicate; *bars*, SD.

Inhibition of DNA repair was also found in SHP-77 and NCI-H727 cells (appendix 2C-2D). In contrast, gefitinib treatment in the RIN-5F cell line had no effect on the kinetics of DNA repair. In the CRI-G1 cell line inhibition of DNA repair was found following treatment with cetuximab with a 27% difference in tail moment at 40 minutes after radiation, which falls at 11% at 120 minutes. However in the RIN-5F cell line, as with gefitinib, treatment with cetuximab had no effect on repair of radiation-induced DNA damage.

5.2.3 Radiation induces EGFR phosphorylation and translocation to the nucleus

Recent reports have associated gefitinib or cetuximab with DNA repair enzyme DNA-PK_{CS} (Benhar *et al.*, 2002; Dittmann *et al.*, 2005; Friedmann *et al.*, 2006), via inhibition of radiation-induced activation and translocation of EGFR to the nucleus. Based on these reports and our results on DNA repair inhibition by gefitinib and cetuximab, we decided to investigate whether ionising radiation has such an effect on EGFR activity and localization in neuroendocrine tumour cells.

For this, cells were irradiated at 4Gy apart from NCI-H727 cells, for which the dose of 30Gy was applied as in the proliferation studies. Expression of EGFR was analysed by immunoblotting at 5 and 20 minutes after treatment. After irradiation treatment and incubation at 37°C for 5 or 20 minutes, nuclear and cytosolic fractions were isolated and immunoblotted for P-EGFR. In addition to the use of α -tubulin as a loading control, blots were stripped and re-probed for lamin β 1. Lamin β 1 interacts with nuclear membrane components and nuclear chromatin and is a commonly used as a loading control for nuclear proteins (Dittmann *et al.*, 2005). The amounts of phosphorylated EGFR were calculated by densitometry analysis of the bands.

As shown in figures 53-54, basal expression of EGFR was detectable in the nucleus of all cells although expression was predominantly cytoplasmic. Within 5 minutes after irradiation treatment, increased EGFR was detectable in the nucleus, and this persists at 20 minutes post-irradiation. This occurs in all cell lines except the RIN-5F cells, where, nuclear EGFR levels show no significant change. In the cytosolic fractions, EGFR is decreased in the 3 cell lines showing increase in nuclear EGFR, while RIN-5F cells show a slight increase in cytosolic EGFR.

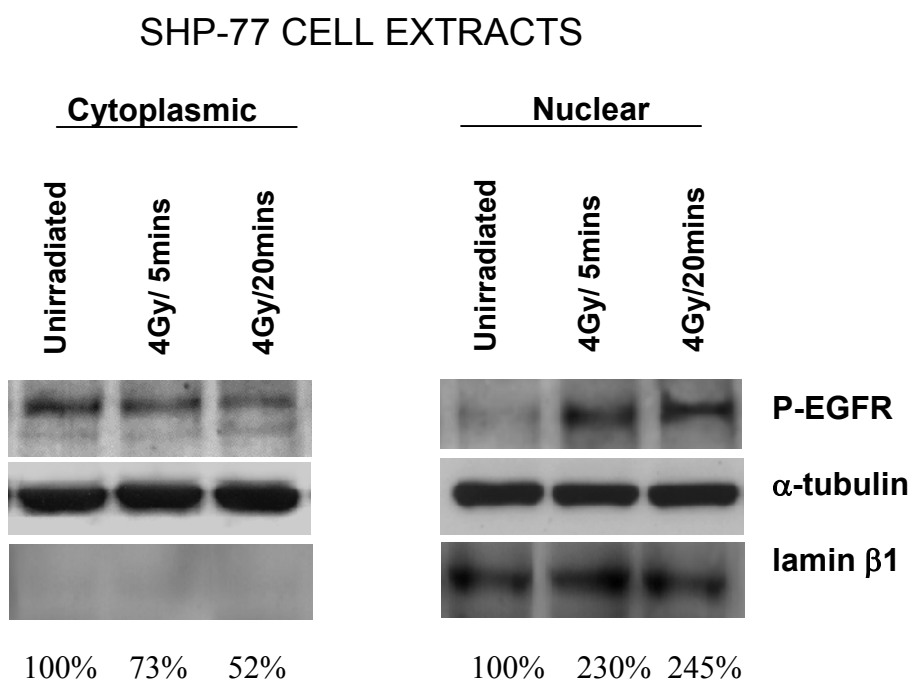
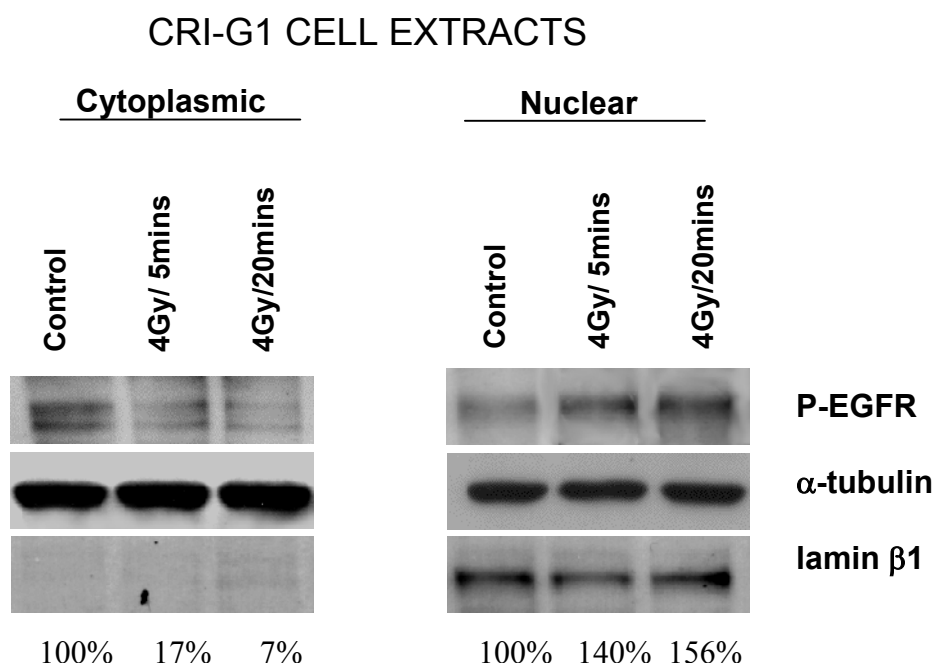
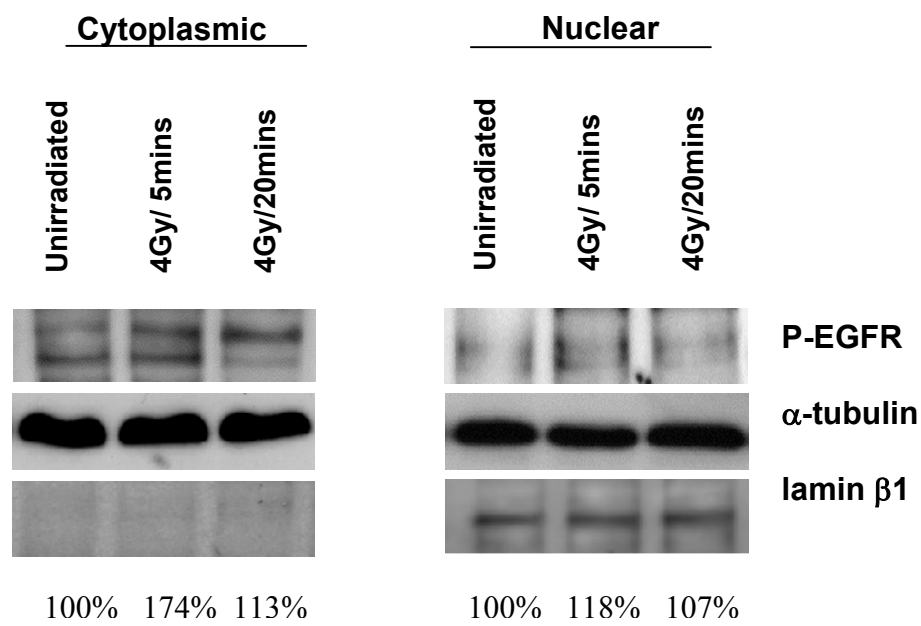


Figure 53: CRI-G1 and SHP-77 cells were irradiated (4Gy) and incubated for up to 20 minutes at 37°C. Cytosolic and nuclear extracts were immunoblotted for P-EGFR. Alpha-tubulin was used as a loading control. Lamin β1 was used as a nuclear marker. Amounts of P-EGFR in percentages were determined by densitometry analysis.

RIN-5F CELL EXTRACTS



NCI-H727 CELL EXTRACTS

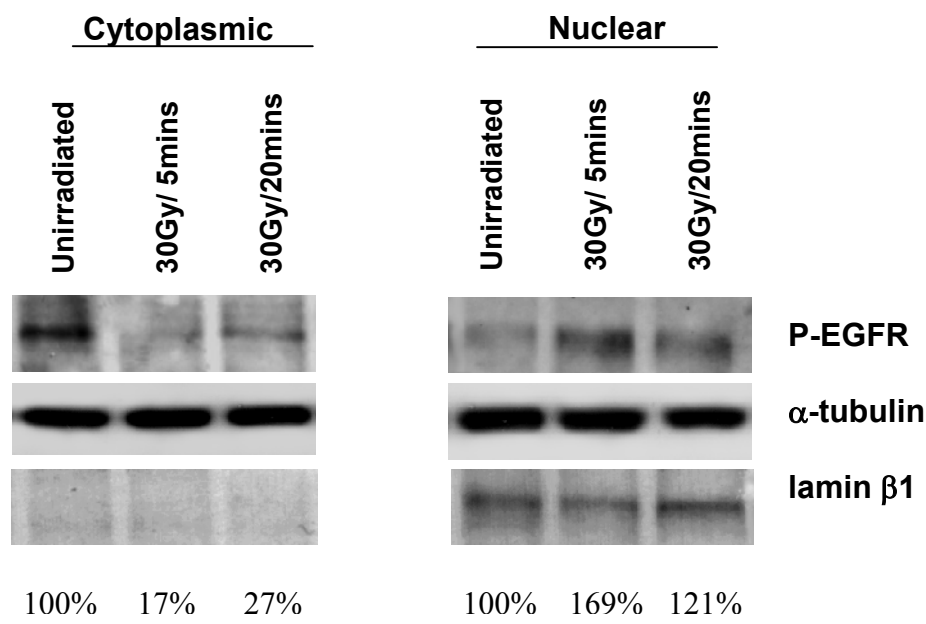


Figure 54: RIN-5F and NCI-H727 cells were irradiated at 4Gy and 30Gy respectively and incubated for up to 20 minutes at 37°C. Cytosolic and nuclear extracts were immunoblotted for P-EGFR and EGFR. Alpha-tubulin was used as a loading control. Lamin β 1 was used as a nuclear marker.

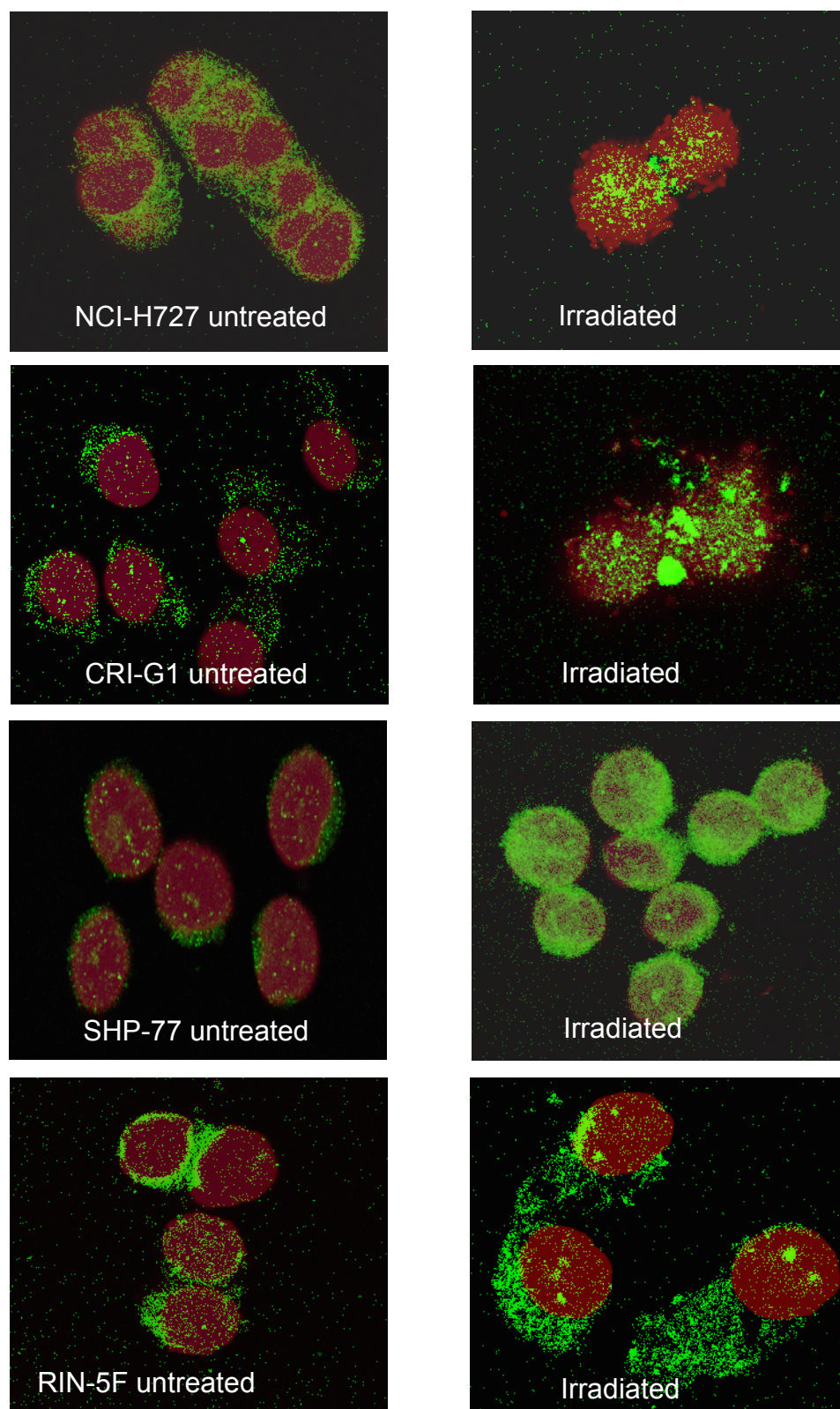


Figure 55: CRI-G1, SHP-77, and RIN-5F cells were irradiated at 4 Gy, and NCI-H727 cells were irradiated at 30 Gy, followed by incubation at 37°C for 5 minutes. Cells were then fixed and stained for EGFR (green) using a fluorescein isothiocyanate (FITC) conjugated antibody and nucleus was stained with propidium iodide (red).

The observed translocation of EGFR by irradiation was further validated by immunofluorescent staining using a confocal microscope (figure 55). Cells were irradiated as before and the presence of EGFR was identified using a FITC-labelled antibody. Propidium iodide was used for nuclear counter staining and is shown in red. EGFR in untreated cells is present in the cytoplasm (shown in green). However, within 5 minutes after irradiation treatment EGFR is redistributed to the nucleus in NCI-H727, CRI-G1 and SHP-77 cells but not in RIN-5F cells.

5.2.4 Gefitinib or Cetuximab inhibits radiation-induced EGFR nuclear translocation

To examine whether EGFR inhibitors could prevent radiation-induced EGFR activation and shift to the nucleus, we treated cells with gefitinib at 10 μ M and cetuximab at 30nM for 3 hours before irradiation, and detected EGFR by immunofluorescent staining. As shown in figures 56-59, gefitinib and cetuximab abrogated radiation-induced EGFR import to the nucleus in cells pre-treated with the above agents prior to irradiation. Since In RIN-5F cells with no EGFR nuclear translocation, treatment with EGFR inhibitors had no effect on EGFR locality within the cells, but nevertheless inhibited activation of the receptor.

Furthermore, gefitinib in unirradiated cells (bottom left pictures) caused a decrease in EGFR activation in all cell lines. Cetuximab alone (middle left pictures) caused downregulation of the receptor in all cells except NCI-H727 cells, which might be more resistant to cetuximab compared to the other cell lines. Interestingly, in RIN-5F cells incubation with gefitinib or cetuximab alone, not only inhibited EGFR phosphorylation, but also caused an assembly of EGFR molecules in the perinuclear region (figure 59).

5.2.4.1 Electron microscopy analysis

It has been suggested that nuclear EGFR identified by confocal microscopy may be contaminated by EGFR present in the endoplasmatic reticulum, which is closely attached to the nuclear membrane. To investigate this hypothesis, radiation-induced EGFR import to the nucleus was also analysed by electron microscopy using ultrathin sections of CRI-G1 and RIN-5F cells and labelling EGFR with 15nm gold particles (figures 60-61).

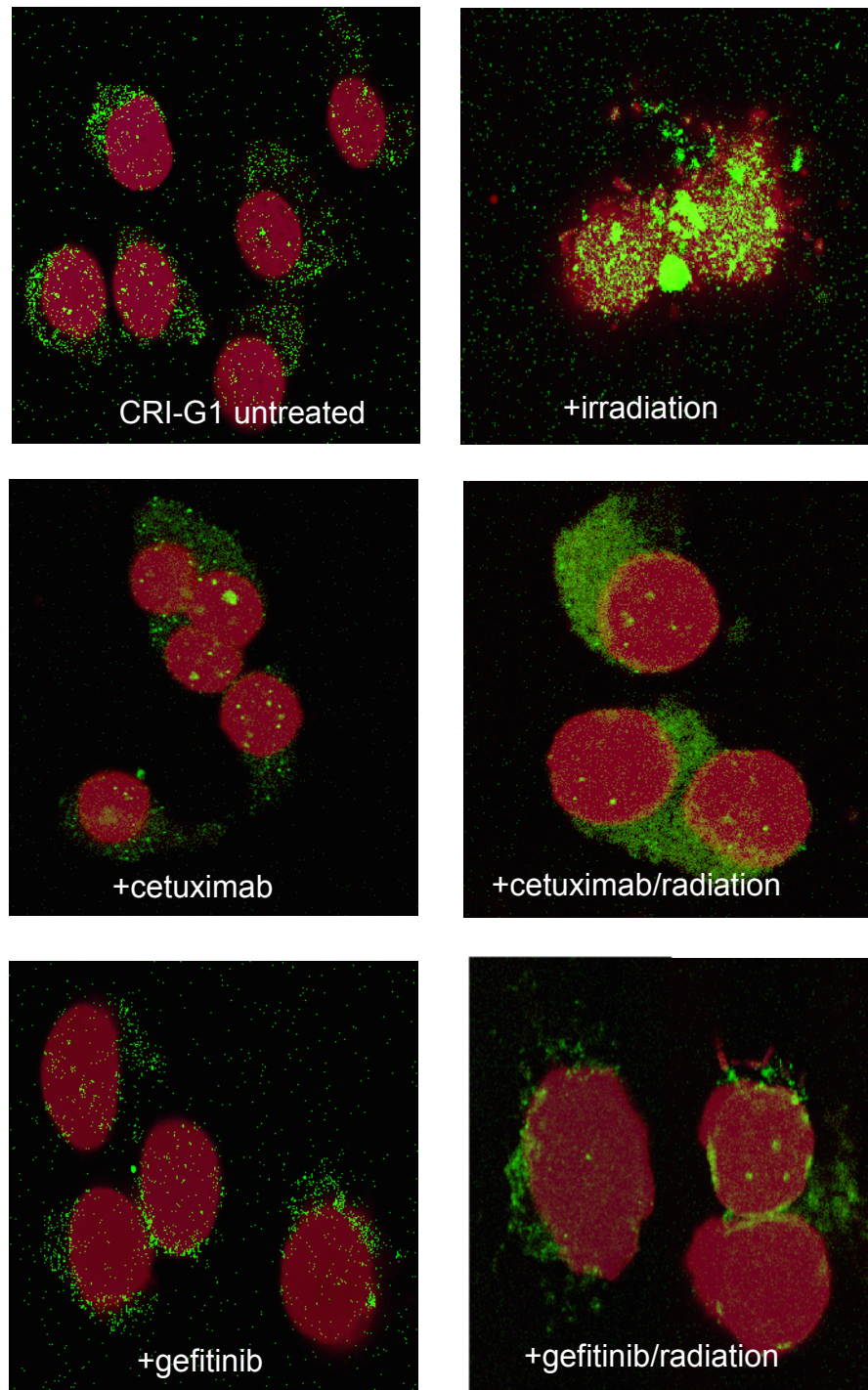


Figure 56: CRI-G1 cells were treated with gefitinib at 10 μ M or cetuximab at 30nM for 3 hours followed by irradiation at 4Gy and incubation at 37°C for 5 minutes. Cells were then fixed and stained for EGFR (green) and nucleus was stained with propidium iodide (red).

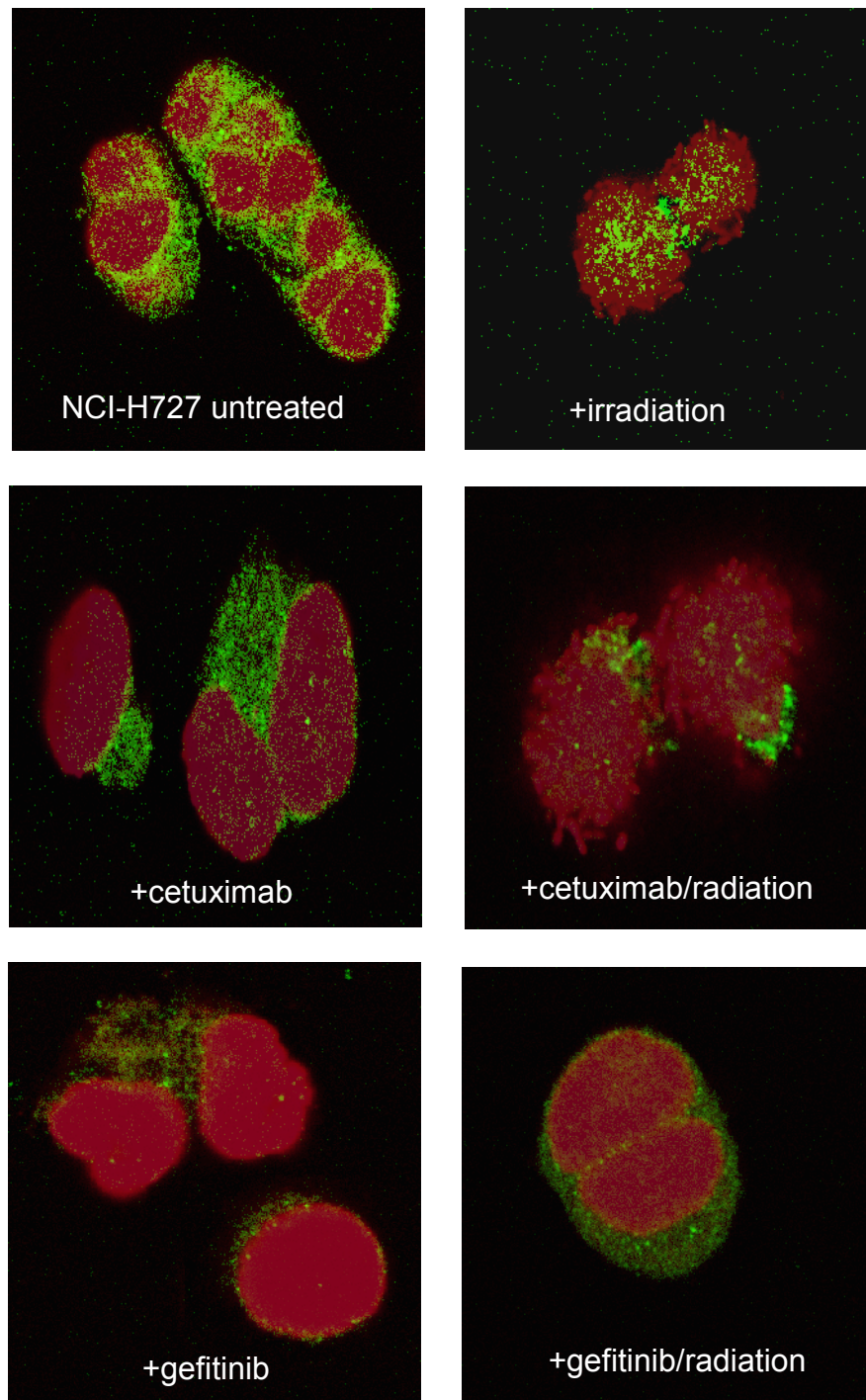


Figure 57: NCI-H727 cells were treated with gefitinib at 10 μ M or cetuximab at 30nM for 3 hours followed by irradiation at 4 Gy and incubation at 37°C for 5 minutes. Cells were then fixed and stained for EGFR (green) and nucleus was stained with propidium iodide (red).

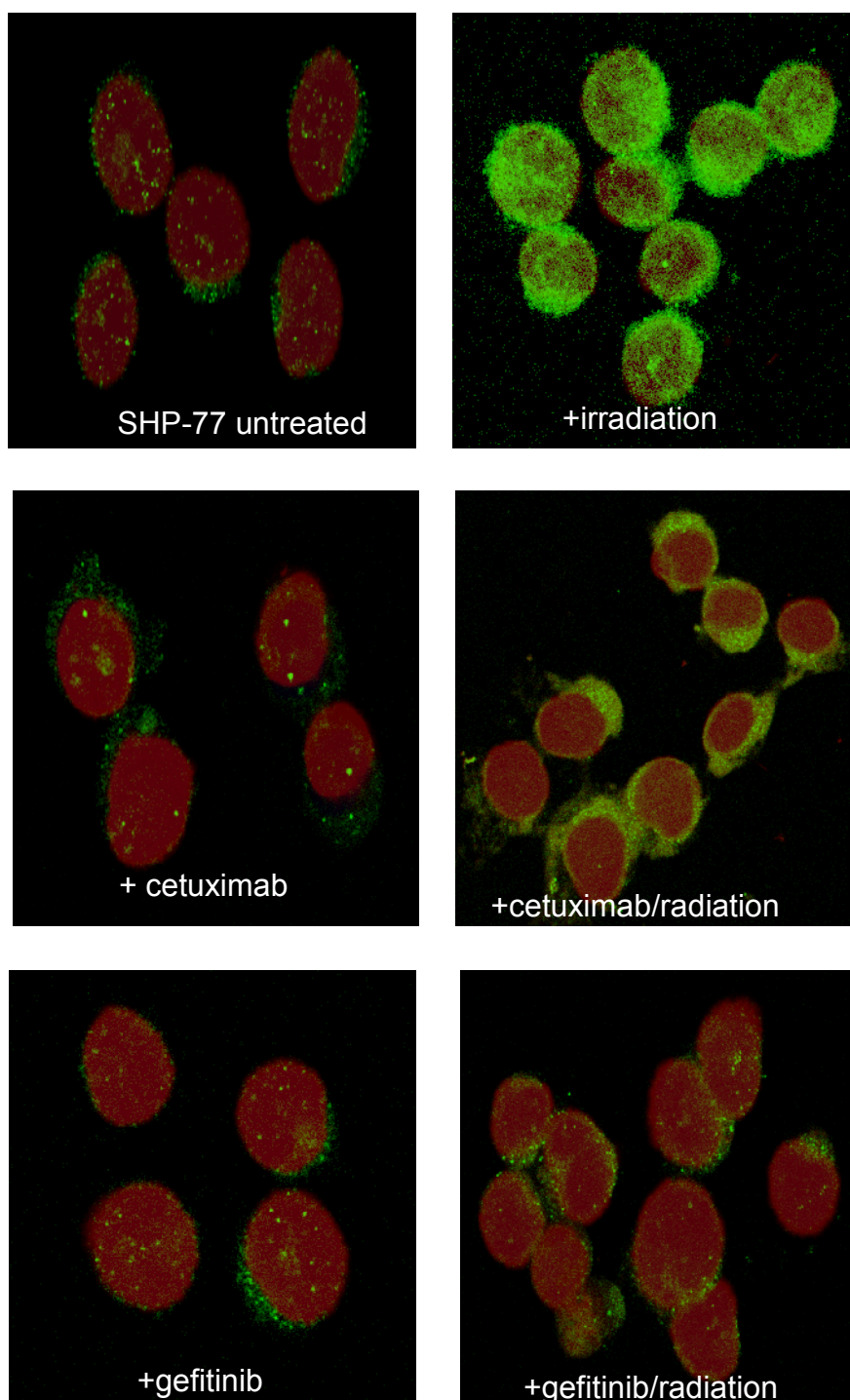


Figure 58: SHP-77 cells were treated with gefitinib at 10 μ M or cetuximab at 30nM for 3 hours followed by irradiation at 4 Gy and incubation at 37°C for 5 minutes. Cells were then fixed and stained for EGFR (green) and nucleus was stained with propidium iodide (red).

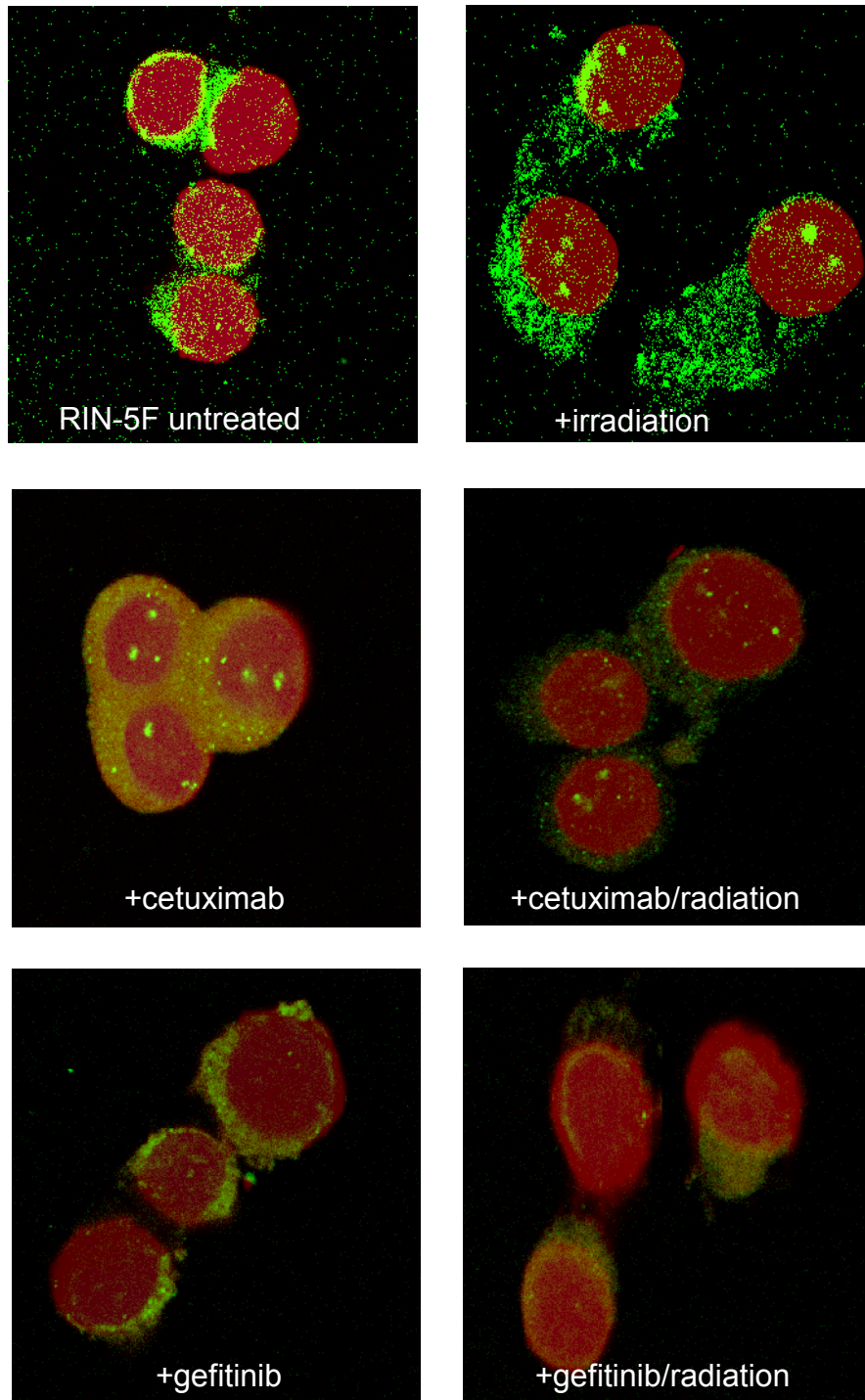


Figure 59: RIN-5F cells were treated with gefitinib at 10 μ M or cetuximab at 30nM for 3 hours followed by irradiation at 4Gy and incubation at 37°C for 5 minutes. Cells were then fixed and stained for EGFR (green) and nucleus was stained with propidium iodide (red).

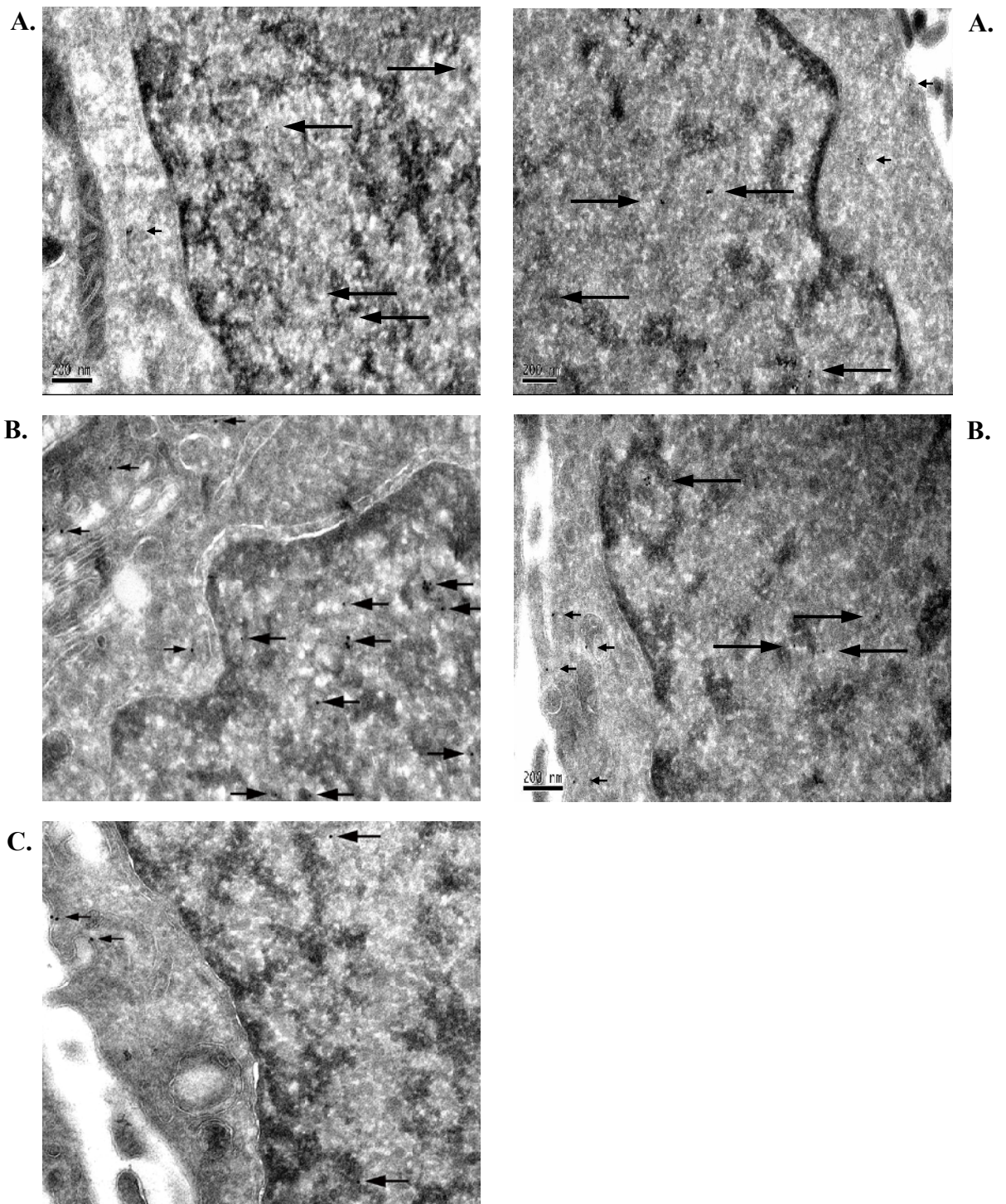


Figure 60: EGFR nuclear import in CRI-G1 cells (left panels) and RIN-5F cells (right panels). Cells were prepared for cryo-immuno-EM 5 min after exposure to 10 μ M gefitinib for 3 hours and irradiation at 4Gy. Ultrathin sections were labelled for EGFR with 15nm gold (arrows). Panel A: control unirradiated cells. Panel B: irradiated cells and Panel C: gefitinib + irradiation. EGFR nuclear labelling (large arrows) and non-nuclear staining (small arrows). Data provided by Emily Eden, UCL Institute of Ophthalmology, London, UK.

Staining of samples and viewing of images was performed by Emily Eden, UCL Institute of Ophthalmology, London, UK. The graph in figure 61 shows that while treatment with x-ray radiation had no effect on the ratio of nuclear to non-nuclear EGFR labelling in RIN-5F cells, irradiation in CRI-G1 cells increased the amounts of nuclear EGFR, making the ratio of nuclear/non-nuclear EGFR increase by a factor of 5 (control cell ratio=0.46 to irradiated cell ratio=2.28). This effect was blocked by treatment with gefitinib, which returned the ratio to control levels (gefitinib-treated and irradiated cell ratio=0.48).

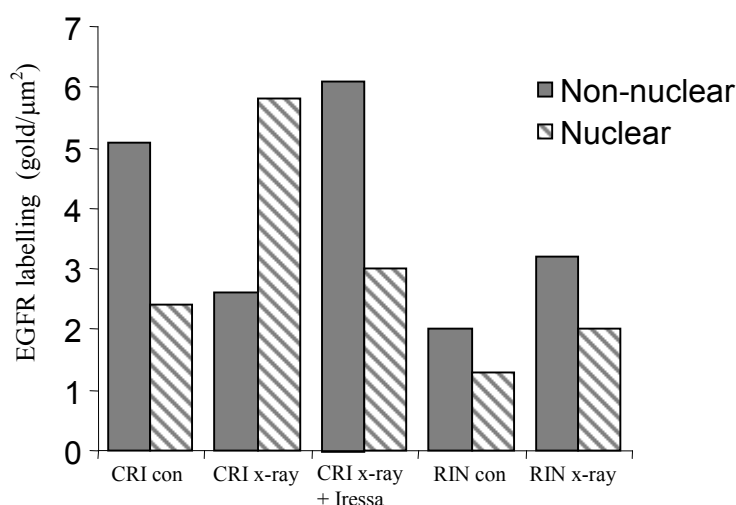


Figure 61: Effect of x-ray radiation on EGFR distribution. EGFR distribution was quantified by cryo-immuno-EM. Non-nuclear (solid bars) and nuclear (striped bars) EGFR staining is expressed as mean (n=10 cells) numbers of gold particles per μm^2 . Con, control cells; x-ray, cells exposed to 4Gy radiation; x-ray + gefitinib, gefitinib-treated and irradiated cells. Data provided by Emily Eden, UCL Institute of Ophthalmology, London, UK.

5.2.5 Cisplatin induces EGFR nuclear translocation

In chapter 4, treatment with cisplatin in neuroendocrine tumour cells induced activation of EGFR, which was associated with activation of growth promoting signalling pathways. To see whether cisplatin (CDDP) had the same effect on EGFR as radiation, we treated cells with cisplatin at $5\mu\text{M}$ for 5 or 20 minutes (figures 62-63). The experiment was initially performed using $50\mu\text{M}$ cisplatin, which showed similar results (data not shown).

EGFR in untreated control cells is mainly detected in the cytoplasm, with small amounts also present in the nucleus. Cisplatin treatment even at 5 μ M induces activation and redistribution of EGFR from the cytoplasm to the nucleus within 5 minutes after treatment in all cells except RIN-5F cells, as with irradiation experiments.

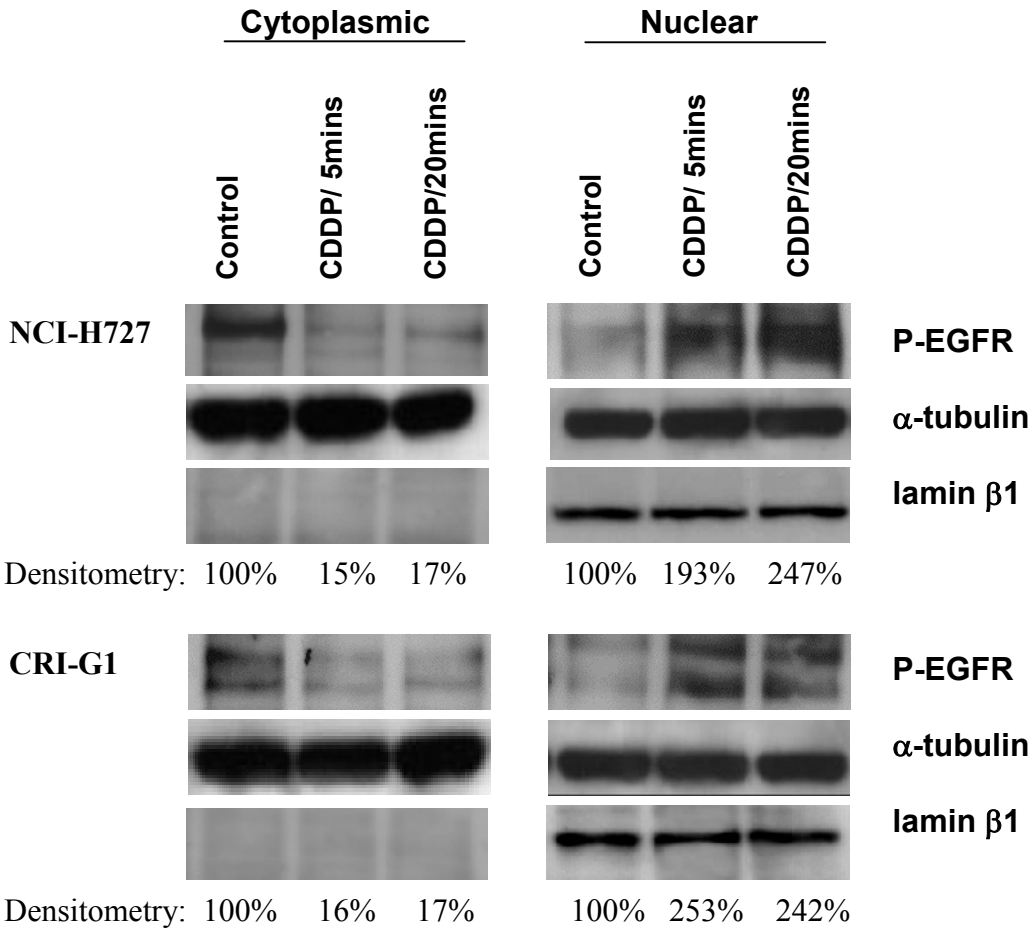


Figure 62: NCI-H727 cells (top panel) and CRI-G1 cells (bottom) were treated with 5 μ M cisplatin for 5 or 20 minutes. Cytosolic and nuclear extracts were isolated and immunoblotted for P-EGFR. Alpha-tubulin was used as a loading control. Lamin β 1 was used as a nuclear marker. Levels of P-EGFR were measured by densitometry.

At 20 minutes post-treatment cisplatin-induced activation persists in NCI-H727 and CRI-G1, but in SHP-77 the levels of nuclear EGFR fall back to control levels. Cytosolic EGFR expression is decreased in CRI-G1, NCI-H727, and SHP-77 cells, while RIN-5F cells show activated EGFR, which remains in the cytoplasm.

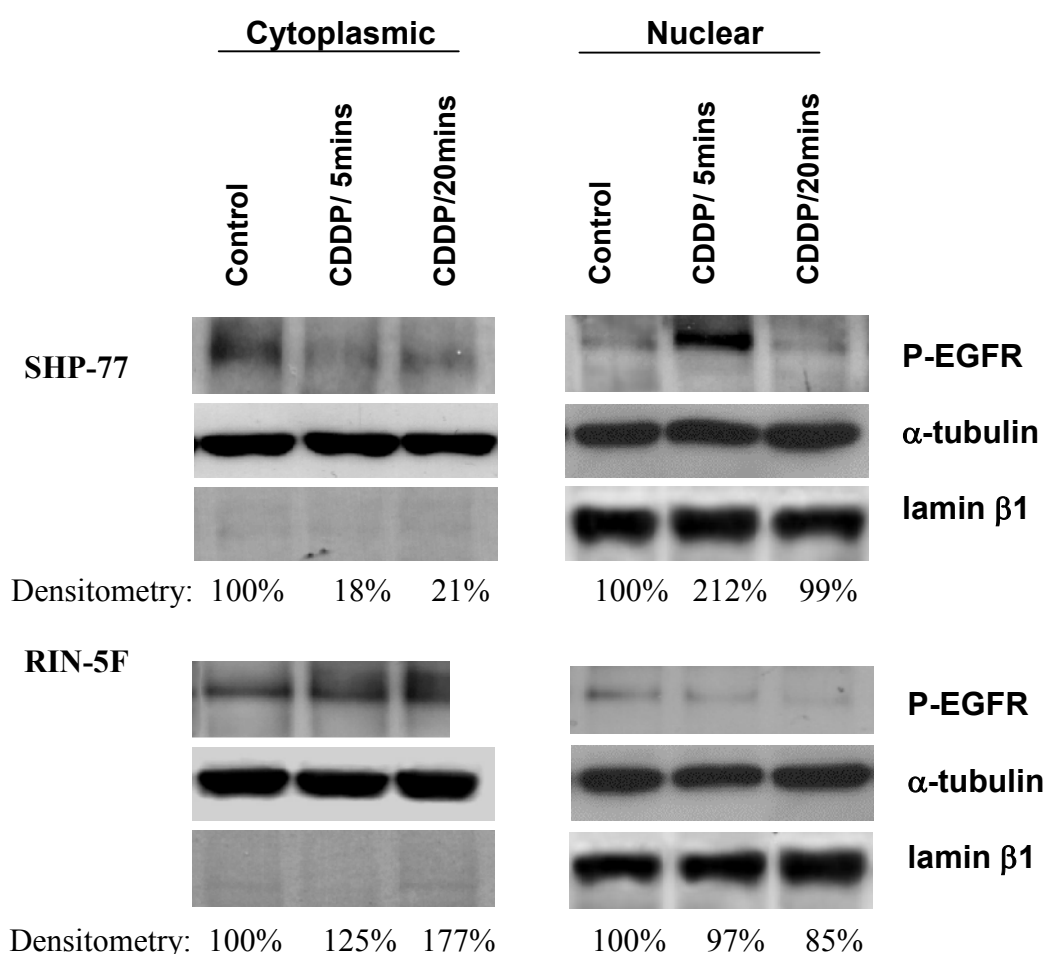


Figure 63: SHP-77 cells (top panel) and RIN-5F cells (bottom) were treated with 5 μ M cisplatin for 5 or 20 minutes. Cytosolic and nuclear extracts were isolated and immunoblotted for P-EGFR. Alpha-tubulin was used as a loading control. Lamin β 1 was used as a nuclear marker. Levels of P-EGFR were measured by densitometry.

5.2.6 EGFR inhibition and DNA-PK_{CS} expression

Cytosolic translocation of DNA-PK_{CS} following inhibition of EGFR by gefitinib or cetuximab has been reported by many groups (Bandyopadhyay *et al.*, 1998; Huang & Harari, 2000; Friedmann *et al.*, 2006). To see if translocation of EGFR is associated with DNA-PK_{CS} redistribution to the cytosol, we treated cells with gefitinib at 10 μ M for 3 hours alone or followed by irradiation and analysed DNA-PK_{CS} expression by immunofluorescent staining (figure 64).

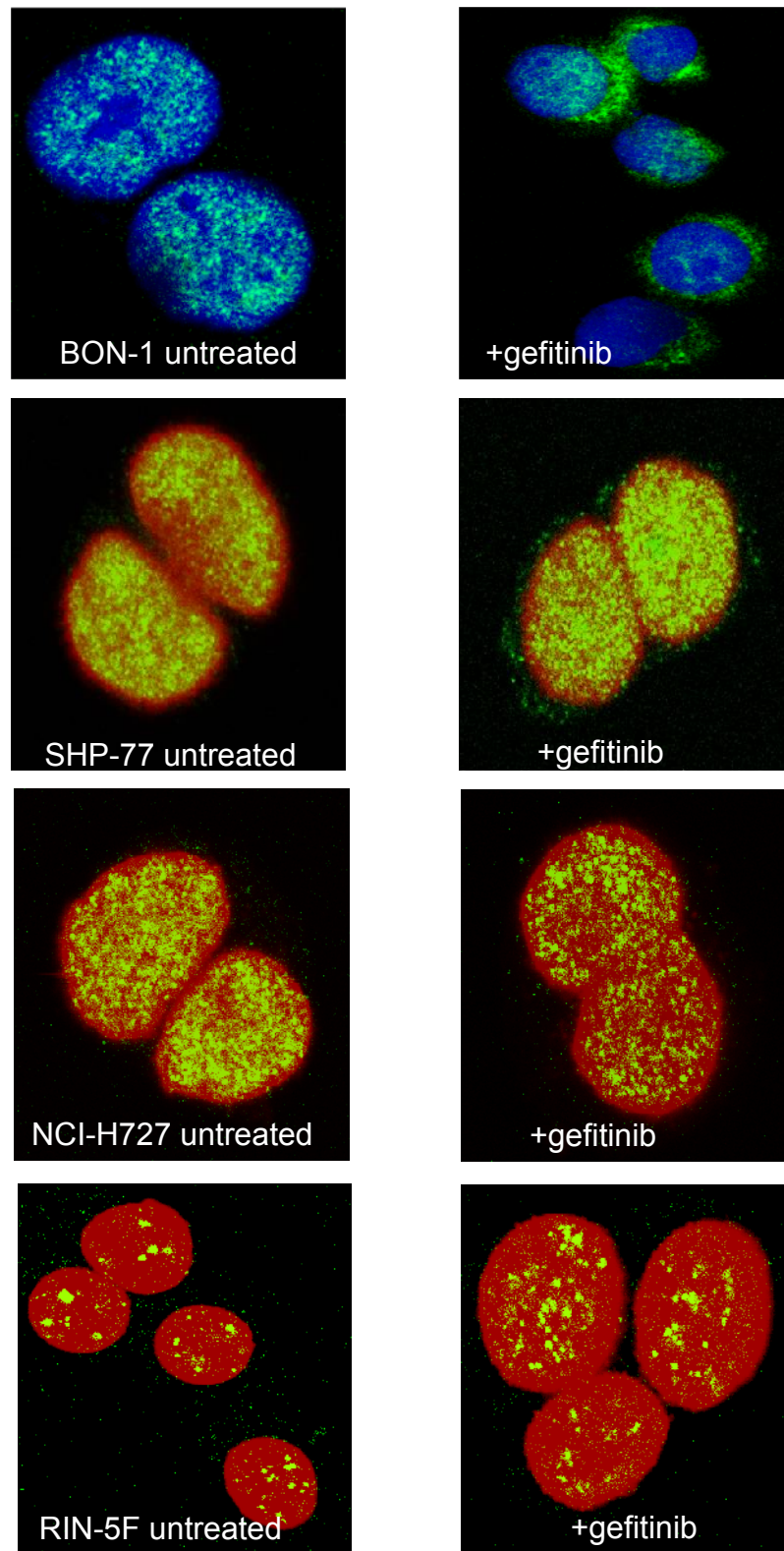


Figure 64: Cells were left untreated or incubated with 10 μ M gefitinib for 3 hours. Cells were then fixed and stained for EGFR (green) and nucleus was stained with propidium iodide (red or blue).

DNA-PK_{CS} in untreated cells is detected in the nucleus. Treatment with gefitinib caused a redistribution of DNA-PK_{CS} from the nucleus to the cytosol in BON-1 cells and to less extent in SHP-77 cells. Gefitinib did not modify DNA-PK_{CS} expression in RIN-5F cells. In NCI-H727 there was no sub-cellular redistribution of DNA-PK_{CS} but a decrease in expression levels was identified.

5.3 Discussion

In the previous chapter, synergy between gefitinib and cisplatin was demonstrated in neuroendocrine cell lines. In addition, cisplatin induced activation of EGFR which lead to activation of cell survival pathways, and this could explain the lack of synergy between gefitinib and chemotherapeutic agents in improving survival of patients in clinical trials. This chapter examines the use of radiation combined with EGFR inhibitors as a novel therapeutic strategy for neuroendocrine tumour patients, based on previous reports of cetuximab and radiotherapy combined effect in prolonging survival and enhancing local control in patients with head and neck squamous cell carcinoma.

5.3.1 Anti-proliferative effect of EGFR inhibitors and radiation

Combined treatments with radiation and EGFR inhibitors demonstrated synergy in inhibition of proliferation in CRI-G1, NCI-H727 and SHP-77 cells (NCI-H727 and SHP-77 cells shown in the appendix 2A-2B). Inhibition of proliferation was increased by 40-50%, showing that EGFR inhibitors sensitise cells to radiotherapy as shown by other groups (Huang *et al.*, 1999; Eller *et al.*, 2005). RIN-5F cells showed an additive effect with a moderate 20% increase of the anti-tumour activity of EGFR inhibitors by radiotherapy. The dose of irradiation used (4Gy) causes approximately 20% inhibition of proliferation in both CRI-G1 and RIN-5F cell lines, therefore the differences observed are probably due to gefitinib or cetuximab, and consequently due to EGFR and its signalling in RIN-5F cells.

5.3.2 Synergy between EGFR inhibitors and radiation in DNA repair

Synergy between EGFR inhibition and ionising radiation has been correlated to impediment of DNA repair (Huang & Harari, 2000; Dittmann *et al.*, 2005b). To understand the mechanism underlying synergism, we investigated radiation and EGFR inhibition dual treatment for any effect in DNA repair. As in proliferation studies,

synergy in DNA repair kinetics was shown in CRI-G1, NCI-H727, and SHP-77 cells. Gefitinib and cetuximab both caused a delay in repair of radiation-induced DNA strand breaks indicating interference of EGFR in DNA repair mechanisms. Radiation-induced strand breaks are repaired by the NHEJ pathway, therefore the results indicate that synergism between gefitinib or cetuximab and radiotherapy is due to modulation of NHEJ, and this is a novel role of EGFR in response to stress stimuli.

No delay in DNA repair was observed in RIN-5F cells treated with EGFR inhibitors, which agrees with the lack of synergy found between radiation and EGFR inhibition in the proliferation assay. This is not the first time a lack of synergy is displayed in RIN-5F cells as this was the only cell line where EGFR inhibitors did not increase the cytotoxicity of four different chemotherapeutic agents tested, which was shown in chapter 4. It seems that the EGFR pathway in RIN-5F cells, which were also the most resistant to gefitinib (with an IC_{50} of $32\mu M$) as seen in chapter 4, is probably of minor consequence to the growth of these cells but also the EGFR pathway is likely independent to the pathways utilized by stress stimuli such as radiation or the chemotherapeutic agents analysed in our study. To understand why EGFR inhibition may affect the radiosensitivity of one cell line but not another, we analysed the effect of radiation on EGFR activity, based on results published by other groups discussed in the next section.

5.3.3 Radiation-induced nuclear EGFR translocation

EGFR is responsive to irradiation and this has been shown to result in translocation of the molecule into the nucleus (Dittmann *et al.*, 2005b). Entry of EGFR into the nucleus in cells exposed to genotoxic stress such as irradiation or cisplatin is done in a ligand-independent manner. On the other hand activation of EGFR by its ligand EGF, results in phosphorylation of the receptor but without entry into the nucleus (Dittmann *et al.*, 2005a). Nuclear EGFR has also been detected in various tissues and cell lines with a different role, that of a transcription factor, which will be discussed in detail in the next chapter (Lin *et al.*, 2001). We have clearly shown that after 5 minutes of irradiation treatment at 4 Gy (or 30Gy in NCI-H727 cells) EGFR enters the nucleus of $\frac{3}{4}$ NET cells except in RIN-5F cells. This was shown by three methods: immunoblotting, immunofluorescent staining, and visualization of cells with the help of electron

microscopy. The EGFR entering the nucleus is phosphorylated as shown by immunoblotting, and the increase in total EGFR demonstrated by immunofluorescent staining is accompanied by activation of the receptor. These results may explain the association of EGFR with DNA repair reported previously. Furthermore, it accounts for the absence of delay in repair of radiation-induced strand breaks by gefitinib and cetuximab in RIN-5F cells. Therefore, in RIN-5F cells EGFR does not enter the nucleus in response to radiation and there are probably other mechanisms activated. Different mechanisms can therefore be evoked by stress stimuli, which reflect cell type specific differences that could form a future step in our study.

5.3.4 Nuclear EGFR translocation is blocked by EGFR inhibitors

EGFR nuclear entry was completely abrogated by gefitinib and cetuximab in CRI-G1, NCI-H727 and SHP-77 cells, whereas in RIN-5F cells, in which EGFR does not enter the nucleus, gefitinib as a single agent stimulated gathering of EGFR in the area around the nucleus. This is a phenomenon not demonstrated before and it is unclear why it happens. Inhibition of EGFR nuclear import by cetuximab indicates that EGFR transferred to the nucleus comes from the plasma membrane of cells where the antibody binds to the extracellular portion of EGFR, and not from cytoplasmic sites of EGFR synthesis such as ribosomes of the endoplasmic reticulum. One of the events following irradiation is activation of the intracellular Ras/MAPK signalling pathway which is traditionally initiated by ligand binding to EGFR (Dent *et al.*, 2003). To examine the relation between signalling initiated by EGFR and double strand break (DSB) repair after exposure to ionising radiation Grądzka *et al.* examined the effect of PD98059, a specific inhibitor of MEK1/2 kinases, on two glioma cell lines: M059K and M059J. M059J cells are deficient in DNA-PKcs and are more sensitive to radiation than the M059K cells. PD98059 did not significantly affect the rate of DSB repair in both cell lines, indicating that DNA repair targeted signals initiated by EGFR activation after irradiation are not transduced to the nucleus by means of the EGFR kinase cascade but by internalisation and nuclear translocation of EGFR (Szumiel, 2006, reference therein). Examination of this hypothesis could form the next step in our research.

5.3.5 Effect of EGFR inhibitors on DNA-PK

Blockade of EGFR has been shown to cause redistribution of DNA-PK_{CS} from the nucleus to the cytosol (Huang & Harari, 2000; Dittmann *et al.*, 2005b; Friedmann *et al.*,

2006). This phenomenon was not proven in NET cells. Radiation did not increase DNA-PK expression, and co-treatment with gefitinib did not stimulate exit of DNA-PK amounts from the nucleus. Gefitinib alone caused a redistribution of DNA-PK in BON-1 cells, a human pancreatic endocrine tumour. These cells were then analysed for radiation-induced EGFR import and synergy with radiotherapy and EGFR inhibitors showing results similar to CRI-G1 cells (data not shown). Gefitinib also caused downregulation of DNA-PK in NCI-H727 cells, but this was not associated with DNA-PK subcellular redistribution. Therefore association of EGFR with gefitinib might actually exist in our cells but could not be proven under the conditions used. Our results though, provoked the hypothesis that nuclear EGFR in NET cells might also have a different role such as that of a transcription factor, which has been reported previously (Lin *et al.*, 2001). These experiments will be discussed in the next chapter.

5.3.6 Cisplatin-induced EGFR nuclear translocation

Cisplatin was also tested for its effect on translocation of EGFR based on results from chapter 4 showing phosphorylation of EGFR by cisplatin. In our study cisplatin, like radiation, induced activation and translocation of EGFR to the nucleus in $\frac{3}{4}$ NET cell lines, as shown previously by others (Dittmann *et al.*, 2005; Friedmann *et al.*, 2006). Since both cisplatin and radiation stimulate entry of EGFR into the nucleus, it is not double strand breaks that generate this response, but DNA damage in general. In fact, production of radicals such as reactive oxygen species may have a role since addition of the radical scavenger acetylcysteine was able to abrogate the radiation-induced EGFR translocation (Dittmann *et al.*, 2005a; Dittmann *et al.*, 2005b).

The role of DNA-PK_{CS} in repair of DNA crosslinks produced by cisplatin is unclear, but cellular sensitisation to cisplatin has been related to DNA-PK inhibition by vanillin. Vanillin, a natural plant-derived compound, inhibited DNA-PK activity via interaction with specific lysine residues in the active site of the enzyme and was shown to be specific to NHEJ and selective for DNA-PK_{CS} over other members of the family of phosphatidylinositol-3 kinase-related kinases (PIKK) such as ATM and ATR (Durant & Karran, 2003). In RIN-5F cells cisplatin stimulated EGFR phosphorylation, but this did not result in EGFR transport to the nucleus. A possible explanation could be that EGFR upregulation by cisplatin in these cells leads to transient activation of EGFR-dependent cell survival pathways, but this does not include activation of DNA repair

mechanisms or any other nuclear function by the receptor due to impaired mechanisms for nuclear transport or mutations in the receptor hindering its nuclear transport, which could be a future step in our study.

5.3.7 Conclusions

Nuclear EGFR, a phenomenon provoked by cytotoxic drugs or ionising radiation is a protection mechanism that enhances DNA repair. The discovery of the described mechanism opens a renewed perspective on factors affecting the intrinsic radiation sensitivity of mammalian cells. In concert with the initiation of signalling pathways and EGFR internalisation, nuclear translocation of DSB repair proteins (Ku 70/80 subunits) from the cytoplasmic stores takes place; therefore agents that disturb trafficking of EGFR can be expected to act as radiosensitisers. Efficiency of such defence may vary between cell types, depending on the status of EGFR, on how many supplementary DNA-PK subunits are stored for use under stress conditions, to what extent does the cell rely on NHEJ for DSB repair (this also depends on position in the cell cycle) and how effective is the translocation machinery. Our study proved that anti-EGFR therapy can block translocation of EGFR to the nucleus and sensitise neuroendocrine tumour cells to radiotherapy. These results provide a rationale for EGFR inhibition in combination with radiotherapy for the treatment of neuroendocrine tumours.

CHAPTER 6

CHARACTERISATION OF NUCLEAR EGFR IMPORT MECHANISM AND NUCLEAR TARGETS IN NET CELLS

6.1 Introduction

6.1.1 Nuclear EGFR function

In the previous chapter results provided evidence for a new mode of action of EGFR in response to radiation and cisplatin that involves nuclear translocation and modulation of DNA repair, via interaction with DNA repair genes which could include DNA-PK_{CS}. Gefitinib and cetuximab both blocked this nuclear translocation, causing a delay in the repair of radiation-induced DNA damage. This mechanism is different from EGFR's well characterised signalling pathway that mediates mitogenic signals through multiple signalling pathways. However, nuclear EGFR and its ligands have long before been identified in cancer cell lines, the human placenta and in regenerating liver, but its function was unknown (Lin *et al.*, 2001). Additionally, EGFR is not the only receptor tyrosine kinase with nuclear activity. Other kinases including HER-2, HER-3, truncated C-terminal HER-4, fibroblast growth factor receptor and cytokine receptors have also been identified in the nucleus of cells, and their nuclear expression has been linked to enhanced tumour proliferation and progression (Lo & Hung, 2006). Recently, expression of nuclear EGFR in breast cancer was shown to correlate positively with increased levels of Ki-67, showing an inverse correlation between high nuclear EGFR and overall survival. Nuclear EGFR therefore has a prognostic value in breast cancer (Lo *et al.*, 2005a).

Another role of nuclear EGFR, identified recently, involves regulation of gene expression by transcriptional activation. Figure 65 summarises reported cytoplasmic and nuclear EGFR signalling pathways. Nuclear entry of EGFR functioning as a transcription factor involves translocation of the receptor in a ligand-dependent fashion. EGFR was shown to activate gene transcription by binding indirectly through its C-terminal transactivation domain (involving formation of an EGFR complex) to the promoter of cyclin D1 leading to its increased expression (Lin *et al.*, 2001). Furthermore, nuclear EGFR was shown to interact with signal transducers and activators of transcription 3 (STAT3) on the promoter of inducible nitric oxide synthase (iNOS), or with E2F1 transcription factor on the promoter of B-Myb, leading to their transcriptional activation (Lo *et al.*, 2005b; Hanada *et al.*, 2006). All the above genes are frequently overexpressed in human cancers; upregulation of cyclin D1 and B-Myb is involved in increased cell proliferation by accelerating the G1/S phase progression,

while elevated iNOS is associated with tumour proliferation, angiogenesis, and metastasis (Lo & Hung, 2006). Inducible NOS expression has also been found to be a powerful prognostic indicator in breast cancer and this correlates with nuclear expression of EGFR (Lo *et al.*, 2005b).

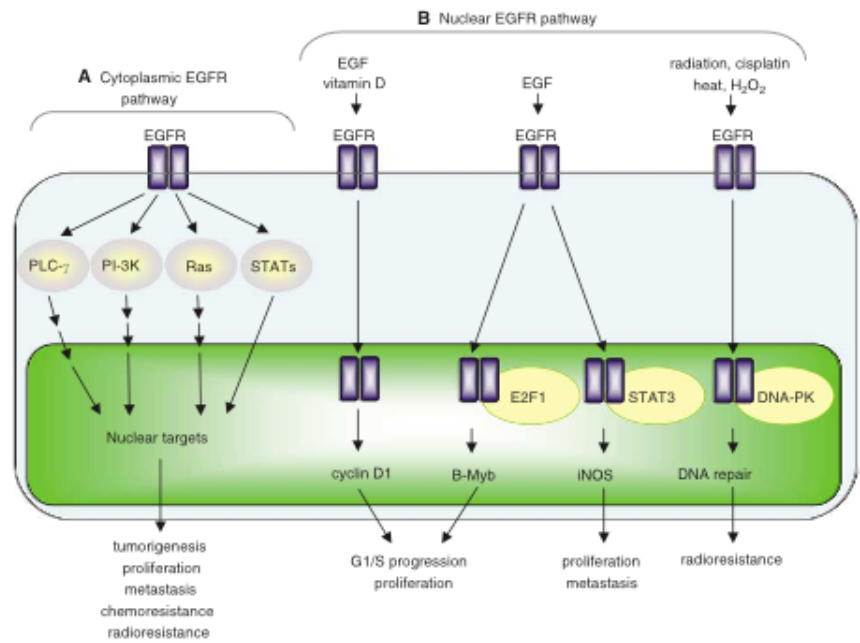


Figure 65: The EGFR cytoplasmic and nuclear signalling pathways.
Source: H-W Lo & MC Hung, British Journal of Cancer, 2006

However, EGFR's transcriptional activity is not independent to DNA repair as shown by us and other groups (Huang & Harari, 2000; Dittmann *et al.*, 2005). Nitric oxide synthase (NOS) activity has been detected in many human tumours and has been shown to significantly increase expression of DNA-PK_{CS} thus protecting cells from the toxic effects of NO and DNA-damaging agents such as cisplatin and radiation (Xu *et al.*, 2000). On the other hand, EGFR interaction with STAT3 in the nucleus was shown to lead to transcriptional activation of iNOS, thus providing another link between EGFR and DNA repair following cisplatin and irradiation treatment (Lo *et al.*, 2005b; Xu *et al.*, 2000). Therefore EGFR inhibition could result in inhibition of the DNA-PK pathway and subsequently of DNA repair both by physical association with DNA-PK_{CS} and by transcriptional activation of iNOS.

6.1.2 Mechanisms of EGFR nuclear translocation

Further investigation of the radiation-induced EGFR nuclear import led to the analysis of the molecular mechanisms underlying this event. EGFR at the plasma membrane is known to be localised with caveolin-1 in lipid rafts and caveolae (Pike, 2005). Lipid rafts are specialised membrane microdomains enriched in sphingolipids and cholesterol that integrate proteins participating in endocytosis, cholesterol traffic and signal transduction from receptors. After stimulation by a specific ligand, EGFR is rapidly internalised into clathrin-coated pits and the signalling continues from the early endosomes (Miaczynska *et al.*, 2004). EGFR may then either be recycled back to the cell surface from the early endosomes, or become polyubiquitinated and degraded in late endosomes fused with lysosomes (Le Roy & Wrana, 2005). Additionally, EGF-dependent nuclear translocation of EGFR may occur (Lo & Hung, 2006).

The fate of EGFR is different after ligand-independent activation. Phosphorylation of EGFR is increased at tyrosine 845 and abrogated at tyrosine 1045; the latter is the docking site for the ubiquitin ligase, c-Cbl. Thus, EGFR is unable to recruit c-Cbl and be ubiquitinated and degraded (Ravid *et al.*, 2002). Internalisation however was shown to take place under oxidative stress when caveolin-1 is phosphorylated at tyrosine 14 by c-Src kinase. In this case EGFR remains complexed with caveolin-1 and is moved to a perinuclear compartment (Khan *et al.*, 2006). It seems possible that the same chain of events takes place after exposure to ionising radiation and it precedes the transport of EGFR into the nucleus. Dittmann *et al.* showed that treatment with 20mM β -methyl cyclodextrin, which inhibits the well documented EGFR internalisation from the cell surface by clathrin-coated pits, had no effect on EGFR nuclear transport suggesting that nuclear EGFR may originate mainly from the perinuclear region and not only the cell surface (Dittmann *et al.*, 2005a), which agrees with the results obtained from our study with confocal microscopy (see figure 83), where EGFR was not specifically localised to the cell membrane in control untreated cells.

This assumption was supported by a recent observation that Src tyrosine kinase inhibitor (PP2) suppresses ERK1/2 activation and EGFR transactivation by irradiation (Li *et al.*, 2006). Figure 66 summarises the fate of EGFR after ligand-dependent or independent activation, as described in recent reports. Since clathrin-dependent

internalisation also involves EGFR molecules from lipid rafts (Puri *et al.*, 2005) and there may be a relation between early endosomes and caveosomes (Helms & Zurzolo, 2004), these two scenarios may not be necessarily exclusive.

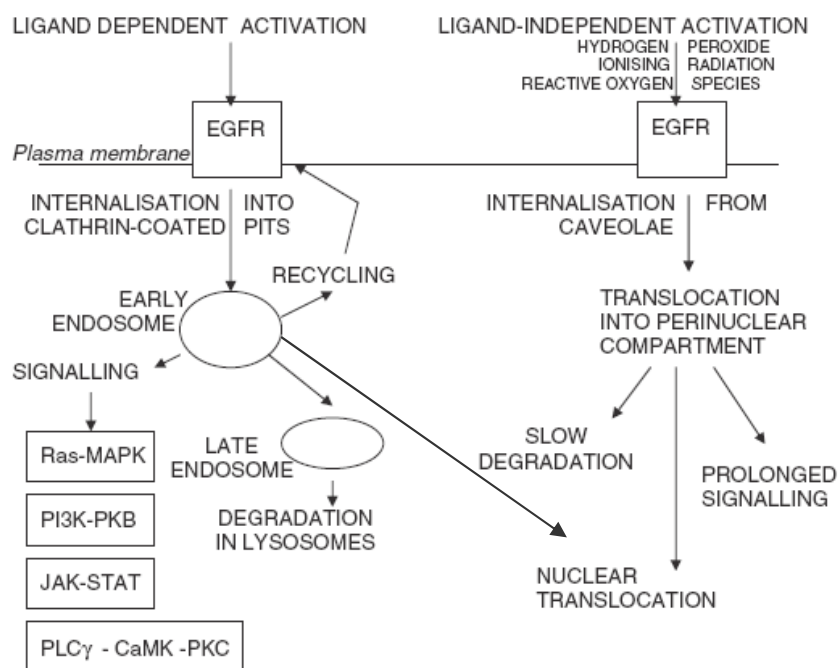


Figure 66: The fate of EGFR after ligand dependent or independent activation.
Source: I Szumiel, Cellular Signalling, 2006

An arginine rich putative nuclear localisation signal (NLS) sequence was identified in amino acids 645-657 of the EGFR's juxtamembrane region. The EGFR putative NLS contains a polypeptide sequence with three clusters of basic amino acids, and is conserved among the EGFR family members (Lin *et al.*, 2001; Hsu & Hung, 2007). Fusing β -galactosidase to this polypeptide led to its nuclear translocation through the nuclear pore. Thus EGFR nuclear entry could be through the conventional nuclear importing system, an energy dependent system that is associated with the nuclear pore complex (Importin/ Ran pathway³) (Lin *et al.*, 2001). Indeed, two separate studies have

³ Classical NLS-protein importation begins with importin α first binding to the NLS sequence, and acts as a bridge for importin β to attach. The importin β -importin α - cargo complex is then directed towards the nuclear pore and diffuses through it. In the nucleus, RanGTP binds to Importin β and displaces it from the complex. Then CAS, an exportin which in the nucleus is bound to RanGTP, displaces importin α from the cargo. The NLS-protein is thus free in the nucleoplasm. The Importin β -RanGTP and importin α -CAS-RanGTP complex diffuses back to the cytoplasm where GTPs are hydrolyzed to GDP leading to the release of importin β and importin α which become available for a new NLS-protein import round (Peters, 2006).

shown interaction of EGFR with importin α (karyopherin α), Ran, and importin β 1, which are essential for the formation of the nuclear import complex needed for import of proteins exhibiting the NLS (Dittmann *et al.*, 2005a; Lo *et al.*, 2006). Nuclear pore entry of proteins can be inhibited by wheat germ agglutinin (WGA), a lectin (sugar binding protein) which inhibits nuclear import of proteins containing the NLS. WGA specifically inhibits active protein import rather than passive diffusion of proteins into the nucleus (Yoneda *et al.*, 1987). Further evidence of a NLS sequence in EGFR was provided by complete blockade of radiation-induced EGFR nuclear entry by incubation with WGA (Dittmann *et al.*, 2005a).

In the classical export scheme, proteins with a nuclear export sequence (NES) can bind inside the nucleus to form a heterotrimeric complex with an exportin (i.e. the exportin chromosome region maintenance protein CRM1) and RanGTP (Peters, 2006). Export via the exportin CRM1 can be inhibited by leptomycin B. Leptomycin B is an unsaturated, branched-chain fatty acid, and is a specific inhibitor of proteins containing the NES. The suggested inhibition mechanism involves the direct binding of leptomycin B to exportin CRM1, which blocks the binding of CRM1 to proteins containing the NES, via the interaction with a cysteine residue in the conserved CRM1 control region (Fukuda *et al.*, 1997). Existence of a NES has not been identified in EGFR, but association with CRM1 was suggested as inhibition with leptomycin B led to increased nuclear levels of EGFR (Lo *et al.*, 2006; Dittmann *et al.*, 2005a).

6.1.3 DNA repair protein targets of EGFR

As mentioned previously, iNOS expression can be modulated by nuclear EGFR acting as a transcription factor and this may lead to increased DNA-PK_{CS} expression and resistance to stress stimuli such as cisplatin and irradiation. Furthermore, altered expression of Rad51, a protein involved in homologous recombination of DNA double strand breaks, was shown by addition of an EGFR inhibitor, erlotinib. Erlotinib used in combination with radiation inhibited Rad51 expression and increased radiosensitivity, providing another evidence of modulation of DNA repair mechanisms by EGFR inhibitors (Chinnaiyan *et al.*, 2005). Therefore, not only non-homologous end joining, but also homologous recombination can be modulated by anti-EGFR therapy.

Aims

Based on the above studies and the results from chapter 5 showing EGFR translocation to the nucleus following irradiation or cisplatin, we decided to investigate the mechanism of EGFR transport using nuclear import and export inhibitors WGA and leptomycin B. We also transfected CRI-G1 and RIN-5F cells with an NLS mutant to enable the mapping of the EGFR regions involved in nuclear translocation. Finally, we investigated possible activation of iNOS or rad51 by nuclear EGFR.

6.2 Results

6.2.1 DNA repair modulation by WGA and leptomycin B

To investigate the mechanism of EGFR nuclear translocation CRI-G1, RIN-5F, NCI-H727, and SHP-77 cells were incubated as before with gefitinib at 10 μ M for 3 hours, and/or WGA or leptomycin for 30 minutes prior to radiation treatment. Cells were then irradiated at 15Gy, or at 30Gy for NCI-H727 cells and DNA damage was quantitated using the comet assay (section 5.2.2, figure 50). Figures show results for CRI-G1 and RIN-5F cells only (the rest of the cell lines are shown in appendix 3A-3B).

As shown in figure 67, pre-treatment with WGA alone prior to irradiation, inhibited DNA repair in CRI-G1 cells by 26% and 16% at 80 and 120 minutes after irradiation. A double treatment of gefitinib and WGA induced an additional delay in DNA repair by 37% at 80 minutes after irradiation, which remains at 37% at 120 minutes post radiation. In contrast, leptomycin B in CRI-G1 cells led to a slight increase of 19% in DNA repair at 40 minutes after irradiation, with DNA repair kinetics falling to levels similar to radiation alone in later time points. In RIN-5F cells (figure 68) WGA or leptomycin B had no effect in the kinetics of strand break repair. These results indicate that radiation-induced EGFR import may utilise proteins associated with the nuclear pore complex.

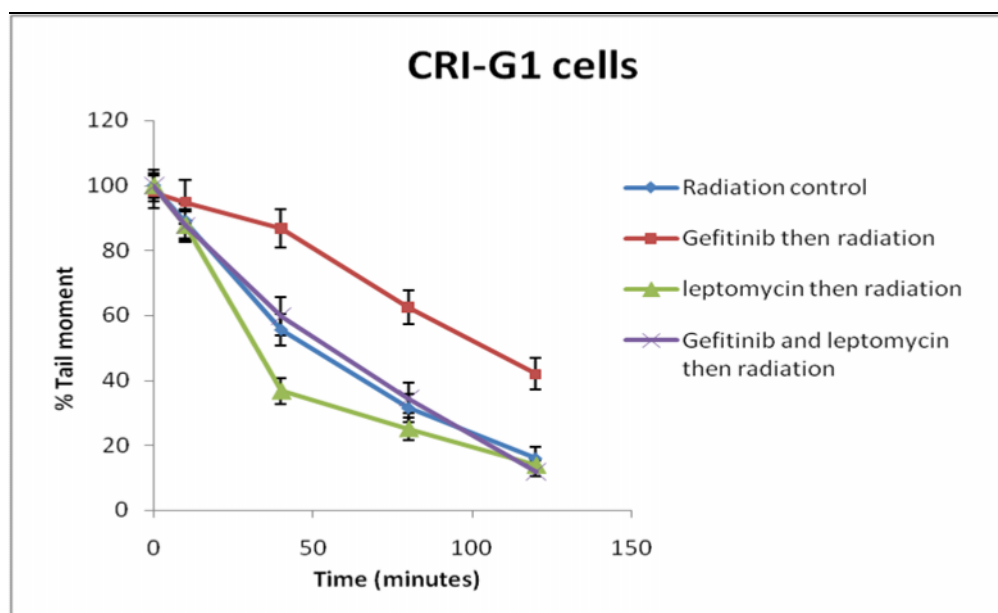
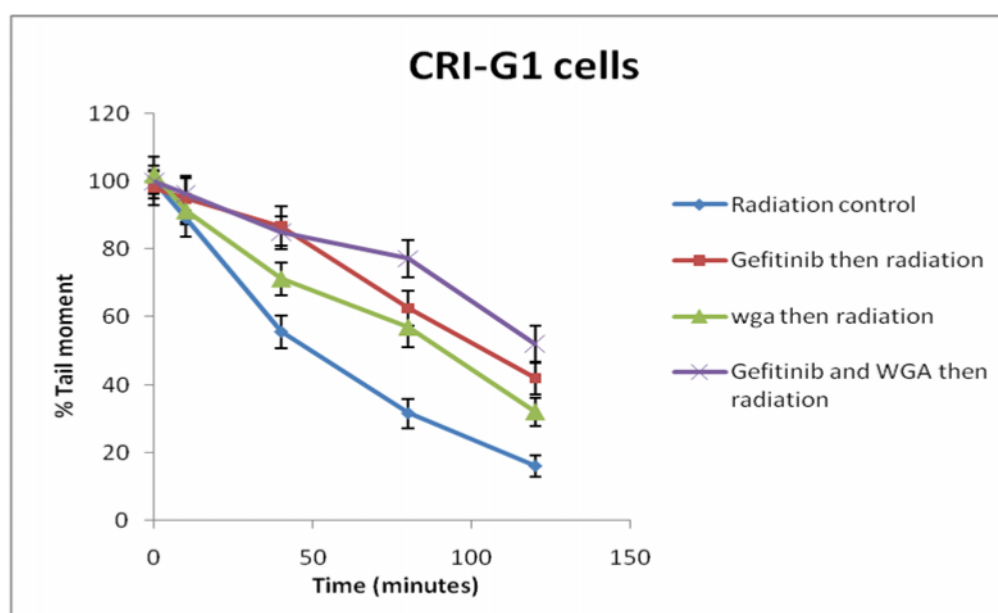


Figure 67: Measurement of irradiation-induced DNA strand breaks and their repair in CRI-G1 cells. Strand break formation quantitated as percentage of control cell tail moment, plotted against time after irradiation. Cells were treated with gefitinib at 10 μ M for 3 hours, with WGA (0.05mg/ml) or leptomycin B (2nM) added in the last 30 minutes. Drug was removed, and then cells were irradiated at 15 Gy (a dose which produces a tail moment of approximately 16) and incubated for up to 120 minutes at 37°C. Data represents the averages of three different experiments, each performed in triplicate; bars, SD

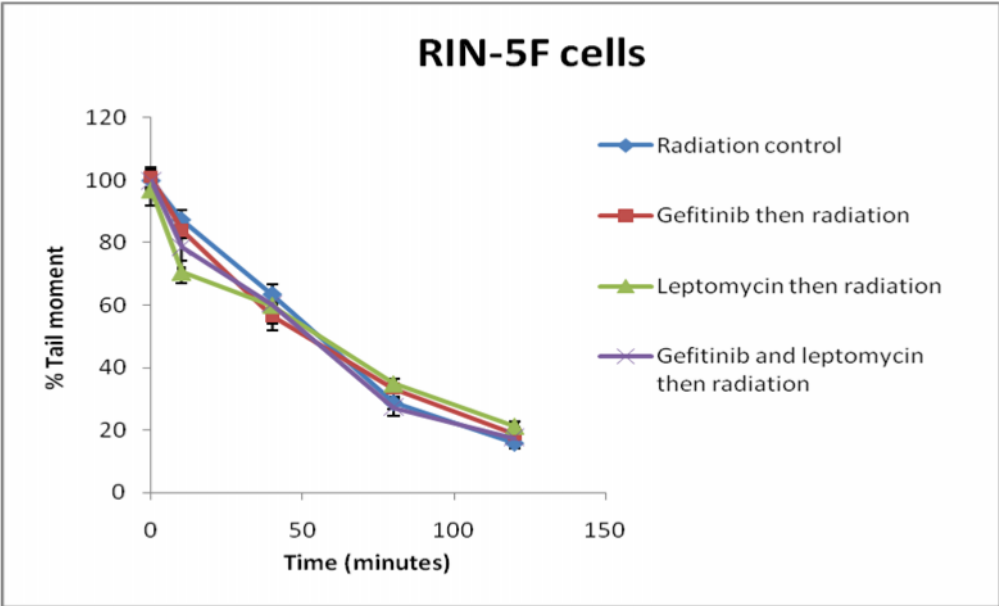
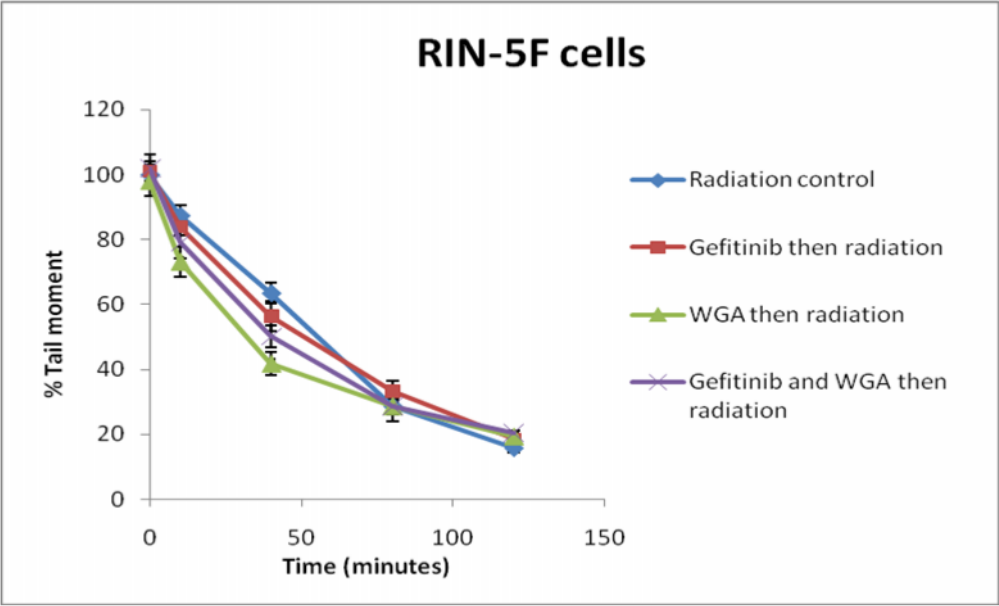


Figure 68: Measurement of irradiation-induced DNA strand breaks and their repair in RIN-5F cells. Strand break formation quantitated as percentage of control cell tail moment, plotted against time after irradiation. Cells were treated with gefitinib at 10 μ M, followed by 30 minutes treatment with WGA (0.05mg/ml) or leptomycin B (2nM). Drug was removed, and then cells were irradiated at 15 Gy (a dose which produces a tail moment of approximately 16) and incubated for up to 120 minutes at 37°C. Data represents the averages of three different experiments, each performed in triplicate; bars, SD

6.2.2 WGA and Leptomycin B effect on EGFR localisation

The effect of WGA and leptomycin B on EGFR localization in CRI-G1 and RIN-5F cells was established by immunohistochemistry. For this, cells were treated as before with gefitinib and/or WGA or leptomycin B and irradiated at 4Gy, and EGFR was detected by immunofluorescent staining using a confocal microscope. Data is shown for CRI-G1 and RIN-5F cells only with the rest of the cell lines shown in appendix 3C-3D. As shown in figure 69, WGA alone had no effect on EGFR localization in CRI-GI cells, but in combination with radiation WGA blocked the radiation-induced EGFR nuclear entry in a similar fashion to gefitinib. On the other hand leptomycin B as a single agent had no effect on locality of EGFR in CRI-GI cells, but when it was added prior to irradiation it led to increased levels of nuclear EGFR compared to untreated cells. In RIN-5F cells (figure 70) which do not express nuclear EGFR, WGA or leptomycin B had no effect EGFR locality in the cell. These results confirmed the employment of nuclear pore complex proteins for EGFR transportation to and out of the nucleus.

The data from comet analysis and immunofluorescent staining were also confirmed by immunoblotting in cytoplasmic and nuclear extracts. CRI-GI and RIN-5F cells were treated with WGA or leptomycin for 30 minutes prior to irradiation at 4Gy. After irradiation treatment and incubation at 37°C for 5 minutes, nuclear and cytosolic fractions were isolated and immunoblotted for EGFR. In addition to the use of α -tubulin as a loading control, blots were stripped and re-probed for lamin β 1, which was used as a loading control for nuclear proteins (Dittmann *et al.*, 2005). The amounts of EGFR were calculated by densitometry analysis of the bands.

As seen in figure 71, WGA completely blocked radiation-induced EGFR import to the nucleus in CRI-G1 cells, while leptomycin led to increased nuclear EGFR levels. Even as a single agent, WGA led to decreased nuclear EGFR levels. Cytoplasmic EGFR levels were decreased in irradiated cells, but were unaffected by WGA or leptomycin. In RIN-5F cells shown in figure 72, no nuclear EGFR is detected. WGA or leptomycin had no effect on the amounts of nuclear EGFR except for an increase in cytoplasmic EGFR by WGA as a single agent.

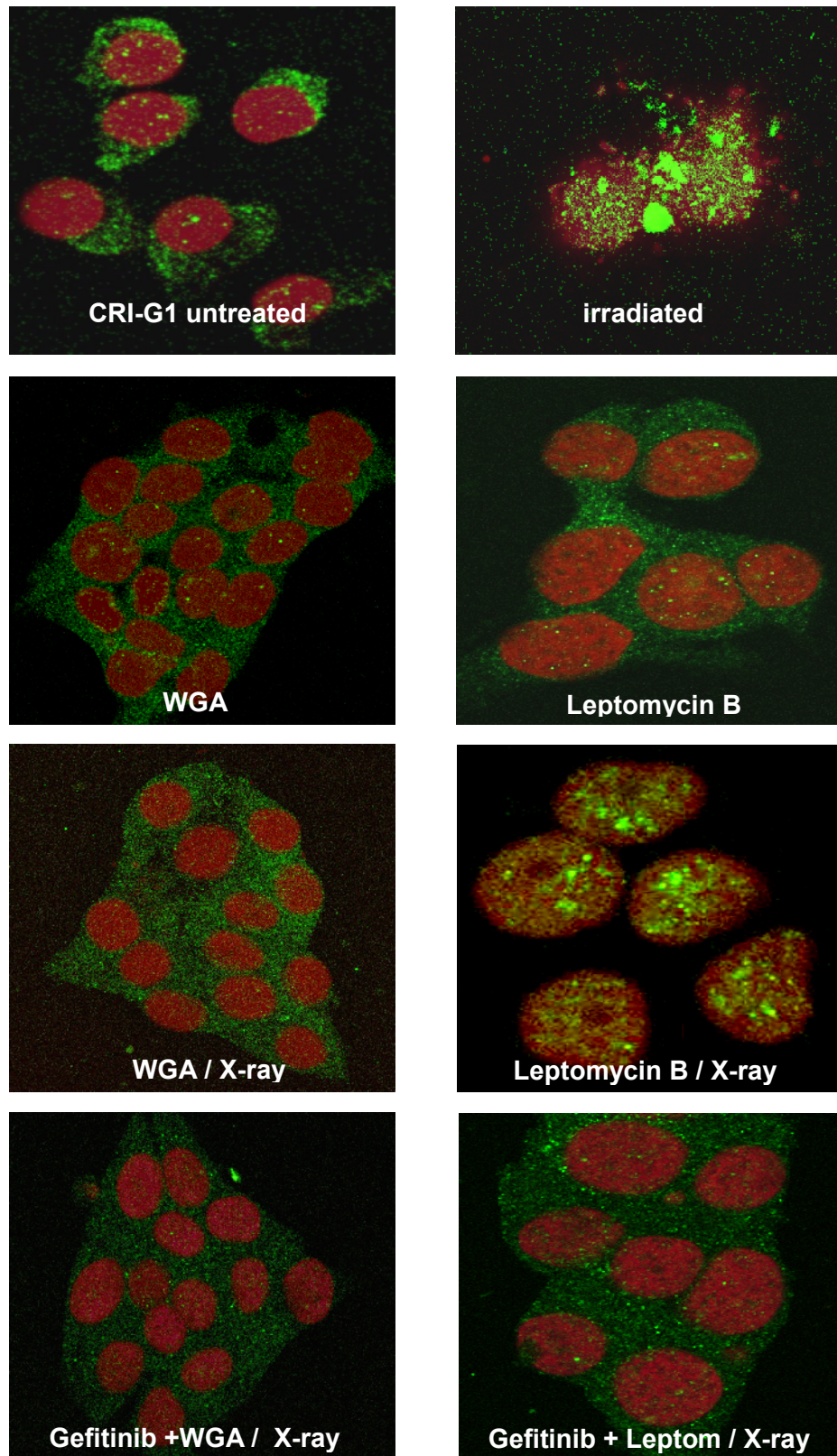


Figure 69: CRI-G1 cells were treated with gefitinib at 10 μ M for 3 hours and/or WGA (0.05mg/ml) or leptomycin B (2nM) added in the last 30 minutes. Cells were then irradiated at 4Gy and incubated for 5 minutes at 37°C. Cells were then fixed and stained for EGFR (green) and nucleus was stained with propidium iodide (red).

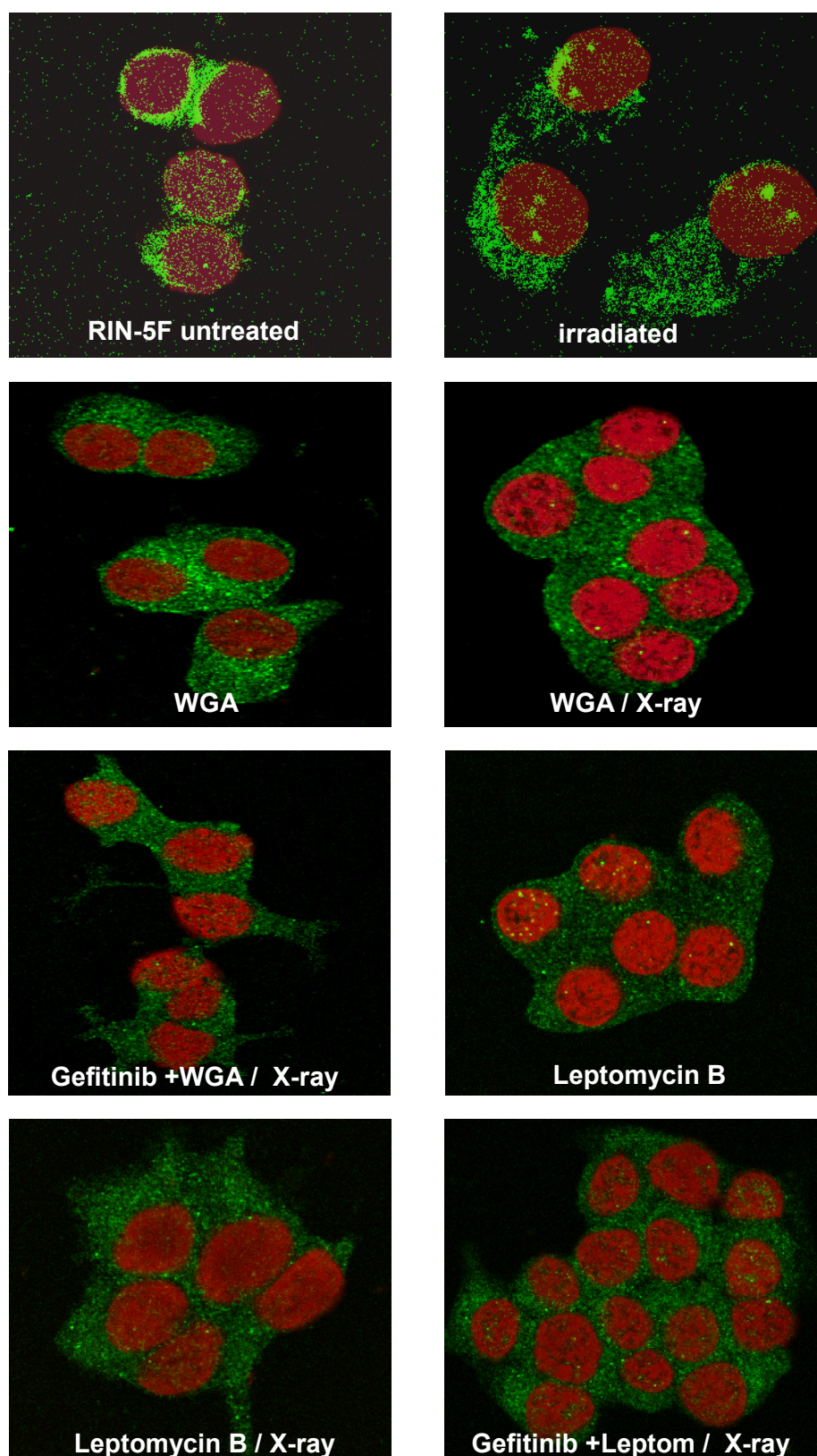
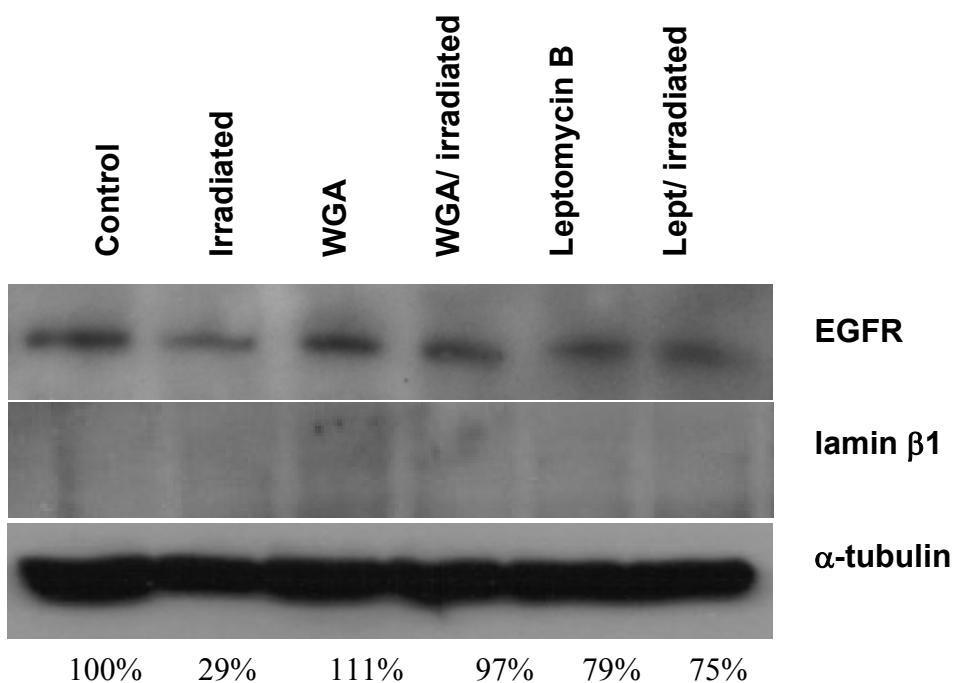


Figure 70: RIN-5F cells were treated with gefitinib at 10 μ M for 3 hours and/or WGA (0.05mg/ml) or leptomycin B (2nM) added in the last 30 minutes. Cells were then irradiated at 4Gy and incubated for 5 minutes at 37°C. Cells were then fixed and stained for EGFR (green) and nucleus was stained with propidium iodide (red).

CRI-G1 CELL EXTRACTS

Cytoplasmic



Nuclear

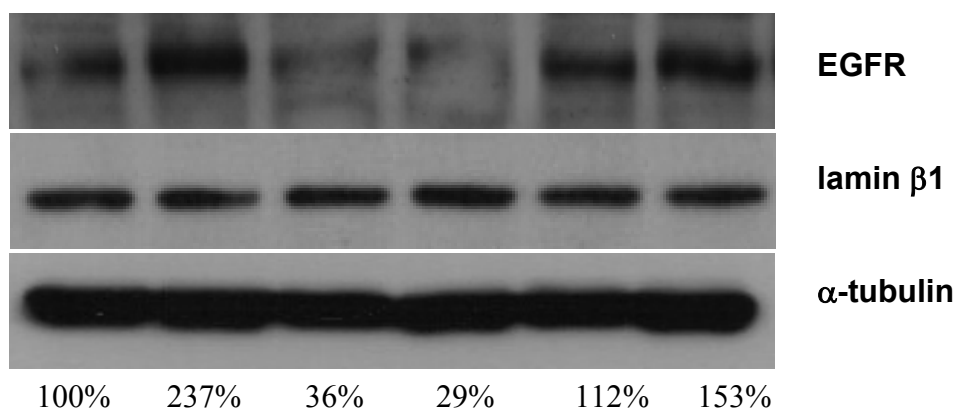


Figure 71: CRI-G1 cells were treated with WGA (0.05mg/ml) or leptomycin B (2nM) for 30 minutes, irradiated at 4Gy and incubated for 5 minutes at 37°C. Cytosolic and nuclear extracts were immunoblotted for EGFR. Alpha-tubulin was used as a loading control. Lamin β 1 was used as a nuclear marker. Amounts of EGFR in percentages were determined by densitometry analysis.

RIN-5F CELL EXTRACTS

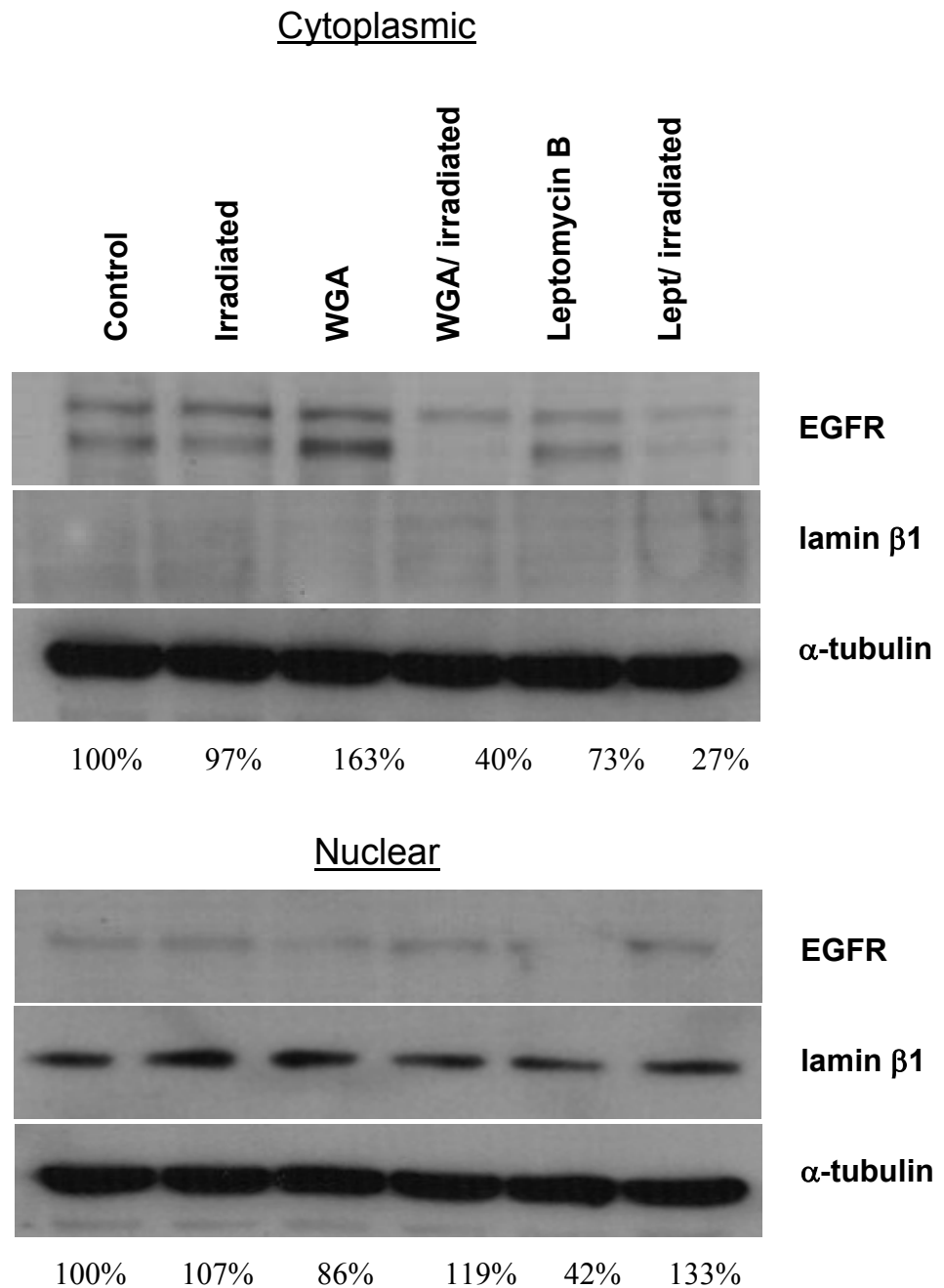


Figure 72: RIN-5F cells were treated with WGA (0.05mg/ml) or leptomycin B (2nM) for 30 minutes, irradiated at 4Gy and incubated for 5 minutes at 37°C. Cytosolic and nuclear extracts were immunoblotted for EGFR. Alpha-tubulin was used as a loading control. Lamin β 1 was used as a nuclear marker. Amounts of EGFR in percentages were determined by densitometry analysis.

6.2.3 Transfection of *wt* and *mutNLS EGFR*

To investigate whether the putative nuclear localisation signal (NLS) sequence was involved in the transport of EGFR to the nucleus, we transfected CRI-G1 and RIN-5F

cells with wt EGFR or an NLS mutant to enable the mapping of the EGFR regions involved in nuclear translocation. The NLS sequence in the juxtamembrane domain of EGFR is RRRHIVRKRTLRR (Hsu & Hung, 2007) containing three clusters (underlined) of basic arginine (R) and lysine (K) amino acids. The sequence was changed into AAAHIVAKATLAA, with hydrophobic alanine replacing the arginine residue. Replacing any of the three clusters with alanine (one cluster at a time), as examined by Hsu & Hung, led to inhibition of EGFR entry to the nucleus (Hsu & Hung, 2007).

CRI-G1 and RIN-5F cells were transfected for 48 hours, followed by treatment with gefitinib at 10 μ M and irradiation at 15Gy for DNA repair analysis by the comet assay (figure 73), or at 4Gy for immunofluorescent staining and the use of confocal microscopy (figures 74-75).

As seen in figure 73, CRI-G1 cells transfected with wtEGFR and irradiated at 15Gy repair DNA strand breaks in approximately 120 minutes as with untransfected cells (dark blue). When CRI-G1 cells are treated with gefitinib (light blue), the repair of radiation-induced DNA damage is delayed by 25% at 80 minutes post irradiation and by 22% at 120 minutes. Irradiation-induced DNA strand breaks in CRI-G1 cells transfected with the mutant NLS EGFR (dark green) repair more slowly compared to the cells transfected with wtEGFR showing 15% more strand breaks at 80 minutes after radiation treatment, but at 120 minutes DNA strand breaks are completely repaired. Addition of gefitinib before irradiation in cells transfected with mut NLS EGFR (light green) did not change significantly the kinetics of DNA repair compared to cells transfected with mut NLS EGFR and irradiated (dark green), but compared to cells transfected with wtEGFR there is a small delay of 13% at 80 minutes post irradiation which remains at 13% at 120 minutes. This difference is probably due to wt EGFR molecules already present in the CRI-G1 cell line before and after transfection.

In RIN-5F cells (figure 73), DNA repair kinetics between cells transfected with wt (dark and light blue) and mutant NLS EGFR (dark and light green) are almost identical, with the former showing 5-10% increased repair activity at 80 and 120 minutes post-irradiation compared to the latter. Addition of gefitinib did not produce any further

delay compared to the respective radiation control cells. These results indicate that the putative NLS sequence may be involved in EGFR transport to the nucleus in CRI-G1 cells.

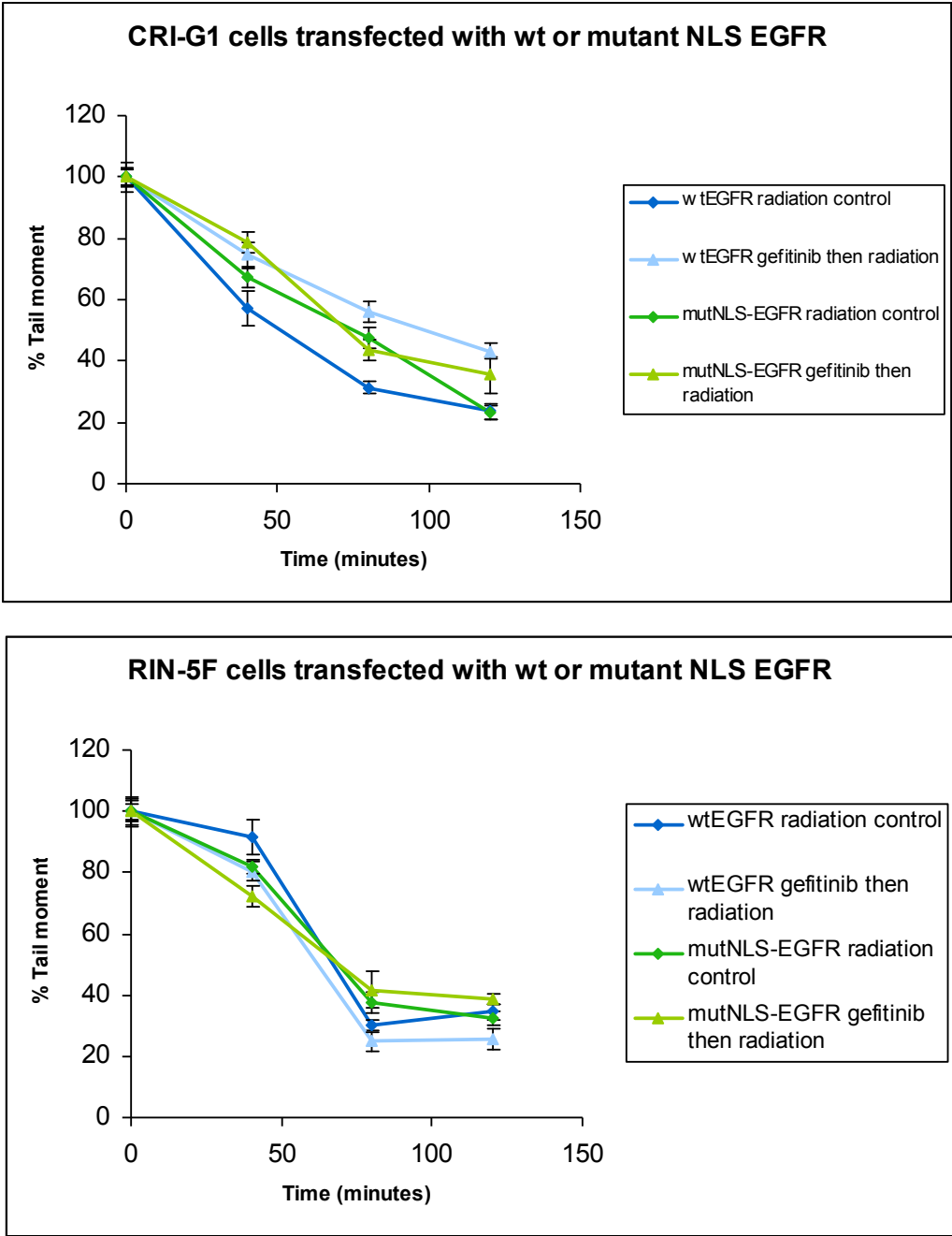


Figure 73: Measurement of irradiation-induced DNA strand breaks and their repair by comet analysis. Strand break formation was quantitated as percentage of control cell tail moment, plotted against time after irradiation. CRI-G1 and RIN-5F cells were transfected with wt or mutNLS-EGFR for 48hours. Cells were then treated with 10 μ M gefitinib for 3 hours, irradiated at 15Gy and incubated for 0-120 minutes at 37°C. Data represents the averages of three different experiments, each performed in triplicate; bars, SD

The effect of irradiation on CRI-G1 and RIN-5F cells transfected with wt or mut NLS EGFR was also studied by immunohistochemistry. Cells were transfected as previously and treated with gefitinib followed by irradiation and labelling for wt and mutant EGFR.

CRI-G1 cells (figure 74) demonstrated wt EGFR but not mutant EGFR entering the nucleus at 5 minutes after irradiation. However, amounts of cytoplasmic EGFR were also present with wt EGFR, probably due to the excess amount of EGFR present inside the cells. Addition of gefitinib abrogated EGFR nuclear entry in cells transfected with wt EGFR as with control untransfected cells, but had no effect in CRI-G1 cells transfected with the mut NLS EGFR.

In RIN-5F cells however (figure 75), no nuclear EGFR was observed after irradiation in either wt or mutant EGFR transfected cells. As expected, gefitinib had no effect in EGFR localization but inhibited activation of the receptor in both wt and mutant EGFR transfected cells.

6.2.4 Nuclear targets of EGFR

Previous reports have stated that EGFR may alter the expression of genes associated with DNA repair: iNOS and Rad51 (Lo *et al.*, 2005b; Chinnaiyan *et al.*, 2005). Rad51 is involved in homologous recombination and iNOS was shown to lead to activation of DNA-PK_{CS}, a member of NHEJ. Based on these reports we decided to test this hypothesis in neuroendocrine tumour cells. Since nuclear EGFR acting as a transcription factor on the promoter of iNOS needs activation by EGF, we serum starved cells for 12 or 24 hours and treated them with EGF for 6 hours, a length of time shown previously to lead to activation of EGFR.

Figure 76 shows immunoblotting for iNOS in six neuroendocrine tumour cell lines. Serum starvation but not EGF-dependent activation of EGFR caused differences in expression levels of iNOS in all cell lines tested. For Rad51, we stripped the nuclear extract blots for EGFR (shown in section 6.2.2) and re-probed the membranes for Rad51 shown in figure 77. No change in Rad51 expression by irradiation and consequently radiation-induced nuclear EGFR was identified in any of the cell lines. WGA or leptomycin had no effect in Rad51 levels in nuclear extracts isolated.

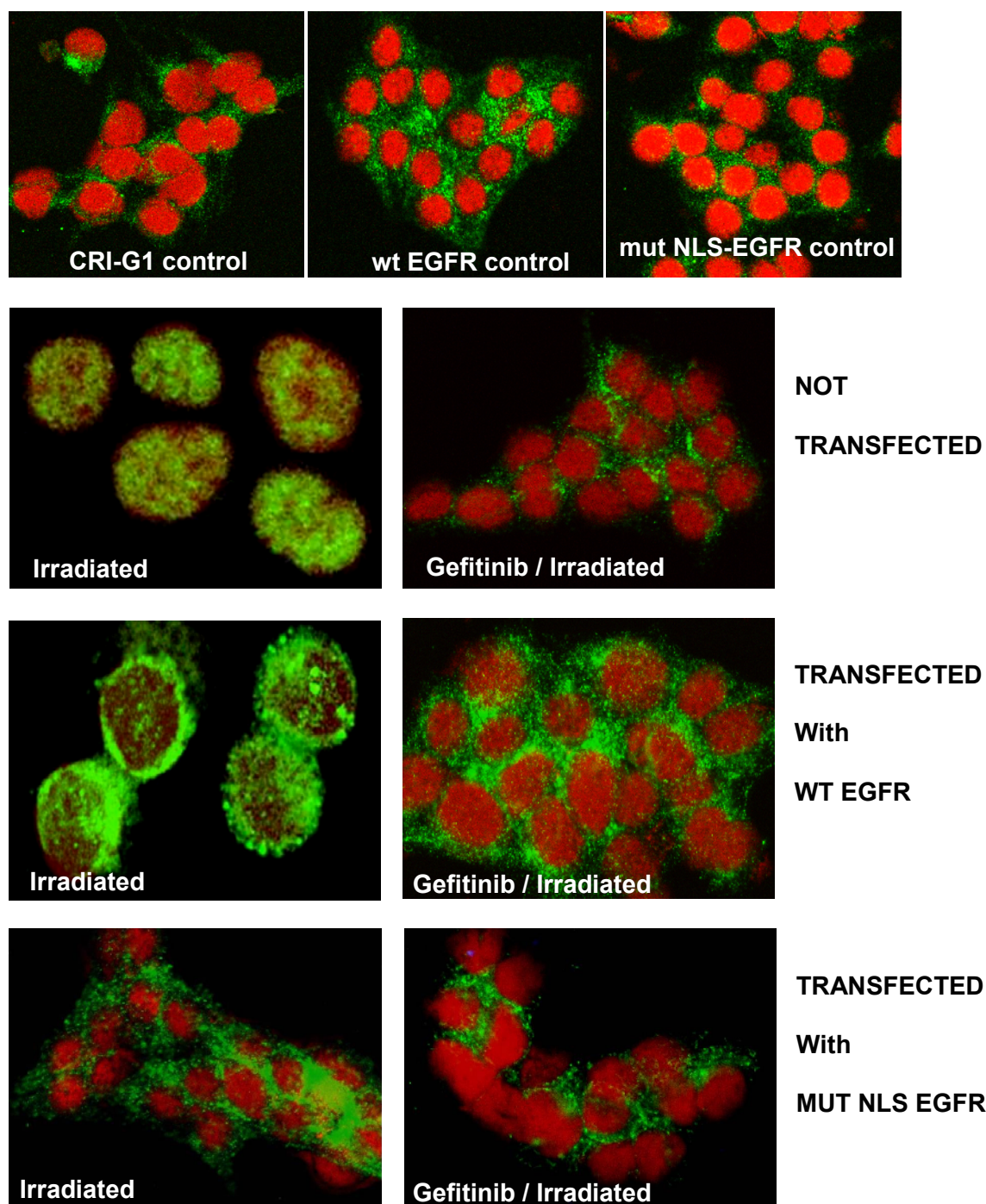


Figure 74: CRI-G1 cells were transfected for 48 hours with wtEGFR or mutant NLS-EGFR. Cells were treated with gefitinib at 10 μ M for 3 hours, irradiated at 4Gy and incubated for 5 minutes at 37°C. Cells were then fixed and stained for EGFR (green) and nucleus was stained with propidium iodide (red).

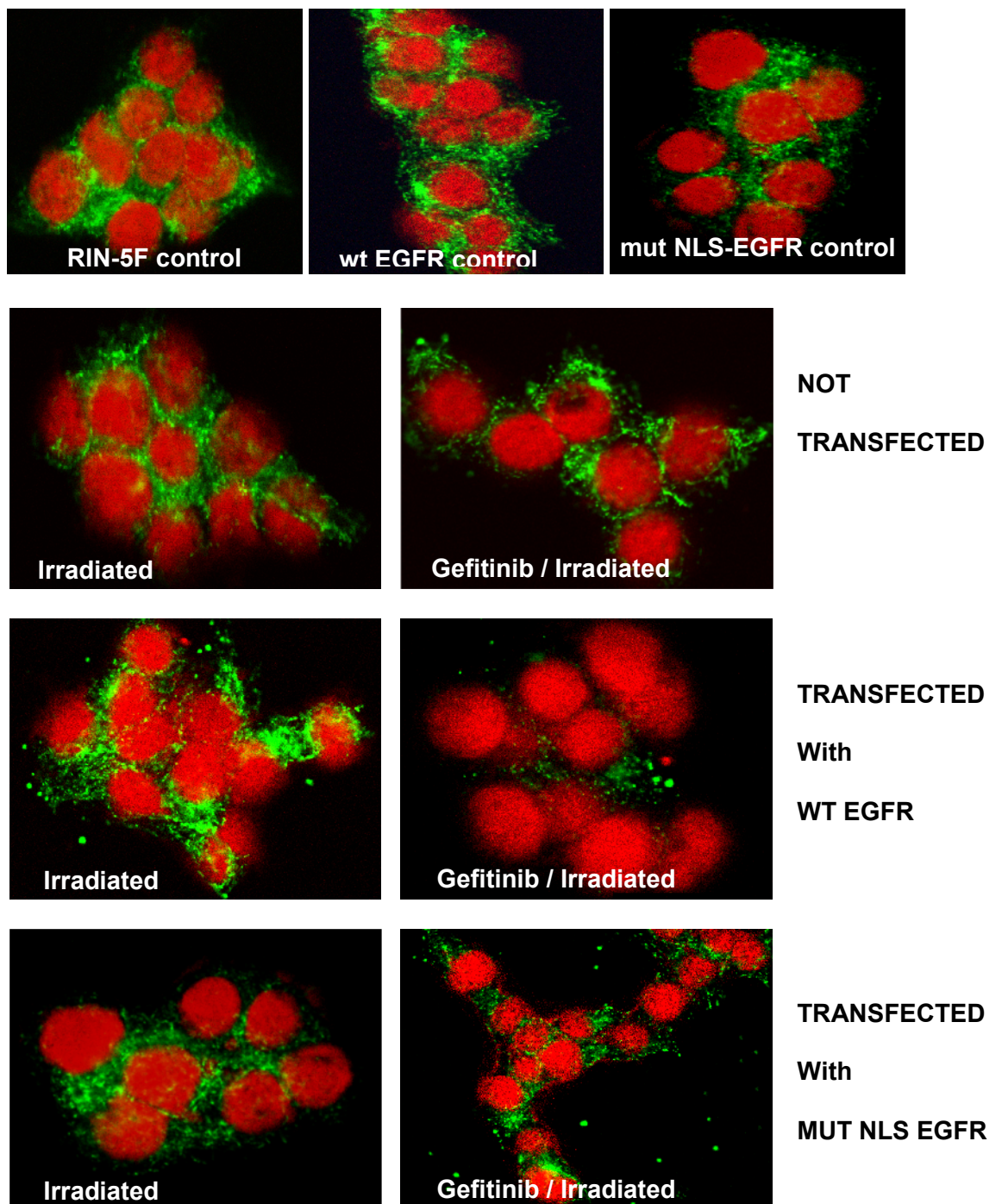


Figure 75: RIN-5F cells were transfected for 48 hours with wtEGFR or mutant NLS-EGFR. Cells were treated with gefitinib at 10 μ M for 3 hours, irradiated at 4Gy and incubated for 5 minutes at 37°C. Cells were then fixed and stained for EGFR (green) and nucleus was stained with propidium iodide (red).

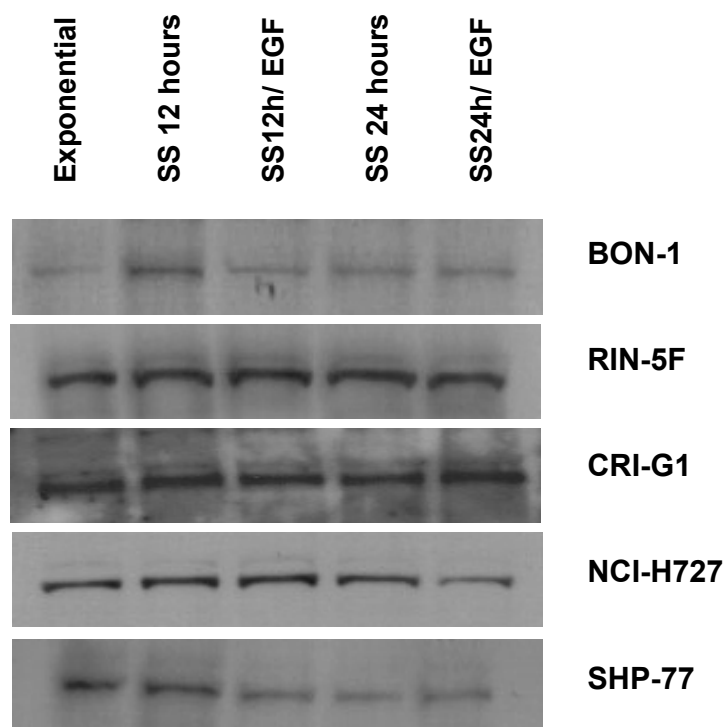


Figure 76: Cells were serum starved (SS) in 0% serum for 12 or 24 hours followed by incubation with EGF (100ng/ml) for 6 hours and immunoblotting of whole cell extracts for iNOS.

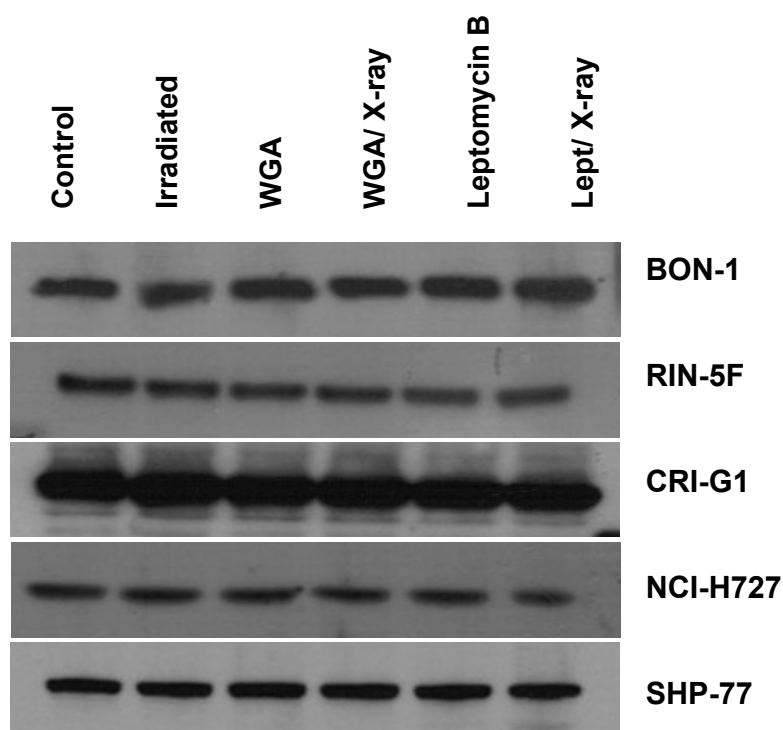


Figure 77: Cells were treated with WGA (0.05mg/ml) or leptomycin B (2nM) for 30 minutes, irradiated at 4Gy (or 30Gy for NCI-H727 cells) and incubated for 5 minutes at 37°C. Nuclear extracts were immunoblotted for Rad51.

6.3 Discussion

The previous chapter demonstrated EGFR movement to the nucleus in cells exposed to cisplatin and radiation. Radiation-induced nuclear entry of EGFR was blocked by EGFR inhibitors gefitinib and cetuximab, showing that phosphorylation of EGFR is needed for the nuclear translocation of the receptor. Anti-EGFR therapy also led to radiosensitisation of cells by delaying the repair of radiation-induced DNA damage. Apart from stress-dependent, ligand-dependent nuclear transit of EGFR can occur and this event leads to activation of genes including iNOS, B-Myb, and cyclin D1, which have been associated with increased proliferation of tumour cells, as mentioned in detail in section 6.1.1 (Lo *et al.*, 2005b; Lin *et al.*, 2001; Hanada *et al.*, 2006).

6.3.1 WGA and leptomycin B modulation of DNA repair and EGFR localisation

To understand how EGFR transport occurs, we analysed the effect of two proteins involved in nuclear trafficking through the nuclear pore complex; wheat germ agglutinin (WGA), and leptomycin B. The first is a nuclear import inhibitor cooperating with importins α and β and protein Ran, and the second is a nuclear export inhibitor associated with exportin CRM1 (Yoneda *et al.*, 1987; Fukuda *et al.*, 1997). Our results demonstrated that WGA works in a similar way to gefitinib or cetuximab, by inhibiting nuclear entry of EGFR and causing a delay in repair of radiation-induced DNA strand breaks in all cells except RIN-5F cells, as shown by immunofluorescent staining and comet analysis respectively. Leptomycin B had no effect as a single agent, but abrogated the gefitinib-induced delay in the repair of strand breaks. Furthermore, treatment with radiation and leptomycin led to increased levels of nuclear EGFR. This is in concordance with previous studies postulating that EGFR nuclear entry is via interaction with importin α (karyopherin α), Ran, and importin β 1, while export is via association with exportin CRM1, all of which are constituents of the nuclear pore complex (Dittmann *et al.*, 2005a; Lo *et al.*, 2006).

6.3.2 The role of the NLS sequence in EGFR

The nuclear pore complex facilitated transport is an energy-dependent mechanism that facilitates import of proteins with a nuclear localisation signal (NLS) sequence. Interestingly, a putative NLS sequence (RRRHIVRKRTLRR) was identified in the juxtamembrane domain of EGFR by Hsu & Hung (2007), which contains three clusters

of basic amino acids. The presence of basic amino acids is characteristic of NLS sequences indicating their importance in the mechanism of interaction with nuclear pore importins. Replacing any of the three clusters with the hydrophobic amino acid alanine (one cluster at a time), led to inhibition of EGFR entry to the nucleus (Hsu & Hung, 2007). In our study, CRI-G1 and RIN-5F cells were transfected with the wild type and a mutant EGFR at the NLS (sequence was changed into AAAHIVAKATLAA). Transfection was performed so that transfected EGFR molecules would be in excess compared to EGFR expressed naturally in both cell types. Transfection with wtEGFR, which was used as a control for our experiments, showed similar results with confocal microscopy to untreated cells in both cell lines, with nuclear EGFR presented only in CRI-G1 cells, indicating that its not the receptor itself but the mechanism for nuclear transport that may be impaired in RIN-5F cells. Small amounts of cytoplasmic EGFR were also present in irradiated CRI-G1 cells, but the majority of EGFR molecules were found at the inner side of the nuclear membrane. Treatment with gefitinib abrogated nuclear transfer of EGFR as in untransfected cells. Mutant NLS EGFR CRI-G1 cells showed very little nuclear transit which is probably due to the receptor naturally present in the cells. Gene sequencing analysis of nuclear EGFR would confirm whether the small amounts of EGFR molecules found in the nucleus are wild type (already present in the cells) and not mutant, and this would form the next step in our study.

Measurement of DNA damage repair by the comet assay in cells transfected with the wild type receptor, as expected showed repair of irradiated cells within two hours after exposure, and a gefitinib-induced delay in repair in CRI-G1 but not in RIN-5F cells. CRI-G1 cells transfected with the mutant receptor exposed to irradiation alone also showed delay in DNA repair, which could not be further increased by gefitinib. This shows that lack of the NLS inhibits EGFR nuclear entry associated with an increase in DNA-PK_{CS} activity and this leads to the impediment of DNA repair (Dittmann *et al.*, 2005a; Dittmann *et al.*, 2005b). In RIN-5F cells, transfection with the wild type or mutant EGFR had no effect in DNA repair kinetics. Gefitinib did not alter DNA repair in RIN-5F cells transfected with either EGFR construct, supporting the view that EGFR does not modulate DNA repair in these cells due to impaired nuclear traffic.

6.3.3 EGFR nuclear targets?

Further analysis of EGFR nuclear transport led to the search for possible nuclear target proteins. Of the proteins already identified including iNOS, B-Myb, and cyclin D1 (Lo & Hung, 2006), the most interesting target for our study was iNOS. EGFR was shown to interact with STAT3 on the promoter of iNOS and this led to transcriptional activation of the enzyme (Lo *et al.*, 2005b). iNOS has been associated with increased proliferation as have the other two target proteins, but is the only of the three to be also associated with DNA repair by increasing the expression of DNA-PK_{CS}, an event shown to provide protection to cells from the cytotoxicity of nitric oxide and DNA-damaging agents such as cisplatin and radiation (Xu *et al.*, 2000). Since association of EGFR and DNA-PK_{CS} was not identified (even though gefitinib caused DNA-PK_{CS} downregulation in some cells), it was suggested that modulation of DNA repair might not be by direct physical association of EGFR to DNA-PK_{CS} but indirectly through transcriptional activation of iNOS. EGF-dependent activation of EGFR did not have any effect in the expression of iNOS. Minor changes were caused by serum starvation in some cell lines, but no significant upregulation was seen by EGF. Perhaps, in neuroendocrine tumour cells ligand dependent activation does not induce nuclear import of EGFR. This was also shown by Dittmann *et al.* who found increased phosphorylation of the receptor by EGF treatment but no increase in nuclear EGFR amounts (Dittmann *et al.*, 2005a). The next step would thus be to analyse the effect of EGF on EGFR localisation, as done with cisplatin and radiation. It would be interesting to see whether this pathway leads to EGFR import in RIN-5F cells, which would prove that the mechanisms of ligand dependent or independent transport are distinct as previously postulated (Szumiel, 2006).

EGFR has also been shown to modulate expression of another DNA repair protein, Rad51 (Chinnaiyan *et al.*, 2005). This protein has a role in homologous recombination, which also repairs DNA strand breaks. Radiation or gefitinib had no effect in Rad51 expression, indicating that EGFR may not be associated with the homologous recombination system in neuroendocrine tumour cells.

6.3.4 Conclusions

The results obtained in our study demonstrate that cisplatin and radiation induce EGFR entry to the nucleus and activation of DNA repair mechanisms that protect cells from

the toxic effects of radiation. Apart from activating traditional signalling pathways such as the PI-3 kinase and the MAPK pathway, EGFR probably undergoes internalisation in caveosomes and transferred to the perinuclear compartment (Khan *et al.*, 2006). From that area, as shown from confocal microscopy, nuclear transport commences that is mediated by the nuclear pore complex. EGFR nuclear entry may utilise the putative NLS sequence of the receptor. Nuclear presence of EGFR is associated with DNA repair, since gefitinib or cetuximab block EGFR entry, an event leading to the impediment of DNA repair. Our study has tried to elucidate the mechanism behind nuclear EGFR. The identification of novel EGFR nuclear targets following radiation would form a next step in our research which would help understand the role of this receptor under stress conditions.

In the next chapter we investigate c-KIT, a tyrosine kinase receptor found in haematopoietic stem cells, as a putative receptor target in neuroendocrine tumour patients.

CHAPTER 7

INVESTIGATION OF C-KIT EXPRESSION IN NEUROENDOCRINE TUMOUR PATIENTS: COMPARISON OF MONOCLONAL & POLYCLONAL ANTIBODIES

7.1 Introduction

Tyrosine phosphorylation by protein tyrosine kinases is of particular importance in cellular signalling and can mediate signals for major cellular processes, such as proliferation, differentiation, apoptosis, attachment, and migration. Tumour growth is based on deregulation of the above tasks, suggesting that targeting these enzymes could help inhibit cancer growth and induce apoptosis of malignant cells (Traxler *et al.*, 2001). *C-KIT*, the human homologue of the v-kit Hardy-Zuckerman 4 feline sarcoma viral oncogene, codes for a receptor tyrosine kinase normally expressed by a variety of cell types including the interstitial cells of Cajal, germ cells, bone marrow stem cells, melanocytes, breast epithelium and mast cells (Besmer *et al.*, 1986). The role of C-KIT expression has mainly been studied in haematological and solid tumours, such as acute leukaemias (Cortes *et al.*, 2003), and gastrointestinal stromal tumours (GIST) (Fletcher *et al.*, 2002). C-KIT may also have a role in germ cell tumours, breast adenocarcinomas, malignant melanomas, small cell lung cancers, and in the malignant transformation of mast cells.

The clinical importance of C-KIT expression in malignant tumors relies on the existence of imatinib (STI571, Gleevec®, Novartis Pharma AG Basel, Switzerland), a compound which specifically inhibits C-KIT (Lefevre *et al.*, 2004), as well as other tyrosine kinase receptors such as the fusion BCR-ABL protein in chronic myelogenous leukaemia (CML). The receptor targets of imatinib are described in detail in section 2.2.2 (p.52). Moreover, a clinically relevant breakthrough has been the finding of notable anti-tumour effects by imatinib in GISTs, a group of tumours regarded as being generally resistant to conventional chemotherapy (De Silva & Reid, 2003). Imatinib has been approved by the United States FDA for the treatment of C-KIT positive GISTs and Philadelphia chromosome - positive chronic myelogenous leukaemias (Cohen *et al.*, 2005; Dagher *et al.*, 2002).

On the other hand, the data regarding C-KIT expression by immunohistochemistry have shown variability with no C-KIT detected in neuroendocrine tumours by various groups including Tsuura *et al.*, (1994) and Welin *et al.*, (2006). On the other hand, 92% of PNETs were found immunoreactive to C-KIT by Fjallskog *et al.*, (2003) and 26% of neuroendocrine carcinomas were found positive for C-KIT by Ishikubo *et al.*, (2006).

Marked differences in the expression of C-KIT have also been found in other types of tumours such as pancreatic adenocarcinomas and soft tissue sarcomas which may resemble GISTs (Sabah *et al.*, 2003; Bateman *et al.*, 2008), and in cases of desmoid fibromatosis (Hornick & Fletcher, 2003), and this has been ascribed to the differences in immunostaining protocols as well as antibodies used by each group.

Aims

The purpose of this study was to study the immunoexpression of C-KIT in NET patients and raise the possibility of treating these tumours with imatinib. The additional purpose was to determine if there was any difference in expression between the monoclonal and polyclonal antibodies. For this, we stained a variety of NET tissue samples using two different antibodies (one polyclonal and one monoclonal), but the same immunohistochemical protocol. The two antibodies used, which have also been used by other groups, recognise and bind to two different regions of the antigen.

As described in the methods section (see p.92), the first antibody is the polyclonal anti C-KIT/ CD117 antibody from DAKO, a rabbit antibody against the 963 to 976 amino acid residues at the C-terminus of the human C-KIT oncoprotein. The second antibody is a monoclonal anti C-KIT antibody from Novocastra which recognizes the three C2-like extracellular domains at the N-terminus of C-KIT and was raised in mice. For simplicity, the two antibodies are referred in the text as ‘polyclonal’ and ‘monoclonal’. In the second part, the presence of C-KIT was also investigated in human and rat neuroendocrine cell lines by immunoblotting, with the intention to analyze the anti-proliferative effect of imatinib in these cell lines. For immunoblotting, a rabbit polyclonal C-KIT antibody from Santa Cruz with an epitope mapping to the C-terminus was used.

7.2 Results

Immunohistochemistry was performed in specimens from 85 NETs patients. Of these 39 patients had foregut NETs including 3 ampullary NETs, 7 bronchial carcinoids, 1 duodenal carcinoid, 6 gastric carcinoids, 1 oesophageal carcinoid, and 21 pancreatic neuroendocrine tumours. 27 patients were presented with midgut carcinoids including 7 appendiceal carcinoids, 18 ileal carcinoids, 1 caecal carcinoid, and 1 jejunal carcinoid. The 4 hindgut carcinoid patients included 1 colon carcinoid, 2 rectal carcinoids, and 1

cervical carcinoid. Finally we analysed 15 more patients with 5 paragangliomas, 5 medullary carcinomas of the thyroid and 5 NETs of unknown primary site. The patients and their tumour type are shown in table 17.

Staining was repeated twice to three times depending on the availability of tissue. Staining was scored as strong to weak, diffuse or present in nests of tumour cells rather than covering the whole tumour area. GIST tumour samples were used as positive control. In most cases, mast cells found in the arterial vessels of the tumours or in the surrounding epithelium provided an additional positive control. The differentiation between mast cells and tumour cells was based on the morphology of the cells as well as their topology in the tissue.

Table 17: Neuroendocrine tumour types of patients

Neuroendocrine Tumour types (No of patients)	
Foregut NETs (39)	Ampullary NETs (3)
	Bronchial carcinoids (7)
	Duodenal carcinoids (1)
	Gastric carcinoids (6)
	Oesophageal carcinoids (1)
	Pancreatic NETs (21)
Midgut NETs (27)	Appendiceal carcinoids (7)
	Ileal carcinoids (18)
	Caecal carcinoids (1)
	Jejunal carcinoids (1)
Hindgut NETs (4)	Colon carcinoids (1)
	Rectal carcinoids (2)
	Cervical carcinoids (1)
Medullary Thyroid Carcinomas (5)	-
Paragangliomas (5)	-
Unknown Primary (5)	-

7.2.1 Polyclonal antibody

Staining with the polyclonal antibody revealed C-KIT expression in 24% (20 out of 85) of the patients (examples shown in figure 78 (b-f), positive control GIST section in 78a). The detailed results of the staining with the polyclonal antibody are outlined in table 18, where the intensity of the staining in comparison to the positive control GIST is also demonstrated.

Positive tumour samples included 5/11 upper gastrointestinal NETs, 8/27 midgut NETs, and 4/21 patients with pancreatic neuroendocrine tumours. The rest of the positive samples were 1 case of hindgut NET, and 2 cases of NET of unknown primary site. Staining with the polyclonal anti-C-KIT antibody revealed lack of C-KIT expression in patients with paragangliomas and medullary thyroid carcinomas as shown in figure 78e-f.

Staining with the polyclonal antibody identified C-KIT primarily in the cytoplasm, except in 4 cases where the receptor was also identified in the nucleus or the perinuclear region. Nuclear staining did not correlate with the type of neuroendocrine tumour. For example, figure 79 shows two patients with ileal carcinoid (a-b) with cytoplasmic staining in case (a), and cytoplasmic and nuclear staining in case (b). Paradigms of nuclear staining are also illustrated in figure 79c-d, in nests of tumours cells of a patient with appendiceal carcinoid. Figure 78 also provides two examples of perinuclear staining seen in a patient with oesophageal carcinoid (c), and a patient with ampullary NET (d), in comparison to cytoplasmic staining in a patient with a NET of unknown primary site (b). In 2 of the patients with a gastric carcinoid and a PNET respectively, neuronal staining was also observed (data not shown).

Table 18: Staining with the polyclonal antibody

Specimen (No of +ve patients/total)		Intensity	Comments
Foregut	Ampullary NET (1/3)	2	Perinuclear staining
	Bronchial carcinoid (0/7)	0	
	Duodenal carcinoid (1/1)	0.5	
	Gastric carcinoid (2/6)	2	1 case with cytoplasmic and neuronal staining
	Oesophageal carcinoid (1/1)	2.5	Perinuclear staining
	Pancreatic NET (4/21)	1.5	1 case with cytoplasmic, neuronal and islet staining
Midgut	Appendiceal carcinoid (3/7)	1	1 case with cytoplasmic and nuclear staining
	Ileal carcinoid (5/18)	1.5	1 case with cytoplasmic and nuclear staining
	Caecal carcinoid (0/1)	0	
	Jejunal carcinoid (0/1)	0	
Hindgut	Colon carcinoid (0/1)	0	
	Rectal carcinoid (1/2)	0	
	Cervical carcinoid (0/1)	0	
MTC (0/5)	-	0	
Paraganglioma (0/5)	-	0	
Unknown primary (2/5)	-	1.5	

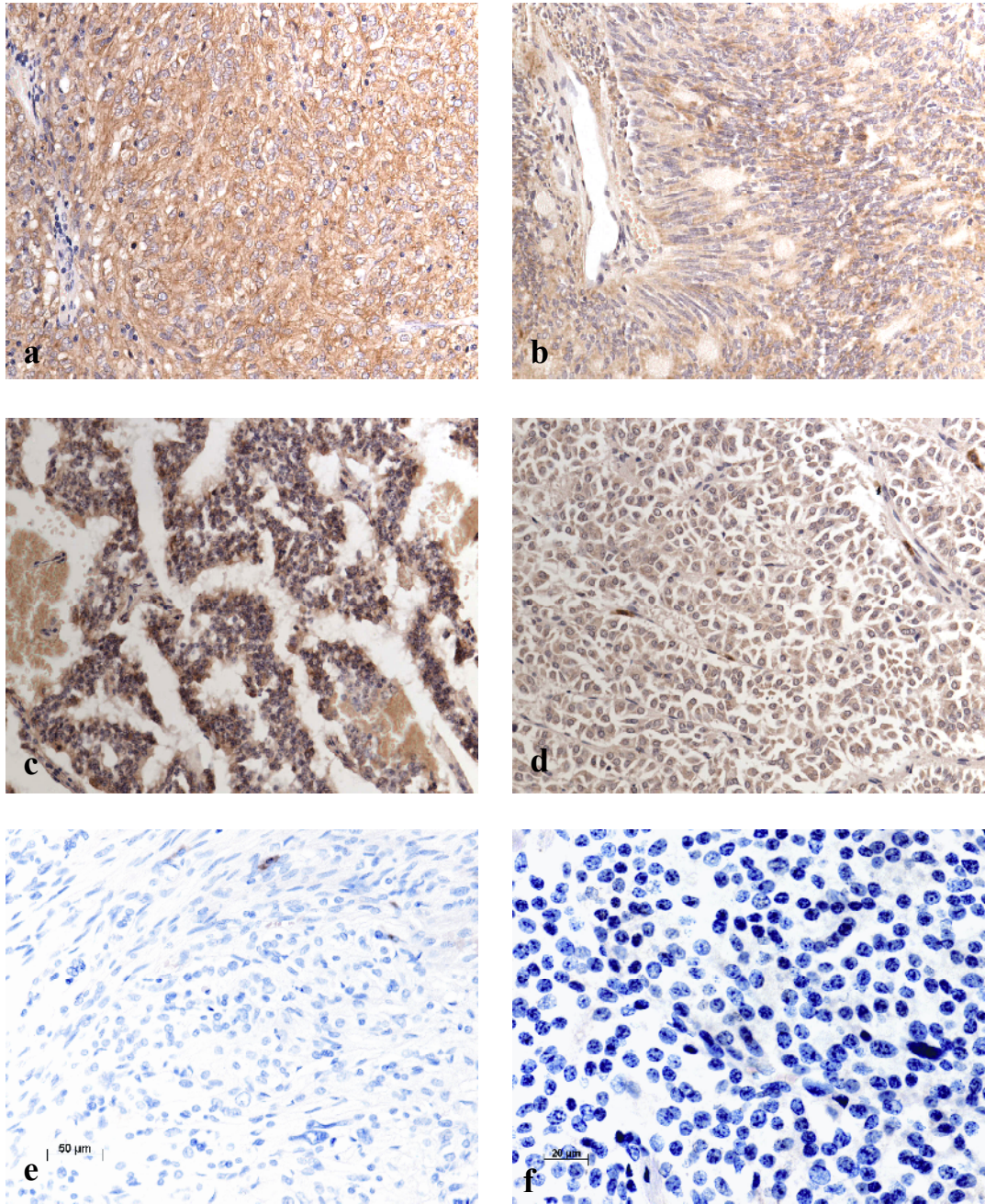


Figure 78: Cases of positive and negative staining with the polyclonal anti-C-KIT antibody. (a) Gastrointestinal stromal tumour (used as a positive control) with strong cytoplasmic staining of tumour cells, (b) Retroperitoneal mass NET of unknown primary site containing partly crushed epithelial cells with moderate to strong cytoplasmic staining, (c) Oesophageal carcinoid with moderate to strong cytoplasmic and perinuclear staining of tumour cells, (d) Ampullary NET with staining of the cytoplasm and nuclear membranes, (e) Paraganglioma where we have no staining of the tumour but positive staining of mast cells, (f) Medullary carcinoma of thyroid negative for C-KIT. Magnification a-e: (x20) and f: (x40)

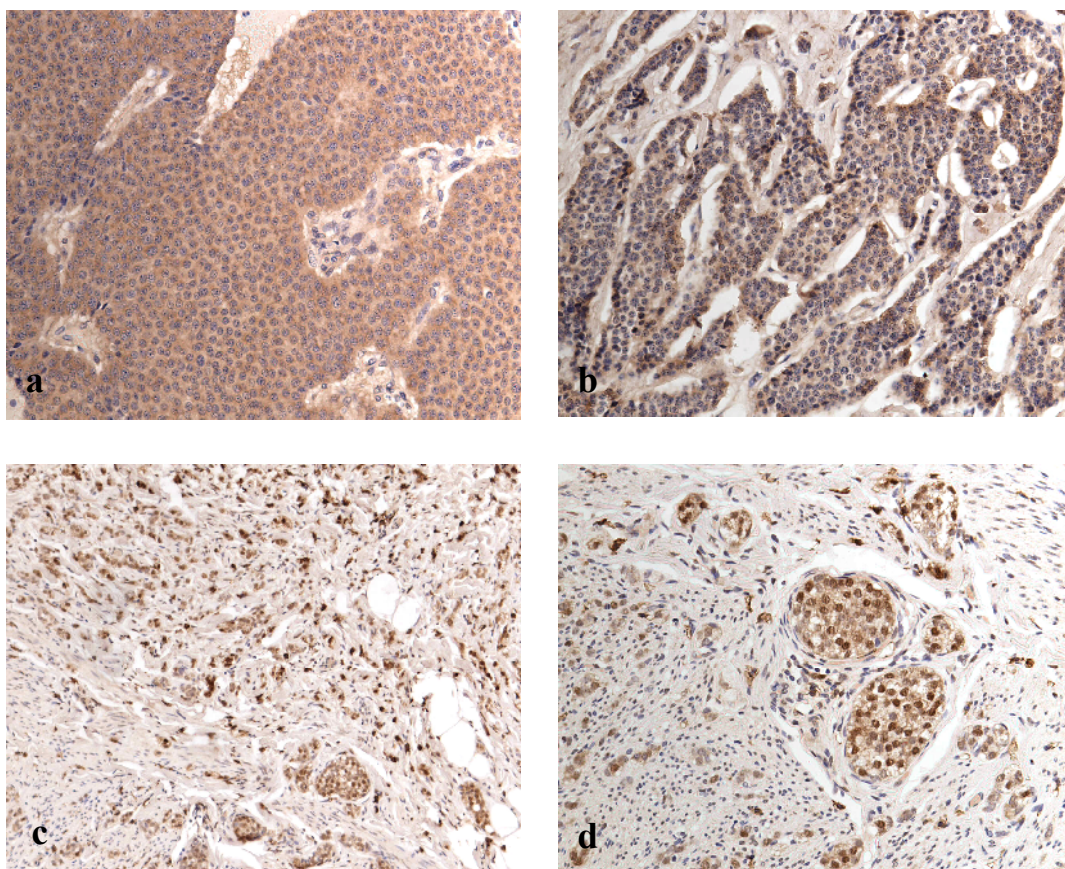


Figure 79: Examples of cytoplasmic and nuclear C-KIT staining with the polyclonal anti-C-KIT antibody. (a) Ileal carcinoid with strong cytoplasmic staining of tumour cells, (b) Ileal carcinoid with cytoplasmic staining and sporadic nuclear staining, (c-d) Appendiceal carcinoids (photos from same patient) of positively stained tumour cells infiltrating the submucosa of the appendix, where nuclei also stain positive. Magnification a,b,d: (x20) and c: (x10)

7.2.2 Monoclonal antibody

The results for the staining with the monoclonal antibody are outlined in detail in table 19. A significant increase in C-KIT expression was identified in the immunohistochemical analysis with the monoclonal antibody, with 64% (50 out of 79 – due to lack of available tissue) of the patients expressing the receptor. C-KIT expression was predominantly increased in pancreatic NETs and in NETs of unknown primary site, which were both 80% positive (16/20 PNETs and 4/5 unknown). High levels of expression were also found in midgut NETs (19/26), and upper G.I NETs (7/11). Staining with the monoclonal antibody also identified the receptor in one patient with bronchial carcinoid and one patient with paraganglioma, both of which types of NETs were negative for the polyclonal antibody.

Table 19: Staining with the monoclonal antibody

Specimen (No of +ve patients/total)		Intensity	Comments
Foregut	Ampullary NET (2/3)	1.5	1 case with apical staining
	Bronchial carcinoid (1/4)	1.5	
	Duodenal carcinoid (1/1)	1	
	Gastric carcinoid (3/6)	2	1 case with nuclear staining
	Oesophageal carcinoid (1/1)	1	
	Pancreatic NET (16/20)	2	7 cases with apical staining and 1 with both cytoplasmic and apical staining
Midgut	Appendiceal carcinoid (5/6)	2.5	3 cases with apical staining
	Ileal carcinoid (13/18)	3	7 cases with apical staining and 2 with both cytoplasmic and apical staining
	Caecal carcinoid (1/1)	2	Apical staining
	Jejunal carcinoid (0/1)		
Hindgut	Colon carcinoid (1/1)	1	
	Rectal carcinoid (1/1)	2	Cytoplasmic and apical staining
	Cervical carcinoid (0/1)	0	
MTC (0/5)		0	
Paraganglioma (1/5)		2	
Unknown primary (4/5)		2.5	1 case with apical staining

With the monoclonal antibody, the expression of the receptor in half of the patients was markedly increased around the edges of tumour nests, with low concentrations in the cytoplasm. Examples of this so called apical staining are shown in figure 81a and 81c.

Nuclear staining was identified in one patient only with gastric carcinoid. Medullary thyroid carcinoma sections were all negative with the monoclonal antibody as with the polyclonal one.

7.2.3 Comparison of the two immunohistochemical studies

As the aim was to determine any differences in C-KIT expression between the polyclonal and monoclonal antibody, we used sequential tissue sections from each patient (tissue for comparison was available in 79/85 patients). The differences in staining of neuroendocrine tumour cell types between the two antibodies are outlined in table 20.

Table 20: Expression C-KIT in NET patients using the monoclonal and the polyclonal anti C-KIT antibodies

Specimen	Specimen	Monoclonal	Polyclonal
Foregut NETs	Bronchial NETs	1/4 (25%)	0/7 (0%)
	Upper G.I NETs	7/11 (64%)	5/11 (45%)
	Pancreatic NETs	16/20 (80%)	4/21 (19%)
Midgut NETs		19/26 (73%)	8/27 (30%)
Hindgut NETs		2/3 (66%)	1/4 (25%)
MTCs		0/5 (0%)	0/5 (0%)
Paragangliomas		1/5 (20%)	0/5 (0%)
Unknown primary		4/5 (80%)	2/5 (40%)

Comparison between the two immunostainings revealed 13 patients showing positivity with both antibodies (examples shown in figure 80), 37 patients showing expression of C-KIT with the monoclonal antibody only (examples shown in figure 81), 7 patients being positive for C-KIT with the polyclonal antibody only, and 27 cases negative for both antibodies, most notably all cases of medullary thyroid carcinoma (examples shown in figure 82). The main divergence between the two antibodies is seen in pancreatic NETs and midgut NETs, where positivity is increased by a factor of 4 and 2.4 respectively with the monoclonal antibody.

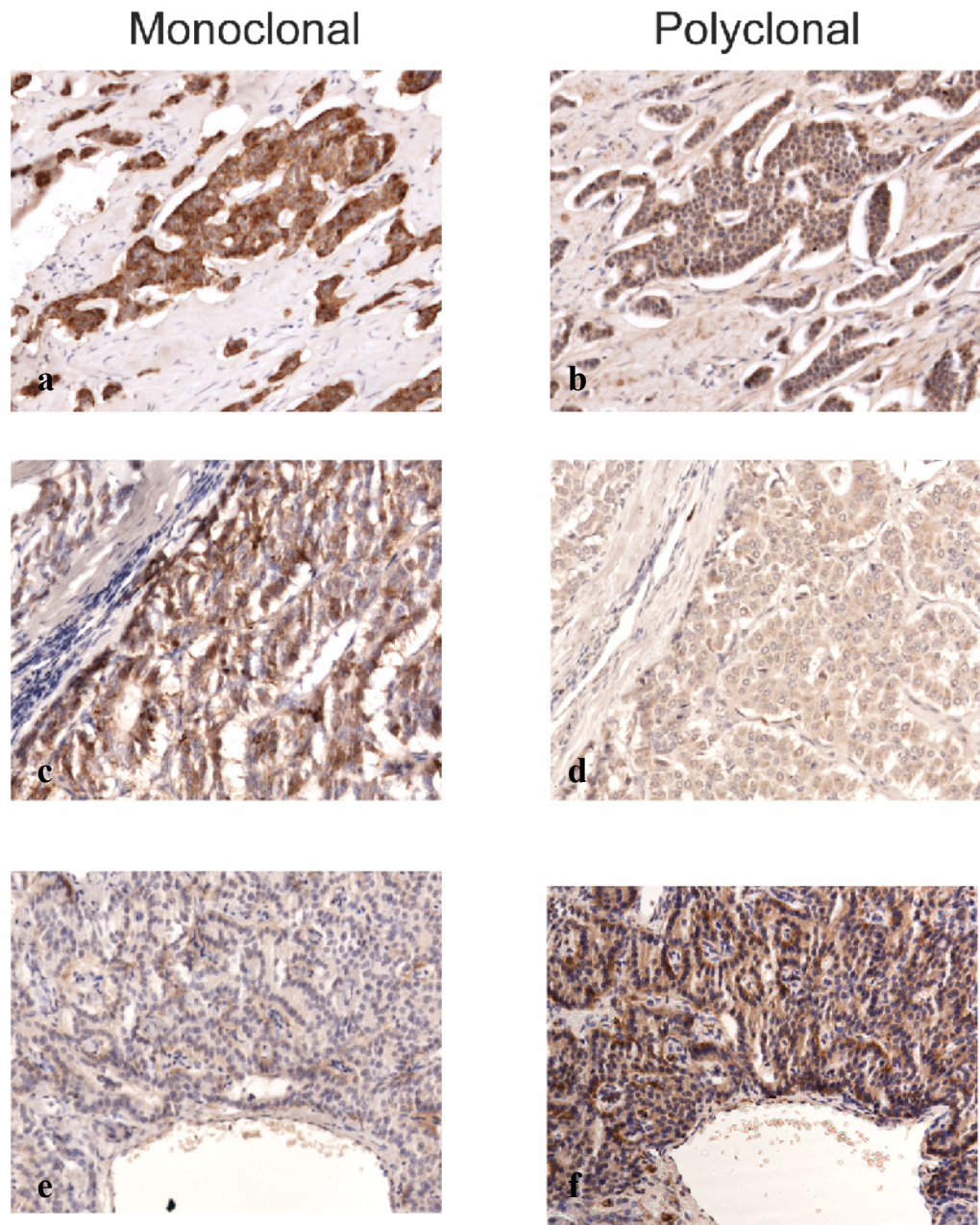
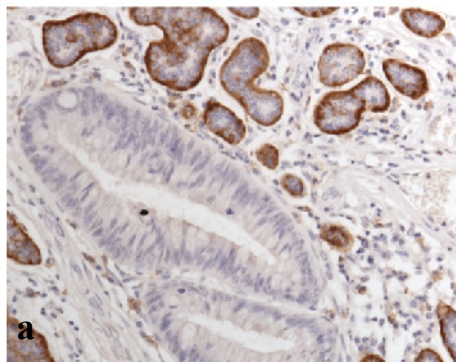


Figure 80: C-KIT expression by both antibodies: (a-b) Ileal carcinoid where strong cytoplasmic staining is seen in tumour cells, (c-d) pancreatic neuroendocrine tumour with strong cytoplasmic staining with the monoclonal antibody and medium staining with the polyclonal antibody, (e-f) pancreatic neuroendocrine tumour where stronger cytoplasmic staining is seen with the polyclonal antibody. Magnification a-f: (x20)

Monoclonal



Polyclonal

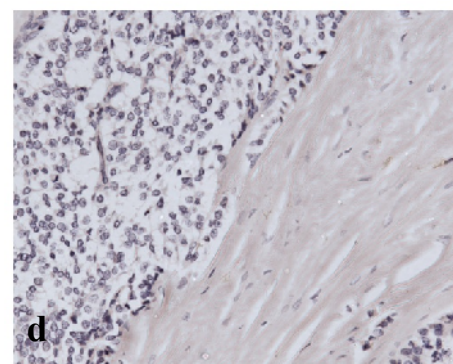
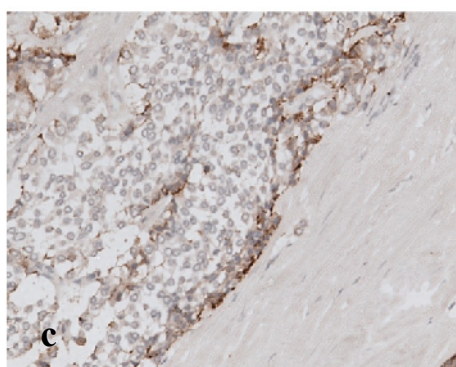
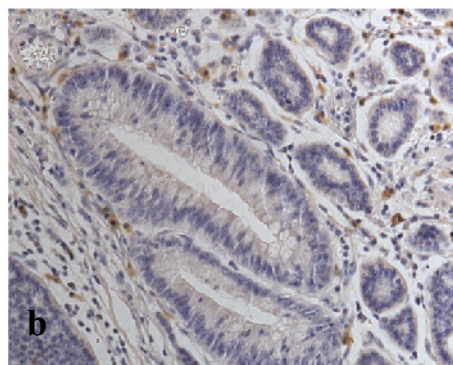


Figure 81: C-KIT expression with the monoclonal antibody only: (a-b) Ileum carcinoid where the more common apical staining of tumour cells is seen with the monoclonal antibody, but no cells stain positive with the polyclonal antibody (C-KIT positive mast cells are seen that serve as an internal positive control), (c-d) carcinoid tumour of the pancreas with moderate apical staining of tumour cells with the monoclonal antibody and again no staining with the polyclonal one. Magnification a-d: (x20)

Monoclonal

Polyclonal

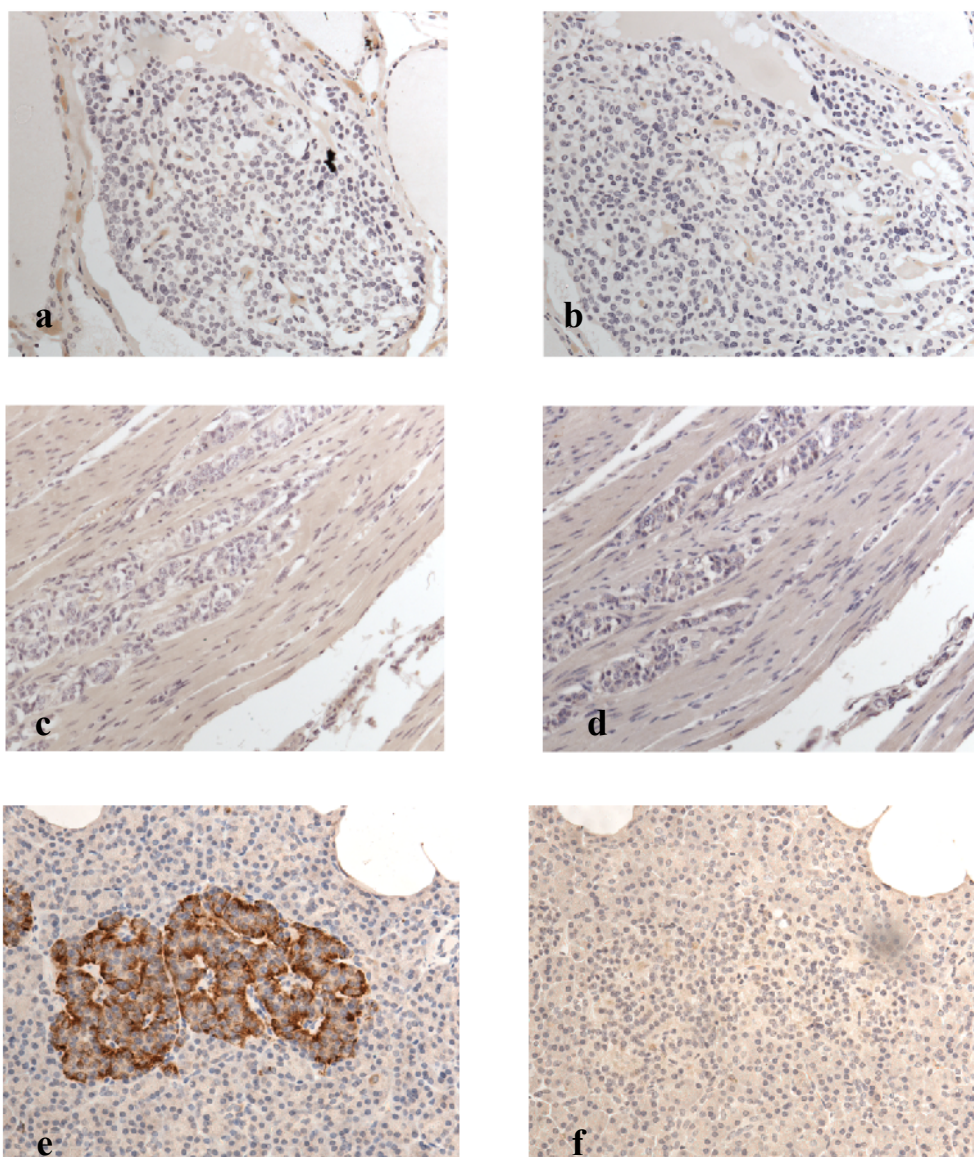


Figure 82: No C-KIT expression of tumour cells with either antibody: (a-b) medullary thyroid carcinoma, (c-d) carcinoid tumour of the duodenum, (e-f) PNETs showing normal pancreatic islets expressing C-KIT when stained with the monoclonal antibody, but no staining of tumour cells with either antibody. Magnification a-f: (x20)

The expression of C-KIT was also analysed in a panel of neuroendocrine tumour cell lines including the human bronchial carcinoid NCI-H727 cells, the human small cell lung cancer SHP-77 cells, and the rat islet CRI-G1 and RIN-5F cell lines, as shown in appendix 4. Following the established expression of C-KIT in our cells, we conducted preliminary experiments to examine the anti-proliferative effect of imatinib in these

cells. Imatinib showed no effective cytotoxic activity in any of the cell lines used and experiments were discontinued.

7.3 Discussion

7.3.1 *C-KIT* prognostic value in cancer

For the past decade C-KIT has been identified in a variety of tumour cells and its expression could be associated with a poor outcome for patients. C-KIT has therefore become an attractive target for the use of tyrosine kinase inhibitors such as imatinib that is used for the treatment of C-KIT positive GISTs.

Although much research has been performed on the expression of C-KIT in tumour cells, information in the literature about the significance of the receptor's mutations or autocrine activation in tumour progression is not comprehensive. In a study by Scotlandi *et al.*, (2003) C-KIT had no significant prognostic or therapeutic value in Ewing's sarcoma, which is characterised by autocrine/paracrine activation of the receptor. Treatment with STI-571 yielded a low degree of inhibition with small clinical importance but could be used in patients that overexpress C-KIT. In addition, no correlation was found between developmental stage of endocrine pancreatic tumours and expression of C-KIT (Fjallskog *et al.*, 2003). No examination of mutations or overexpression of the oncoprotein was demonstrated by this group to account for the role of C-KIT in tumour development. Analysis of *C-KIT* mutations in tumour development by Sakurai *et al.*, (1999) showed that the mutated form of the receptor (activating mutation in exon 11 of the *C-KIT* gene) was found equally in low- and high-risk groups of GIST patients, showing no correlation to the Ki-67 labelling index. Based on these results C-KIT may be considered a target for therapy with tyrosine kinase inhibitors but its role in tumour growth remains unclear.

In contrast to Sakurai's results, clinical analysis of 48 patients with GISTs by a different group (Blanke *et al.*, 2001) proved that the type of *C-KIT* mutation may predict the behaviour of the tumour. Deletions/insertions in exon 11 had the lowest recurrent free survival rate of all other mutations including missense mutations in exon 11 or mutations in exons 9, 13 or 17 or when compared with patients who had no identified mutations. Also, treatment with imatinib was shown to be more effective in GIST patients that carry a mutation in *C-KIT* than in those without a mutation, which

proves the significance of mutations in the clinical outcome of GISTs (Blanke *et al.*, 2001). Furthermore, *C-KIT* mutations appear to be important in tumour progression of mast cells in dogs (Zemke *et al.*, 2002). In this study mutations in the juxtamembrane domain of the oncoprotein were found in 12/64 grade II and grade III tumours but none were found in grade I tumours (grade I being the least aggressive tumour type, grade II intermediate, and grade III characterises poorly differentiated tumour cells, which grow rapidly). The mutations were mainly duplications and deletions which lead to constitutive activation of the receptor. Interestingly, a study in 36 GIST patients, which were all C-KIT positive, showed co-expression of the C-KIT ligand SCF in 21 cases, and this was associated with a higher MIB-1 proliferation index, indicating that co-expression of receptor and ligand could be a marker of tumour proliferation (Hirano *et al.*, 2008). In addition, a study by Erler *et al.* showed that C-KIT was overexpressed in a high percentage (66%, 54/82) of high-grade NETs but was not overexpressed in low or intermediate-grade NETs. Overexpression of C-KIT did not appear though to affect the aggressiveness of the tumour growth in terms of affecting survival (Erler *et al.*, 2004).

Recent studies have demonstrated association of C-KIT expression with neuroendocrine tumour development. C-KIT expression was related to poor prognosis in patients with small cell lung cancer (SCLC) and large cell neuroendocrine carcinoma (LCNEC), as it was associated with advanced disease and poor response to chemotherapy for SCLC patients or decreased survival and recurrence in LCNEC patients (Micke *et al.*, 2003; Casali *et al.*, 2004). In addition, C-KIT immunoreactivity was also identified in 26% of patients with gastrointestinal neuroendocrine carcinoma, a tumour characterised by aggressive behaviour and poor prognosis (Ishikubo *et al.*, 2006). Finally, Ferrari *et al.* evaluated the correlation between C-KIT and the Ki-67 proliferation index in neuroendocrine tumours and showed that 8 out of 11 samples immunoreactive for C-KIT had poorly differentiated histology, which is associated with a high proliferation index. No reference was made on mutations present in the C-KIT oncoprotein (Ferrari *et al.*, 2006). Based on the above results, and the therapeutic efficacy of imatinib in GISTs expressing C-KIT, we investigated the expression of C-KIT in a large number of NET patients with the aim to justify the use of imatinib for therapy.

As discussed earlier in this chapter, our primary interest was to study the variability in C-KIT immunoexpression in neuroendocrine tumour cells, which has been previously demonstrated by other groups (Tsuura *et al.*, 1994; Welin *et al.*, 2006; Fjallskog *et al.*, 2003; Ishikubo *et al.*, 2006). As these differences have been attributed to different antibodies or different immunohistochemical protocols used, we decided to use two commonly used antibodies, one polyclonal and one monoclonal antibody, while keeping the same protocol for the two staining procedures.

7.3.2 Comparison of monoclonal and polyclonal immunohistochemical studies

Our immunohistochemical analysis identified the C-KIT receptor in 24% of the patients with the polyclonal antibody and in 64% of the patients with the monoclonal antibody. This difference was not correlated with the type of tumour carried by the patient or with the organ affected by the tumour. With the polyclonal antibody from DAKO, C-KIT immunoreactivity was mostly observed in carcinoids. On the other hand, the monoclonal antibody from Novocastra identified the expression of C-KIT mostly in PNETs. By comparing the two immunohistochemical procedures we conclude that the monoclonal antibody showed a 2-fold increase in C-KIT expression in carcinoid patients (65% mAb versus 28% pAb) and a 4-fold increase in PNET patients (80% mAb versus 19% pAb).

The difference could not be accounted for by lack of specificity of the polyclonal antibody (DAKO). Assessment of the two most common antibodies from DAKO and Santa Cruz used in research against C-KIT supported the view of the DAKO product being the more specific antibody (Lucas *et al.*, 2003). The polyclonal antibody by DAKO is widely used and in a large comparative study of seven C-KIT antibodies in more than 3000 tumours, the DAKO antibody was found to be the most specific (Went *et al.*, 2004). Is the variability due to the different epitope being recognised by the two antibodies? If it is easier for an antibody to bind the extracellular portion of an antigen (recognised by the monoclonal antibody), heat-induced epitope retrieval should diminish such a possibility. On the other hand, the tissue sections used in this study derived from tumour tissue samples which were formalin fixed and embedded in paraffin, and were up to 5 years old. Prolonged storage has been associated with epitope fading and this could explain the fewer positive cases observed with the polyclonal antibody, if its particular epitope was affected. Finally, mutations present in

the cytoplasmic part of the receptor, which is recognised by the polyclonal antibody, could account for the smaller number of positive cases observed. In this case the difference could only be explained by mutation studies in both extracellular and intracellular sequences recognised by the two antibodies in all patients tested and this forms the next step in our research.

For analysis of the two antibody stainings, proper precautions were taken to ensure accuracy of the results. Firstly, sections of GIST, which is known to overexpress C-KIT, were used as a primary positive control. In addition, since C-KIT is a haematopoietic stem cell marker, mast cells present in the tissue served as a supplementary internal positive control, and have been used as such by other groups (Lucas *et al.*, 2003; Miettinen & Lasota, 2005). For negative controls, we used sequential sections for each sample where the primary antibody was omitted. GIST and mast cells strongly expressed C-KIT with both antibodies used. Analysis of the sections was carried out by two separate histopathologists at the Royal Free Hospital, with years of experience in immunohistochemistry. To further prove the accuracy of our results, it is a well known fact that one characteristic element of true positive staining is the difference in the intensity of staining among cells, commonly known as ‘cell to cell heterogeneity’, a feature observed in all of our sections with both antibodies. Finally, for each antibody appropriate titrations were made to identify the most appropriate dilution, in order to avoid non-specific binding of the antibody.

It is worth noting that the polyclonal antibody has positioned C-KIT mainly in the cytoplasm whereas the monoclonal antibody has, in more than half the cases, identified the receptor mostly in the plasma membrane with low concentrations in the cytoplasm. C-KIT is a plasma membrane protein which would justify the accuracy of the monoclonal antibody. On the other hand, although the polyclonal antibody identified the protein mostly in the cytoplasm, there were cases where C-KIT was also identified in the plasma membrane with the same antibody. In addition, C-KIT cytoplasmic staining was also identified with the monoclonal antibody, but in fewer cases. Finally, the polyclonal antibody also revealed nuclear or perinuclear staining in 4 patients, not correlating to the type of NET present, while the monoclonal antibody shown nuclear

C-KIT expression in one patient, a phenomenon which, to our knowledge, has not been discussed previously.

Nevertheless, diagnosis of NETs is not based solely on a single marker. Patients tested with both antibodies should combine this with identification of other NETs markers such as the chromogranins, the NSE or CEA (Lamberts *et al.*, 2001, Eriksson *et al.*, 2000), the secretion of peptide hormones and amines such as serotonin, insulin, gastrin, glucagon, or VIP, as well as the presence of clinical syndromes associated with NETs.

7.3.3 Comparison of this study with results from other groups

Our immunohistochemical study demonstrated the presence of C-KIT (CD117) in gastroenteropancreatic neuroendocrine tumours. Positive immunoreactivity was established in a range of tumours that included foregut NETs (mainly pancreatic NETs and gastric carcinoids), midgut NETs (mainly ileal and appendiceal carcinoids), hindgut NETs, and NETs of unknown primary site. This is in contrast with a study by Tsuura *et al.*, (1994) where no expression of C-KIT was detected in NETs. The antibody used by Tsuura and co-workers (1994) was the same polyclonal DAKO antibody used in our analysis, so any discrepancy observed may be due to the method employed or other reagents used.

The difference in results obtained by different scientific groups is difficult to examine, not only due to different immunohistochemical procedures being used but also due to the biological heterogeneity of NETs. NETs are divided into many different groups according to the tissue type they arise from and they have different receptor expression patterns, and this could also depend on whether the tumour is malignant or not. Welin *et al.* found no immunoreactivity to C-KIT in malignant midgut carcinoid tumours (Welin *et al.*, 2006). On the other hand, a group from Sweden showed a 92% expression of C-KIT in malignant endocrine pancreatic tumours (Fjallskog *et al.*, 2003).

7.3.4 Imatinib as a therapeutic option for NET patients

In vitro studies have demonstrated positive antitumour activity by imatinib in a variety of tumours. Imatinib was shown to inhibit the growth of aggressive neuroblastic tumours (Vitali *et al.*, 2003). Furthermore, Lankat-Buttgereit *et al.* showed that imatinib

inhibits the cell growth of insulinomas, gastrinomas, and carcinoids independently of KIT expression (Lankat-Buttgereit *et al.*, 2005). Preliminary proliferation studies in neuroendocrine tumour cell lines expressing C-KIT showed no effect on growth of cells by imatinib (data not shown). As a result, this part of the study was not pursued any further.

For patients with neuroendocrine tumours, treatment with imatinib as a single agent has not shown promising response rates. In a phase II trial of imatinib in patients with advanced carcinoid tumour, only a modest effect on tumour growth was shown (Carr *et al.*, 2004). C-KIT is overexpressed in up to 70% of cases of small cell lung cancer. Based on this fact 29 patients with recurrent and refractory small cell lung cancer immunoreactive to C-KIT were treated with imatinib at 400 mg twice a day for 28 days. Imatinib did not demonstrate an objective response or confirm stable disease (Dy *et al.*, 2005). Similar results were obtained in a phase II clinical trial by Krug *et al.* (Krug *et al.*, 2005). In another phase II trial in patients with advanced metastatic melanoma imatinib demonstrated lack of efficacy (Ugurel *et al.*, 2005). Finally, in a phase II multi-center study of 15 patients with disseminated endocrine tumours including medullary thyroid carcinomas (MTC), adrenocortical carcinomas (ACC), malignant pheochromocytomas, carcinoids, and neuroendocrine tumours, imatinib was not found useful for treatment and caused increased toxicity in the group of patients (Gross *et al.*, 2006).

The above findings might suggest that the use of imatinib as a single agent does not prove sufficient antitumour activity, but combination with other chemotherapeutic agents could be of benefit. Gronchi *et al.* recently showed auxiliary treatment with imatinib in patients with GISTs can delay the progression of the disease (Gronchi *et al.*, 2007). In addition, Blackstein *et al.* demonstrated that the response rate and progression-free survival in patients with GISTs that are C-KIT negative was not different from those with C-KIT positive GISTs, implying that a therapeutic trial of imatinib may be helpful for all patients with GISTs regardless of C-KIT expression (Blackstein *et al.*, 2006).

Finally, a most recently identified problem with imatinib treatment is that GIST patients treated with imatinib usually develop resistance to the drug after about 2 years of drug

administration (Braconi *et al.*, 2008; Jiang *et al.*, 2008). This is mainly due to the acquisition of secondary mutations in the tyrosine kinase domain of C-KIT, which is recognized by the drug. This problem has led to the development of new tyrosine kinase inhibitors with multiple targets, such as sunitinib, which targets C-KIT, PDGFR, VEGFR, and FMS-related tyrosine kinase 3 receptor, and has shown efficacy in a number of relapsing patients (Braconi *et al.*, 2008; Jiang *et al.*, 2008). Recent clinical trials of sunitinib in NETs have shown very promising results (Kulke *et al.*, 2008), and most recently a study of sunitinib versus placebo in non-functioning NET patients had to be stopped early after interim analysis demonstrated a significant survival benefit in the sunitinib treated group (Raymond *et al.*, 2009).

7.3.5 Conclusions

Based on our study C-KIT may play a pivotal role in neuroendocrine tumour growth and affect the clinical outcome. We have identified C-KIT expression using immunohistochemical studies with two antibodies against different epitopes in a significant percentage of patients with NETs. Further exploration of its expression status as well as sequence analysis is needed in order to investigate its role in the pathology of NETs. Generally, the lack of clinically relevant anti-proliferative activity by imatinib in neuroendocrine tumour patients could be because C-KIT is not the driving force in these tumours. Expression of an oncogene in specific tumour cell types may not necessarily imply therapeutic potential of drugs against this oncogene, and a prime example for this is gefitinib, a widely used inhibitor of EGFR that failed to prolong survival in 90% of patients with non-small cell lung cancer overexpressing EGFR, in contrast to preclinical studies. Another reason could be the presence of mutations in the tyrosine kinase domain of the receptor that disable efficacy of the drug in neuroendocrine tumour cells. This justifies the need for analysis of the C-KIT receptor for mutations in individual patients to help prognosis and evaluation of the appropriate therapeutic modes. Finally, it is a well known fact that tyrosine kinase inhibitors may cross-react with other tyrosine kinases, in the case of imatinib with PDGFR (both α and β), and this may result in different activity profiles. Therefore identification of other tyrosine kinases such as PDGFR, which have also shown response to imatinib, may help unravel the mechanism of drug action in these patients.

CHAPTER 8

INVESTIGATION OF COMBINATION TREATMENTS USING OCTREOTIDE WITH CHEMOTHERAPEUTIC AGENTS IN NET CELLS

8.1 Introduction

The final receptor target analysed for any anti-proliferative effect in NETs was the group of somatostatin receptors. Somatostatin (SST) is a gastrointestinal and hypothalamic peptide hormone found in the gastric mucosa, the pancreatic islets, the nerves of the gastrointestinal tract, and in the central nervous system. It inhibits endocrine and exocrine secretions, intestinal motility and cell proliferation (Bousquet *et al.*, 2004). Somatostatin binds somatostatin receptors (SSTR1-SSTR5), which belong to the family of G-protein coupled receptors. Somatostatin receptors are expressed in neuroendocrine tumours, with the SSTR2 subtype being the most frequently expressed. The presence of SST receptors has greatly aided diagnosis and treatment of neuroendocrine tumours via binding of SST analogues. These compounds are not only used for symptomatic relief of patients but also for the localisation and treatment of primary and metastatic tumours expressing SSTRs via somatostatin receptor scintigraphy (SRS) and somatostatin receptor-targeted radiotherapy respectively. Of all existing somatostatin analogues, octreotide has been the most extensively investigated.

Octreotide, binds SSTR2 and SSTR5 with high affinity, SSTR3 with moderate affinity, but does not bind SSTR1 and SSTR4 subtypes. Somatostatin analogues have demonstrated anti-neoplastic activity in a variety of experimental models *in vitro* and *in vivo* including mammary, pancreatic, colorectal, and lung cancers (Weckbecker *et al.*, 1993). Octreotide has also shown anti-proliferative effects *in vitro* against gastric and pancreatic adenocarcinoma cells (Hofsli *et al.*, 2002, Wang *et al.*, 2003). In addition, combinations of octreotide with cytotoxic drugs such as 5-fluorouracil, mitomycin C, paclitaxel, and doxorubicin resulted in synergistic or additive interactions in AR42J cells (Weckbecker *et al.*, 1996), and with rofecoxib in gastric cancer SGC-7901 cells (Tang *et al.*, 2004). In human studies the effects have been variable with tumour growth stabilisation reported in up to 50% of NET patients. Less than 10% of the patients demonstrated tumour regression, and in most of these cases octreotide treatment was combined with chemotherapy, chemoembolisation or alpha-interferon, making it difficult to assess the anti-proliferative effect of octreotide alone (Leong & Pasieka, 2002).

Aims

Our aim was to investigate the role of somatostatin receptors in neuroendocrine tumour cell growth. To this end, we examined the expression of SST receptors in neuroendocrine tumours cell lines and whether such receptors, when expressed, may transmit growth inhibitory signals following binding of the somatostatin analogue octreotide. Treatments included octreotide acting as a single agent or together with commonly used chemotherapy drugs cisplatin, etoposide, melphalan as well as the non-covalent DNA binding agent doxorubicin. The SRB proliferation assay was used to determine survival in octreotide-treated cells with or without the cytotoxic agents. Flow cytometry was also used to investigate any effect of octreotide on the cell cycle of NET cells. The presence of SSTR2A and SSTR5, but not SSTR1 or SSTR3 was identified by immunoblotting.

8.2 Results

8.2.1 *SSTR expression in NETs*

Initially, the expression of SSTR2A and SSTR5 but not SSTR1 or SSTR3 was demonstrated by immunoblotting in NCI-H727 human bronchial carcinoid, BON-1 human pancreatic endocrine cells, and the two rat islet tumour cells RIN-5F and CRI-G1 (figure 83). The expression of SST receptors was also identified in HCT-116 colon cancer cell line. For this, we used four monoclonal rabbit antibodies against human SSTR1, SSTR2A, SSTR3 and SSTR5 from Gramsch Laboratories, Germany. This experiment confirmed the expression of SST receptors with high affinity to octreotide in neuroendocrine tumours cells, justifying the use of octreotide in our proliferation studies.

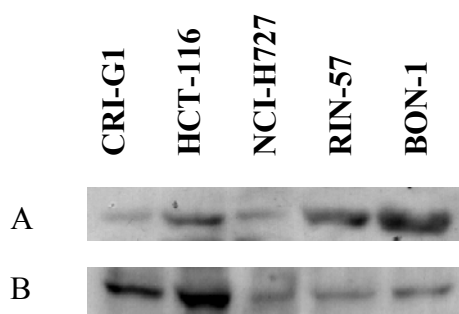


Figure 83: Total cell lysates of CRI-G1, HCT-116, NCI-H727, RIN-5F and BON-1 cells were immunoblotted for A. SSTR2A (80kDa) B: SSTR5 (65kDa). The antibodies were used at a 1:4000 dilution from a 25µl stock in distilled water.

8.2.2 Proliferation studies using octreotide with chemotherapy

Octreotide, alone or in combination with cisplatin, etoposide, doxorubicin or melphalan, was tested for its cytotoxic effect in NCI-H727, CRI-G1, BON-1, and RIN-5F cells. Graphs show results for NCI-H727 cells only, with results for the other cell lines added in the appendix 5A-5D.

Administered schedules included:

- Simultaneous addition of octreotide (at 10 or 1000nM) and cisplatin, etoposide doxorubicin or melphalan for a period of 72 hours
- Incubation of cells with octreotide (at 10 or 1000nM) for 24 hours, followed by 48 hour incubation with cisplatin, etoposide doxorubicin or melphalan
 - Cytotoxic drugs were added at 0-100µM for cisplatin, etoposide and melphalan, and at 0-10µM for doxorubicin
 - Drug incubations were followed by 2 days incubation in drug-free media before analysis

Single treatments

Octreotide was added at 0-1000nM for 24 or 72 hours. Treatment with octreotide as a single agent had no effect on the proliferation of NCI-H727, CRI-G1, BON-1 and RIN-5F cells (figure 84, appendix 5A for all other cell lines). All chemotherapy drugs used had a dose-dependent effect on all four cell lines tested (figures 85-86, appendix 5B-5D for all other cell lines). The IC₅₀s of cytotoxic drugs for the standard 3-day experiment are outlined in table 21.

Doxorubicin is the most effective drug with an average IC₅₀ of less than 1µM in all 4 cell lines. Cisplatin follows with an average IC₅₀ of less than 10µM in 3 out of the 4 cell lines used, but is less potent in BON-1 cells, where 50% decrease in cell proliferation is seen at ~50µM. Etoposide and melphalan are most effective against the rat islet tumour cells CRI-G1 and RIN-5F, with an average IC₅₀ of less than 10µM. Etoposide is also effective in NCI-H727 bronchial carcinoid cells where proliferation was inhibited by 50% at ~9µM. Melphalan is the least cytotoxic drug for NCI-H727 and BON-1 cell lines.

Table 21: IC₅₀s of chemotherapy drugs in NET cell lines

	BON-1	CRI-G1	NCI-H727	RIN-5F
Cisplatin (μM)	53 ± 6.21	8.2 ± 0.75	8.9 ± 0.87	1.7 ± 0.48
Etoposide (μM)	55 ± 5.63	3.5 ± 0.39	9.2 ± 0.68	2.3 ± 0.63
Doxorubicin (μM)	0.33 ± 0.051	0.37 ± 0.072	0.67 ± 0.084	0.028 ± 0.003
Melphalan (μM)	82 ± 7.25	8.1 ± 0.93	51 ± 4.34	3.1 ± 0.64

Note: IC₅₀s of treatments with drugs for a period of 3 days followed by 2 days in complete media. The values represent means of 3 independent experiments, each done in triplicate, with standard deviation.

Double treatments

To test whether addition of octreotide to the chemotherapy treatment would increase the anti-proliferative effect of either single treatment, we decided to treat cells with octreotide and each chemotherapeutic agent either simultaneously or with one type of drug treatment following the second as mentioned in the administered schedules above.

In simultaneous combination treatments (figures 85-86) with cisplatin, etoposide, doxorubicin or melphalan, octreotide -at 10 or 1000nM- did not increase the anti-proliferative effect of the anti-cancer drugs. Data are shown for NCI-H727 cells while treatments for all other cell lines are included in the appendix 5B-5D. Cytotoxic drugs had a dose-dependent effect on cell proliferation in all cell lines. The most cytotoxic drug was doxorubicin with IC₅₀s below 1μM in all cells. Cisplatin and etoposide have a similar cytotoxic effect in all cell lines, with NCI-H727 bronchial carcinoid cells and CRI-G1 and RIN-5F rat islet cells being more sensitive to these agents compared to BON-1 cells. BON-1 pancreatic endocrine cells are more chemo-resistant compared to all other cell lines used, while CRI-G1 and RIN-5F cells are the most chemo-sensitive.

In sequential combination treatments (figures 87-88, data shown for NCI-H727 cells only), octreotide or medium alone (control) was added to the cells for 24 hours, followed by addition of chemotherapy drugs for 48 hours. Again, as in the simultaneous double treatments, addition of octreotide did not increase the cytotoxic effect of chemotherapy alone. All chemotherapeutic agents were less cytotoxic in this

experiment as they were added for 48 hours instead of 72. Pre-treatment with chemotherapeutic agents before addition of octreotide was also tested with similar results in all cell lines (data not shown).

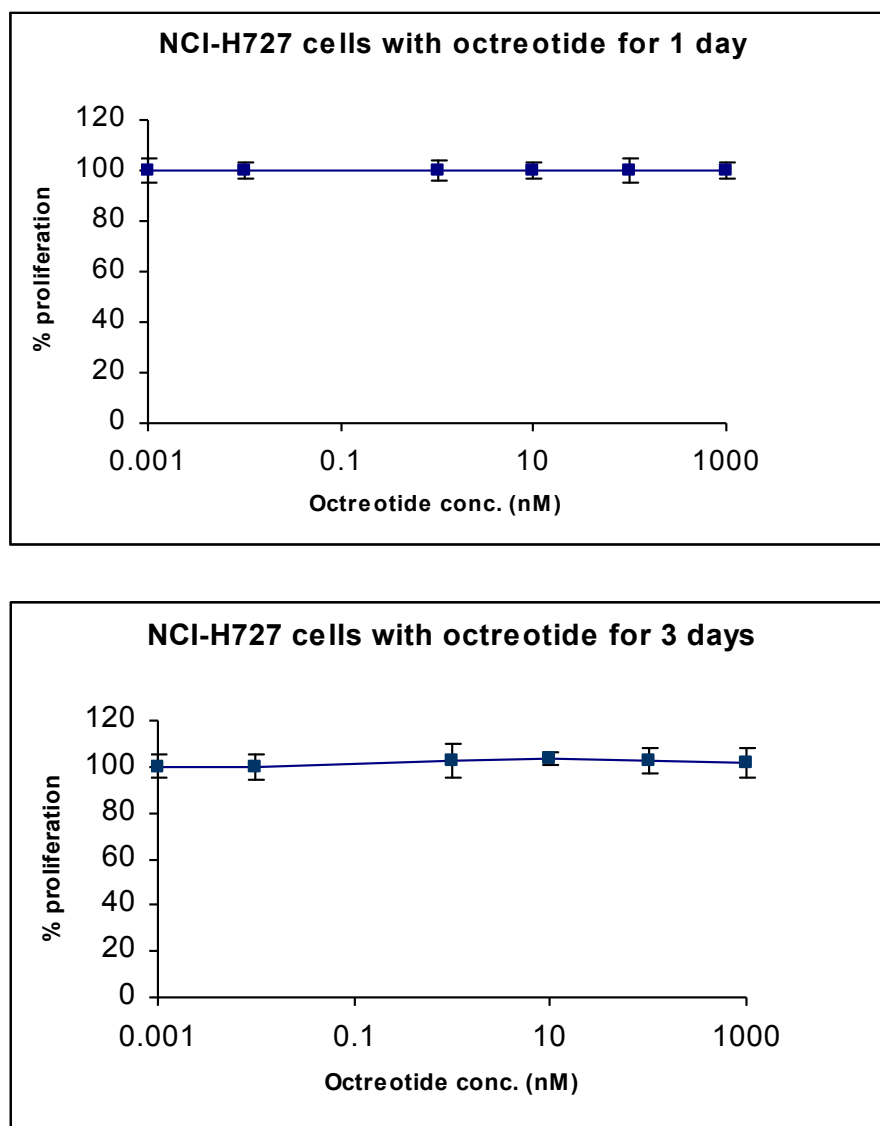


Figure 84: Titration of octreotide in NCI-H727 cells. Cells were treated with octreotide at 0-1000nM for 24 or 72 hours followed by 2 days incubation in drug free media. In the graphs, the '0' point of the x-axis is represented as '0.001' due to the logarithmic scale of the x-axis. Proliferation was calculated as a % of control untreated cells. The values represent averages of 3 different experiments, each performed in triplicate; *bars*, SD.

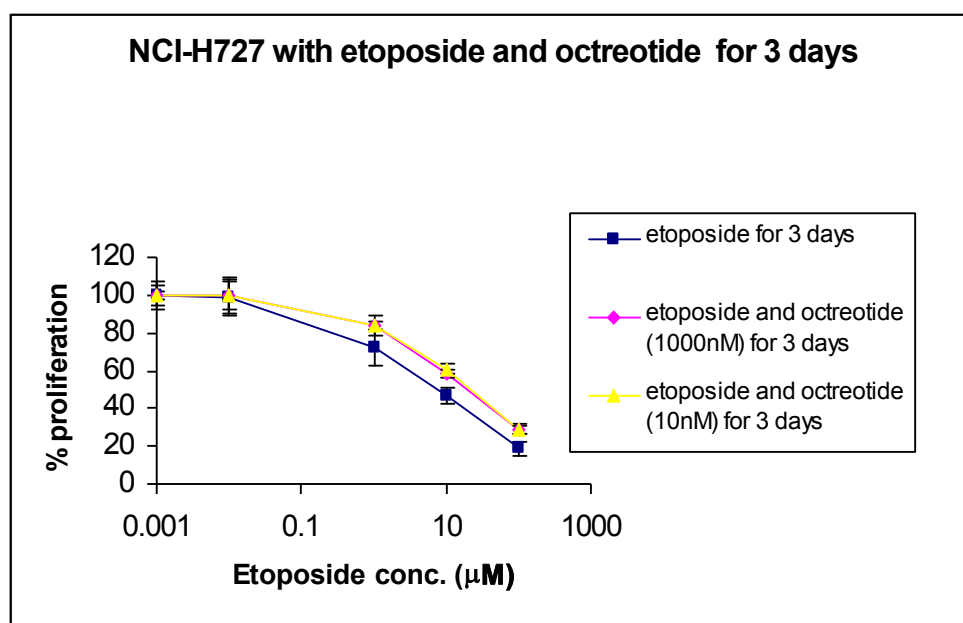
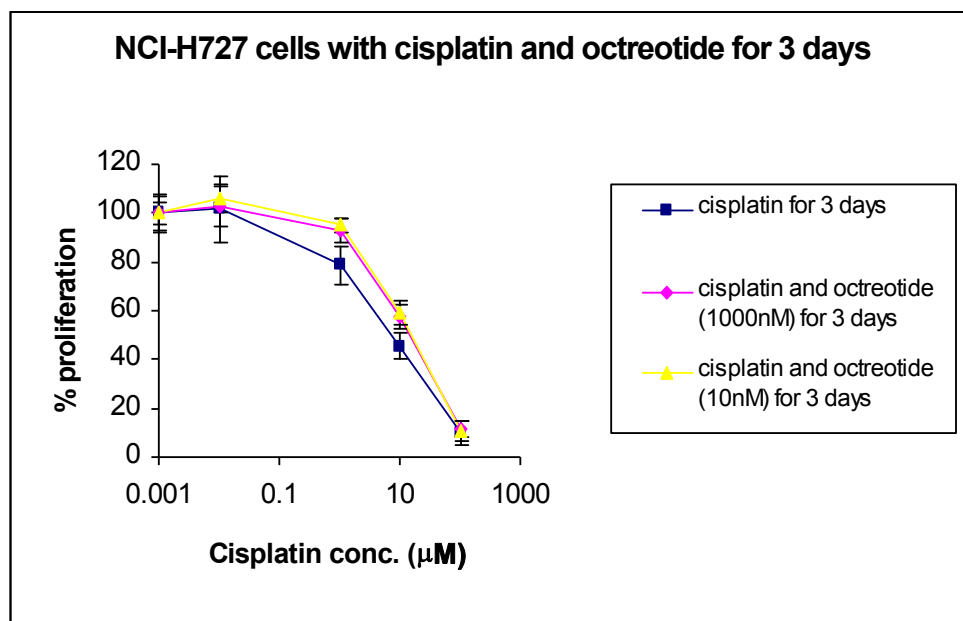


Figure 85: NCI-H727 cells were treated with octreotide (at 10 or 1000nM) and cisplatin or etoposide (both at 0-100 μM) for 72 hours, followed by 48 hours in drug-free media. In the graphs, the '0' point of the x-axis is represented as '0.001' due to the logarithmic scale of the x-axis. Proliferation was calculated as a % of control untreated cells. The values represent averages of 3 different experiments, each performed in triplicate; bars, SD.

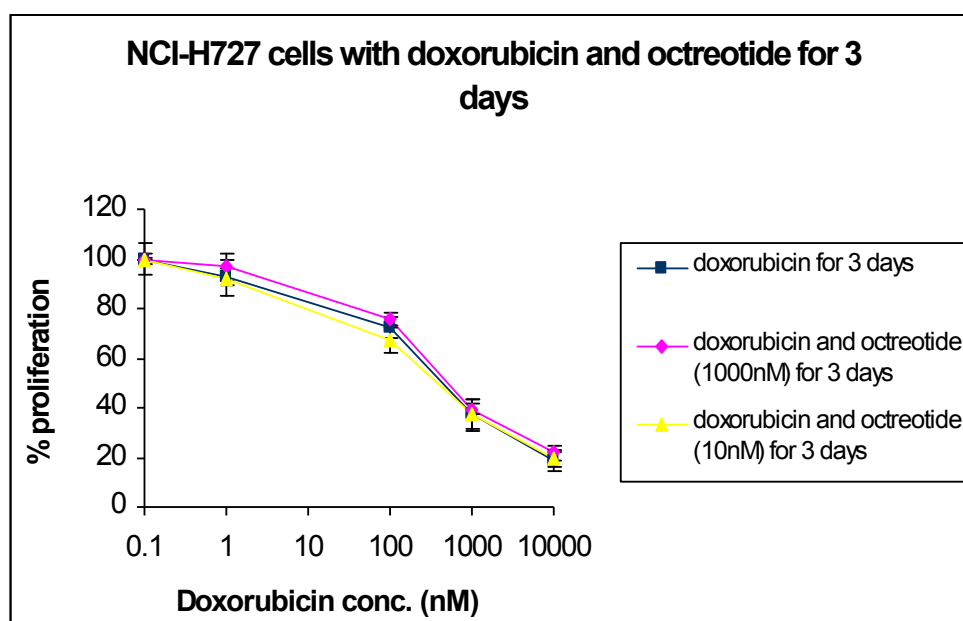
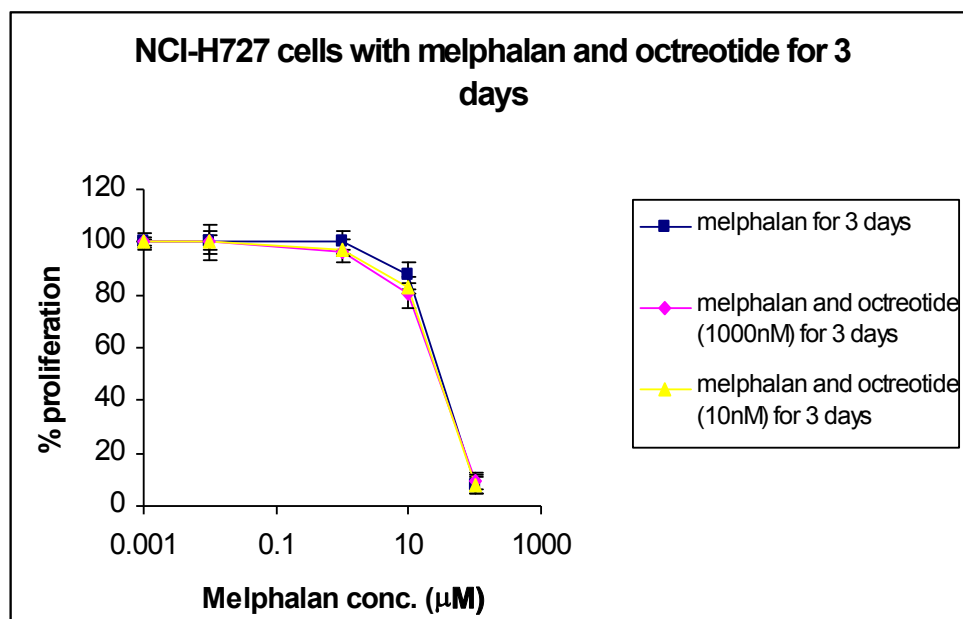


Figure 86: NCI-H727 cells were treated with octreotide (at 10 or 1000nM) and melphalan (0-100μM) or doxorubicin (0-10μM) for 72 hours, followed by 48 hours in drug-free media. In the graphs, the '0' point of the x-axis is represented as '0.1' or '0.001' due to the logarithmic scale of the x-axis. Proliferation was calculated as a % of control untreated cells. The values represent averages of 3 different experiments, each performed in triplicate; bars, SD.

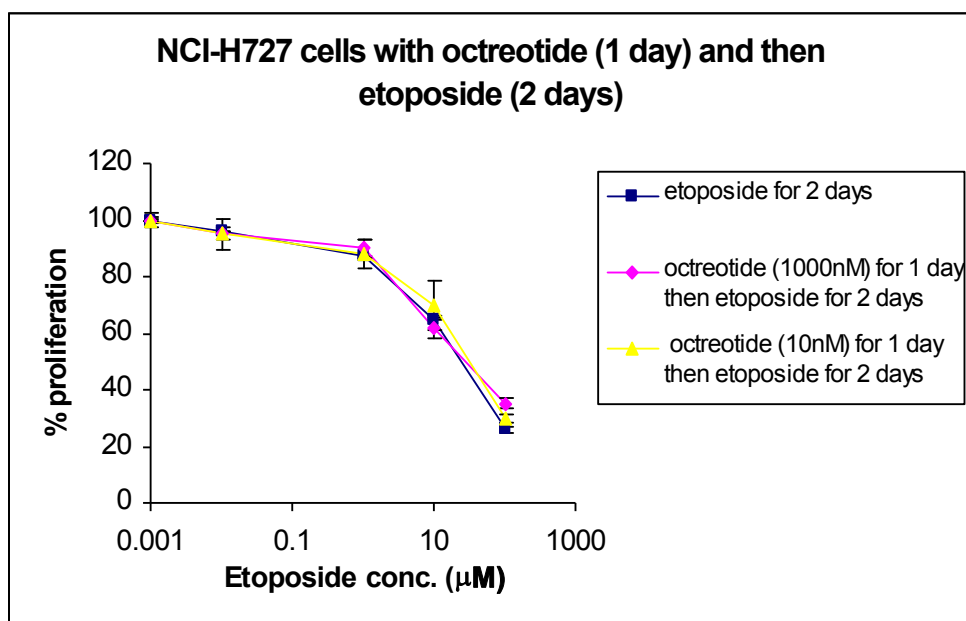
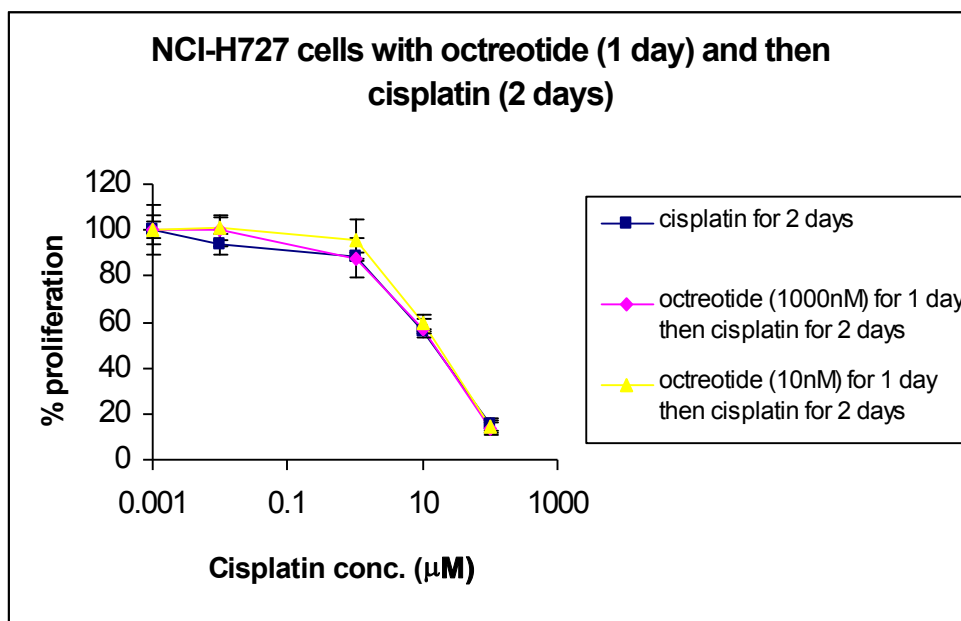


Figure 87: NCI-H727 cells were treated with octreotide (at 10 or 1000nM) for 24 hours and then cisplatin or etoposide (both at 0-100 μM) for 72 hours, followed by 48 hours in drug-free media. In the graphs, the '0' point of the x-axis is represented as '0.001' due to the logarithmic scale of the x-axis. Proliferation was calculated as a % of control untreated cells. The values represent averages of 3 different experiments, each performed in triplicate; *bars*, SD.

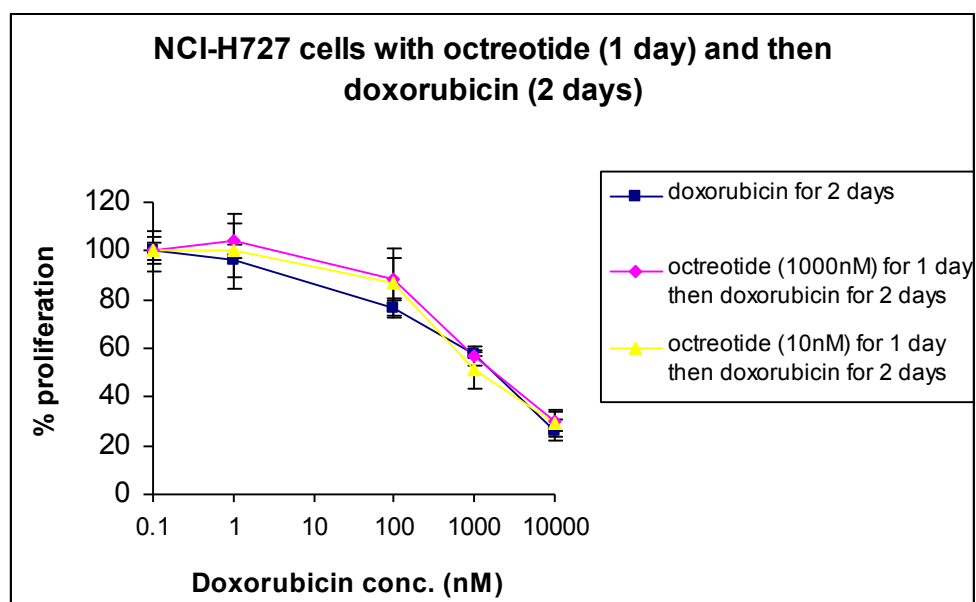
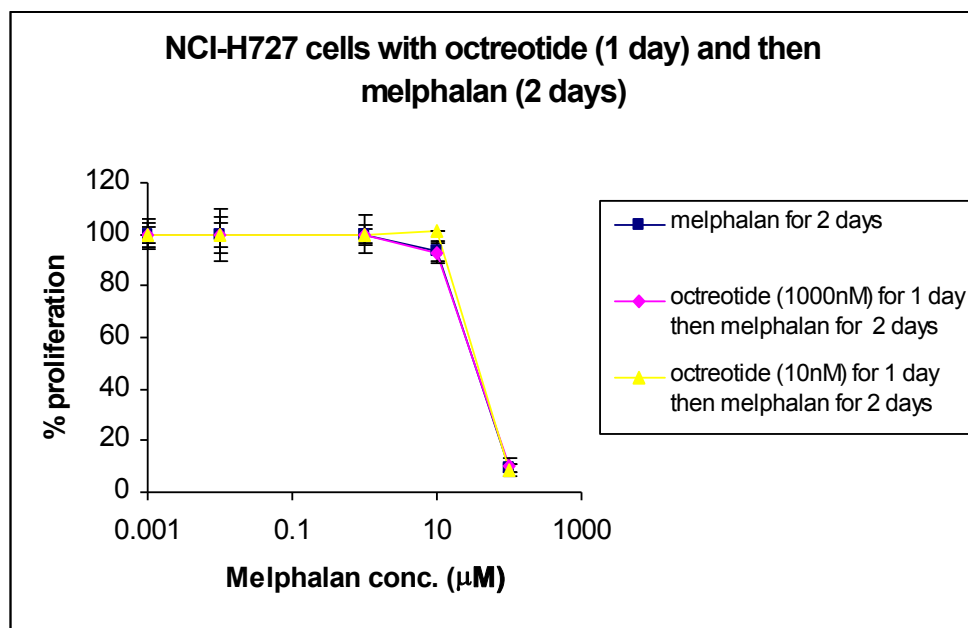


Figure 88: NCI-H727 cells were treated with octreotide (at 10 or 1000nM) for 24 hours and then melphalan (0-100 μM) or doxorubicin (0-10 μM) for 72 hours, followed by 48 hours in drug-free media. In the graphs, the '0' point of the x-axis is represented as '0.1' or '0.001' due to the logarithmic scale of the x-axis. Proliferation was calculated as a % of control untreated cells. The values represent averages of 3 different experiments, each performed in triplicate; *bars*, SD.

Many studies analysing the effect of drugs in cellular proliferation use drugs dissolved in serum-free media to avoid any interaction of the drug with serum proteins, which might affect the results. To assess whether lack of serum could have any effect in the cytotoxicity of octreotide, we treated cells with octreotide at 0-10 μ M for 24, 48 or 72 hours in media containing 5, 0.5 or 0% serum. In addition, octreotide in this study was added fresh daily to enhance effectiveness. An example of this experiment is shown for NCI-H727 cells in appendix 5E. Any anti-proliferative effect seen was due to the lack of serum, confirming that octreotide is not cytotoxic to the cell lines used.

8.2.3 Octreotide effect on cell cycle of NET cell lines

Octreotide demonstrated lack of an anti-proliferative effect. As the results of the SRB proliferation assay depend on the *rate* of cellular proliferation and not proliferation itself, the lack of cytotoxicity shown by octreotide could have occurred for the reason that the effect of octreotide is cytostatic, causing the cells to arrest in a specific phase of the cell cycle. To test this hypothesis, cells were treated with octreotide and analysed by flow cytometry for DNA content, which denotes the cell cycle phase.

As seen in the upper left graph of figure 89, untreated cells in a histogram plot of events (counts) vs fluorescence intensity (FL2-H) are presented as two peaks. The first peak (on the left) represents cells in phase G1/S of the cell cycle, while the second peak represents cells in the G2/M phase of the cell cycle. In any given cell population, more cells are found in the G1/S phase of the cell cycle than in the G2/M phase. Any drug causing cell cycle arrest will shift cells from one to the other peak of the histogram.

NCI-H727 cells were treated with octreotide at 0-10 μ M for 72 hours. Even at the highest dose, octreotide did not induce cell cycle arrest in NCI-H727 cells, as there is no difference in cell counts between treated and untreated cells. A similar effect was seen in the rest of the cell lines (appendix 5F-5H). The only difference was that at the highest dose of octreotide (10 μ M), which is at toxic and clinically irrelevant levels, BON-1 cells move to the beginning of the x-axis, which indicates cell death by apoptosis. This did not occur with any of the other cell lines tested which did not undergo apoptosis at any dose given.

NCI-H727

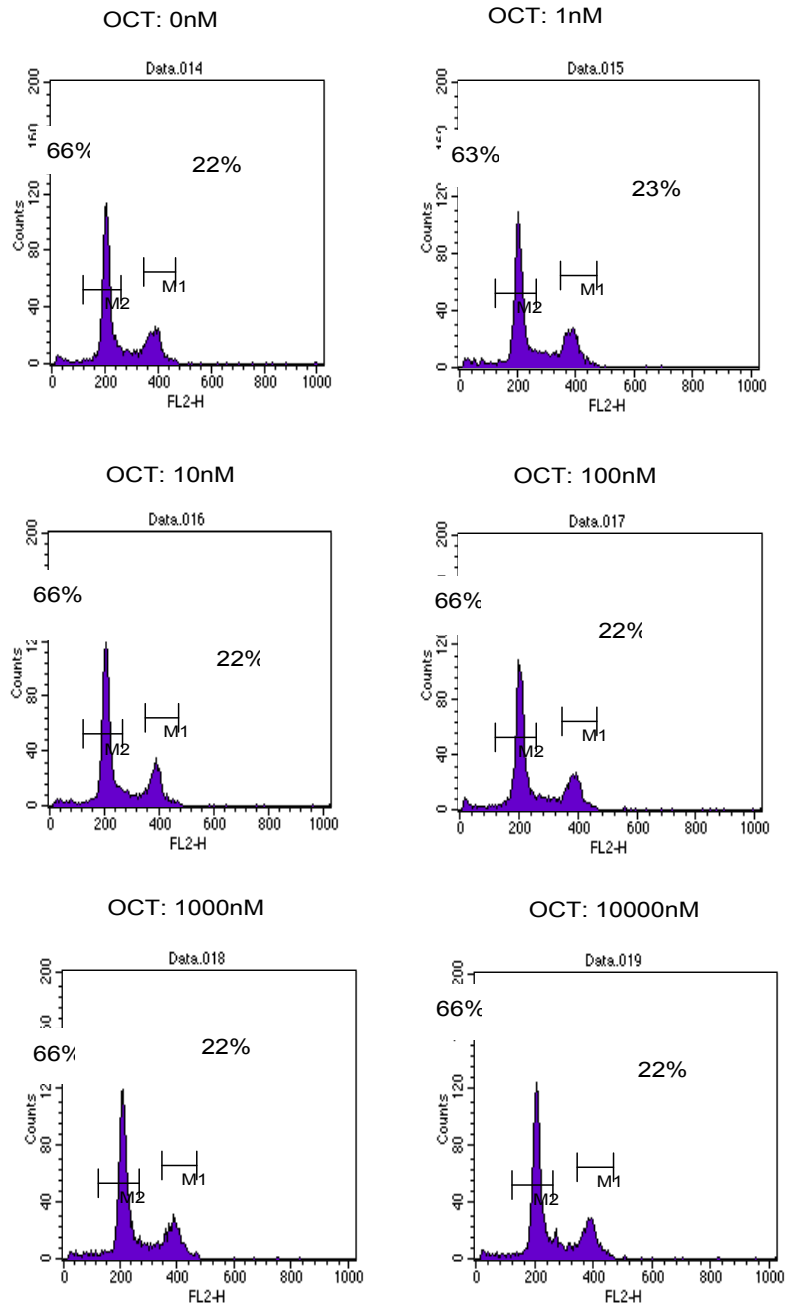


Figure 89: NCI-H727 cells were treated with octreotide at 0-10,000nM for 24 hours. 'FL2-H' denotes DNA content by propidium iodide staining, while 'counts' denotes cell number. Bars M1 and M2 indicate populations of cells at phases G1 and G2/M of the cell cycle respectively.

8.3 Discussion

8.3.1 Proliferation studies

In the second part of this study, the somatostatin analogue octreotide was assessed for its effect on the cell growth of two rat islet tumour cell lines CRI-G1 and RIN-5F, the NCI-H727 human lung carcinoid cell line and the BON-1 human pancreatic endocrine cell line. Although, the receptors selective for octreotide were expressed in all cell lines, octreotide treatment did not demonstrate any anti-proliferative or cytostatic activity under the conditions used. All cell lines displayed resistance to octreotide even at toxic doses.

Somatostatin analogues and in particular octreotide have been widely tested for their effect on growth of cells *in vitro* and in xenograft models. The proliferation of AR42J pancreatic cells was abolished by octreotide at concentrations as low as 0.1nM. The growth of AR42J cells was either induced by EGF or gastrin, all of which promote the growth of pancreatic cells (Charland *et al.*, 2001; Hofslis *et al.*, 2002). A similar effect was seen in pancreatic growth in rats induced by caerulein (Charland *et al.*, 2001). Octreotide also inhibited the serum and bFGF stimulated growth of NIH3T3 cells transfected with human SSTR2 receptor at doses up to 1nM via activation of tyrosine phosphatases (Buscail *et al.*, 1994). In our study the effect of the drugs was investigated on the basal proliferation of neuroendocrine tumour cells, without induction by external growth factors. The presence of exogenous factors may justify cytotoxicity observed by the other groups.

8.3.2 Drug treatments in serum-free media

The cells in our study were also treated with drugs dissolved in complete media containing 10% foetal calf serum. In both studies mentioned above using AR42J cells, octreotide decreased proliferation of cells deprived of serum (Charland *et al.*, 2001; Hofslis *et al.*, 2002). Cholangiocarcinoma cells also grown in serum-free conditions or transplanted in nude mice showed reduction in tumour growth when octreotide was added for 48 hours at $1\text{-}10^4$ ng/ml (Zhao, 2002). A similar effect was seen in serum deprived gastric adenocarcinoma SGC-7901 cells and in xenograft models with octreotide added at concentrations up to 10^4 nM (Wang, 2003). Based on these facts, we also treated cells with octreotide in 5, 0.5 or 0% serum-containing media. In this

case, cell proliferation was inhibited by the lack of serum and not by octreotide, confirming our previous results.

On the other hand, studies exist which, in concordance with our results have shown no effect of octreotide on cell proliferation. Liebow and co-workers showed inhibition of growth of the pancreatic cells Mia PaCa-2 by another somatostatin analogue, the RC-160, but not by octreotide which was also tested (Liebow *et al.*, 1989). Octreotide also inhibited the GLP-1 induced insulin secretion in RIN-5F cells, but showed no effect on basal or GLP-1 induced proliferation even in 1% serum, which agrees with our results (Stark & Mentlein, 2002). Most recently, Ono *et al.* showed that the somatostatin analogue SOM230 inhibited proliferation of NCI-H727 cells but octreotide did not which confirms our results (Ono *et al.*, 2007).

8.3.3 Apoptosis and cell cycle analysis

Other groups have shown an apoptotic or a cytostatic effect of octreotide. Oberg showed that a high-dose octreotide treatment in a xenograft model resulted in an increase of apoptotic cells, but tumour growth inhibition was related to cell cycle arrest and not induction of apoptosis by octreotide (Imam *et al.*, 1997). Octreotide treatment in IL-6 dependent and independent multiple myeloma cells at 0-1000nM resulted in inhibition of growth by blocking the cell cycle rather than decreasing the cell viability (Georgii-Hemming, 1999). Finally, apoptosis and inhibition of angiogenesis was induced in human rectal neuroendocrine carcinoma cells *in vitro* and *in vivo* by octreotide, which resulted in tumour necrosis (Koizumi *et al.*, 2002). In contrast to the above groups, our results showed no blocking of the cell cycle or induction of apoptosis by octreotide in four neuroendocrine cell lines.

8.3.4 Conclusions

Octreotide is a somatostatin analogue that is widely used for the detection of neuroendocrine tumours due to its high affinity binding to somatostatin receptor 2A. As part of the therapeutic treatment of gastrointestinal endocrine tumours it is mainly used for the control of symptoms resulting from excessive hormone release in patients with carcinoid, Verner-Morrison and glucagonoma syndromes. Despite the promising results in *in vitro* models (Hofslie *et al.* 2002, Wang Chun-Hui *et al.*, 2003), and the stabilisation of tumour growth in 30 – 70% of neuroendocrine tumour patients (Behr *et*

al., 2002), in our study, octreotide showed no cytotoxic or cytostatic activity. As previously mentioned, the doses chosen were based on preclinical studies. Combined treatment with chemotherapy had no added value in inhibition of proliferation of neuroendocrine cells. As a result, a further examination of the conditions used will be needed to examine the role of somatostatin receptors in the molecular biology of neuroendocrine tumours.

CHAPTER 9

CONCLUSIONS AND FUTURE WORK

Three therapeutic targets in neuroendocrine tumours have been analysed in this study. In chapters 4-6 we analysed the therapeutic potency of a well-known receptor tyrosine kinase; EGFR. EGFR is expressed in many cancers and is associated with poor prognosis. EGFR is frequently expressed in neuroendocrine tumours and has been implicated with tumour growth and progression in gastrointestinal carcinoids and PNETs (Wang *et al.*, 1997; Nilsson *et al.*, 1995; Rusch *et al.*, 1996; Papouchado *et al.*, 2005; Wulbrand *et al.*, 1998; Peghini *et al.*, 2002). Blockade therefore of EGFR signalling pathways represents a promising strategy for anti-cancer therapy. Gefitinib (Iressa or ZD1839) is a specific tyrosine kinase inhibitor of EGFR used for the treatment of non-small cell lung cancer as well as for other solid tumours. Antineoplastic activity has been shown in a variety of human cancers including prostate, breast, ovarian, colon and lung cancer cells (Schiller, 2003; Herbst, 2002; Blackledge & Averbuch, 2004).

Gefitinib alone or in combination with other anti-cancer therapies, such as chemotherapy drugs and radiation therapy has demonstrated efficacy against tumour growth in a variety of cancer cell lines and in xenograft models (Ciardiello *et al.*, 2000; Ciardiello *et al.*, 2001b; Huang, 2002; Magne, *et al.*, 2002; Sirotnak, *et al.*, 2000). In our study, gefitinib displayed a dose-response cytotoxic effect in four neuroendocrine tumour cell lines, though in very high and clinically irrelevant doses. Gefitinib is known to inhibit EGFR homodimers but not EGFR heterodimers, therefore the presence of EGFR heterodimers could explain the relative resistance of the neuroendocrine tumour cell lines to gefitinib. This is a theory worth further exploration. Gefitinib anti-proliferative effect was associated with induction of apoptosis but no cell cycle arrest. Gefitinib was also used in combination with anticancer drugs with a variety of mechanisms of action, including the DNA cross-linking compound cisplatin, the topoisomerase II poison etoposide, the mitotic inhibitor paclitaxel, and the antimetabolite methotrexate. Gefitinib demonstrated synergy with etoposide in 3/4 NET cell lines and with cisplatin in NCI-H727 cell line. Gefitinib-induced apoptosis did not result in synergy with all cytotoxic drugs used, therefore apoptosis alone cannot account for the presence or absence of synergy.

The reason why gefitinib co-treatment led to synergistic anti-tumour effect with etoposide but not methotrexate or paclitaxel, or why cisplatin increased the anti-

proliferative effect of gefitinib in one cell line but not in the rest is unclear. It would be interesting to see whether synergy shown with etoposide is also seen with other topoisomerase II inhibitors such as teniposide or even doxorubicin, which intercalates DNA resulting in impediment of topoisomerase II and DNA biosynthesis. In the same mode, do other alkylating-like agents such as carboplatin or oxaliplatin have the same effect as cisplatin, and is it cell type specific? This investigation would help understand whether synergy occurs with anti-cancer agents according to their mechanism of action and their direct or indirect effect on DNA, and lead to better combinations that can be exploited in the clinic.

Analysis of the effect of chemotherapeutic drugs on EGFR activity showed transient activation of EGFR after 3 hours of cisplatin treatment in all the NET cell lines, after 3 hours of incubation with etoposide in CRI-G1 and NCI-H727 cell lines, and after 6 hours of incubation with paclitaxel in RIN-5F cell line. Activation of EGFR by cisplatin was mediated through the Ras/MAPK and PI-3K/Akt signalling cascades that promote cell proliferation and survival. Therefore cisplatin may induce EGFR-dependent survival pathways in neuroendocrine tumour cells. The etoposide-induced activation of EGFR has not been assessed for downstream signalling and this could form a future step in our research to see whether activation of EGFR-dependent survival pathways applies to other anti-cancer drugs as well. Again the question why cisplatin, which synergised with gefitinib in one cell line only, led to EGFR activation but not paclitaxel or methotrexate remains unanswered. The reason behind this may be associated with the mode of action of each drug, and more agents of the same class with cisplatin should be tested to delineate this effect. On the other hand, small molecule inhibitors of Akt and MAPK are also currently under development. The demonstration of activated Akt and MAPK after exposure to cisplatin identifies therapeutic potential in combination of chemotherapy with Akt/MAPK inhibitors in neuroendocrine tumours.

This study has shown that sensitivity to chemotherapeutic agents can be enhanced significantly by inhibition of growth factor pathways such as the EGFR signalling pathway. In contrast to the preclinical data from other groups and ours, four large phase III clinical trials in patients with either locally advanced stage III disease or stage IV NSCLC failed to show any benefit for combined treatment of gefitinib with cisplatin, carboplatin, gemcitabine or paclitaxel (Giaccone *et al.*, 2004; Herbst *et al.*, 2004;

Gatzemeier *et al.*, 2004; Moore *et al.*, 2005). The upregulation of phosphorylated receptor following treatment with chemotherapeutic agents shown by us and other groups (Benhar *et al.*, 2002) could explain the failure of combination treatments in clinical trials, and further analysis of combined treatment scheduling as well as dosage is needed for optimal results. In addition, recent studies have indicated that EGFR mutations, including the commonly occurring EGFRvIII deletion mutation, can determine tumour behaviour and response to anti-EGFR therapy. In particular, a number of mutations have been discovered, occurring at the region encoding for the ATP binding site of EGFR, which result in enhanced EGFR activation as well as a higher susceptibility to TKIs (Lynch *et al.*, 2004; Paez *et al.*, 2004). These mutations however, have been shown not to occur in neuroendocrine tumours (Gilbert *et al.*, 2005), whereas the role of EGFRvIII in neuroendocrine tumours has not yet been determined. Whether specific mutations affect response to a chemotherapeutic agent is still unclear and should be investigated.

To understand modulation of EGFR by cisplatin we analysed the effect of this agent on EGFR localisation based on previous reports showing cisplatin-induced EGFR translocation to the nucleus (Dittmann *et al.*, 2005a). Also based on the clinical failure of gefitinib with chemotherapy, but the success of cetuximab in radiosensitising patients with head and neck squamous cell carcinoma (Bonner *et al.*, 2006), we investigated whether any interaction exists between radiation treatment and EGFR inhibition. Cisplatin induced translocation in $\frac{3}{4}$ NET cell lines within 5 minutes after drug exposure. X-ray irradiation at 4Gy induced EGFR nuclear entry in the same cell lines as cisplatin also within 5 minutes after irradiation. This event was completely abrogated by EGFR inhibitors gefitinib and cetuximab. Abortion of EGFR nuclear entry was associated with a delay in the repair of radiation-induced double DNA strand breaks. Inhibition of EGFR has previously been correlated to a decrease in DNA-PK_{CS} activity along with redistribution of this non-homologous end joining (NHEJ)-DNA repair enzyme to the cytosol (Huang & Harari, 2000; Dittmann *et al.*, 2005b; Friedmann *et al.*, 2006). Gefitinib treatment in neuroendocrine cells led to a small increase in cytosolic amounts of DNA-PK but no direct association between EGFR inhibition and DNAPK have been proved so far. Since there is a definite effect of anti-EGFR therapy on DNA repair, the effect of nuclear EGFR and its inhibitors on DNAPK will be studied further. Any physical association of the EGFR and DNA-PK

can be analysed by immunoprecipitation experiments after irradiation and gefitinib treatment. To further examine the relation between EGFR and DNA-PKcs activity after exposure to ionising radiation, DNA repair can be examined by the comet assay using two glioma cell lines: M059K and M059J. M059J cells are deficient in DNA-PKcs and are more sensitive to radiation than the M059K cells, therefore any effect by EGFR inhibitors should be identified in M059K cells only.

Further studies should also be carried out to determine whether cisplatin-induced EGFR nuclear translocation is inhibited by co-treatment with gefitinib or cetuximab, and whether anti-EGFR agents have any effect on DNA repair of interstrand cross-links (ICL) produced by exposure to cisplatin. Although pathways of ICL repair have been reported to involve excision repair (Sarkar *et al.*, 2006), inhibition of the DNA-PK was shown to modulate resistance to cisplatin (Durant & Karran, 2003). DNA-PK involvement in ICL repair can be analysed as before by co-immunoprecipitations with EGFR after cisplatin as well as quantitation of ICL repair by the comet assay. Apart from DNA-PK, other DNA repair enzymes can also be analysed including ERCC1 and XRCC1 (both involved in excision repair) to investigate whether other DNA repair pathways can be modulated by nuclear EGFR.

Nuclear translocation of EGFR in response to irradiation or cisplatin is a novel function of EGFR even though nuclear EGFR has been identified in breast cancer cells and its locality has been associated with increased expression of Ki-67 proliferation index (Lo *et al.*, 2005a). Another mode of EGFR nuclear translocation is by ligand binding. EGF-dependent translocation of EGFR was shown to lead to transcriptional activation of genes involved in increased proliferation of tumours, including cyclin D1, B-Myb, and inducible nitric oxide synthase (iNOS) (Lo & Hung, 2006). The last protein was shown to induce activation of DNA-PK, thus connecting proliferation with increased DNA repair (Xu *et al.*, 2000). This mode of EGFR nuclear transfer has not been investigated in neuroendocrine tumour cells, although activation of EGFR by EGF was shown not to induce alterations in iNOS expression. It would be interesting to see whether EGF can induce EGFR translocation and if this is associated with activation of proliferation genes or with DNA repair.

RIN-5F rat islet tumour cells was the only cell line not demonstrating EGFR nuclear transfer by radiation or cisplatin, and treatment with EGFR inhibitors had no effect on EGFR localisation or the kinetics of DNA repair of radiation-induced strand breaks. Activation though of EGFR by cisplatin (but not radiation) was shown, even though it had no effect on EGFR localisation, but it led to activation of Akt and MAPK survival pathways. Taken together, the results in RIN-5F cells indicate a non-significant role of EGFR in the growth of RIN-5F cells, or even an impairment of their nuclear transport mechanism and this should be further investigated. It would be interesting to see whether EGF leads to EGFR import in RIN-5F cells, which would prove that the mechanisms of ligand dependent or independent transport are distinct as previously postulated (Szumiel, 2006).

Chapter 6 analysed the possible mechanisms for EGFR nuclear transport using RIN-5F cells as a negative control. Nuclear transport of EGFR is mediated through the nuclear pore complex via association with karyopherins (nuclear importins and exportins). The inhibitor of nuclear import wheat germ agglutinin (WGA) blocked EGFR import in CRI-G1 but not in RIN-5F cells and caused a delay in repair of radiation-induced DNA strand breaks, while nuclear export inhibitor leptomycin B had no effect as a single agent, but abrogated the gefitinib-induced delay in the repair of strand breaks. Association with nuclear importins requires a nuclear localisation signal (NLS) sequence. Transfection with mutant EGFR in the putative NLS identified by Hsu & Hung (2007), inhibited EGFR nuclear transit, confirming the involvement of the NLS sequence in EGFR nuclear transport. Furthermore, similar studies on the mutant EGFR cell lines and other specific EGFR deletion constructs will enable the mapping of the EGFR regions that may be involved in transcriptional activation of genes by EGFR.

Further investigation is needed to understand where the EGFR nuclear transport is initiated and what mechanisms are involved, for example if internalisation of EGFR takes place in clathrin-coated pits or caveosomes (see section 6.1.2 for details). For this, the inhibitor of clathrin-coated pit formation β -methyl cyclodextrin can be used. In addition, we don't know whether radiation-induced EGFR nuclear transport involves activation of downstream EGFR signalling pathways. Thus, the effect of SR13668

inhibitor of Akt, or of PD98059 specific inhibitor of MEK1/2 kinases can be analysed to identify connection between EGFR signalling and nuclear entry.

It must be noted that this study has been qualitative rather than quantitative as time was a limiting factor. Statistical analysis of the results obtained would involve the use of comparative tests such as the ANOVA (analysis of variance) and the *t*-test.

A. The three-way ANOVA test would be used for statistical analysis of dose response curves shown in proliferation studies of:

1. Gefitinib alone or in combination with chemotherapeutic agents
2. Radiation alone or in combination with gefitinib or cetuximab

The three-way ANOVA is based on the equation $y = x_1 + x_2 + x_3 + \varepsilon$, where the dependent variable *y* denotes the % proliferation, x_1 is the concentration of the single or double treatments (values of the *x*-axis), x_2 denotes the presence or absence of treatment A (1=gefitinib, 2=radiation) with values of 1 or 0 respectively, x_3 denotes the presence or absence of treatment B (1=chemotherapeutic agent, 2=gefitinib) with values of 1 or 0 respectively, and ε is the error.

The reason for using the three way ANOVA is because the *y* value can predicted when the values of the *x* factors called independent variables or fixed factors is known. The level of significance, which is the probability to reject the null hypothesis (the null hypothesis always states that there is no difference between two sets of data) is 0.05. *P* values are calculated for x_1 , x_2 , and x_3 . If for any of the fixed factors $p > 0.05$ then the fixed factor is not statistically significant.

B. For comet analysis data of double treatments using radiation alone, or radiation in combination with gefitinib, or of triple treatments (chapter 6) using radiation with gefitinib and WGA/leptomycin, the three-way ANOVA and the five-way ANOVA tests would be used. The equations would be in the form of $y = x_1 + x_2 + x_3 + \varepsilon$, $y = x_1 + x_2 + x_3 + x_4 + x_5 + \varepsilon$, where the dependent variable *y* denotes the % tail moment, the independent variable x_1 denotes the time (values of the *x*-axis), x_2 denotes the presence or absence of treatment A (radiation) with values of 1 or 0 respectively, x_3 denotes the presence or absence of treatment B (gefitinib) with values of 1 or 0

respectively, x_4 denotes the presence or absence of treatment C (WGA) with values of 1 or 0 respectively, x_5 denotes the presence or absence of treatment D (leptomycin) with values of 1 or 0 respectively, and ε is the error. The level of significance is 0.05 and p values are calculated for each of the x factors. Statistical significant factors have $p < 0.05$.

- C. For comet analysis in cells transfected with wild type or mutant EGFR the four-way ANOVA test would be used. In the equation $y = x_1 + x_2 + x_3 + x_4 + \varepsilon$, y denotes the % tail moment, x_1 - x_4 factors denote the time, presence or absence of radiation, presence or absence of gefitinib, and presence of wild type or mutant EGFR, and ε is the error. The calculation of p values is same as above.
- D. For western blots, the amounts of P-EGFR, P-MAPK, and P-Akt would be quantified in relation to alpha tubulin control and total unphosphorylated protein level in each case. In this study the densitometry analysis amounts were quantified only in relation to the untreated control band and this quantification may be different to the results that would be obtained with the new quantification. To assess the statistical significance of treatments with chemotherapeutic agents at different doses or for different time intervals the two-way ANOVA test would be employed, as only two factors (concentration and time) affect the y value (level of protein). The equation would be $y = x_1 + x_2 + \varepsilon$, where x_1 denotes the concentration, x_2 denotes the time, and ε is the error. The calculation of p values is same as above.
- E. For western blots of EGFR in cells treated with radiation alone or in combination with WGA or leptomycin, the level of the protein would be compared with each one of the factors (radiation, WGA, or leptomycin or combinations of two) separately. As the amount of each band separately (three sets of experiments for each sample), which is called the test variable, follows a normal distribution, the t -test can be employed. The equation would be $y = x_1 + \varepsilon$, where x would denote the appropriate factor and ε is the error. The calculation of p values is same as above.

NOTE: The equations presented above represent the relation between the dependent (y) and independent (x) variables and are not the actual equations used in the statistical analysis, which are much more complex and are not dealt with in this study.

In chapter 7, we examined C-KIT, a tyrosine kinase inhibitor that has also been identified in a variety of tumour cells including gastrointestinal stromal tumours (GISTs) (Fletcher *et al.*, 2002), and its expression has been associated with a poor outcome for patients (Ferrari *et al.*, 2006). Based on the clinical efficacy of imatinib mesylate tyrosine kinase inhibitor (TKI) against C-KIT in GISTs (Cohen *et al.*, 2005) we investigated the presence of C-KIT in neuroendocrine tumour patients by immunohistochemistry.

Expression of C-KIT was established in a range of tumours that included foregut NETs (mainly pancreatic NETs and gastric carcinoids), midgut NETs (mainly ileal and appendiceal carcinoids), hindgut NETs, and NETs of unknown primary site. Therefore, C-KIT has been identified as a receptor tyrosine kinase with therapeutic potential. Unfortunately, clinical trials for imatinib mesylate as a single agent have not demonstrated objective responses or stability of disease in patients with neuroendocrine tumours (Carr *et al.*, 2004; Dy *et al.*, 2005; Krug *et al.*, 2005; Gross *et al.*, 2006). The efficacy of imatinib mesylate being used as an adjuvant therapy is still not clear. Some investigators have suggested using C-KIT expression as a prognostic marker (Erler *et al.*, 2004; Ferrari *et al.* 2006), but whether this is true for neuroendocrine tumours remains to be shown.

Nevertheless, new tyrosine kinase inhibitors with multiple targets including C-KIT have been synthesised, proving that therapies interacting with C-KIT-signalling pathway should be taken into account for possible future clinical trials. A recently developed drug named sunitinib (SU011248; Sutent) is a multi-targeted tyrosine kinase inhibitor with selectivity for PDGF receptors, VEGF receptors, FMS-like tyrosine kinase 3 (FLT3), and C-KIT, that was known to inhibit angiogenesis (Chow & Eckhardt, 2007). Sunitinib has demonstrated *in vitro* inhibition of C-KIT phosphorylation and cell proliferation at nanomolar concentrations, and is therefore 10 times more potent than imatinib (Abrams *et al.*, 2003). Compared with imatinib, sunitinib is also more effective against PDGFR and inhibits additional receptors including VEGFR2, and this may account for its efficacy in imatinib-resistant GISTs (Demetri *et al.*, 2009). Recently completed phase II and III trials in renal cell carcinoma (RCC) and imatinib-refractory GISTs, respectively, have led to approval of sunitinib by

the US FDA for these diseases in 2006. Additionally, phase II clinical trials with sunitinib have shown anti-tumour activity in patients with advanced malignancies, including neuroendocrine tumours, breast cancer, and colorectal cancer (Chow & Eckhardt, 2007). Clinical trials of sunitinib in NETs have shown very promising results (Kulke *et al.*, 2008). The most successful outcome was recently released in a clinical trial of sunitinib in patients with non-functioning NET, which had to be stopped early after interim analysis demonstrated a significant survival benefit in the sunitinib treated group (Raymond *et al.*, 2009). Therefore, targeting C-KIT in combination with other biomarkers may prove useful for the treatment of neuroendocrine tumour patients.

Chapter 8 included assessment of somatostatin analogue octreotide for any effect on growth of neuroendocrine tumour cells. Somatostatin binds somatostatin receptors (SSTR1-SSTR5), all of which are overexpressed in NET patients with the SSTR2 subtype being the most frequently expressed. The molecular cloning of five distinct subtypes of somatostatin receptors in the 1980s significantly increased our insight into the biology of somatostatin and its receptor subtypes and led to the development of subtype-selective peptides and nonpeptide agonists and antagonists (Öberg, 2004). Somatostatin analogues octreotide and lanreotide are widely accepted as the main treatment for symptomatic relief of NET patients, especially those tumours characterised by hypersecretion of hormones such as VIPoma, glucagonoma and carcinoid syndrome. Somatostatin receptor scintigraphy is the main imaging technique for the localization and staging procedure in these tumours (Melen-Mucha *et al.*, 2006).

Clinical trials with long-term somatostatin analogues have not demonstrated significant anti-tumour activity with less than 5% of patients showing objective tumour regression, although about 50% of patients showed stabilisation of tumour size (Modlin *et al.*, 2008). In agreement with this, our results showed no effect on tumour growth of neuroendocrine tumour cells by octreotide. Octreotide was used at high concentrations and added to cells in both serum-free and serum-containing media. No effect on cell proliferation or cell cycle was observed in any of the cells tested. However, somatostatin receptors are biologically specific receptor-targets to NETs and new strategies are being developed for their utilisation. Somatostatin receptors targeted with somatostatin analogues conjugated to cytotoxic drugs have shown promising results and are being further developed in clinical trials (Melen-Mucha *et al.*, 2006; Modlin *et*

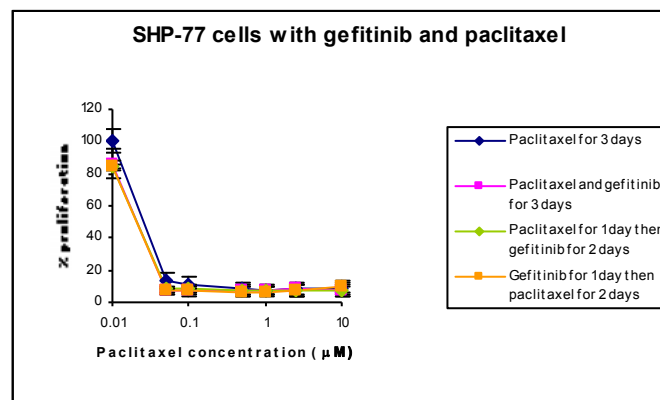
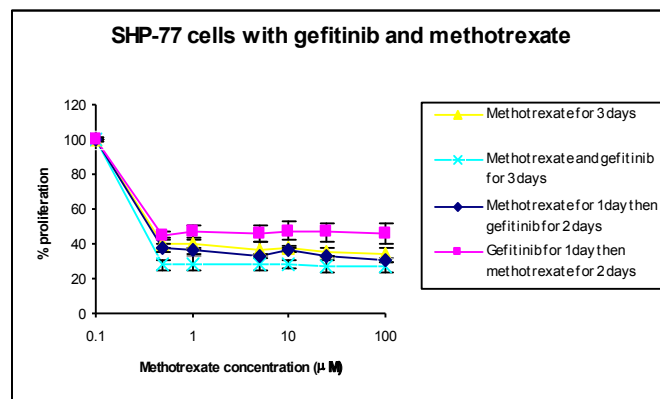
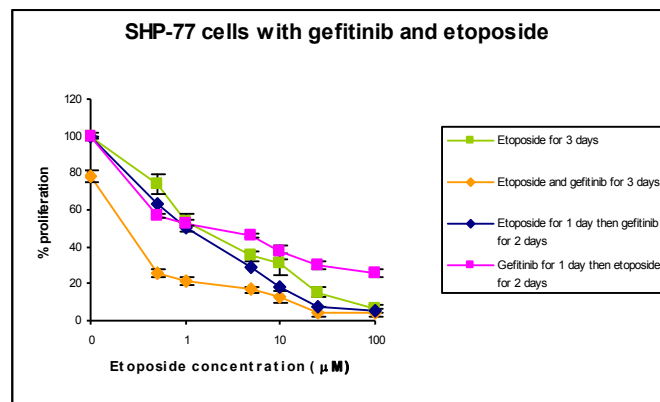
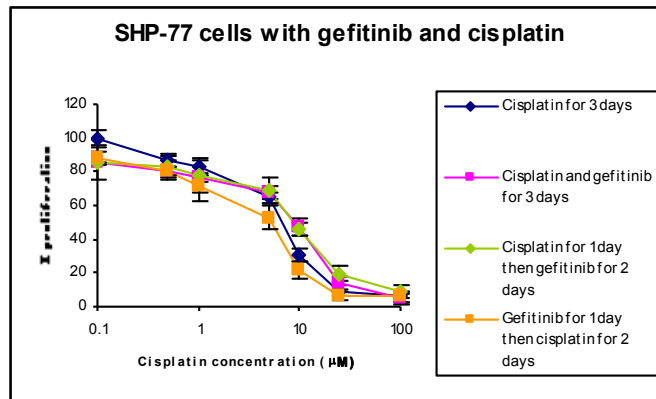
al., 2008). New biological agents and somatostatin-tagged radionuclides are under investigation. Furthermore, treatment of neuroendocrine gut tumours with ultra-high doses of somatostatin analogues has demonstrated significant clinical effects in patients resistant to standard-dose treatment with the same somatostatin analogue. Finally, new somatostatin analogues are being designed with specificity to one somatostatin receptor subtype or all subtypes (pan-receptor analogues) that can bind the receptor(s) with higher affinity but causing less toxic effects (Öberg, 2004; Modlin *et al.*, 2008). Somatostatin receptors are molecular targets closely associated to NETs and novel treatment regimens for NET patients should take advantage of this distinctive relationship.

Finally, apart from the three receptors analysed in this study, other protein targets have been identified in neuroendocrine tumours including the proangiogenic VEGFR and its ligand, PI-3K and Akt, and the mammalian target of rapamycin (mTOR). Drugs against these proteins have been developed and some have been tested in clinical trials, and these could be analysed for efficacy in combination with chemotherapy or radiotherapy as with EGFR.

Taken together, our results may explain why EGFR has been associated with chemo- or radioresistance of tumour cells, and it may also explain the lack of efficacy of chemotherapy or radiotherapy in neuroendocrine tumour patients. We conclude by suggesting a combination modality using radiotherapy and anti-EGFR therapy for the treatment of neuroendocrine tumours. Indeed, based on our study, a clinical trial will take place at the Royal Free Hospital to evaluate the effect of radiotherapy combined with cetuximab in selected neuroendocrine tumour patients.

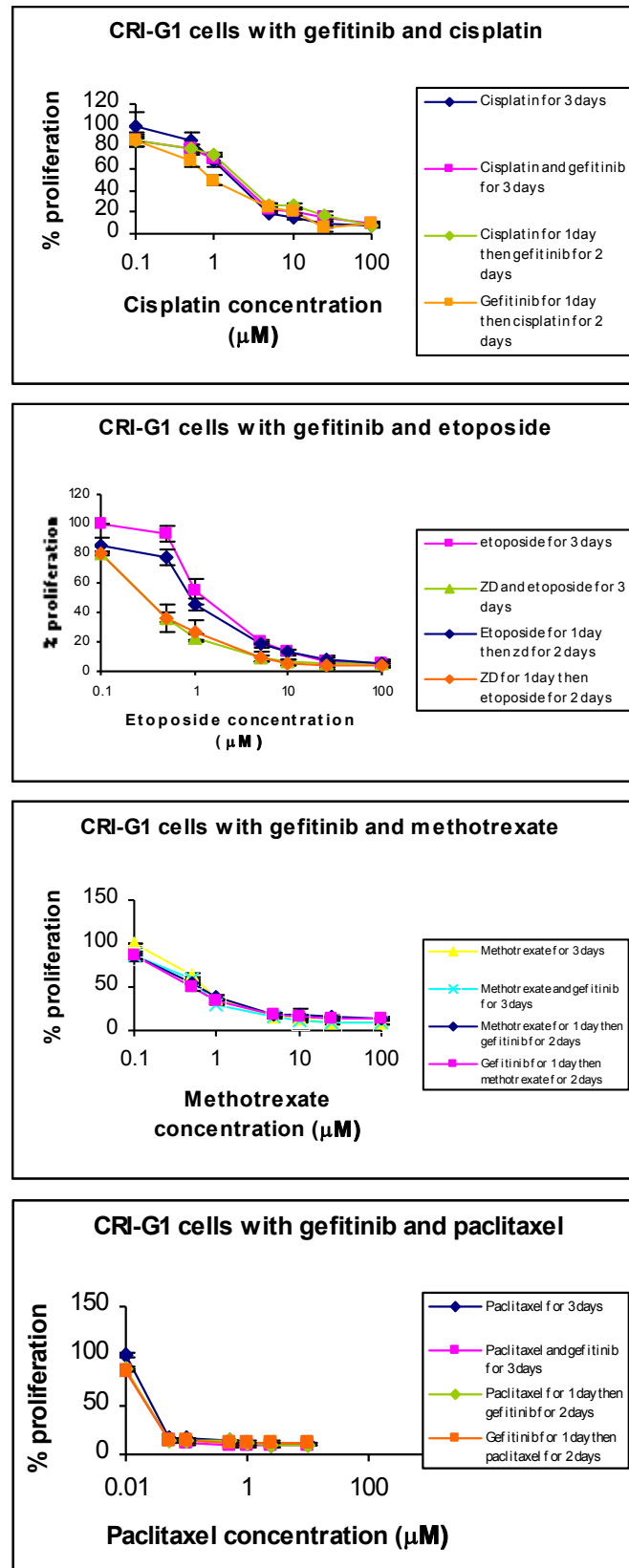
APPENDIX

Appendix 1A: Gefitinib and chemotherapeutic agents in SHP-77 cells



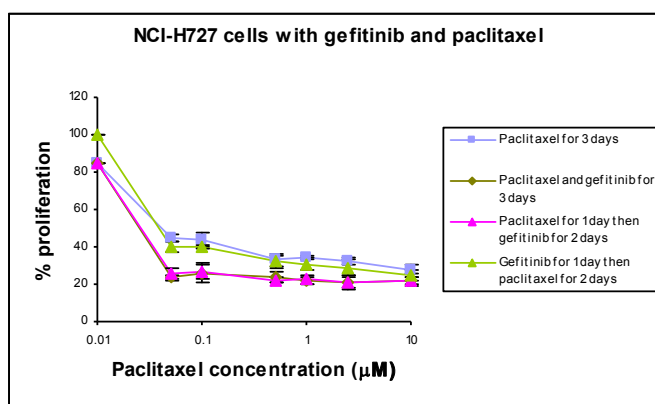
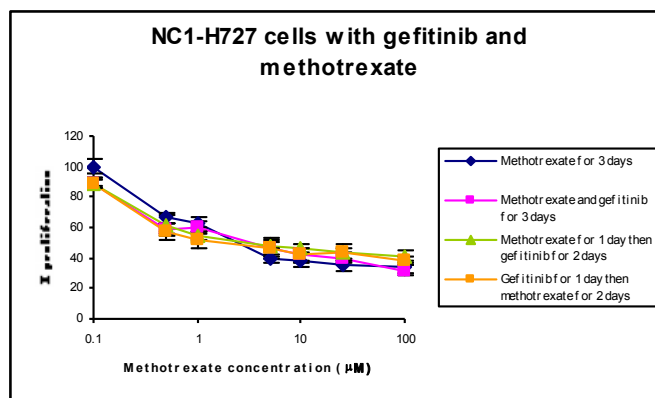
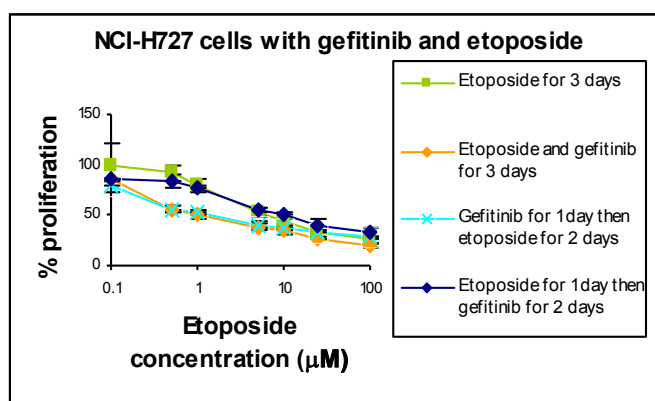
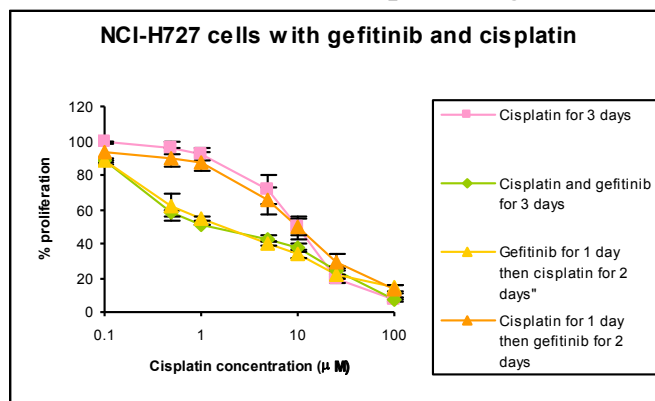
Cells were treated with chemotherapeutic agents at the indicated concentrations alone, simultaneously with gefitinib (10μM) for 72 hours, or with drug A for 1 day followed by drug B for 2 days and vice versa, followed by 48 hours in drug free medium. Proliferation was calculated as a % of control untreated cells. Data represents the averages of three different experiments, each performed in triplicate; bars, SD.

Appendix 1B: Gefitinib and chemotherapeutic agents in CRI-G1 cells



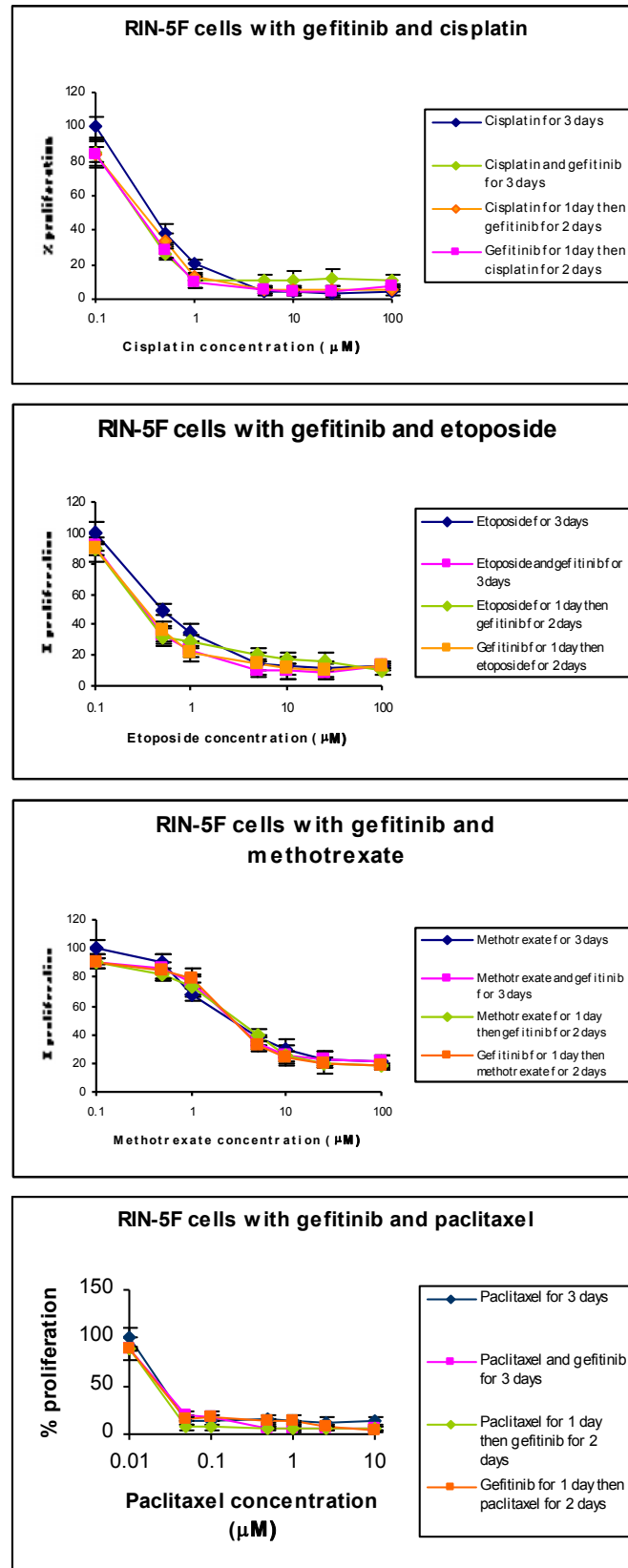
Cells were treated with chemotherapeutic agents at the indicated concentrations alone, simultaneously with gefitinib (10μM) for 72 hours, or with drug A for 1 day followed by drug B for 2 days and vice versa, followed by 48 hours in drug free medium. Proliferation was calculated as a % of control untreated cells. Data represents the averages of three different experiments, each performed in triplicate; *bars*, SD.

Appendix 1C: Gefitinib and chemotherapeutic agents in NCI-H727 cells



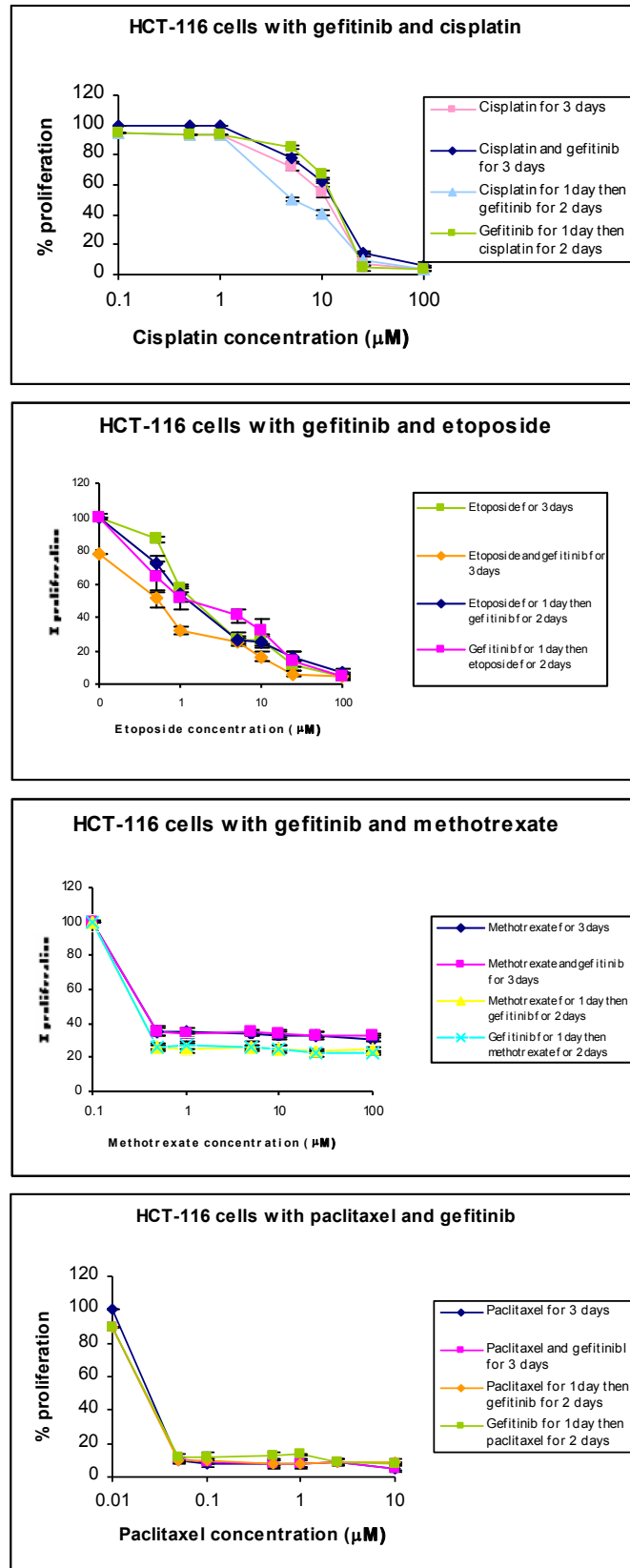
Cells were treated with chemotherapeutic agents at the indicated concentrations alone, simultaneously with gefitinib (10μM) for 72 hours, or with drug A for 1 day followed by drug B for 2 days and vice versa, followed by 48 hours in drug free medium. Proliferation was calculated as a % of control untreated cells. Data represents the averages of three different experiments, each performed in triplicate; bars, SD.

Appendix 1D: Gefitinib and chemotherapeutic agents in RIN-5F cells



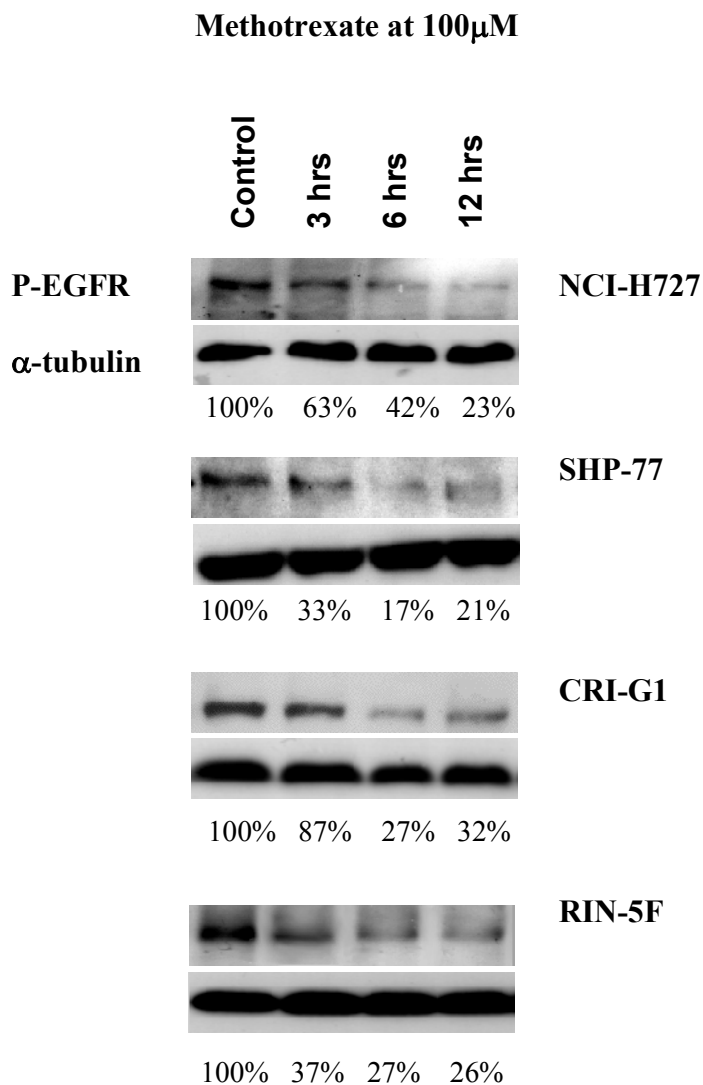
Cells were treated with chemotherapeutic agents at the indicated concentrations alone, simultaneously with gefitinib (10μM) for 72 hours, or with drug A for 1 day followed by drug B for 2 days and vice versa, followed by 48 hours in drug free medium. Proliferation was calculated as a % of control untreated cells. Data represents the averages of three different experiments, each performed in triplicate; bars, SD.

Appendix 1E: Gefitinib and chemotherapeutic agents in HCT-116 cells



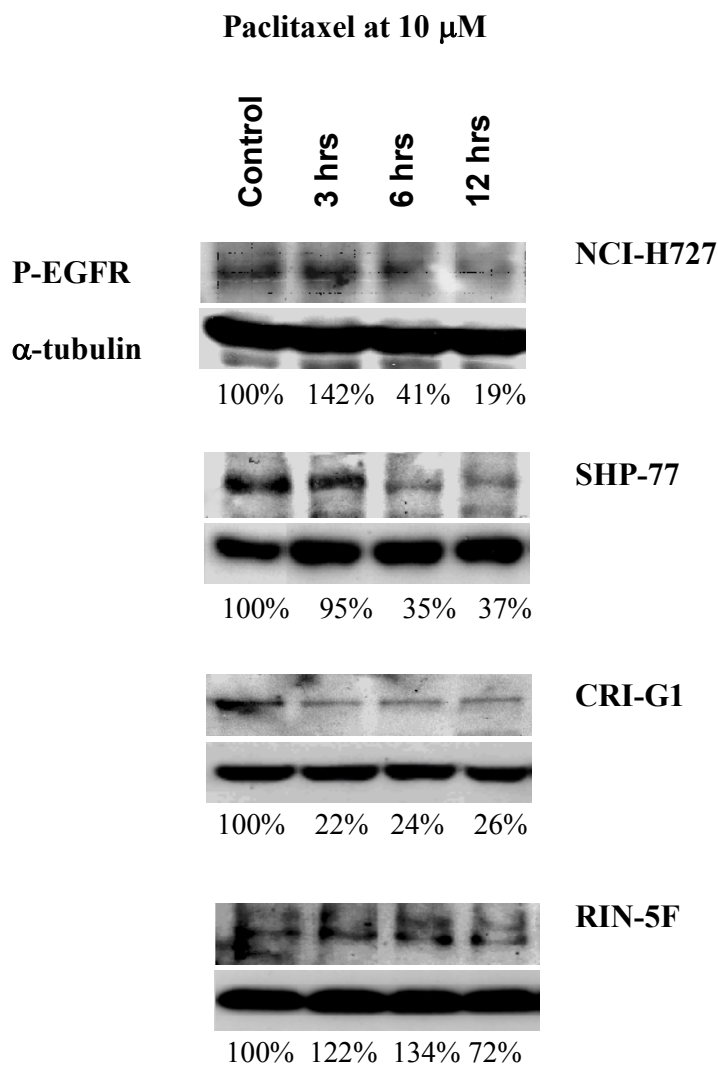
Cells were treated with chemotherapeutic agents at the indicated concentrations alone, simultaneously with gefitinib (10μM) for 72 hours, or with drug A for 1 day followed by drug B for 2 days and vice versa, followed by 48 hours in drug free medium. Proliferation was calculated as a % of control untreated cells. Data represents the averages of three different experiments, each performed in triplicate; bars, SD.

Appendix 1F: Time course analysis of the effect of methotrexate on EGFR activity



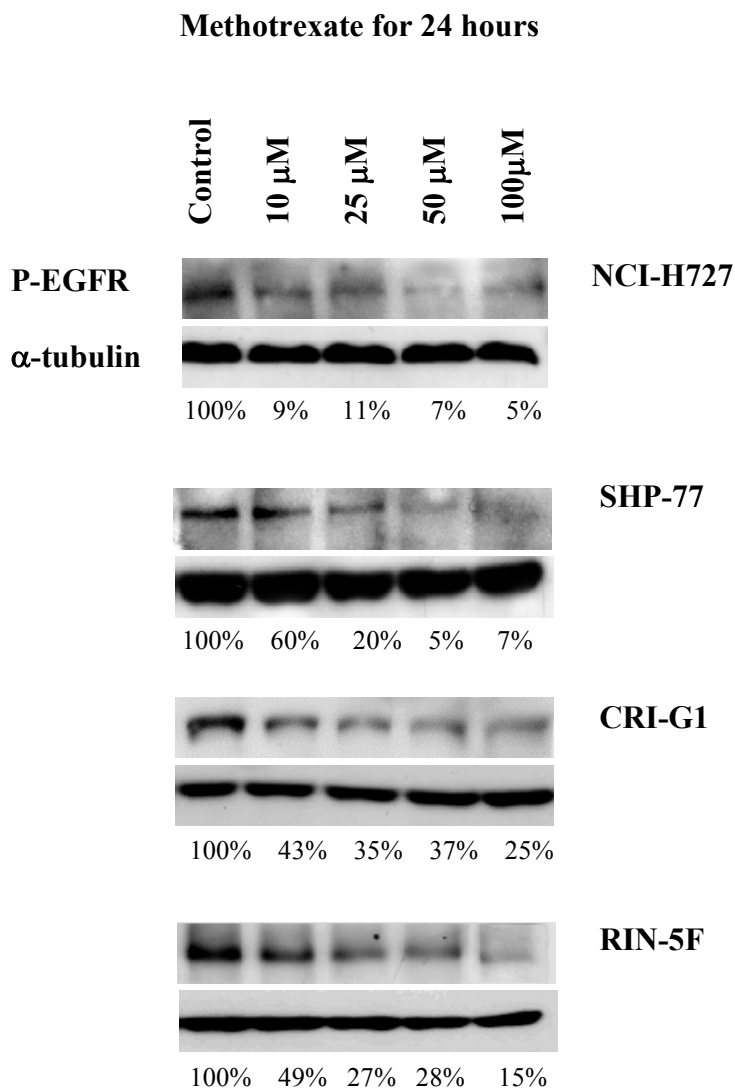
Tyrosine phosphorylation of EGFR in NET cell lines determined by immunoblotting for PY20 (170kDa). Cells were treated with methotrexate at 100 μ M for 3, 6 or 12 hours. Bottom panel shows α -tubulin bands (50kDa) as loading control. Amounts of P-EGFR in percentages were determined by densitometry analysis.

Appendix 1G: Time course analysis of the effect of paclitaxel on EGFR activity



Tyrosine phosphorylation of EGFR in NET cell lines determined by immunoblotting for PY20 (170kDa). Cells were treated with paclitaxel at 10 μ M for 3, 6 or 12 hours. Bottom panel shows α -tubulin bands (50kDa) as loading control. Amounts of P-EGFR in percentages were determined by densitometry analysis.

Appendix 1H: Dose response analysis of the effect of methotrexate on EGFR activity



Tyrosine phosphorylation of EGFR in NET cell lines determined by immunoblotting for PY20 (170kDa). Cells were treated with methotrexate at 0, 10, 25, 50 or 100 μ M for 24 hours. Bottom panel shows α -tubulin bands (50kDa) as loading control. Amounts of P-EGFR in percentages were determined by densitometry analysis.

Appendix 1I: Dose response analysis of the effect of paclitaxel on EGFR activity

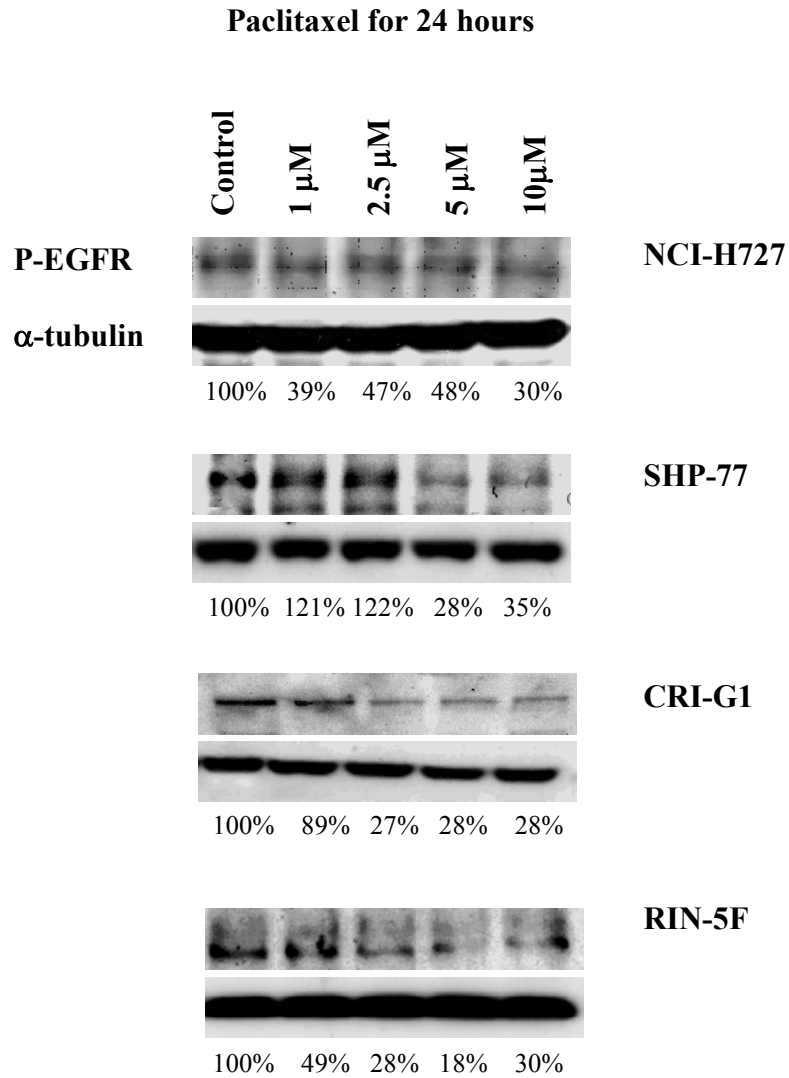
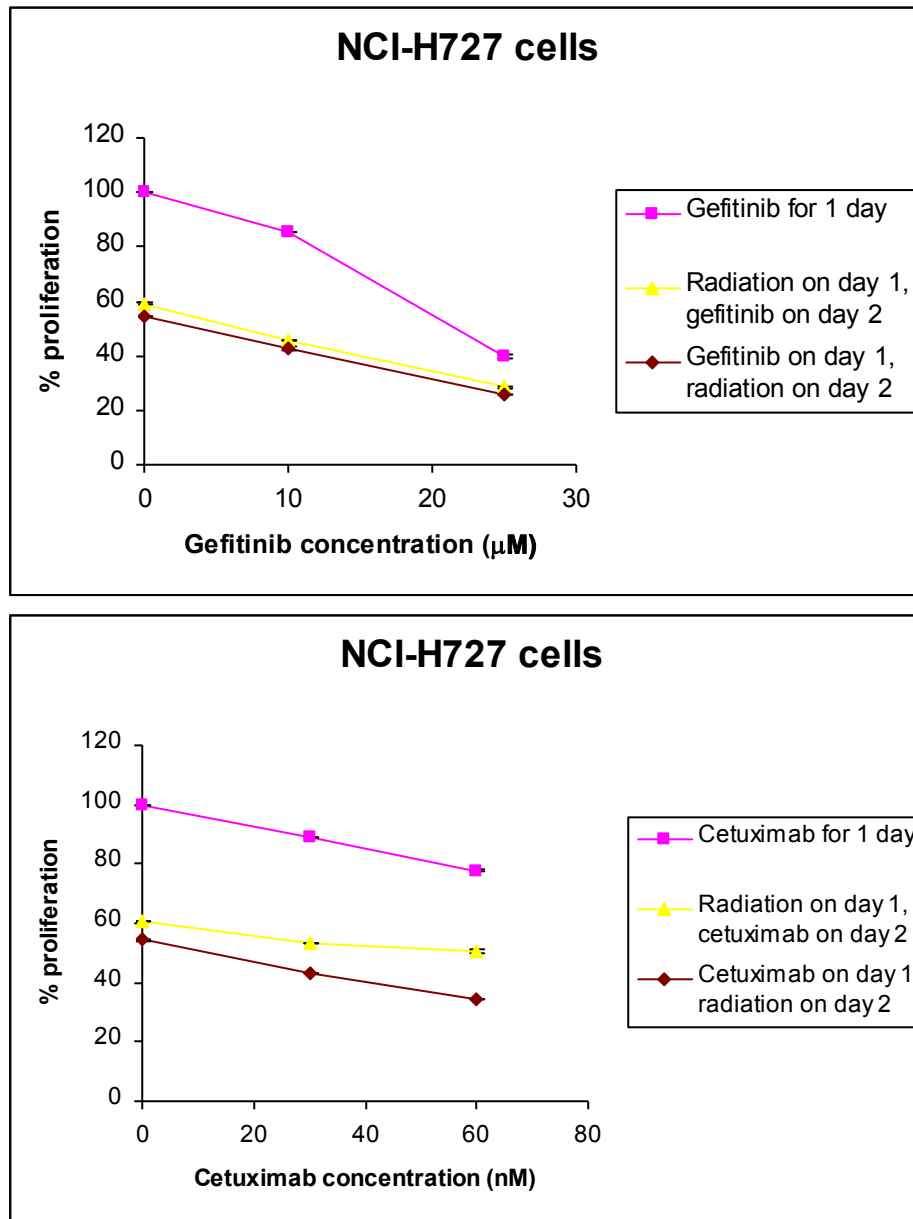


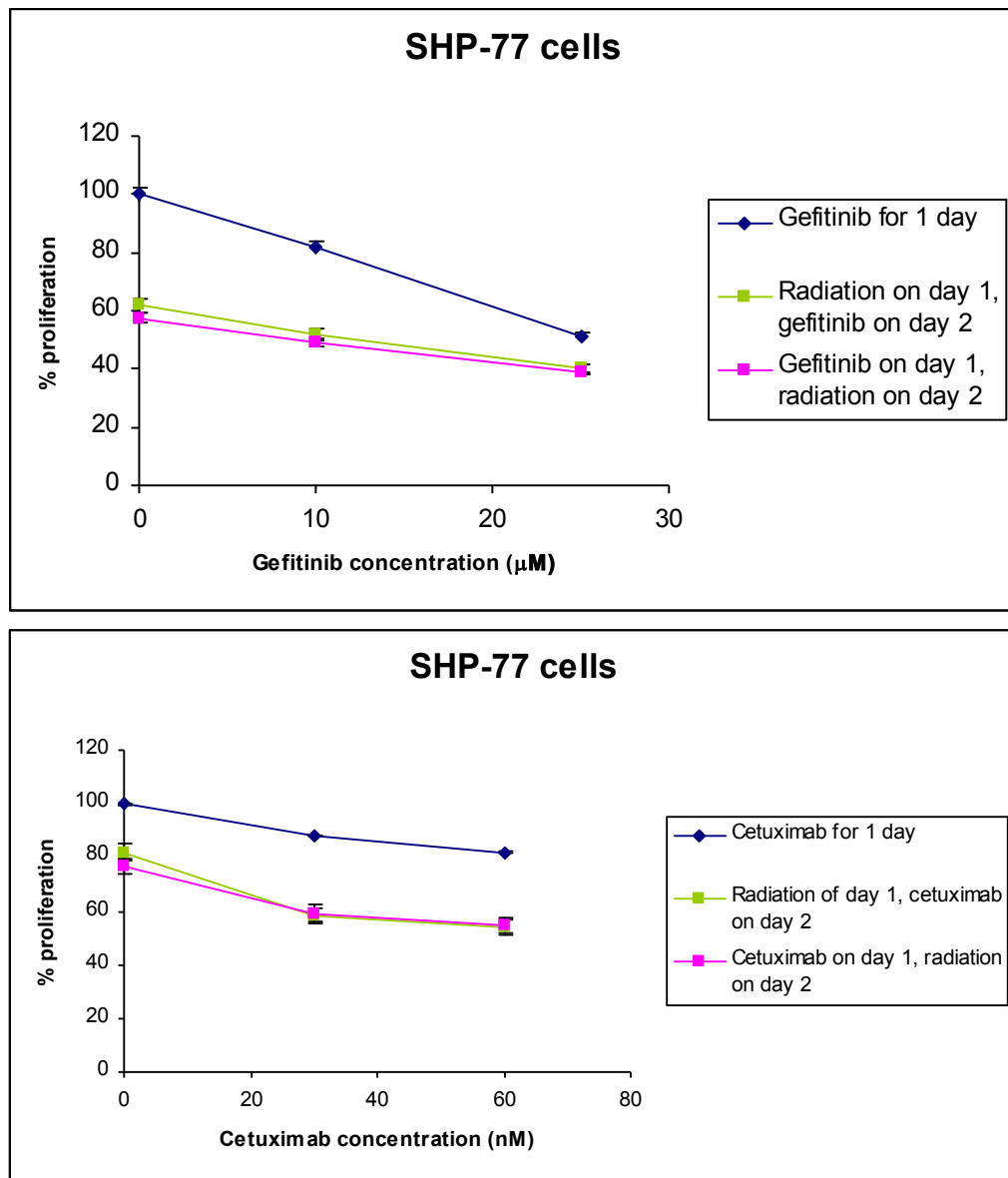
Figure 67: Tyrosine phosphorylation of EGFR in NET cell lines determined by immunoblotting for PY20 (170kDa). Cells were treated with paclitaxel at 0, 1, 2.5, 5 or 10 μ M for 24 hours. Bottom panel shows α -tubulin bands (50kDa) as loading control. Amounts of P-EGFR in percentages were determined by densitometry analysis.

Appendix 2A: Radiation and EGFR inhibitors in proliferation study using NCI-H727 cells



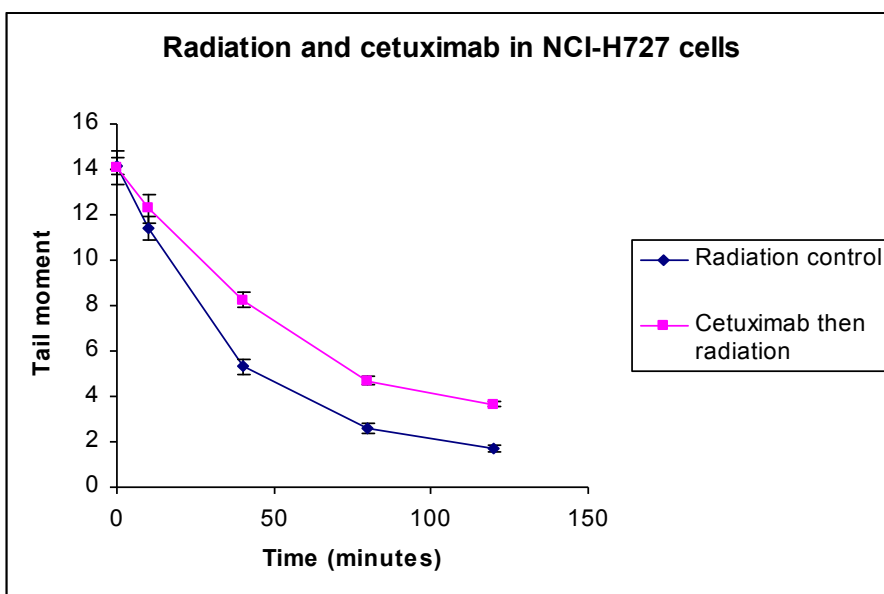
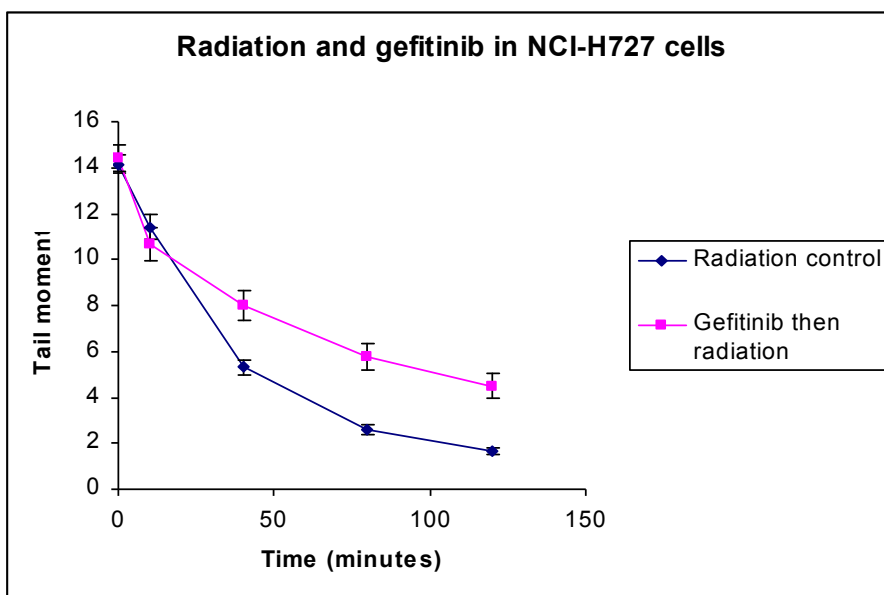
Cells were treated with radiation at 30Gy on day 1 and gefitinib or cetuximab at the indicated concentrations on day 2, or in reverse order, followed by 48 hours in drug free medium. Proliferation was calculated as a % of control untreated cells. Data represents the averages of three different experiments, each performed in triplicate; bars, SD.

Appendix 2B: Radiation and EGFR inhibitors in proliferation study using SHP-77 cells



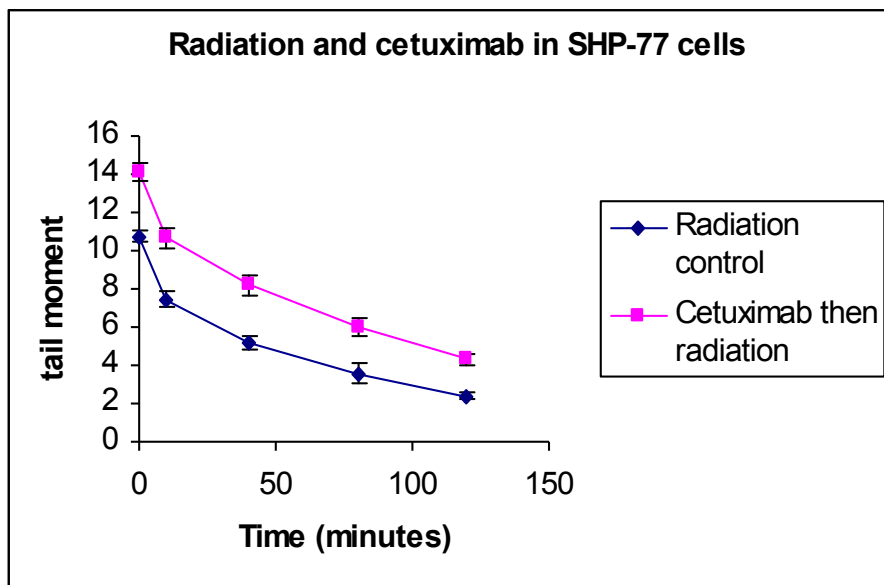
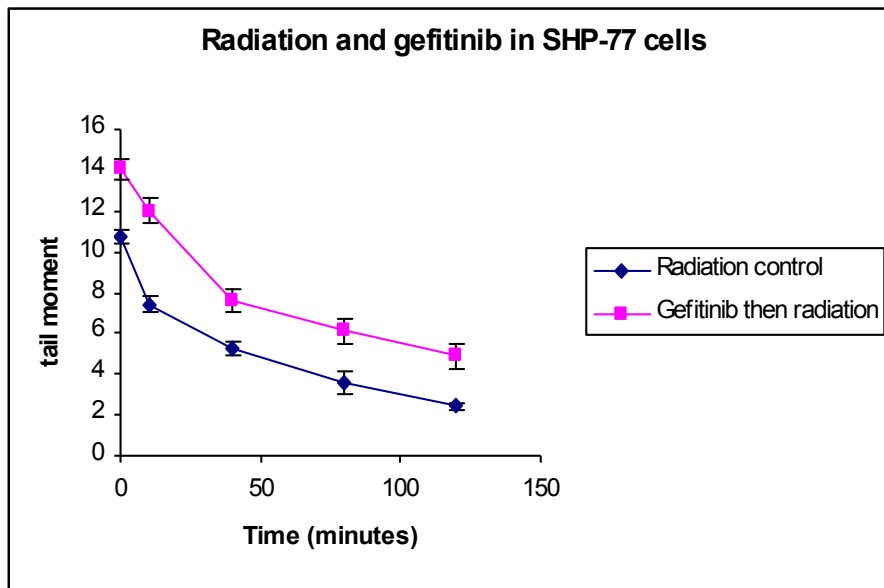
Cells were treated with radiation at 4Gy on day 1 and gefitinib or cetuximab at the indicated concentrations on day 2, or in reverse order, followed by 48 hours in drug free medium. Proliferation was calculated as a % of control untreated cells. Data represents the averages of three different experiments, each performed in triplicate; bars, SD.

Appendix 2C: Radiation and EGFR inhibitors in DNA repair analysis using NCI-H727 cells



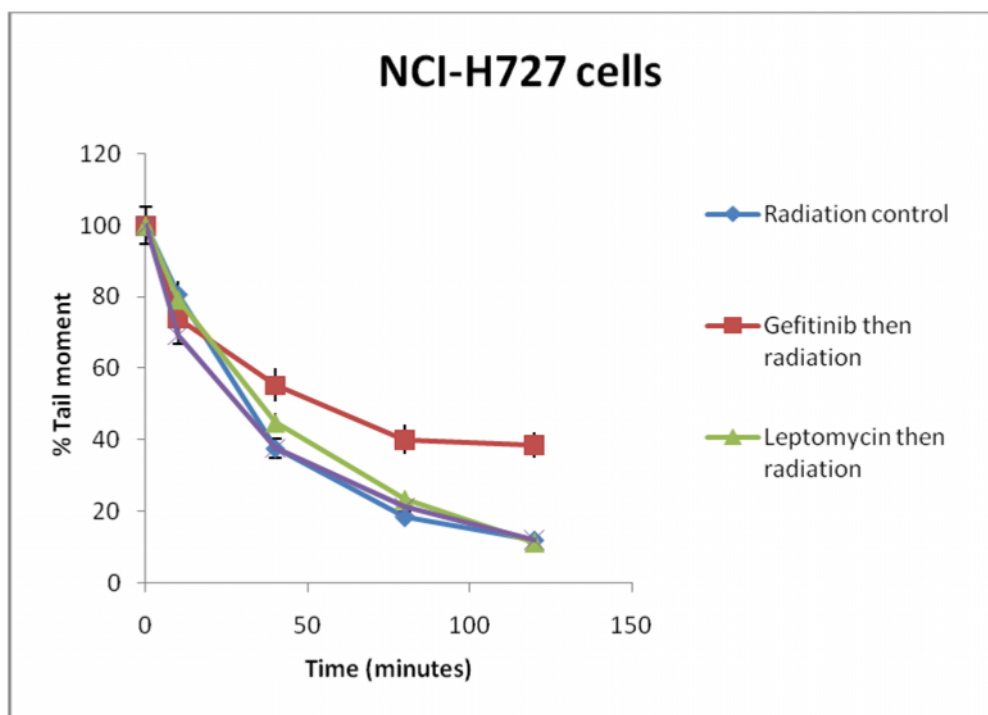
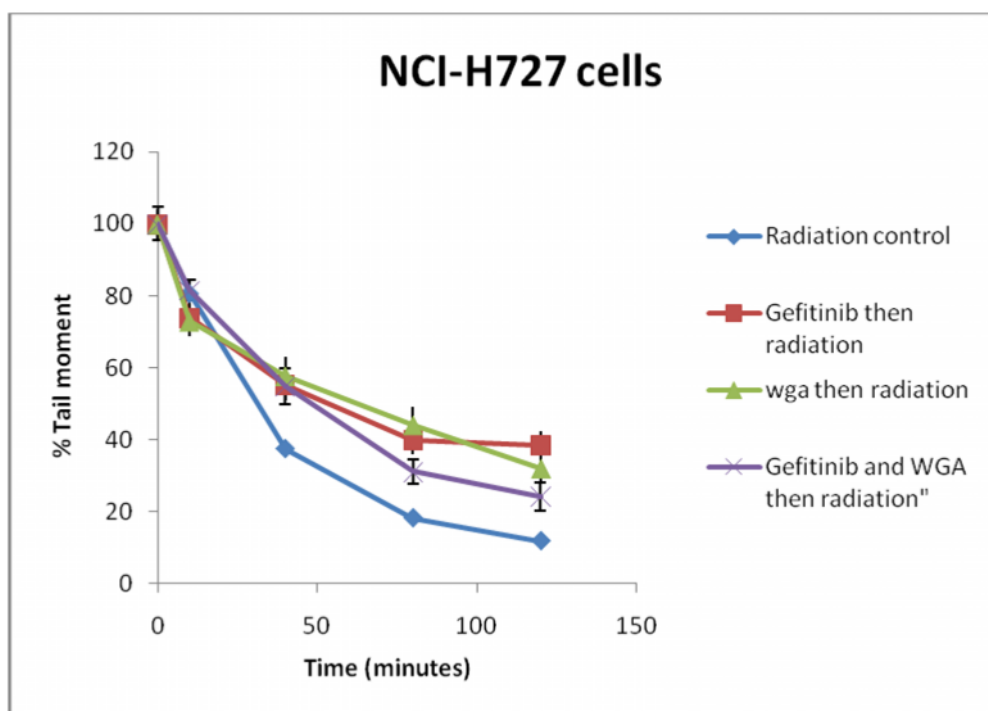
Measurement of irradiation-induced DNA strand breaks and their repair in NCI-H727 cells. Strand break formation quantitated as tail moment, plotted against time after irradiation. Cells were treated with gefitinib at 10 μ M or cetuximab at 30nM for 3 hours, drug was removed, and then cells were irradiated at 30 Gy and incubated for up to 120 minutes at 37°C. Data represents the averages of three different experiments, each performed in triplicate; *bars*, SD.

Appendix 2D: Radiation and EGFR inhibitors in DNA repair analysis using SHP-77 cells



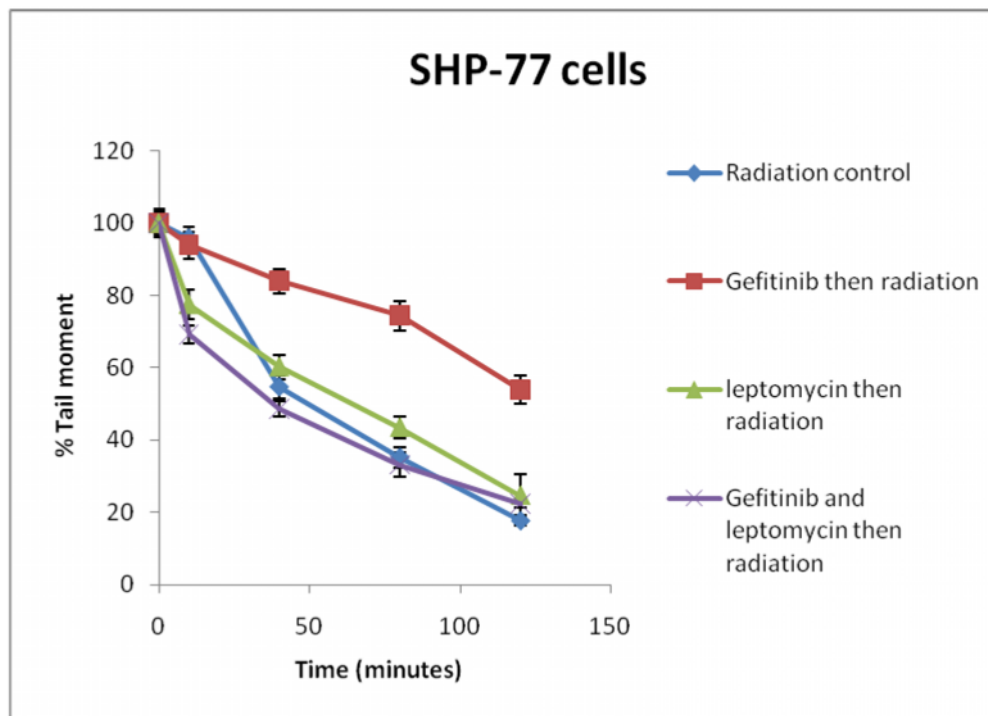
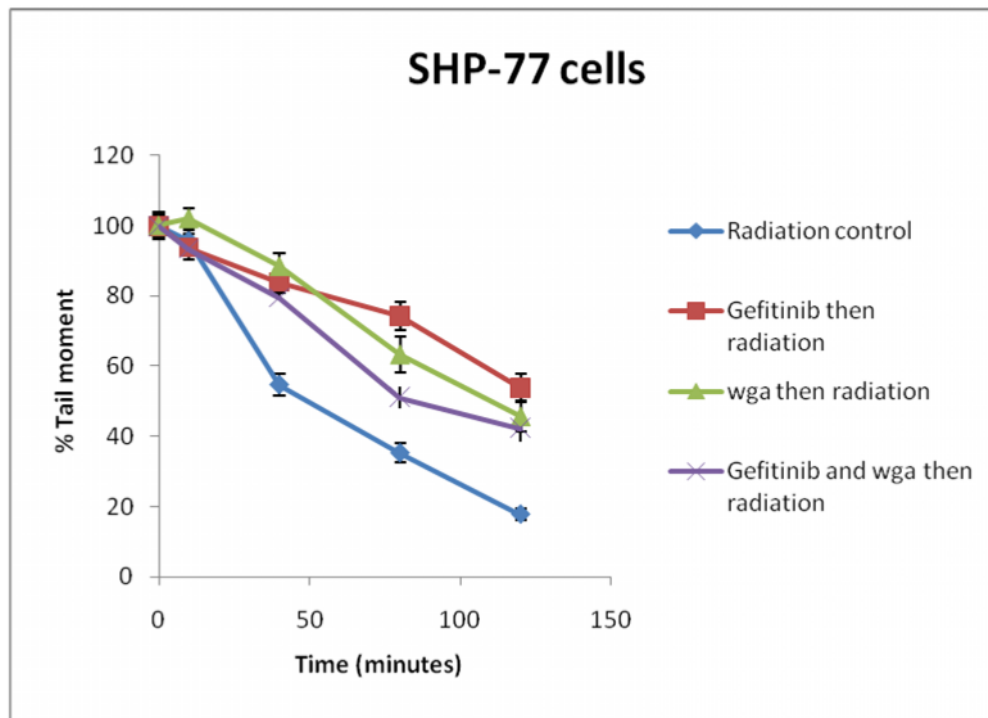
Measurement of irradiation-induced DNA strand breaks and their repair in SHP-77 cells. Strand break formation quantitated as tail moment, plotted against time after irradiation. Cells were treated with gefitinib at 10 μ M or cetuximab at 30nM for 3 hours, drug was removed, and then cells were irradiated at 15 Gy and incubated for up to 120 minutes at 37°C. Data represents the averages of three different experiments, each performed in triplicate; *bars*, SD.

Appendix 3A: Radiation with gefitinib and EGFR nuclear transport inhibitors in DNA repair analysis using NCI-H727 cells



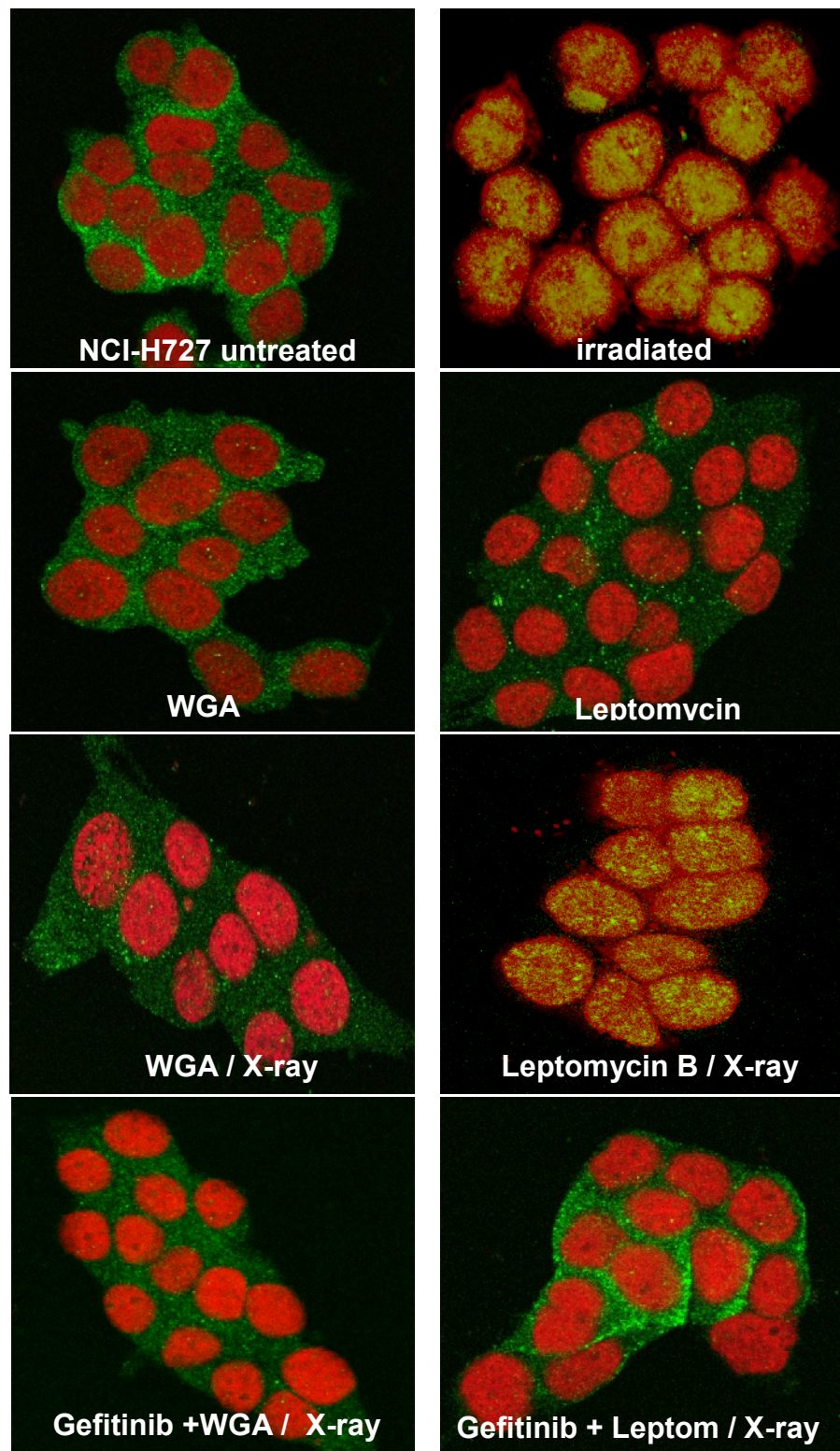
Measurement of irradiation-induced DNA strand breaks and their repair in NCI-H727 cells. Strand break formation quantitated as percentage of control cell (irradiated cell at $t=0$) tail moment, plotted against time after irradiation. Cells were treated with gefitinib at $10\mu\text{M}$ for 3 hours, and/or WGA (0.05mg/ml) or leptomycin B (2nM) for 30 minutes. Drug was removed, and then cells were irradiated at 15Gy and incubated for up to 120 minutes at 37°C . Data represents the averages of three different experiments, each performed in triplicate; bars, SD

Appendix 3B: Radiation with gefitinib and EGFR nuclear transport inhibitors in DNA repair analysis using SHP-77 cells



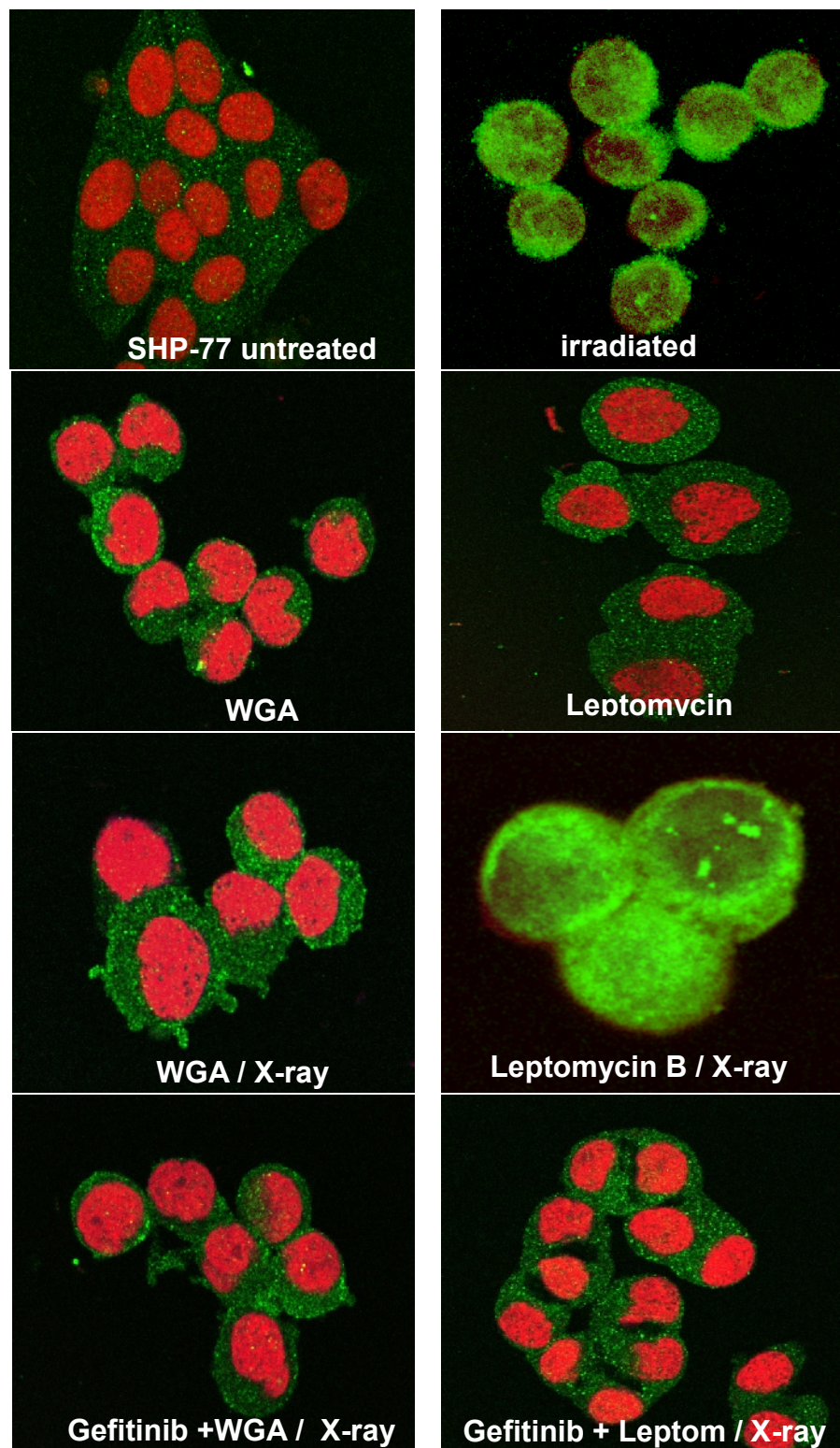
Measurement of irradiation-induced DNA strand breaks and their repair in SHP-77 cells. Strand break formation quantitated as percentage of control cell (irradiated cell at $t=0$) tail moment, plotted against time after irradiation. Cells were treated with gefitinib at $10\mu\text{M}$ for 3 hours, and/or WGA (0.05mg/ml) or leptomycin B (2nM) for 30 minutes. Drug was removed, and then cells were irradiated at 15Gy and incubated for up to 120 minutes at 37°C . Data represents the averages of three different experiments, each performed in triplicate; bars, SD

Appendix 3C: Radiation with gefitinib and EGFR nuclear transport inhibitors in immunofluorescent analysis using NCI-H727 cells



NCI-H727 cells were treated with gefitinib at 10 μ M for 3 hours and/or WGA (0.05mg/ml) or leptomycin B (2nM) added in the last 30 minutes. Cells were then irradiated at 30Gy and incubated for 5 minutes at 37°C. Cells were then fixed and stained for EGFR (green) and nucleus was stained with propidium iodide (red).

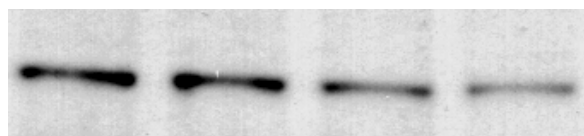
Appendix 3D: Radiation with gefitinib and EGFR nuclear transport inhibitors in immunofluorescent analysis using SHP-77 cells



SHP-77 cells were treated with gefitinib at 10 μ M for 3 hours and/or WGA (0.05mg/ml) or leptomycin B (2nM) added in the last 30 minutes. Cells were then irradiated at 4Gy and incubated for 5 minutes at 37°C. Cells were then fixed and stained for EGFR (green) and nucleus was stained with propidium iodide (red).

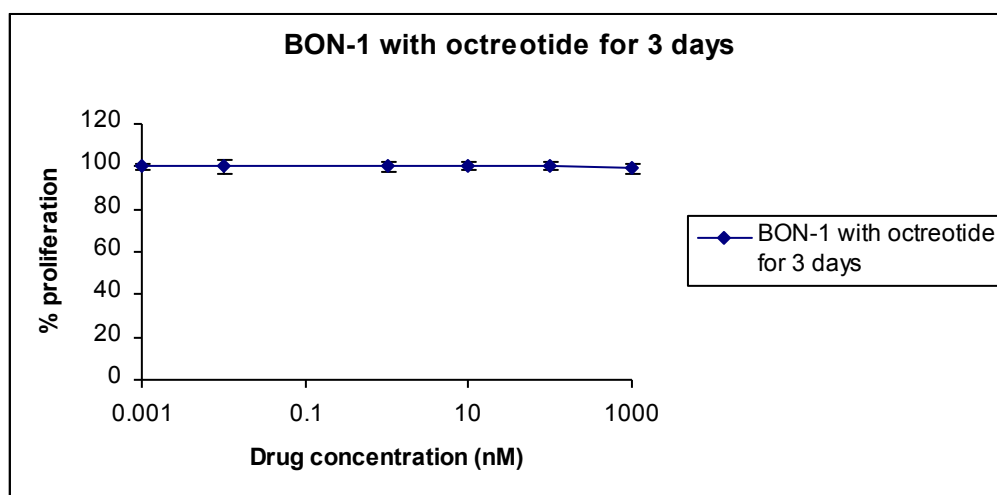
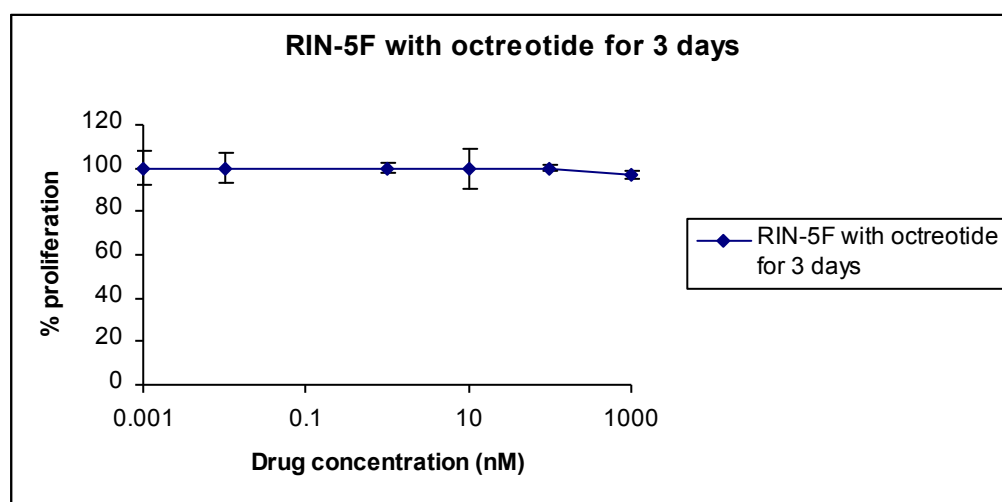
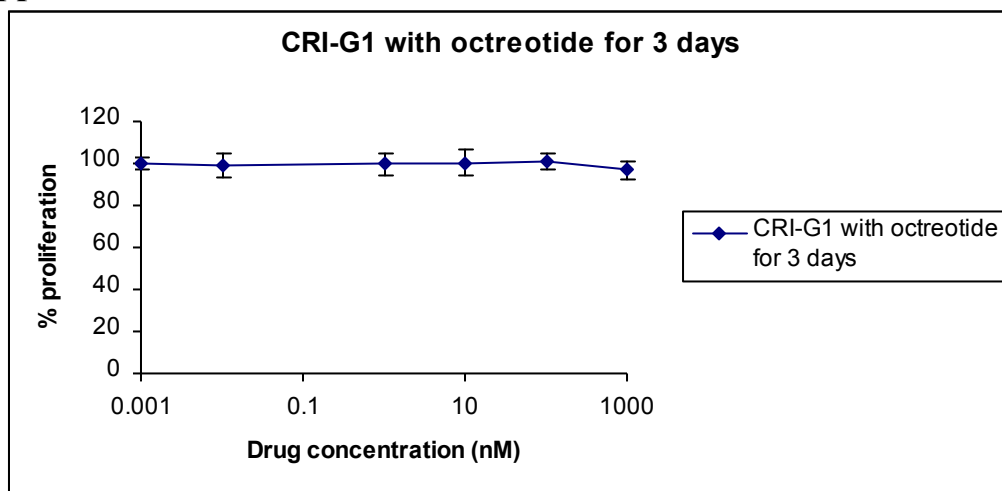
Appendix 4: Titration of anti-gastrin pathway drugs in SW1222 and HCT-116 colon cancer cells

NCI-H727 SHP-77 CRI-G1 RIN-5F



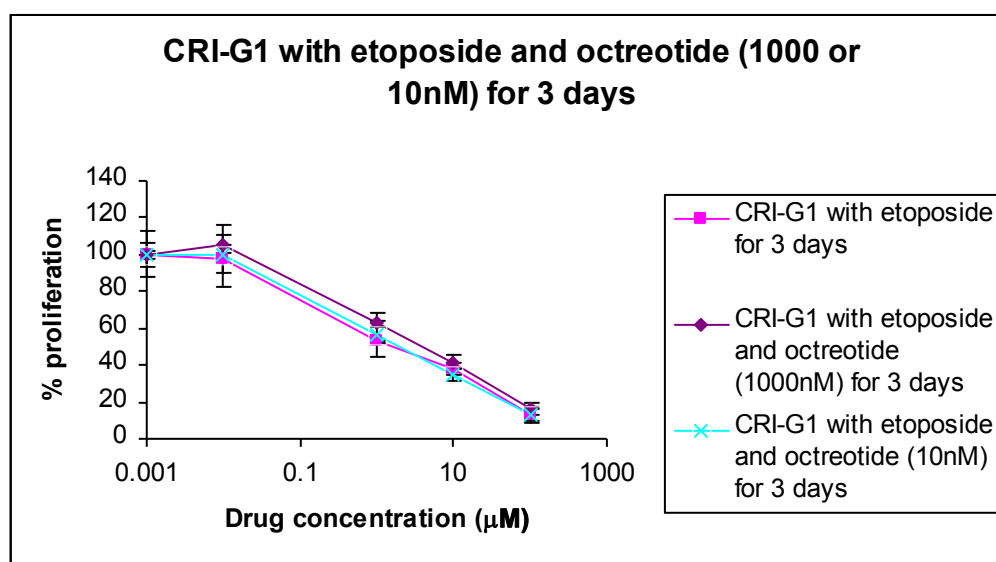
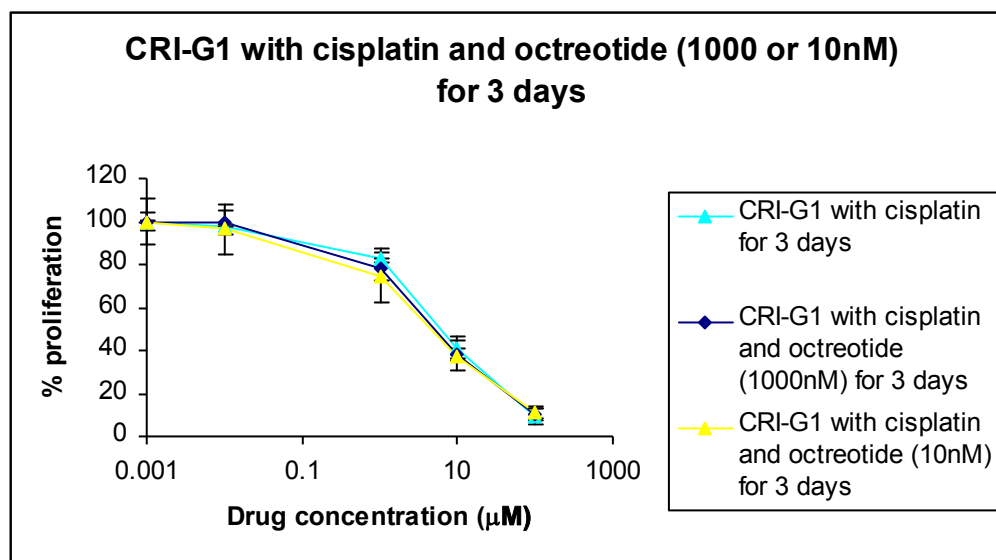
Immunoblot of lysates from CRI-G1, NCI-H727, SHP-77 and RIN-5F cell lines using 1 μ g/ml anti-c-KIT antibody for 2 hours. The bands of 145kDa were revealed using an HRP-conjugated goat anti-rabbit antibody.

Appendix 5A: Titration of octreotide in CRI-G1, RIN-5F and BON-1 cells



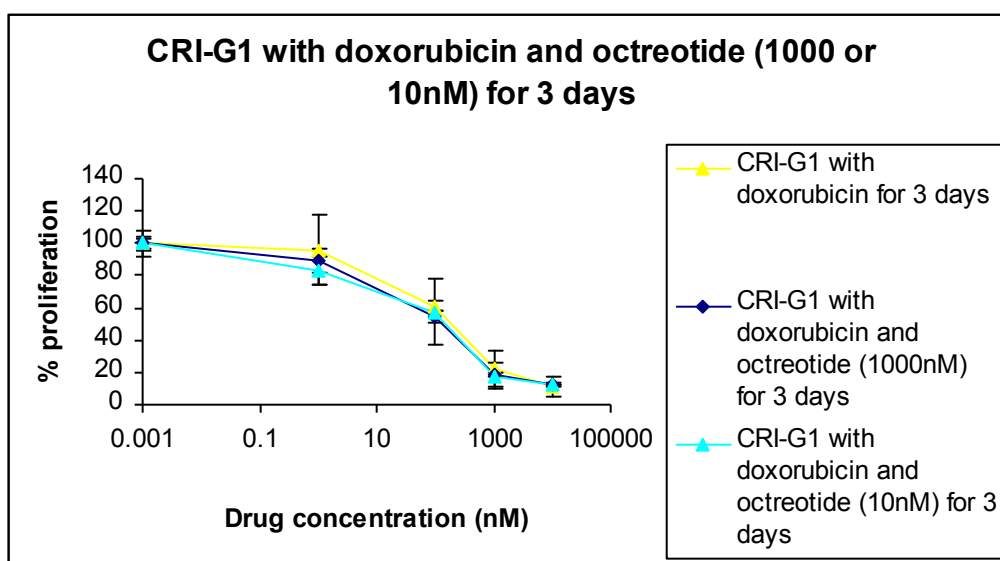
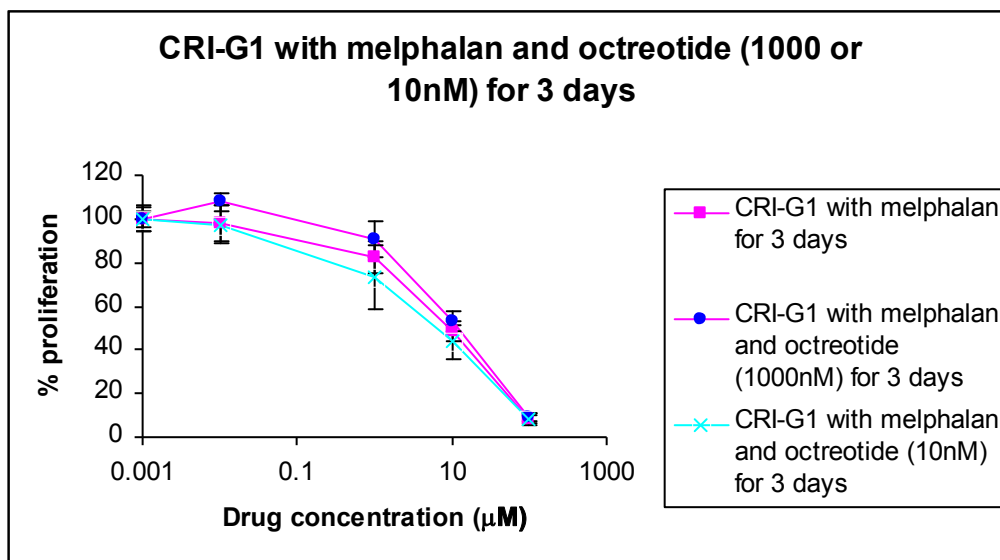
Titration of octreotide in CRI-G1, RIN-5F and BON-1 cells. Cells were treated with octreotide at 0-1000nM for 72 hours followed by 2 days incubation in drug free media. In the graphs, the '0' point of the x-axis is represented as '0.001' due to the logarithmic scale of the x-axis. Proliferation was calculated as a % of control untreated cells. The values represent averages of 3 different experiments, each performed in triplicate; bars, SD.

Appendix 5B (part I): Chemotherapeutic agents with octreotide in CRI-G1 cells



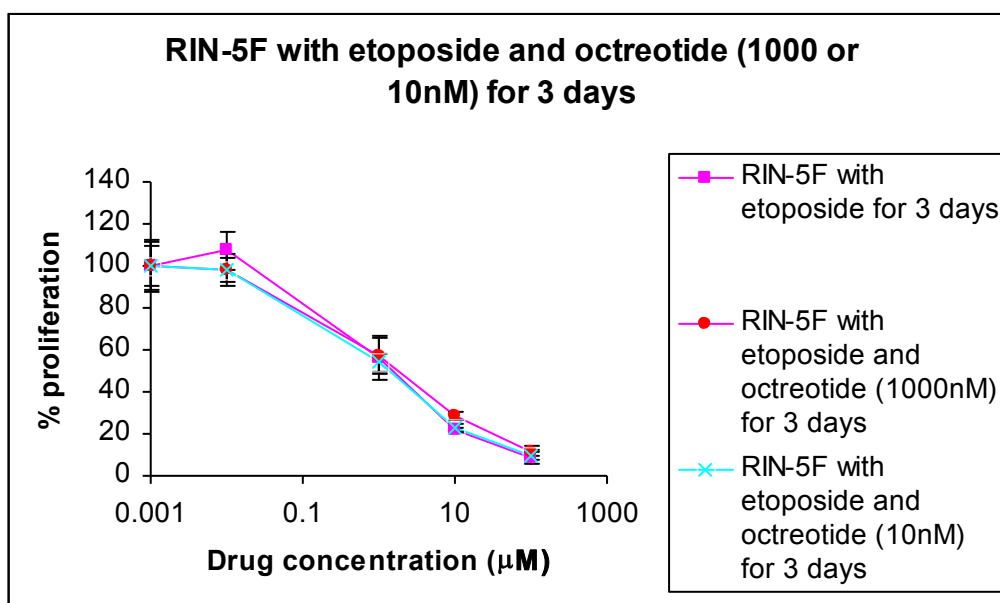
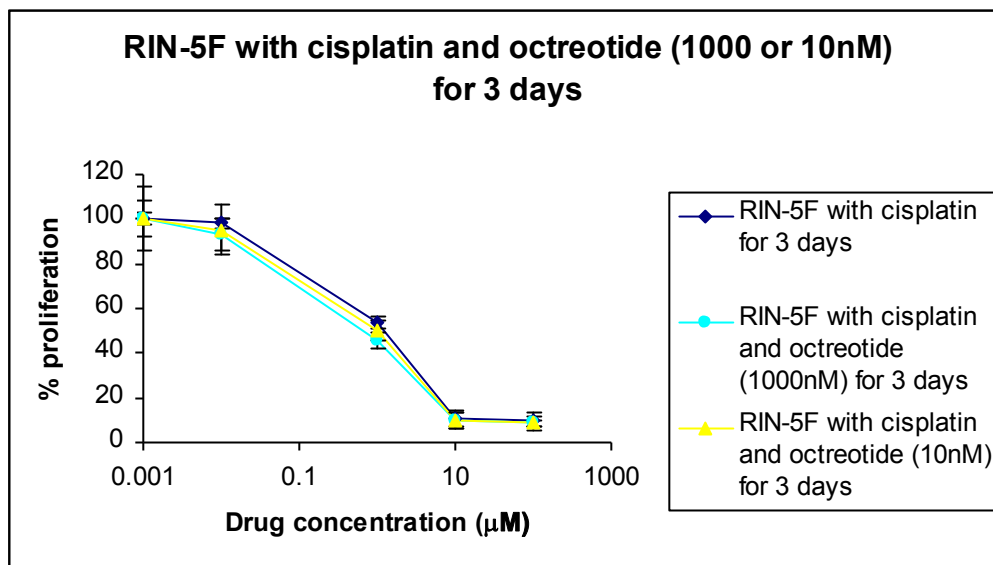
CRI-G1 cells were treated with octreotide (at 10 or 1000nM) and cisplatin or etoposide (both at 0-100μM) for 72 hours, followed by 48 hours in drug-free media. In the graphs, the '0' point of the x-axis is represented as '0.001' due to the logarithmic scale of the x-axis. Proliferation was calculated as a % of control untreated cells. The values represent averages of 3 different experiments, each performed in triplicate; *bars*, SD.

Appendix 5B (part II): Chemotherapeutic agents with octreotide in CRI-G1 cells



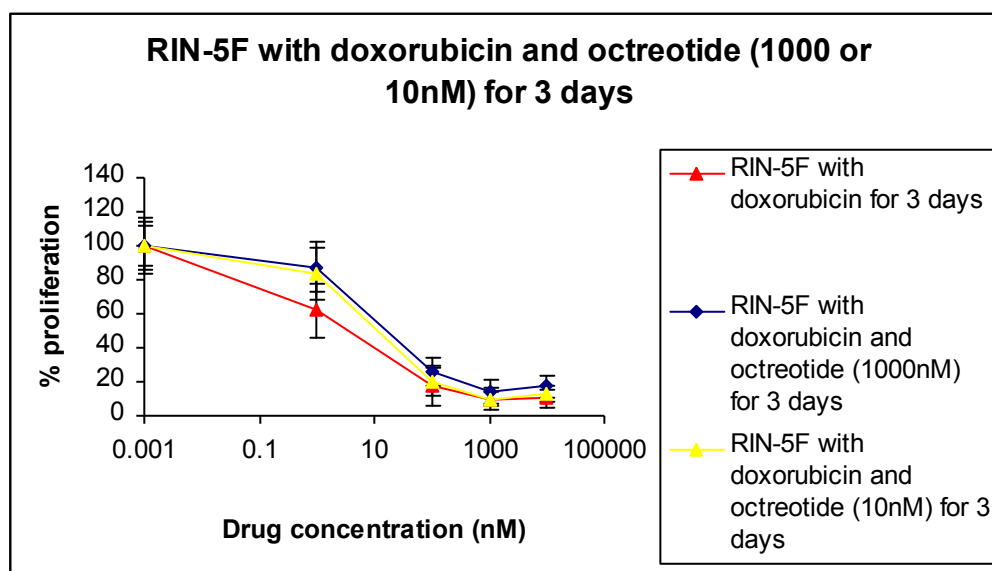
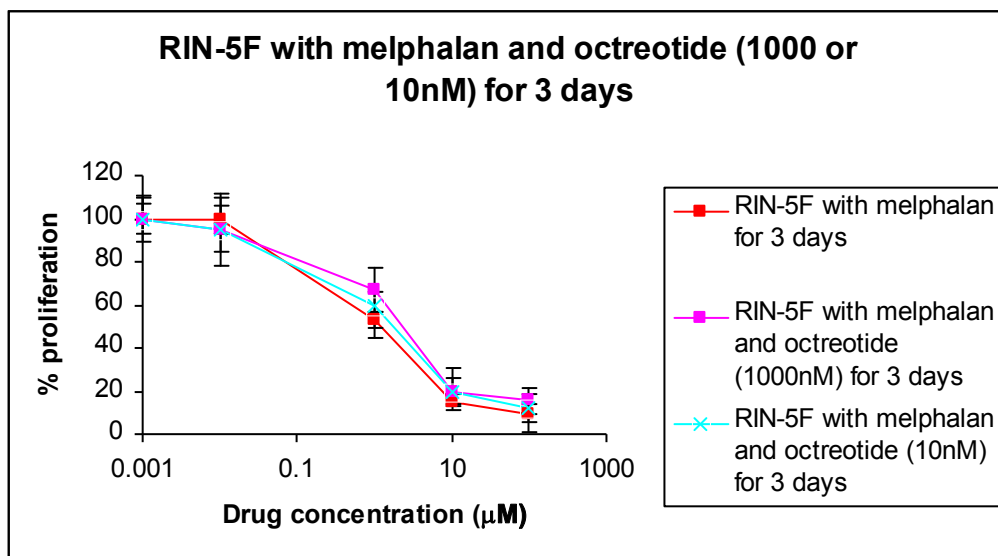
CRI-G1 cells were treated with octreotide (at 10 or 1000nM) and melphalan (0-100μM) or doxorubicin (0-10μM) for 72 hours, followed by 48 hours in drug-free media. In the graphs, the '0' point of the x-axis is represented as '0.001' due to the logarithmic scale of the x-axis. Proliferation was calculated as a % of control untreated cells. The values represent averages of 3 different experiments, each performed in triplicate; *bars*, SD.

Appendix 5C (part I): Chemotherapeutic agents with octreotide in RIN-5F cells



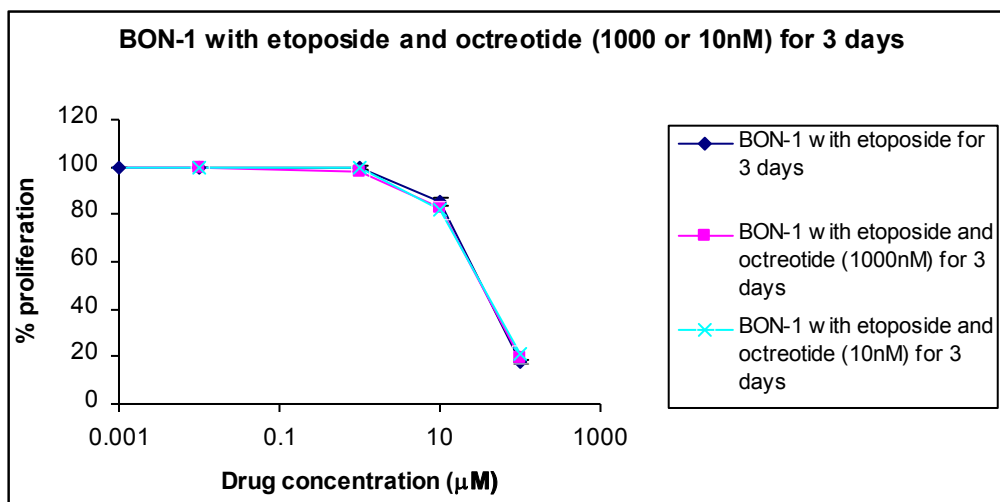
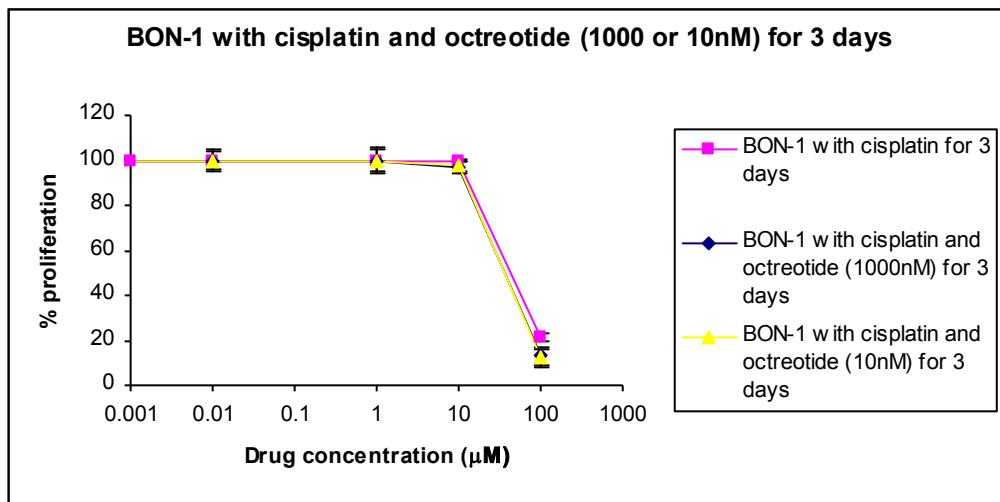
RIN-5F cells were treated with octreotide (at 10 or 1000nM) and cisplatin or etoposide (both at 0-100μM) for 72 hours, followed by 48 hours in drug-free media. In the graphs, the '0' point of the x-axis is represented as '0.001' due to the logarithmic scale of the x-axis. Proliferation was calculated as a % of control untreated cells. The values represent averages of 3 different experiments, each performed in triplicate; *bars*, SD.

Appendix 5C (part II): Chemotherapeutic agents with octreotide in RIN-5F cells



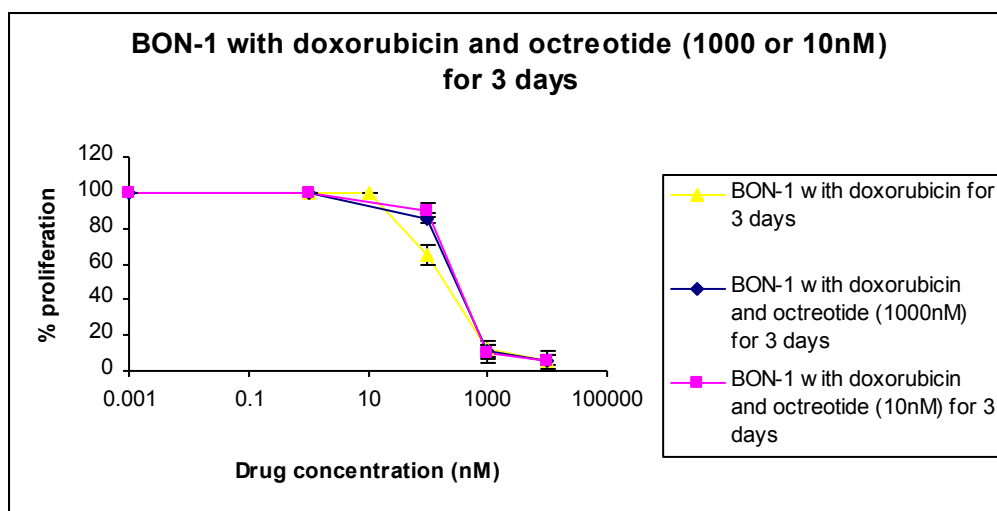
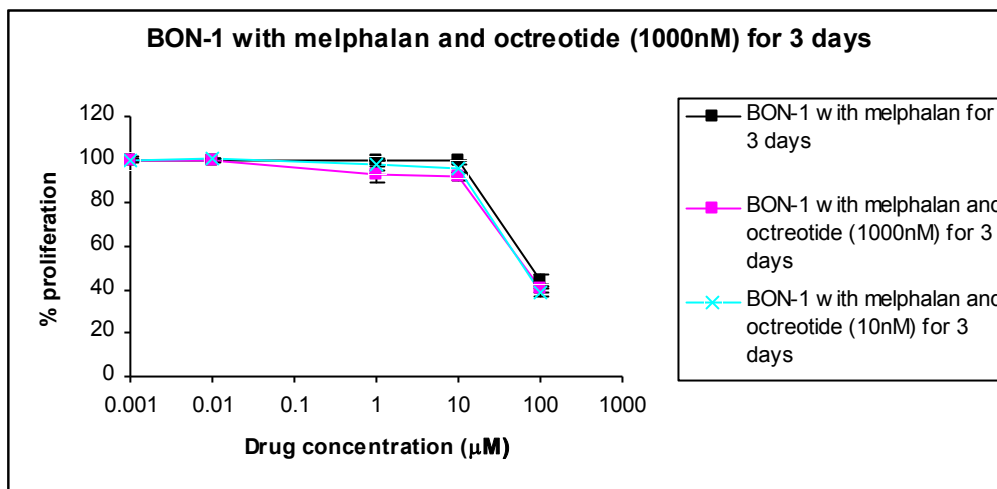
RIN-5F cells were treated with octreotide (at 10 or 1000nM) and melphalan (0-100μM) or doxorubicin (0-10μM) for 72 hours, followed by 48 hours in drug-free media. In the graphs, the '0' point of the x-axis is represented as '0.001' due to the logarithmic scale of the x-axis. Proliferation was calculated as a % of control untreated cells. The values represent averages of 3 different experiments, each performed in triplicate; bars, SD.

Appendix 5D (part I): Chemotherapeutic agents with octreotide in BON-1 cells



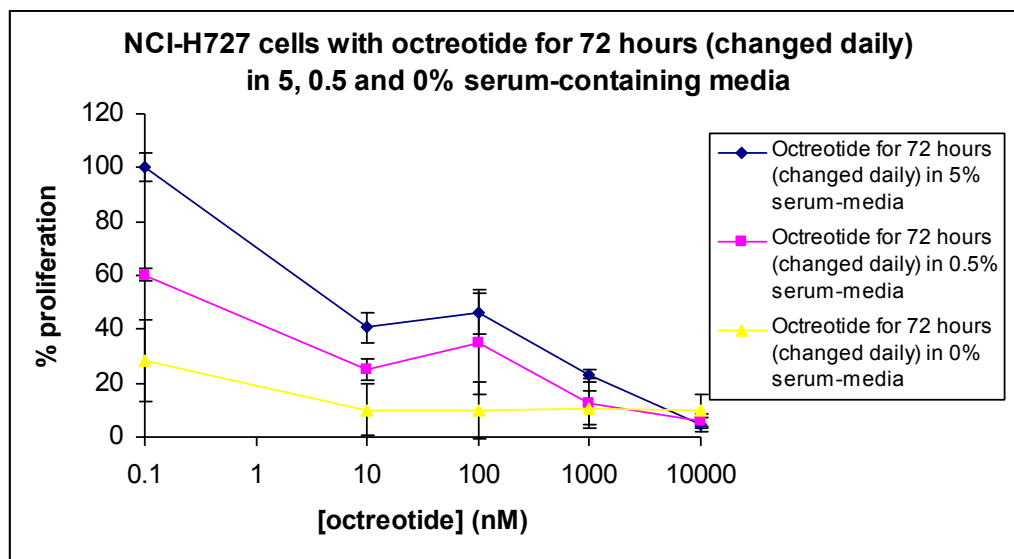
BON-1 cells were treated with octreotide (at 10 or 1000nM) and cisplatin or etoposide (both at 0-100μM) for 72 hours, followed by 48 hours in drug-free media. In the graphs, the '0' point of the x-axis is represented as '0.001' due to the logarithmic scale of the x-axis. Proliferation was calculated as a % of control untreated cells. The values represent averages of 3 different experiments, each performed in triplicate; *bars*, SD.

Appendix 5D (part II): Chemotherapeutic agents with octreotide in BON-1 cells



BON-1 cells were treated with octreotide (at 10 or 1000nM) and melphalan (0-100μM) or doxorubicin (0-10μM) for 72 hours, followed by 48 hours in drug-free media. In the graphs, the '0' point of the x-axis is represented as '0.001' due to the logarithmic scale of the x-axis. Proliferation was calculated as a % of control untreated cells. The values represent averages of 3 different experiments, each performed in triplicate; *bars*, SD.

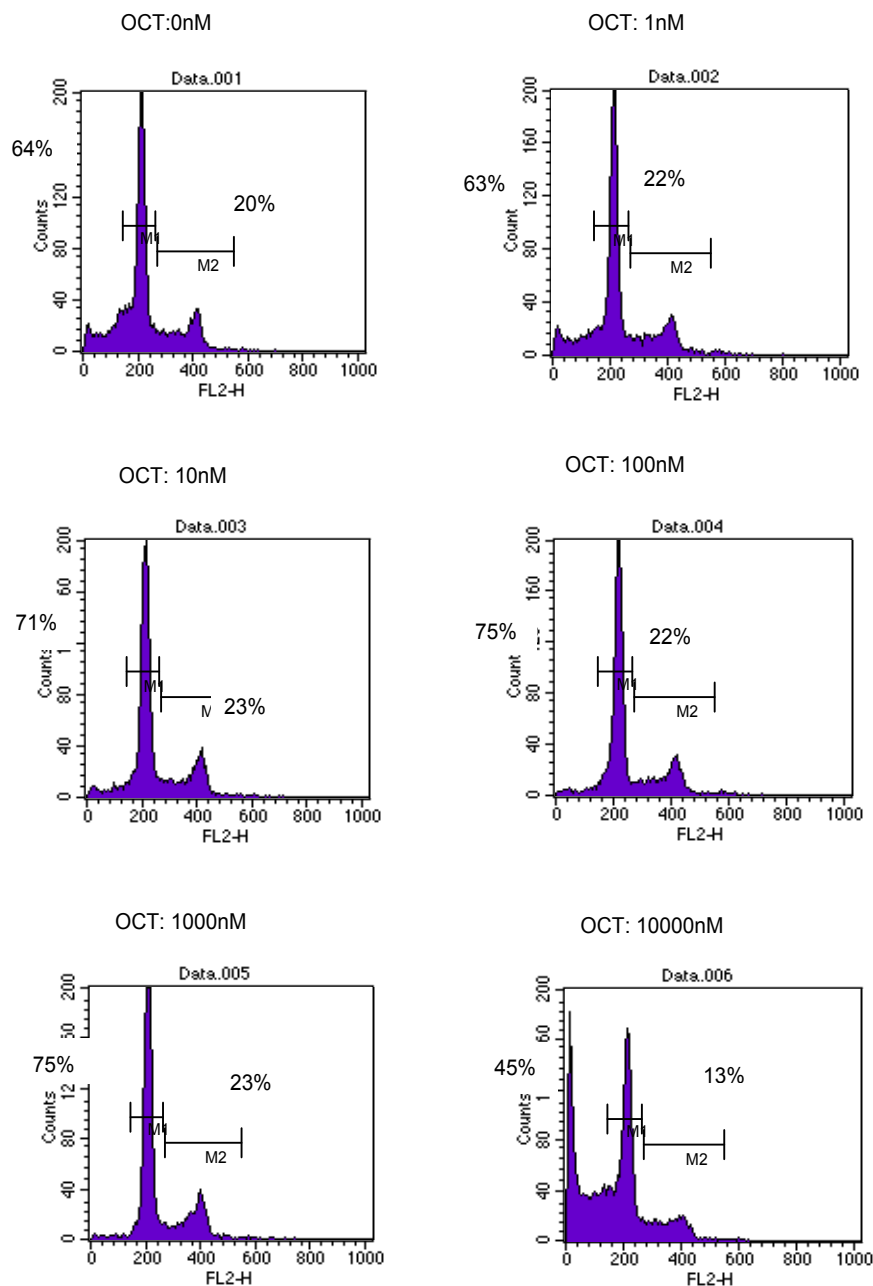
Appendix 5E: Octreotide effect in cell proliferation in media containing 5%, 0.5% or 0% serum



Octreotide at 0-10 μ M added for 72 hours (changed daily) in media containing 5, 0.5 or 0% serum. Proliferation was calculated as a % of control untreated cells. The values represent averages of 2 different experiments, each performed in triplicate; *bars*, SD.

Appendix 5F: Octreotide effect on the cell cycle in BON-1 cells

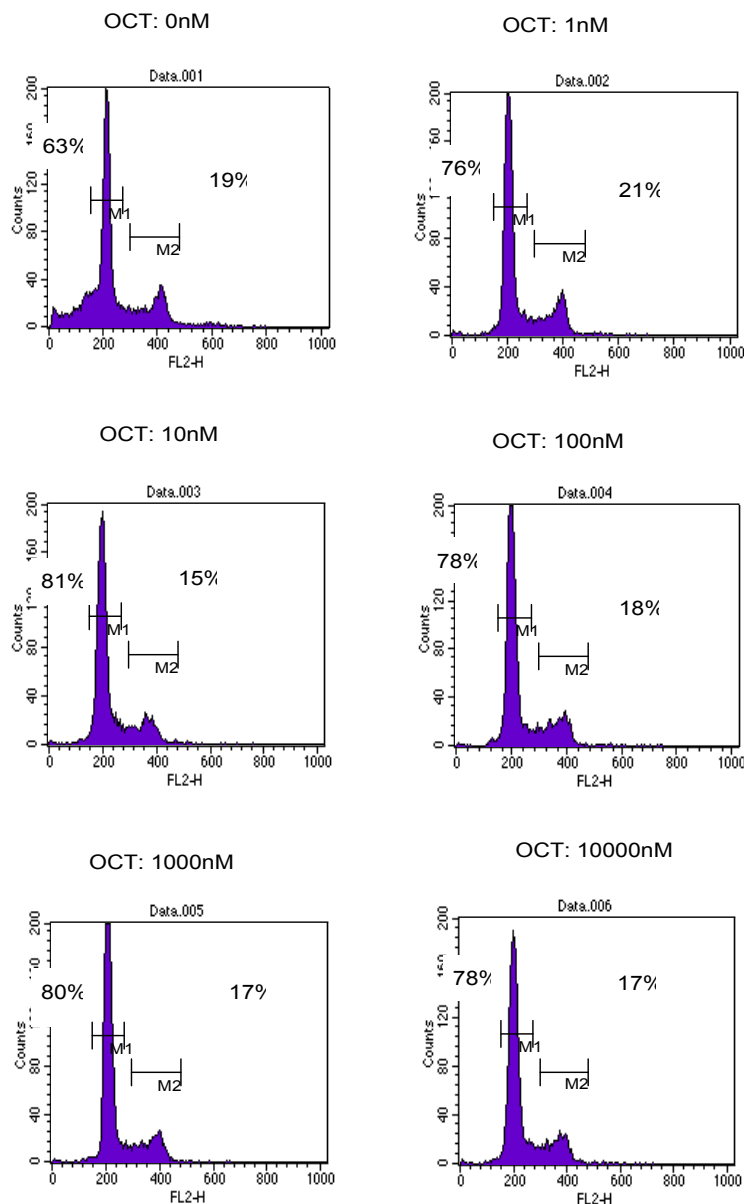
BON-1



BON-1 cells were treated with octreotide at 0-10,000nM for 24 hours. 'FL2-H' denotes DNA content by propidium iodide staining, while 'counts' denotes cell number. Bars M1 and M2 indicate populations of cells at phases G1 and G2/M of the cell cycle respectively.

Appendix 5G: Octreotide effect on the cell cycle in CRI-G1 cells

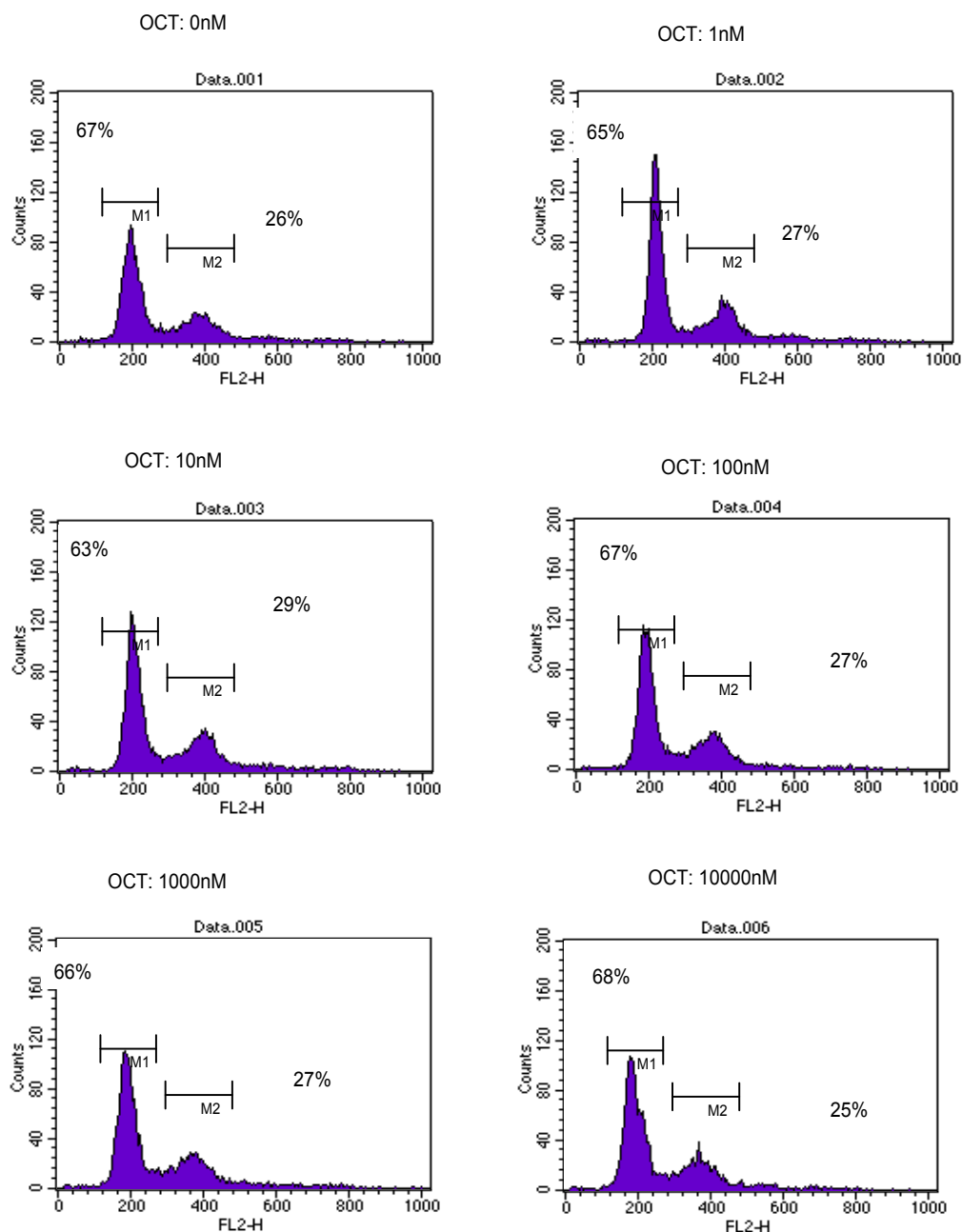
CRI-G1



CRI-G1 cells were treated with octreotide at 0-10,000nM for 24 hours. 'FL2-H' denotes DNA content by propidium iodide staining, while 'counts' denotes cell number. Bars M1 and M2 indicate populations of cells at phases G1 and G2/M of the cell cycle respectively.

Appendix 5H: Octreotide effect on the cell cycle in RIN-5F cells

RIN-5F



RIN-5F cells were treated with octreotide at 0-10,000nM for 24 hours. 'FL2-H' denotes DNA content by propidium iodide staining, while 'counts' denotes cell number. Bars M1 and M2 indicate populations of cells at phases G1 and G2/M of the cell cycle respectively.

BIBLIOGRAPHY

- Abrams, T. J., Lee, L. B., Murray, L. J., Pryer, N. K., and Cherrington, J. M. (2003): SU11248 inhibits KIT and platelet-derived growth factor receptor beta in preclinical models of human small cell lung cancer. *Mol Cancer Ther* **2**, 471-8.
- Alaoui-Jamali MA, Song DJ, Benlimame N, Yen L, Deng X, Hernandez-Perez M, Wang T. (2003): Regulation of multiple tumor microenvironment markers by overexpression of single or paired combinations of ErbB receptors. *Cancer Res.* **63**(13):3764-74.
- Amin DN, Perkins AS, Stern DF. (2004): Gene expression profiling of ErbB receptor and ligand-dependent transcription. *Oncogene.* **23**(7):1428-38.
- Arnold, R., Frank, M., and Kajdan, U. (1994): Management of gastroenteropancreatic endocrine tumors: the place of somatostatin analogues. *Digestion* **55 Suppl 3**, 107-13.
- Ashman LK, Cambareri AC, To LB, Levinsky RJ, Juttner CA. (1991): Expression of the YB5.B8 antigen (c-kit proto-oncogene product) in normal human bone marrow. *Blood.* **78**(1):30-7.
- Ashman LK. (1999): The biology of stem cell factor and its receptor C-kit. *The International Journal of Biochemistry and Cell Biology.* **31**(10):1037-51.
- Atalay, G., Cardoso, F., Awada, A., and Piccart, M. J. (2003): Novel therapeutic strategies targeting the epidermal growth factor receptor (EGFR) family and its downstream effectors in breast cancer. *Ann Oncol* **14**, 1346-63.
- Attoub S, Moizo L, Laigneau JP, Alchepo B, Lewin MJ, Bado A. (1998): YM022, a highly potent and selective CCKB antagonist inhibiting gastric acid secretion in the rat, the cat and isolated rabbit glands. *Fundamental and Clinical Pharmacology.* **12**(3):256-62.
- Baldwin, G. S., and Shulkes, A. (2007): CCK receptors and cancer. *Curr Top Med Chem* **7**, 1232-8.
- Bandyopadhyay, D., Mandal, M., Adam, L., Mendelsohn, J., and Kumar, R. (1998): Physical interaction between epidermal growth factor receptor and DNA-dependent protein kinase in mammalian cells. *J Biol Chem* **273**, 1568-73.
- Baselga, J., Norton, L., Masui, H., Pandiella, A., Coplan, K., Miller, W. H., Jr., and Mendelsohn, J. (1993): Antitumor effects of doxorubicin in combination with anti-epidermal growth factor receptor monoclonal antibodies. *J Natl Cancer Inst* **85**, 1327-33.
- Bateman, A. C., Judd, M., Radenkovic, D., and Johnson, C. D. (2008): CD117/KIT expression in pancreatic adenocarcinoma. *Pancreas* **36**, 76-9.
- Bauer, S., Duensing, A., Demetri, G. D., and Fletcher, J. A. (2007): KIT oncogenic signaling mechanisms in imatinib-resistant gastrointestinal stromal tumor: PI3-kinase/AKT is a crucial survival pathway. *Oncogene* **26**, 7560-8.
- Baulida J, Kraus MH, Alimandi M, Di Fiore PP, Carpenter G. (1996): All ErbB receptors other than the epidermal growth factor receptor are endocytosis impaired. *J Biol Chem.* **271**(9):5251-7.
- Benhar M, Engelberg D, Levitzki A (2002). Cisplatin-induced activation of the EGF receptor. *Oncogene.* **21**(57):8723-31.
- Benhar, M., Dalyot, I., Engelberg, D., and Levitzki, A. (2001): Enhanced ROS production in oncogenically transformed cells potentiates c-Jun N-terminal kinase and p38 mitogen-

- activated protein kinase activation and sensitization to genotoxic stress. *Mol Cell Biol* **21**, 6913-26.
- Bertherat, J., Tenenbaum, F., Perlemoine, K., Videau, C., Alberini, J. L., Richard, B., Dousset, B., Bertagna, X., and Epelbaum, J. (2003): Somatostatin receptors 2 and 5 are the major somatostatin receptors in insulinomas: an in vivo and in vitro study. *J Clin Endocrinol Metab* **88**, 5353-60.
- Besmer P, Murphy JE, George PC, Qiu FH, Bergold PJ, Lederman L, Snyder HW Jr, Brodeur D, Zuckerman EE, Hardy WD. (1986): A new acute transforming feline retrovirus and relationship of its oncogene v-kit with the protein kinase gene family. *Nature*. **320**(6061):415-21.
- Bhola NE, Grandis JR. (2008): Crosstalk between G-protein-coupled receptors and epidermal growth factor receptor in cancer. *Front Biosci*. **13**:1857-65
- Bianco C, Bianco R, Tortora G, Damiano V, Guerrieri P, Montemaggi P, Mendelsohn J, De Placido S, Bianco AR, Ciardiello F. (2000): Antitumor activity of combined treatment of human cancer cells with ionizing radiation and anti-epidermal growth factor receptor monoclonal antibody C225 plus type I protein kinase A antisense oligonucleotide. *Clin Cancer Res*. **6**: 4343-50.
- Bianco, C., Tortora, G., Bianco, R., Caputo, R., Veneziani, B. M., Caputo, R., Damiano, V., Troiani, T., Fontanini, G., Raben, D., Pepe, S., Bianco, A. R., and Ciardiello, F. (2002): Enhancement of antitumor activity of ionizing radiation by combined treatment with the selective epidermal growth factor receptor-tyrosine kinase inhibitor ZD1839 (Iressa). *Clin Cancer Res* **8**, 3250-8.
- Blackledge G, Averbuch S. (2004): Gefitinib ('Iressa', ZD1839) and new epidermal growth factor receptor inhibitors. *British Journal of Cancer*. **90**(3):566-72.
- Blackstein, M. E., Blay, J. Y., Corless, C., Driman, D. K., Riddell, R., Soulieres, D., Swallow, C. J., and Verma, S. (2006): Gastrointestinal stromal tumours: consensus statement on diagnosis and treatment. *Can J Gastroenterol* **20**, 157-63.
- Blanke CD, Von Mehren M, Joensuu H, Roberts PJ, Eisenberg B, Heinrich M, Druker B, Tuveson D, Dimitrijevic S, Silberman S, Demetri GD. (2001): Evaluation of the safety and efficacy of an oral molecularly-targeted therapy, STI571, in patients (Pts) with unresectable or metastatic gastrointestinal stromal tumors (GIST) expressing c-kit (CD117). *Proceedings of the American Society for Clinical Oncology*. 20:1a.
- Block WD, Yu Y, Merkle D, Gifford JL, Ding Q, Meek K, Lees-Miller SP. (2004): Autophosphorylation-dependent remodelling of the DNA-dependent protein kinase catalytic subunit regulates ligation of DNA ends. *Nucleic Acids Res*. **32**: 4351-7.
- Blume-Jensen P and Hunter T. (2001): Oncogenic kinase signalling. *Nature*. **411**: 355-65.
- Blume-Jensen, P., Janknecht, R., and Hunter, T. (1998): The kit receptor promotes cell survival via activation of PI 3-kinase and subsequent Akt-mediated phosphorylation of Bad on Ser136. *Curr Biol* **8**, 779-82.
- Bogdan S, Klämbt C. (2001): Epidermal growth factor receptor signaling. *Curr Biol*. **11**(8):R292-5
- Boissan M, Feger F, Guillosson JJ, Arock M. (2000): C-Kit and c-kit mutations in mastocytosis and other hematological diseases. *Journal of Leukocyte Biology*. **67**(2):135-48.

- Bombardieri, E., Maccauro, M., De Deckere, E., Savelli, G., and Chiti, A. (2001): Nuclear medicine imaging of neuroendocrine tumours, pp. S51-61: *Ann Oncol*.
- Bonner, J. A., Harari, P. M., Giralt, J., Azarnia, N., Shin, D. M., Cohen, R. B., Jones, C. U., Sur, R., Raben, D., Jassem, J., Ove, R., Kies, M. S., Baselga, J., Yousoufian, H., Amellal, N., Rowinsky, E. K., and Ang, K. K. (2006): Radiotherapy plus cetuximab for squamous-cell carcinoma of the head and neck. *N Engl J Med* **354**, 567-78.
- Bousquet C, Guillermet J, Vernejoul F, Lahlou H, Buscail L, Susini C. (2004): Somatostatin receptors and regulation of cell proliferation. *Digestive Liver Diseases*. **36** Suppl 1:S2-7.
- Braconi, C., Bracci, R., and Cellerino, R. (2008): Molecular targets in Gastrointestinal Stromal Tumors (GIST) therapy. *Curr Cancer Drug Targets* **8**, 359-66.
- Brazeau, P., Vale, W., Burgus, R., Ling, N., Butcher, M., Rivier, J., and Guillemin, R. (1973): Hypothalamic polypeptide that inhibits the secretion of immunoreactive pituitary growth hormone. *Science* **179**, 77-9.
- Breeman, W. A., de Jong, M., Kwekkeboom, D. J., Valkema, R., Bakker, W. H., Kooij, P. P., Visser, T. J., and Krenning, E. P. (2001): Somatostatin receptor-mediated imaging and therapy: basic science, current knowledge, limitations and future perspectives. *Eur J Nucl Med* **28**, 1421-9.
- Brown, J. R., and DuBois, R. N. (2005): COX-2: a molecular target for colorectal cancer prevention. *J Clin Oncol* **23**, 2840-55.
- Buscail, L., Delesque, N., Esteve, J. P., Saint-Laurent, N., Prats, H., Clerc, P., Robberecht, P., Bell, G. I., Liebow, C., Schally, A. V., and et al. (1994): Stimulation of tyrosine phosphatase and inhibition of cell proliferation by somatostatin analogues: mediation by human somatostatin receptor subtypes SSTR1 and SSTR2. *Proc Natl Acad Sci U S A* **91**, 2315-9.
- Cabrera, CM; Cobo, F; Nieto, A; Cortés, JL; Montes, RM; Catalina, P; Concha, A. (2006): "Identity tests: determination of cell line cross-contamination". *Cytotechnology*. **51** (2): 45-50.
- Cambier N, Chopra R, Strasser A, Metcalf D, Elefanty AG. (1998): BCR-ABL activates pathways mediating cytokine independence and protection against apoptosis in murine hematopoietic cells in a dose-dependent manner. *Oncogene*. **16**: 335-48.
- Camp, E. R., Summy, J., Bauer, T. W., Liu, W., Gallick, G. E., and Ellis, L. M. (2005): Molecular mechanisms of resistance to therapies targeting the epidermal growth factor receptor. *Clin Cancer Res* **11**, 397-405.
- Caplin ME, Buscombe JR, Hilson AJ, Jones AL, Watkinson AF, Burroughs AK. (1998): Carcinoid tumour. *Lancet*. **352** (9130):799-805.
- Carpenter, G. (2000): The EGF receptor: a nexus for trafficking and signaling. *Bioessays* **22**, 697-707.
- Carr K, Yao JC, Rashid A, Yeung SC, Szklaruk J, Baker J, Vauthey JN, Curley S, Ellis L and Ajani JA. A phase II trial of imatinib in patients with advanced carcinoid tumor *Journal of Clinical Oncology*, 2004 ASCO Annual Meeting Proceedings (Post-Meeting Edition). **Vol 22, No 14S (July 15 Supplement)**, 2004: 4124
- Carroll, M., Ohno-Jones, S., Tamura, S., Buchdunger, E., Zimmermann, J., Lydon, N. B., Gilliland, D. G., and Druker, B. J. (1997): CGP 57148, a tyrosine kinase inhibitor,

- inhibits the growth of cells expressing BCR-ABL, TEL-ABL, and TEL-PDGFR fusion proteins. *Blood* **90**, 4947-52.
- Carson, W. E., Haldar, S., Baiocchi, R. A., Croce, C. M., and Caligiuri, M. A. (1994): The c-kit ligand suppresses apoptosis of human natural killer cells through the upregulation of bcl-2. *Proc Natl Acad Sci U S A* **91**, 7553-7.
- Cartee, L., Vrana, J. A., Wang, Z., Park, J. S., Birrer, M., Fisher, P. B., Grant, S., and Dent, P. (2000): Inhibition of the mitogen activated protein kinase pathway potentiates radiation-induced cell killing via cell cycle arrest at the G2/M transition and independently of increased signaling by the JNK/c-Jun pathway. *Int J Oncol* **16**, 413-22.
- Casali, C., Stefani, A., Rossi, G., Migaldi, M., Bettelli, S., Parise, A., and Morandi, U. (2004): The prognostic role of c-kit protein expression in resected large cell neuroendocrine carcinoma of the lung. *Ann Thorac Surg* **77**, 247-52; discussion 252-3.
- Castellone, M. D., Teramoto, H., Williams, B. O., Druey, K. M., and Gutkind, J. S. (2005): Prostaglandin E2 promotes colon cancer cell growth through a Gs-axin-beta-catenin signaling axis. *Science* **310**, 1504-10.
- Chabot B, Stephenson DA, Chapman VM, Besmer P, Bernstein A. (1988): The proto-oncogene c-kit encoding a transmembrane tyrosine kinase receptor maps to the mouse W locus. *Nature*. **335**(6185):88-9.
- Chakravarti, A., Loeffler, J. S., and Dyson, N. J. (2002): Insulin-like growth factor receptor I mediates resistance to anti-epidermal growth factor receptor therapy in primary human glioblastoma cells through continued activation of phosphoinositide 3-kinase signaling. *Cancer Res* **62**, 200-7.
- Charland, S., Boucher, M. J., Houde, M., and Rivard, N. (2001): Somatostatin inhibits Akt phosphorylation and cell cycle entry, but not p42/p44 mitogen-activated protein (MAP) kinase activation in normal and tumoral pancreatic acinar cells. *Endocrinology* **142**, 121-8.
- Chen, H., Isozaki, K., Kinoshita, K., Ohashi, A., Shinomura, Y., Matsuzawa, Y., Kitamura, Y., and Hirota, S. (2003): Imatinib inhibits various types of activating mutant kit found in gastrointestinal stromal tumors. *Int J Cancer* **105**, 130-5.
- Chian, R., Young, S., Danilkovitch-Miagkova, A., Ronnstrand, L., Leonard, E., Ferrao, P., Ashman, L., and Linnekin, D. (2001): Phosphatidylinositol 3 kinase contributes to the transformation of hematopoietic cells by the D816V c-Kit mutant. *Blood* **98**, 1365-73.
- Chinnaiyan, P., Huang, S., Vallabhaneni, G., Armstrong, E., Varambally, S., Tomlins, S. A., Chinnaiyan, A. M., and Harari, P. M. (2005): Mechanisms of enhanced radiation response following epidermal growth factor receptor signaling inhibition by erlotinib (Tarceva). *Cancer Res* **65**, 3328-35.
- Cho, H. S., and Leahy, D. J. (2002): Structure of the extracellular region of HER3 reveals an interdomain tether. *Science* **297**, 1330-3.
- Chow, L. Q., and Eckhardt, S. G. (2007): Sunitinib: from rational design to clinical efficacy. *J Clin Oncol* **25**, 884-96.
- Ciardiello F, Caputo R, Bianco R, Damiano V, Pomatito G, De Placido S, Bianco AR, Tortora G. (2000): Antitumor effect and potentiation of cytotoxic drugs activity in human cancer cells

by ZD1839 (Iressa), an epidermal growth factor receptor-selective tyrosine kinase inhibitor. *Clin Cancer Res*. **6**: 2053-63.

- Ciardiello F, Tortora G. (2003): Epidermal growth factor receptor (EGFR) as a target in cancer therapy: understanding the role of receptor expression and other molecular determinants that could influence the response to anti-EGFR drugs. *Eur J Cancer*. **39**: 1348-54.
- Ciardiello, F., and Tortora, G. (2001): A novel approach in the treatment of cancer: targeting the epidermal growth factor receptor. *Clin Cancer Res* **7**, 2958-70.
- Ciardiello, F., Caputo, R., Bianco, R., Damiano, V., Fontanini, G., Cuccato, S., De Placido, S., Bianco, A. R., and Tortora, G. (2001): Inhibition of growth factor production and angiogenesis in human cancer cells by ZD1839 (Iressa), a selective epidermal growth factor receptor tyrosine kinase inhibitor. *Clin Cancer Res* **7**, 1459-65.
- Ciardiello, F., Caputo, R., Troiani, T., Borriello, G., Kandimalla, E. R., Agrawal, S., Mendelsohn, J., Bianco, A. R., and Tortora, G. (2001): Antisense oligonucleotides targeting the epidermal growth factor receptor inhibit proliferation, induce apoptosis, and cooperate with cytotoxic drugs in human cancer cell lines. *Int J Cancer* **93**, 172-8.
- Cohen, M. H., Johnson, J. R., and Pazdur, R. (2005): U.S. Food and Drug Administration Drug Approval Summary: conversion of imatinib mesylate (STI571; Gleevec) tablets from accelerated approval to full approval. *Clin Cancer Res* **11**, 12-9.
- Cohen, R. B. (2003): Epidermal growth factor receptor as a therapeutic target in colorectal cancer. *Clin Colorectal Cancer* **2**, 246-51.
- Collis SJ, DeWeese TL, Jeggo PA and Parker AR. (2005): The life and death of DNA-PK. *Oncogene*. **24**: 949-961.
- Cortes, J., Giles, F., O'Brien, S., Thomas, D., Albitar, M., Rios, M. B., Talpaz, M., Garcia-Manero, G., Faderl, S., Letvak, L., Salvado, A., and Kantarjian, H. (2003): Results of imatinib mesylate therapy in patients with refractory or recurrent acute myeloid leukemia, high-risk myelodysplastic syndrome, and myeloproliferative disorders. *Cancer* **97**, 2760-6.
- Csaba, Z., and Dournaud, P. (2001): Cellular biology of somatostatin receptors. *Neuropeptides* **35**, 1-23.
- Cunningham, D., Humblet, Y., Siena, S., Khayat, D., Bleiberg, H., Santoro, A., Bets, D., Mueser, M., Harstrick, A., Verslype, C., Chau, I., and Van Cutsem, E. (2004): Cetuximab monotherapy and cetuximab plus irinotecan in irinotecan-refractory metastatic colorectal cancer. *N Engl J Med* **351**, 337-45.
- Cunningham, M. P., Thomas, H., Fan, Z., and Modjtahedi, H. (2006): Responses of human colorectal tumor cells to treatment with the anti-epidermal growth factor receptor monoclonal antibody ICR62 used alone and in combination with the EGFR tyrosine kinase inhibitor gefitinib. *Cancer Res* **66**, 7708-15.
- Dagher, R., Cohen, M., Williams, G., Rothmann, M., Gobburu, J., Robbie, G., Rahman, A., Chen, G., Staten, A., Griebel, D., and Pazdur, R. (2002): Approval summary: imatinib mesylate in the treatment of metastatic and/or unresectable malignant gastrointestinal stromal tumors. *Clin Cancer Res* **8**, 3034-8.

- De Silva, C. M., and Reid, R. (2003): Gastrointestinal stromal tumors (GIST): C-kit mutations, CD117 expression, differential diagnosis and targeted cancer therapy with Imatinib. *Pathol Oncol Res* **9**, 13-9.
- De Vita, F., Orditura, M., Ciardiello, F., and Catalano, G. (2005): Adjuvant chemotherapy of gastric cancer: which regimens? *Ann Oncol* **16 Suppl 4**, iv102-105.
- De Weerth, A., von Schrenck, T., Gronewold, M., Freudenberg, F., Mirau, S., Schulz, M., and Greten, H. (1997): Characterization of CCK receptors in stomach smooth muscle: evidence for two subtypes. *Biochim Biophys Acta* **1327**, 213-21.
- Debiec-Rychter, M., Dumez, H., Judson, I., Wasag, B., Verweij, J., Brown, M., Dimitrijevic, S., Sciot, R., Stul, M., Vranck, H., Scurr, M., Hagemeyer, A., van Glabbeke, M., and van Oosterom, A. T. (2004): Use of c-KIT/PDGFR α mutational analysis to predict the clinical response to imatinib in patients with advanced gastrointestinal stromal tumours entered on phase I and II studies of the EORTC Soft Tissue and Bone Sarcoma Group. *Eur J Cancer* **40**, 689-95.
- Degen, L., and Beglinger, C. (1999): The role of octreotide in the treatment of gastroenteropancreatic endocrine tumors. *Digestion* **60 Suppl 2**, 9-14.
- Dei Tos, A. P., and Ellis, I. (2005): Assessing epidermal growth factor receptor expression in tumours: what is the value of current test methods? *Eur J Cancer* **41**, 1383-92.
- Deininger, M. W., Goldman, J. M., Lydon, N., and Melo, J. V. (1997): The tyrosine kinase inhibitor CGP57148B selectively inhibits the growth of BCR-ABL-positive cells. *Blood* **90**, 3691-8.
- Dematteo RP, Heinrich MC, El-Rifai WM, Demetri G. (2002): Clinical management of gastrointestinal stromal tumors: before and after STI-571. *Human Pathology*. **33**(5):466-77.
- Demetri GD. (2001): Targeting c-kit mutations in solid tumors: scientific rationale and novel therapeutic options. *Seminars in Oncology*. **8**(5 Suppl 17):19-26.
- Demetri, G. D., Heinrich, M. C., Fletcher, J. A., Fletcher, C. D., Van den Abbeele, A. D., Corless, C. L., Antonescu, C. R., George, S., Morgan, J. A., Chen, M. H., Bello, C. L., Huang, X., Cohen, D. P., Baum, C. M., and Maki, R. G. (2009): Molecular target modulation, imaging, and clinical evaluation of gastrointestinal stromal tumor patients treated with sunitinib malate after imatinib failure. *Clin Cancer Res* **15**, 5902-9.
- Demetri, G. D., von Mehren, M., Blanke, C. D., Van den Abbeele, A. D., Eisenberg, B., Roberts, P. J., Heinrich, M. C., Tuveson, D. A., Singer, S., Janicek, M., Fletcher, J. A., Silverman, S. G., Silberman, S. L., Capdeville, R., Kiese, B., Peng, B., Dimitrijevic, S., Druker, B. J., Corless, C., Fletcher, C. D., and Joensuu, H. (2002): Efficacy and safety of imatinib mesylate in advanced gastrointestinal stromal tumors. *N Engl J Med* **347**, 472-80.
- Dent, P., Yacoub, A., Contessa, J., Caron, R., Amorino, G., Valerie, K., Hagan, M. P., Grant, S., and Schmidt-Ullrich, R. (2003): Stress and radiation-induced activation of multiple intracellular signaling pathways. *Radiat Res* **159**, 283-300.
- Desai, K. K., Khan, M. S., Toumpanakis, C., and Caplin, M. E. (2009): Management of gastroentero-pancreatic neuroendocrine tumors (GEP-NETs). *Minerva Gastroenterol Dietol* **55**, 425-43.

- Deutsch E, Dugray A, AbdulKarim B, Marangoni E, Maggiorella L, Vaganay S, M'Kacher R, Rasy SD, Eschwege F, Vainchenker W, Turhan AG, Bourhis J. (2001): BCR-ABL down-regulates the DNA repair protein DNA-PKcs. *Blood*. **97**: 2084-90.
- Ding Q, Reddy YV, Wang W, Woods T, Douglas P, Ramsden DA, Lees-Miller SP, Meek K. (2003): Autophosphorylation of the catalytic subunit of the DNA-dependent protein kinase is required for efficient end processing during DNA double-strand break repair. *Mol Cell Biol*. **23**: 5836-48.
- Dittmann K, Mayer C, Fehrenbacher B, Schaller M, Raju U, Milas L, Chen DJ, Kehlbach R, Rodemann HP. (2005a): Radiation-induced Epidermal Growth Factor Receptor Nuclear Import Is Linked to Activation of DNA-dependent Protein Kinase. *J Biol Chem*. **280**: 31182-31189.
- Dittmann K, Mayer C, Rodemann HP. (2005b): Inhibition of radiation-induced EGFR nuclear import by C225 (Cetuximab) suppresses DNA-PK activity. *Radiother Oncol*. **76**: 157-161.
- Dorsam, R. T., and Gutkind, J. S. (2007): G-protein-coupled receptors and cancer. *Nat Rev Cancer* **7**, 79-94.
- Dronkert MLG and Kanaar R. (2001): Repair of DNA interstrand crosslinks. *Mut Res*. **486**: 217-247.
- Droogendijk, H. J., Kluin-Nelemans, H. J., van Doormaal, J. J., Oranje, A. P., van de Loosdrecht, A. A., and van Daele, P. L. (2006): Imatinib mesylate in the treatment of systemic mastocytosis: a phase II trial. *Cancer* **107**, 345-51.
- Druker, B. J., Tamura, S., Buchdunger, E., Ohno, S., Segal, G. M., Fanning, S., Zimmermann, J., and Lydon, N. B. (1996): Effects of a selective inhibitor of the Abl tyrosine kinase on the growth of Bcr-Abl positive cells. *Nat Med* **2**, 561-6.
- Dunlop J, Brammer N, Evans N, Ennis C. (1997): YM022 [(R)-1-[2,3-dihydro-1-(2'-methylphenacyl)-2-oxo-5-phenyl-1H-1,4- benzodiazepin-3-yl]-3-(3-methylphenyl)urea]: an irreversible cholecystokinin type-B receptor antagonist. *Biochemical Pharmacology*. **54**(1):81-5.
- Durant S, Karran P. (2003): Vanillins - A novel family of DNA-PK inhibitors. *Nucleic Acids Res*. **31**: 5501-12.
- Dy, G. K., Miller, A. A., Mandrekar, S. J., Aubry, M. C., Langdon, R. M., Jr., Morton, R. F., Schild, S. E., Jett, J. R., and Adjei, A. A. (2005): A phase II trial of imatinib (ST1571) in patients with c-kit expressing relapsed small-cell lung cancer: a CALGB and NCCTG study. *Ann Oncol* **16**, 1811-6.
- El-Deiry, W. S. (1997): Role of oncogenes in resistance and killing by cancer therapeutic agents. *Curr Opin Oncol* **9**, 79-87.
- Eller, J. L., Longo, S. L., Kyle, M. M., Bassano, D., Hicklin, D. J., and Canute, G. W. (2005): Anti-epidermal growth factor receptor monoclonal antibody cetuximab augments radiation effects in glioblastoma multiforme in vitro and in vivo. *Neurosurgery* **56**, 155-62; discussion 162.
- El-Rayes, B. F., and LoRusso, P. M. (2004): Targeting the epidermal growth factor receptor. *Br J Cancer* **91**, 418-24.

- Eriksson B, Oberg K, Stridsberg M. (2000): Tumor markers in neuroendocrine tumors. *Digestion*. **62** Suppl 1:33-8.
- Erler B, Finch M, Hodges A, Horowitz K, Matulewicz T and Topilow AA. (2004): cd117 overexpression in neuroendocrine carcinomas *Journal of Clinical Oncology*, 2004 ASCO Annual Meeting Proceedings (Post-Meeting Edition). **Vol 22, No 14S (July 15 Supplement)**, 2004: 9595
- Escribano L, Ocqueteau M, Almeida J, Orfao A, San Miguel JF. (1998): Expression of the c-kit (CD117) molecule in normal and malignant hematopoiesis. *Leukemia and Lymphoma*. **30**(5-6):459-66.
- Falck, J., Coates, J., and Jackson, S. P. (2005): Conserved modes of recruitment of ATM, ATR and DNA-PKcs to sites of DNA damage. *Nature* **434**, 605-11.
- Fan, Z., Baselga, J., Masui, H., and Mendelsohn, J. (1993): Antitumor effect of anti-epidermal growth factor receptor monoclonal antibodies plus cis-diamminedichloroplatinum on well established A431 cell xenografts. *Cancer Res* **53**, 4637-42.
- Fedi P, Pierce JH, di Fiore PP, Kraus MH. (1994): Efficient coupling with phosphatidylinositol 3-kinase, but not phospholipase C gamma or GTPase-activating protein, distinguishes ErbB-3 signaling from that of other ErbB/EGFR family members. *Mol Cell Biol*. **14**: 492-500.
- Feger F, Ribadeau Dumas A, Leriche L, Valent P, Arock M. (2002): Kit and c-kit mutations in mastocytosis: a short overview with special reference to novel molecular and diagnostic concepts. *International Archives of Allergy and Immunology*. **127**(2):110-4.
- Ferrari, L., Della Torre, S., Collini, P., Martinetti, A., Procopio, G., De Dosso, S., Bajetta, R., and Catena, L. (2006): Kit protein (CD117) and proliferation index (Ki-67) evaluation in well and poorly differentiated neuroendocrine tumors. *Tumori* **92**, 531-5.
- Fichtinger-Shepman AM, Van der Veer JL, Den Hartog JH, Lohman PH and Reedijk J. (1985): Adducts of the anti-tumour drug cis-diamminedichloroplatinum(II) with DN: formation, identification and quantitaion. *Biochemistry*. **24**: 707-13.
- Fjallskog ML, Lejonklou MH, Oberg KE, Eriksson BK, Janson ET. (2003): Expression of molecular targets for tyrosine kinase receptor antagonists in malignant endocrine pancreatic tumors. *Clinical Cancer Research*. **9**(4):1469-73.
- Fletcher, C. D., Berman, J. J., Corless, C., Gorstein, F., Lasota, J., Longley, B. J., Miettinen, M., O'Leary, T. J., Remotti, H., Rubin, B. P., Shmookler, B., Sobin, L. H., and Weiss, S. W. (2002): Diagnosis of gastrointestinal stromal tumors: a consensus approach. *Int J Surg Pathol* **10**, 81-9.
- Fornari, F. A., Randolph, J. K., Yalowich, J. C., Ritke, M. K., and Gewirtz, D. A. (1994): Interference by doxorubicin with DNA unwinding in MCF-7 breast tumor cells. *Mol Pharmacol* **45**, 649-56.
- Foucaud, M., Tikhonova, I. G., Langer, I., Escrieut, C., Dufresne, M., Seva, C., Maigret, B., and Fourmy, D. (2006): Partial agonism, neutral antagonism, and inverse agonism at the human wild-type and constitutively active cholecystokinin-2 receptors. *Mol Pharmacol* **69**, 680-90.
- Friedmann B, Caplin M, Hartley JA, Hochhauser D. (2004): Modulation of DNA repair in vitro after treatment with chemotherapeutic agents by the epidermal growth factor receptor inhibitor gefitinib (ZD1839). *Clinical Cancer Research*. **10**(19):6476-86.

- Friedmann, B. J., Caplin, M., Savic, B., Shah, T., Lord, C. J., Ashworth, A., Hartley, J. A., and Hochhauser, D. (2006): Interaction of the epidermal growth factor receptor and the DNA-dependent protein kinase pathway following gefitinib treatment. *Mol Cancer Ther* **5**, 209-18.
- Fukuda, M., Asano, S., Nakamura, T., Adachi, M., Yoshida, M., Yanagida, M., and Nishida, E. (1997): CRM1 is responsible for intracellular transport mediated by the nuclear export signal. *Nature* **390**, 308-11.
- Galli SJ, Zsebo KM, Geissler EN. (1994): The kit ligand, stem cell factor. *Advances in Immunology*. **55**:1-96.
- Gambacorti-Passerini CB, Gunby RH, Piazza R, Galiotta A, Rostagno R, Scapozza L. (2003): Molecular mechanisms of resistance to imatinib in Philadelphia-chromosome-positive leukaemias. *The Lancet Oncology*. **4**(2):75-85.
- Garrett TP, McKern NM, Lou M, Elleman TC, Adams TE, Lovrecz GO, Zhu HJ, Walker F, Frenkel MJ, Hoyne PA, Jorissen RN, Nice EC, Burgess AW, Ward CW. (2002): Crystal structure of a truncated epidermal growth factor receptor extracellular domain bound to transforming growth factor alpha. *Cell*. **110**: 763-73.
- Gatzemeier, U., Pluzanska, A., Szczesna, A., Kaukel, E., Roubec, J., De Rosa, F., Milanowski, J., Karnicka-Mlodkowski, H., Pesek, M., Serwatowski, P., Ramlau, R., Janaskova, T., Vansteenkiste, J., Strausz, J., Manikhas, G. M., and Von Pawel, J. (2007): Phase III study of erlotinib in combination with cisplatin and gemcitabine in advanced non-small-cell lung cancer: the Tarceva Lung Cancer Investigation Trial. *J Clin Oncol* **25**, 1545-52.
- Geissler EN, Ryan MA, Housman DE. (1988): The dominant-white spotting (W) locus of the mouse encodes the c-kit proto-oncogene. *Cell*. **55**(1):185-92.
- Georgii-Hemming, P., Stromberg, T., Janson, E. T., Stridsberg, M., Wiklund, H. J., and Nilsson, K. (1999): The somatostatin analog octreotide inhibits growth of interleukin-6 (IL-6)-dependent and IL-6-independent human multiple myeloma cell lines. *Blood* **93**, 1724-31.
- Gesbert F and Griffin JD. (2000): Bcr/Abl activates transcription of the Bcl-X gene through STAT5. *Blood*. **96**: 2269-76.
- Giaccone, G., Gonzalez-Larriba, J. L., van Oosterom, A. T., Alfonso, R., Smit, E. F., Martens, M., Peters, G. J., van der Vijgh, W. J., Smith, R., Averbuch, S., and Fandi, A. (2004): Combination therapy with gefitinib, an epidermal growth factor receptor tyrosine kinase inhibitor, gemcitabine and cisplatin in patients with advanced solid tumors. *Ann Oncol* **15**, 831-8.
- Gibril F, Jensen RT. (2004): Diagnostic uses of radiolabelled somatostatin receptor analogues in gastroenteropancreatic endocrine tumours. *Digestive Liver Diseases*. **36** Suppl 1:S106-20.
- Gilbert, J. A., Lloyd, R. V., and Ames, M. M. (2005): Lack of mutations in EGFR in gastroenteropancreatic neuroendocrine tumors. *N Engl J Med* **353**, 209-10.
- Gracey, D. J., Bell, R., and King, D. J. (2000): PD-135,158, a cholecystokinin(B) antagonist, enhances latent inhibition in the rat. *Pharmacol Biochem Behav* **65**, 459-63.
- Grant, S., Qiao, L., and Dent, P. (2002): Roles of ERBB family receptor tyrosine kinases, and downstream signaling pathways, in the control of cell growth and survival. *Front Biosci* **7**, d376-89.

- Gronchi, A., Fiore, M., Miselli, F., Lagonigro, M. S., Coco, P., Messina, A., Pilotti, S., and Casali, P. G. (2007): Surgery of residual disease following molecular-targeted therapy with imatinib mesylate in advanced/metastatic GIST. *Ann Surg* **245**, 341-6.
- Gross, D. J., Munter, G., Bitan, M., Siegal, T., Gabizon, A., Weitzen, R., Merimsky, O., Ackerstein, A., Salmon, A., Sella, A., and Slavin, S. (2006): The role of imatinib mesylate (Glivec) for treatment of patients with malignant endocrine tumors positive for c-kit or PDGF-R. *Endocr Relat Cancer* **13**, 535-40.
- Gupta, R. A., and Dubois, R. N. (2001): Colorectal cancer prevention and treatment by inhibition of cyclooxygenase-2. *Nat Rev Cancer* **1**, 11-21.
- Hakanson R, Chen D, Andersson K, Monstein HJ, Zhao CM, Ryberg B, Sundler F, Mattsson H. (1994): The biology and physiology of the ECL cell. *The Yale Journal of Biology and Medicine*. **67**:123.
- Halfdanarson, T. R., Rabe, K. G., Rubin, J., and Petersen, G. M. (2008): Pancreatic neuroendocrine tumors (PNETs): incidence, prognosis and recent trend toward improved survival. *Ann Oncol* **19**, 1727-33.
- Hanada, N., Lo, H. W., Day, C. P., Pan, Y., Nakajima, Y., and Hung, M. C. (2006): Co-regulation of B-Myb expression by E2F1 and EGF receptor. *Mol Carcinog* **45**, 10-7.
- Hanahan D, and Weinberg RA. (2000): The hallmarks of cancer. *Cell*. **100**: 57-70.
- Hande, K. R. (1998): Etoposide: four decades of development of a topoisomerase II inhibitor. *Eur J Cancer* **34**, 1514-21.
- Harari PM. (2004): Epidermal growth factor receptor inhibition strategies in oncology. *Endocr Rel Cancer*. **11**: 689-708.
- Heinemann A, Jovic M, Holzer-Petsche U, Petho G, Peskar BM, Horwell DC, Holzer P. (1995): Mediation by CCKB receptors of the CCK-evoked hyperaemia in rat gastric mucosa. *British Journal of Pharmacology*. **116**(4):2274-8.
- Heinrich MC, Blanke CD, Druker BJ, Corless CL. (2002): Inhibition of KIT tyrosine kinase activity: a novel molecular approach to the treatment of KIT-positive malignancies. *Journal of Clinical Oncology*. **20**(6):1692-703.
- Heinrich, M. C., Corless, C. L., Blanke, C. D., Demetri, G. D., Joensuu, H., Roberts, P. J., Eisenberg, B. L., von Mehren, M., Fletcher, C. D., Sandau, K., McDougall, K., Ou, W. B., Chen, C. J., and Fletcher, J. A. (2006): Molecular correlates of imatinib resistance in gastrointestinal stromal tumors. *J Clin Oncol* **24**, 4764-74.
- Helms, J. B., and Zurzolo, C. (2004): Lipids as targeting signals: lipid rafts and intracellular trafficking. *Traffic* **5**, 247-54.
- Henderson, D., and Hurley, L. H. (1995): Molecular struggle for transcriptional control. *Nat Med* **1**, 525-7.
- Herbst RS, Shin DM. (2002): Monoclonal antibodies to target epidermal growth factor receptor-positive tumors: a new paradigm for cancer therapy. *Cancer*. **94**: 1593- 611.
- Herbst RS. (2002): ZD1839: targeting the epidermal growth factor receptor in cancer therapy. *Expert Opinion on Investigational Drugs*. **11**(6):837-49.
- Herbst, R. S., Giaccone, G., Schiller, J. H., Natale, R. B., Miller, V., Manegold, C., Scagliotti, G., Rosell, R., Oliff, I., Reeves, J. A., Wolf, M. K., Krebs, A. D., Averbuch, S. D., Ochs, J.

- S., Grous, J., Fandi, A., and Johnson, D. H. (2004): Gefitinib in combination with paclitaxel and carboplatin in advanced non-small-cell lung cancer: a phase III trial--INTACT 2. *J Clin Oncol* **22**, 785-94.
- Hirano, K., Shishido-Hara, Y., Kitazawa, A., Kojima, K., Sumiishi, A., Umino, M., Kikuchi, F., Sakamoto, A., Fujioka, Y., and Kamma, H. (2008): Expression of stem cell factor (SCF), a KIT ligand, in gastrointestinal stromal tumors (GISTs): a potential marker for tumor proliferation. *Pathol Res Pract* **204**, 799-807.
- Hirono, Y., Tsugawa, K., Fushida, S., Ninomiya, I., Yonemura, Y., Miyazaki, I., Endou, Y., Tanaka, M., and Sasaki, T. (1995): Amplification of epidermal growth factor receptor gene and its relationship to survival in human gastric cancer. *Oncology* **52**, 182-8.
- Hirota, S., Isozaki, K., Moriyama, Y., Hashimoto, K., Nishida, T., Ishiguro, S., Kawano, K., Hanada, M., Kurata, A., Takeda, M., Muhammad Tunio, G., Matsuzawa, Y., Kanakura, Y., Shinomura, Y., and Kitamura, Y. (1998): Gain-of-function mutations of c-kit in human gastrointestinal stromal tumors. *Science* **279**, 577-80.
- Hofsl E, Thommesen L, Norsett K, Falkmer S, Syversen U, Sandvik A, Laegreid A. (2002): Expression of chromogranin A and somatostatin receptors in pancreatic AR42J cells. *Molecular and Cellular Endocrinology*. **194**(1-2):165-73.
- Holbro, T., Civenni, G., and Hynes, N. E. (2003): The ErbB receptors and their role in cancer progression. *Exp Cell Res* **284**, 99-110.
- Holtz MS, Slovak ML, Zhang F, Sawyers CL, Forman SJ, Bhatia R. (2002): Imatinib mesylate (STI571) inhibits growth of primitive malignant progenitors in chronic myelogenous leukemia through reversal of abnormally increased proliferation. *Blood*. **99**(10):3792-800.
- Hopfner M, Sutter AP, Gerst B, Zeitz M, Scherubl H. (2003): A novel approach in the treatment of neuroendocrine gastrointestinal tumours. Targeting the epidermal growth factor receptor by gefitinib (ZD1839). *British Journal of Cancer*. **89**(9):1766-75.
- Hornick, J. L., and Fletcher, C. D. (2003): Validating immunohistochemical staining for KIT (CD117). *Am J Clin Pathol* **119**, 325-7.
- Hsu, S. C., and Hung, M. C. (2007): Characterization of a novel tripartite nuclear localization sequence in the EGFR family. *J Biol Chem* **282**, 10432-40.
- Huang SM, Li J, Armstrong EA, Harari PM. (2002): Modulation of radiation response and tumor-induced angiogenesis after epidermal growth factor receptor inhibition by ZD1839 (Iressa) *Cancer Res*. **62**: 4300-6.
- Huang, S. M., and Harari, P. M. (1999): Epidermal growth factor receptor inhibition in cancer therapy: biology, rationale and preliminary clinical results. *Invest New Drugs* **17**, 259-69.
- Huang, S. M., and Harari, P. M. (2000): Modulation of radiation response after epidermal growth factor receptor blockade in squamous cell carcinomas: inhibition of damage repair, cell cycle kinetics, and tumor angiogenesis. *Clin Cancer Res* **6**, 2166-74.
- Huang, S. M., Bock, J. M., and Harari, P. M. (1999): Epidermal growth factor receptor blockade with C225 modulates proliferation, apoptosis, and radiosensitivity in squamous cell carcinomas of the head and neck. *Cancer Res* **59**, 1935-40.
- Hughes, J., Boden, P., Costall, B., Domeney, A., Kelly, E., Horwell, D. C., Hunter, J. C., Pinnock, R. D., and Woodruff, G. N. (1990): Development of a class of selective

- cholecystokinin type B receptor antagonists having potent anxiolytic activity. *Proc Natl Acad Sci U S A* **87**, 6728-32.
- Huizinga JD, Thuneberg L, Kluppel M, Malysz J, Mikkelsen HB, Bernstein A. (1995): W/kit gene required for interstitial cells of Cajal and for intestinal pacemaker activity. *Nature*. **373**(6512):347-9.
- Hurley LH. (2002): DNA and its associated processes as targets for cancer therapy. *Nature Reviews Cancer*. **2**: 188-200.
- Hynes NE, Lane HA. (2005): ERBB receptors and cancer: the complexity of targeted inhibitors. *Nat Rev Cancer*. **5**: 341-54.
- Imam, H., Eriksson, B., Lukinius, A., Janson, E. T., Lindgren, P. G., Wilander, E., and Oberg, K. (1997): Induction of apoptosis in neuroendocrine tumors of the digestive system during treatment with somatostatin analogs. *Acta Oncol* **36**, 607-14.
- Ishikubo, T., Akagi, K., Kurosumi, M., Yamaguchi, K., Fujimoto, T., Sakamoto, H., Tanaka, Y., and Ochiai, A. (2006): Immunohistochemical and mutational analysis of c-kit in gastrointestinal neuroendocrine cell carcinoma. *Jpn J Clin Oncol* **36**, 494-8.
- Janmaat, M. L., Kruyt, F. A., Rodriguez, J. A., and Giaccone, G. (2003): Response to epidermal growth factor receptor inhibitors in non-small cell lung cancer cells: limited antiproliferative effects and absence of apoptosis associated with persistent activity of extracellular signal-regulated kinase or Akt kinase pathways. *Clin Cancer Res* **9**, 2316-26.
- Jensen RT. (2000): Carcinoid and pancreatic endocrine tumors: recent advances in molecular pathogenesis, localization, and treatment. *Current Opinion in Oncology*. **12**(4):368-77.
- Jiang, Y., Ming, L., Montero, A. J., Kimchi, E., Nikfarjam, M., and Staveley-O'Carroll, K. F. (2008): Optimizing imatinib mesylate treatment in gastrointestinal stromal tumors. *Gastrointest Cancer Res* **2**, 245-50.
- Jiang, Y., Ming, L., Montero, A. J., Kimchi, E., Nikfarjam, M., and Staveley-O'Carroll, K. F. (2008): Optimizing imatinib mesylate treatment in gastrointestinal stromal tumors. *Gastrointest Cancer Res* **2**, 245-50.
- Johnston, A., Gudjonsson, J. E., Sigmundsdottir, H., Ludviksson, B. R., and Valdimarsson, H. (2005): The anti-inflammatory action of methotrexate is not mediated by lymphocyte apoptosis, but by the suppression of activation and adhesion molecules. *Clin Immunol* **114**, 154-63.
- Kaltsas GA, Mukherjee JJ, Grossman AB. (2001): The value of radiolabelled MIBG and octreotide in the diagnosis and management of neuroendocrine tumours. *Annals of Oncology*. **12** Suppl 2:S47-50.
- Kaltsas, G. A., Besser, G. M., and Grossman, A. B. (2004): The diagnosis and medical management of advanced neuroendocrine tumors. *Endocr Rev* **25**, 458-511.
- Kaltsas, G. A., Papadogias, D., Makras, P., and Grossman, A. B. (2005): Treatment of advanced neuroendocrine tumours with radiolabelled somatostatin analogues. *Endocr Relat Cancer* **12**, 683-99.
- Kaltsas, G., Rockall, A., Papadogias, D., Reznick, R., and Grossman, A. B. (2004): Recent advances in radiological and radionuclide imaging and therapy of neuroendocrine tumours. *Eur J Endocrinol* **151**, 15-27.

- Kanakura Y, Ikeda H, Kitayama H, Sugahara H, Furitsu T. (1993): Expression, function and activation of the proto-oncogene c-kit product in human leukemia cells. *Leukemia and Lymphoma*. **10**(1-2):35-41.
- Katakura Y, Alam S, Shirahata S. (1998): immortalization by gene transfection. *Methods Cell Biol*. **57**:69-91.
- Khan, E. M., Heidinger, J. M., Levy, M., Lisanti, M. P., Ravid, T., and Goldkorn, T. (2006): Epidermal growth factor receptor exposed to oxidative stress undergoes Src- and caveolin-1-dependent perinuclear trafficking. *J Biol Chem* **281**, 14486-93.
- Khanna KK and Jackson SP. (2001): DNA double-strand breaks: signalling, repair and the cancer connection. *Nature Genet*. **27**: 247-254.
- Kharbanda S, Pandey P, Jin S, Inoue S, Bharti A, Yuan ZM, Weichselbaum R, Weaver D, Kufe D. (1997): Functional interaction between DNA-PK and c-Abl in response to DNA damage. *Nature*. **386**: 732-5.
- Kim ES, Khuri FR, Herbst RS. (2001): Epidermal growth factor receptor biology (IMC-C225). *Curr Opin Oncol*. **13**: 506-13.
- Kitano, M., Norlen, P., Ding, X. Q., Nakamura, S., and Hakanson, R. (2000): Long-lasting cholecystokinin(2) receptor blockade after a single subcutaneous injection of YF476 or YM022. *Br J Pharmacol* **130**, 699-705.
- Kobayashi S, Boggon TJ, Dayaram T, Janne PA, Kocher O, Meyerson M, Johnson BE, Eck MJ, Tenen DG, Halmos B. (2005): EGFR mutation and resistance of non-small-cell lung cancer to gefitinib. *N Engl J Med*. **352**: 786-92.
- Koizumi, M., Onda, M., Tanaka, N., Seya, T., Yamada, T., and Takahashi, Y. (2002): Antiangiogenic effect of octreotide inhibits the growth of human rectal neuroendocrine carcinoma. *Digestion* **65**, 200-6.
- Krenning, E. P., de Jong, M., Kooij, P. P., Breeman, W. A., Bakker, W. H., de Herder, W. W., van Eijck, C. H., Kwekkeboom, D. J., Jamar, F., Pauwels, S., and Valkema, R. (1999): Radiolabelled somatostatin analogue(s) for peptide receptor scintigraphy and radionuclide therapy. *Ann Oncol* **10 Suppl 2**, S23-9.
- Krug, L. M., Crapanzano, J. P., Azzoli, C. G., Miller, V. A., Rizvi, N., Gomez, J., Kris, M. G., Pizzo, B., Tyson, L., Dunne, M., and Heelan, R. T. (2005): Imatinib mesylate lacks activity in small cell lung carcinoma expressing c-kit protein: a phase II clinical trial. *Cancer* **103**, 2128-31.
- Krystal GW, Hines SJ, Organ CP. (1996): Autocrine growth of small cell lung cancer mediated by coexpression of c-kit and stem cell factor. *Cancer Research*. **56**(2):370-6.
- Krystal GW, Honsawek S, Litz J, Buchdunger E. (2000): The selective tyrosine kinase inhibitor STI571 inhibits small cell lung cancer growth. *Clinical Cancer Research*. **6**(8):3319-26.
- Kulaksiz, H., Eissele, R., Rossler, D., Schulz, S., Holtt, V., Cetin, Y., and Arnold, R. (2002): Identification of somatostatin receptor subtypes 1, 2A, 3, and 5 in neuroendocrine tumours with subtype specific antibodies. *Gut* **50**, 52-60.
- Kulik, G., Klippel, A., and Weber, M. J. (1997): Antiapoptotic signalling by the insulin-like growth factor I receptor, phosphatidylinositol 3-kinase, and Akt. *Mol Cell Biol* **17**, 1595-606.

- Kulke, M. H., Lenz, H. J., Meropol, N. J., Posey, J., Ryan, D. P., Picus, J., Bergsland, E., Stuart, K., Tye, L., Huang, X., Li, J. Z., Baum, C. M., and Fuchs, C. S. (2008): Activity of sunitinib in patients with advanced neuroendocrine tumors. *J Clin Oncol* **26**, 3403-10.
- Kumar, N. (1981): Taxol-induced polymerization of purified tubulin. Mechanism of action. *J Biol Chem* **256**, 10435-41.
- Kwekkeboom, D. J., de Herder, W. W., Kam, B. L., van Eijck, C. H., van Essen, M., Kooij, P. P., Feelders, R. A., van Aken, M. O., and Krenning, E. P. (2008): Treatment with the radiolabeled somatostatin analog [177 Lu-DOTA 0,Tyr3]octreotate: toxicity, efficacy, and survival. *J Clin Oncol* **26**, 2124-30.
- Lamberts SW, Hofland LJ, Nobels FR. (2001): Neuroendocrine tumor markers. *Frontiers in Neuroendocrinology*. **22**(4):309-39.
- Lankat-Buttgereit, B., Horsch, D., Barth, P., Arnold, R., Blocker, S., and Goke, R. (2005): Effects of the tyrosine kinase inhibitor imatinib on neuroendocrine tumor cell growth. *Digestion* **71**, 131-40.
- Lassila, M., Allen, T. J., Cao, Z., Thallas, V., Jandeleit-Dahm, K. A., Candido, R., and Cooper, M. E. (2004): Imatinib attenuates diabetes-associated atherosclerosis. *Arterioscler Thromb Vasc Biol* **24**, 935-42.
- Le Coutre, P., Mologni, L., Cleris, L., Marchesi, E., Buchdunger, E., Giardini, R., Formelli, F., and Gambacorti-Passerini, C. (1999): In vivo eradication of human BCR/ABL-positive leukemia cells with an ABL kinase inhibitor. *J Natl Cancer Inst* **91**, 163-8.
- Le Roy, C., and Wrana, J. L. (2005): Signaling and endocytosis: a team effort for cell migration. *Dev Cell* **9**, 167-8.
- Learn CA, Hartzell TL, Wikstrand CJ, Archer GE, Rich JN, Friedman AH, Friedman HS, Bigner DD, Sampson JH. (2004): Resistance to tyrosine kinase inhibition by mutant epidermal growth factor receptor variant III contributes to the neoplastic phenotype of glioblastoma multiforme. *Clin Cancer Res*. **10**: 3216-24.
- Learn, C. A., Hartzell, T. L., Wikstrand, C. J., Archer, G. E., Rich, J. N., Friedman, A. H., Friedman, H. S., Bigner, D. D., and Sampson, J. H. (2004): Resistance to tyrosine kinase inhibition by mutant epidermal growth factor receptor variant III contributes to the neoplastic phenotype of glioblastoma multiforme. *Clin Cancer Res* **10**, 3216-24.
- Lefevre, G., Glotin, A. L., Calipel, A., Mouriaux, F., Tran, T., Kherrouche, Z., Maurage, C. A., Auclair, C., and Mascarelli, F. (2004): Roles of stem cell factor/c-Kit and effects of Glivec/STI571 in human uveal melanoma cell tumorigenesis. *J Biol Chem* **279**, 31769-79.
- Lennartsson, J., Jelacic, T., Linnekin, D., and Shivakrupa, R. (2005): Normal and oncogenic forms of the receptor tyrosine kinase kit. *Stem Cells* **23**, 16-43.
- Leong, W. L., and Pasieka, J. L. (2002): Regression of metastatic carcinoid tumors with octreotide therapy: two case reports and a review of the literature. *J Surg Oncol* **79**, 180-7.
- Levitzki A. (2003): Protein kinase inhibitors as a therapeutic modality. *Acc Chem Res*. **36**: 462-469.

- Li, Z., Hosoi, Y., Cai, K., Tanno, Y., Matsumoto, Y., Enomoto, A., Morita, A., Nakagawa, K., and Miyagawa, K. (2006): Src tyrosine kinase inhibitor PP2 suppresses ERK1/2 activation and epidermal growth factor receptor transactivation by X-irradiation. *Biochem Biophys Res Commun* **341**, 363-8.
- Liebow, C., Reilly, C., Serrano, M., and Schally, A. V. (1989): Somatostatin analogues inhibit growth of pancreatic cancer by stimulating tyrosine phosphatase. *Proc Natl Acad Sci U S A* **86**, 2003-7.
- Lin, S. Y., Makino, K., Xia, W., Matin, A., Wen, Y., Kwong, K. Y., Bourguignon, L., and Hung, M. C. (2001): Nuclear localization of EGF receptor and its potential new role as a transcription factor. *Nat Cell Biol* **3**, 802-8.
- Lindstrom E, Bjorkqvist M, Hakanson R. (1999): Pharmacological analysis of CCK2 receptor antagonists using isolated rat stomach ECL cells. *British Journal of Pharmacology*. **127**(2):530-6.
- Linnekin, D. (1999): Early signaling pathways activated by c-Kit in hematopoietic cells. *Int J Biochem Cell Biol* **31**, 1053-74.
- Lo, H. W., Ali-Seyed, M., Wu, Y., Bartholomeusz, G., Hsu, S. C., and Hung, M. C. (2006): Nuclear-cytoplasmic transport of EGFR involves receptor endocytosis, importin beta1 and CRM1. *J Cell Biochem* **98**, 1570-83.
- Lo, H. W., and Hung, M. C. (2006): Nuclear EGFR signalling network in cancers: linking EGFR pathway to cell cycle progression, nitric oxide pathway and patient survival. *Br J Cancer* **94**, 184-8.
- Lo, H. W., Hsu, S. C., Ali-Seyed, M., Gunduz, M., Xia, W., Wei, Y., Bartholomeusz, G., Shih, J. Y., and Hung, M. C. (2005): Nuclear interaction of EGFR and STAT3 in the activation of the iNOS/NO pathway. *Cancer Cell* **7**, 575-89.
- Lo, H. W., Xia, W., Wei, Y., Ali-Seyed, M., Huang, S. F., and Hung, M. C. (2005): Novel prognostic value of nuclear epidermal growth factor receptor in breast cancer. *Cancer Res* **65**, 338-48.
- Loehrer PJ and Einhorn LH. (1984): Drugs five years later. Cisplatin. *Ann Intern Med*. **100**: 704-713.
- Loehrer, P. J., and Einhorn, L. H. (1984): Drugs five years later. Cisplatin. *Ann Intern Med* **100**, 704-13.
- Lou Z, Chen BP, Asaithamby A, Minter-Dykhouse K, Chen DJ, Chen J. (2004): MDC1 regulates DNA-PK autophosphorylation in response to DNA damage. *J Biol Chem*. **279**: 46359-62.
- Lu Z, Jiang G, Blume-Jensen P, Hunter T. (2001): Epidermal growth factor-induced tumor cell invasion and metastasis initiated by dephosphorylation and downregulation of focal adhesion kinase. *Mol Cell Biol*. **21**: 4016-31.
- Lucas DR, Al-Abbadi M, Tabaczka P, Hamre MR, Weaver DW, Mott MJ. (2003): c-Kit expression in desmoid fibromatosis. Comparative immunohistochemical evaluation of two commercial antibodies. *American Journal of Clinical Pathology*. **119**(3):339-45.

- Lucero H, Gae D, Taccioli GE. (2003): Novel localization of the DNA-PK complex in lipid rafts: a putative role in the signal transduction pathway of the ionizing radiation response. *J Biol Chem*. **278**: 22136-43.
- Lynch TJ, Lilenbaum R, Bonomi P, Ansari R, Govindan R, Janne PA, *et al.* (2004): A phase II trial of cetuximab as therapy for recurrent non-small cell lung cancer (NSCLC). *Proc Am Soc Clin Oncol* 2004; abstr 7084.
- Lyons, J., Landis, C. A., Harsh, G., Vallar, L., Grunewald, K., Feichtinger, H., Duh, Q. Y., Clark, O. H., Kawasaki, E., Bourne, H. R., and *et al.* (1990): Two G protein oncogenes in human endocrine tumors. *Science* **249**, 655-9.
- Magne, N., Fischel, J. L., Dubreuil, A., Formento, P., Marcie, S., Lagrange, J. L., and Milano, G. (2002): Sequence-dependent effects of ZD1839 ('Iressa') in combination with cytotoxic treatment in human head and neck cancer. *Br J Cancer* **86**, 819-27.
- Magne, N., Fischel, J. L., Dubreuil, A., Formento, P., Marcie, S., Lagrange, J. L., and Milano, G. (2002): Sequence-dependent effects of ZD1839 ('Iressa') in combination with cytotoxic treatment in human head and neck cancer. *Br J Cancer* **86**, 819-27.
- Magne, N., Fischel, J. L., Tiffon, C., Formento, P., Dubreuil, A., Renee, N., Formento, J. L., Francoual, M., Ciccolini, J., Etienne, M. C., and Milano, G. (2003): Molecular mechanisms underlying the interaction between ZD1839 ('Iressa') and cisplatin/5-fluorouracil. *Br J Cancer* **89**, 585-92.
- Mahadevan, D., Cooke, L., Riley, C., Swart, R., Simons, B., Della Croce, K., Wisner, L., Iorio, M., Shakalya, K., Garewal, H., Nagle, R., and Bearss, D. (2007): A novel tyrosine kinase switch is a mechanism of imatinib resistance in gastrointestinal stromal tumors. *Oncogene* **26**, 3909-19.
- Maki RG. (2004): Gastrointestinal Stromal Tumors Respond to Tyrosine Kinase-targeted Therapy. *Current Treatment Options in Gastroenterology*. **7**(1):13-17.
- Marinissen, M. J., and Gutkind, J. S. (2001): G-protein-coupled receptors and signaling networks: emerging paradigms. *Trends Pharmacol Sci* **22**, 368-76.
- Marmor, M. D., Skaria, K. B., and Yarden, Y. (2004): Signal transduction and oncogenesis by ErbB/HER receptors. *Int J Radiat Oncol Biol Phys* **58**, 903-13.
- Masuda M, Toh S, Koike K, Kuratomi Y, Suzui M, Deguchi A, Komiyama S, Weinstein IB. (2002): The roles of JNK1 and Stat3 in the response of head and neck cancer cell lines to combined treatment with all-trans-retinoic acid and 5- fluorouracil. *Jpn J Cancer Res*. **93**: 329-39.
- Masumoto N, Nakano S, Fujishima H, Kohno K, Niho Y. (1999): v-src induces cisplatin resistance by increasing the repair of cisplatin-DNA interstrand cross-links in human gallbladder adenocarcinoma cells. *Int J Cancer*. **80**: 731-7.
- Mayrhofer G, Gadd SJ, Spargo LD, Ashman LK. (1987): Specificity of a mouse monoclonal antibody raised against acute myeloid leukaemia cells for mast cells in human mucosal and connective tissues. *Immunology and Cell Biology*. **65**(Pt 3):241-50.
- McArthur, G. (2007): Dermatofibrosarcoma protuberans: recent clinical progress. *Ann Surg Oncol* **14**, 2876-86.

- McKillop, D., Partridge, E. A., Kemp, J. V., Spence, M. P., Kendrew, J., Barnett, S., Wood, P. G., Giles, P. B., Patterson, A. B., Bichat, F., Guilbaud, N., and Stephens, T. C. (2005): Tumor penetration of gefitinib (Iressa), an epidermal growth factor receptor tyrosine kinase inhibitor. *Mol Cancer Ther* **4**, 641-9.
- Melen-Mucha, G., Lawnicka, H., Kierszniewska-Stepien, D., Komorowski, J., and Stepien, H. (2006): The place of somatostatin analogs in the diagnosis and treatment of the neuroendocrine glands tumors. *Recent Pat Anticancer Drug Discov* **1**, 237-54.
- Mendelsohn J. (2001): The epidermal growth factor receptor as a target for cancer therapy. *Endocr Reat Cancer*. **8**: 3-9.
- Miaczynska, M., Pelkmans, L., and Zerial, M. (2004): Not just a sink: endosomes in control of signal transduction. *Curr Opin Cell Biol* **16**, 400-6.
- Micke, P., Basrai, M., Faldum, A., Bittinger, F., Ronnstrand, L., Blaukat, A., Beeh, K. M., Oesch, F., Fischer, B., Buhl, R., and Hengstler, J. G. (2003): Characterization of c-kit expression in small cell lung cancer: prognostic and therapeutic implications. *Clin Cancer Res* **9**, 188-94.
- Miettinen, M., and Lasota, J. (2005): KIT (CD117): a review on expression in normal and neoplastic tissues, and mutations and their clinicopathologic correlation. *Appl Immunohistochem Mol Morphol* **13**, 205-20.
- Mignon M. (2000): Natural history of neuroendocrine enteropancreatic tumors. *Digestion*. **62** Suppl 1:51-8.
- Milas L, Mason K, Hunter N, Petersen S, Yamakawa M, Ang K, Mendelsohn J, Fan Z. (2000): In vivo enhancement of tumor radioresponse by C225 antiepidermal growth factor receptor antibody. *Clin Cancer Res*. **6**: 701-8.
- Moasser, M. M., Basso, A., Averbuch, S. D., and Rosen, N. (2001): The tyrosine kinase inhibitor ZD1839 ("Iressa") inhibits HER2-driven signaling and suppresses the growth of HER2-overexpressing tumor cells. *Cancer Res* **61**, 7184-8.
- Modlin IM, Lawton GP, Miu K, Kidd M, Luque EA, Sandor A, Tang LH. (1996): Pathophysiology of the fundic enterochromaffin-like (ECL) cell and gastric carcinoid tumours. *Annals of the Royal College of Surgeons of England*. **78**(2):133-8.
- Modlin, I. M., Kidd, M., Drozdov, I., Siddique, Z. L., and Gustafsson, B. I. (2008): Pharmacotherapy of neuroendocrine cancers. *Expert Opin Pharmacother* **9**, 2617-26.
- Modlin, I. M., Oberg, K., Chung, D. C., Jensen, R. T., de Herder, W. W., Thakker, R. V., Caplin, M., Delle Fave, G., Kaltsas, G. A., Krenning, E. P., Moss, S. F., Nilsson, O., Rindi, G., Salazar, R., Ruszniewski, P., and Sundin, A. (2008): Gastroenteropancreatic neuroendocrine tumours. *Lancet Oncol* **9**, 61-72.
- Modlin, IM., Kidd, M., and Lye, K. D. (2002): Biology and management of gastric carcinoid tumours: a review. *Eur J Surg* **168**, 669-83.
- Moore, M. J., Goldstein, D., Hamm, J., Figer, A., Hecht, J. R., Gallinger, S., Au, H. J., Murawa, P., Walde, D., Wolff, R. A., Campos, D., Lim, R., Ding, K., Clark, G., Voskoglou-Nomikos, T., Ptasynski, M., and Parulekar, W. (2007): Erlotinib plus gemcitabine compared with gemcitabine alone in patients with advanced pancreatic cancer: a phase III trial of the National Cancer Institute of Canada Clinical Trials Group. *J Clin Oncol* **25**, 1960-6.

- Naramura, M., Gillies, S. D., Mendelsohn, J., Reisfeld, R. A., and Mueller, B. M. (1993): Mechanisms of cellular cytotoxicity mediated by a recombinant antibody-IL2 fusion protein against human melanoma cells. *Immunol Lett* **39**, 91-9.
- Neves, S. R., Ram, P. T., and Iyengar, R. (2002): G protein pathways. *Science* **296**, 1636-9.
- Nilsson O, Wangberg B, Kolby L, Schultz GS, Ahlman H. (1995): Expression of transforming growth factor alpha and its receptor in human neuroendocrine tumours. *International Journal of Cancer*. **60**(5):645-51.
- Niu G, Wright KL, Huang M, Song L, Haura E, Turkson J, Zhang S, Wang T, Sinibaldi D, Coppola D, Heller R, Ellis LM, Karras J, Bromberg J, Pardoll D, Jove R, Yu H. (2002): Constitutive Stat3 activity up-regulates VEGF expression and tumor angiogenesis. *Oncogene*. **21**: 2000-8.
- Noble, F., and Roques, B. P. (1999): CCK-B receptor: chemistry, molecular biology, biochemistry and pharmacology. *Prog Neurobiol* **58**, 349-79.
- Noble, F., Wank, S. A., Crawley, J. N., Bradwejn, J., Seroogy, K. B., Hamon, M., and Roques, B. P. (1999): International Union of Pharmacology. XXI. Structure, distribution, and functions of cholecystokinin receptors. *Pharmacol Rev* **51**, 745-81.
- Nocka K, Majumder S, Chabot B, Ray P, Cervone M, Bernstein A, Besmer P. (1989): Expression of c-kit gene products in known cellular targets of W mutations in normal and W mutant mice--evidence for an impaired c-kit kinase in mutant mice. *Genes Development*. **3**(6):816-26.
- Oberg, K. (1996): Biological aspects of neuroendocrine gastro-enteropancreatic tumours. *Digestion* **57 Suppl 1**, 42-4.
- Oberg, K. (2001): Chemotherapy and biotherapy in the treatment of neuroendocrine tumours. *Ann Oncol* **12 Suppl 2**, S111-4.
- Oberg, K. (2004): Management of neuroendocrine tumours. *Ann Oncol* **15 Suppl 4**, iv293-8.
- Olayioye MA, Graus-Porta D, Beerli RR, Rohrer J, Gay B, Hynes NE. (1998): ErbB-1 and ErbB-2 acquire distinct signaling properties dependent upon their dimerization partner. *Mol Cell Biol*. **18**(9):5042-51.
- Olive PL. (2002): The Comet Assay – An overview of techniques. *Methods in Molecular Biology*. **203**:179-94.
- Ono, K., Suzuki, T., Miki, Y., Taniyama, Y., Nakamura, Y., Noda, Y., Watanabe, M., and Sasano, H. (2007): Somatostatin receptor subtypes in human non-functioning neuroendocrine tumors and effects of somatostatin analogue SOM230 on cell proliferation in cell line NCI-H727. *Anticancer Res* **27**, 2231-9.
- Paez JG, Janne PA, Lee JC, Tracy S, Greulich H, Gabriel S, Herman P, Kaye FJ, Lindeman N, Boggon TJ, Naoki K, Sasaki H, Fujii Y, Eck MJ, Sellers WR, Johnson BE, Meyerson M. (2004): EGFR mutations in lung cancer: correlation with clinical response to gefitinib therapy. *Science*. **304**: 1497-500.
- Pal, S. K., and Pegram, M. (2005): Epidermal growth factor receptor and signal transduction: potential targets for anti-cancer therapy. *Anticancer Drugs* **16**, 483-94.

- Papouchado, B., Erickson, L. A., Rohlinger, A. L., Hobday, T. J., Erlichman, C., Ames, M. M., and Lloyd, R. V. (2005): Epidermal growth factor receptor and activated epidermal growth factor receptor expression in gastrointestinal carcinoids and pancreatic endocrine carcinomas. *Mod Pathol* **18**, 1329-35.
- Parrott JA, Kim G, Skinner MK. (2000): Expression and action of kit ligand/stem cell factor in normal human and bovine ovarian surface epithelium and ovarian cancer. *Biology of Reproduction*. **62**(6):1600-9.
- Patel, Y. C. (1999): Somatostatin and its receptor family. *Front Neuroendocrinol* **20**, 157-98.
- Patel, Y. C., and Srikant, C. B. (1986): Somatostatin mediation of adenohypophysial secretion. *Annu Rev Physiol* **48**, 551-67.
- Patel, Y. C., Greenwood, M. T., Panetta, R., Demchyshyn, L., Niznik, H., and Srikant, C. B. (1995): The somatostatin receptor family. *Life Sci* **57**, 1249-65.
- Peghini, P. L., Iwamoto, M., Raffeld, M., Chen, Y. J., Goebel, S. U., Serrano, J., and Jensen, R. T. (2002): Overexpression of epidermal growth factor and hepatocyte growth factor receptors in a proportion of gastrinomas correlates with aggressive growth and lower curability. *Clin Cancer Res* **8**, 2273-85.
- Perrotte, P., Matsumoto, T., Inoue, K., Kuniyasu, H., Eve, B. Y., Hicklin, D. J., Radinsky, R., and Dinney, C. P. (1999): Anti-epidermal growth factor receptor antibody C225 inhibits angiogenesis in human transitional cell carcinoma growing orthotopically in nude mice. *Clin Cancer Res* **5**, 257-65.
- Peters, R. (2006): Introduction to nucleocytoplasmic transport: molecules and mechanisms. *Methods Mol Biol* **322**, 235-58.
- Pierce, A. C., Sandretto, K. L., and Bemis, G. W. (2002): Kinase inhibitors and the case for CH...O hydrogen bonds in protein-ligand binding. *Proteins* **49**, 567-76.
- Pike, L. J. (2005): Growth factor receptors, lipid rafts and caveolae: an evolving story. *Biochim Biophys Acta* **1746**, 260-73.
- Pirollo, K. F., Hao, Z., Rait, A., Ho, C. W., and Chang, E. H. (1997): Evidence supporting a signal transduction pathway leading to the radiation-resistant phenotype in human tumor cells. *Biochem Biophys Res Commun* **230**, 196-201.
- Pollak, M. N., and Schally, A. V. (1998): Mechanisms of antineoplastic action of somatostatin analogs. *Proc Soc Exp Biol Med* **217**, 143-52.
- Porter, A. C., and Vaillancourt, R. R. (1998): Tyrosine kinase receptor-activated signal transduction pathways which lead to oncogenesis. *Oncogene* **17**, 1343-52.
- Povirk LF, and Shuker DE. (1994): DNA damage and mutagenesis induced by nitrogen mustards. *Mutation Research*. **318**: 205-26.
- Pratt WB, Ruddon RW, Ensminger WD, Maybaum J. (1994): *The Anticancer Drugs*. Oxford University Press: New York
- Prenzel N, Fischer OM, Streit S, Hart S, Ullrich A. (2001): The epidermal growth factor receptor family as a central element for cellular signal transduction and diversification. *Endocr Relat Cancer*. **8**: 11-31.

- Prewett MC, Hooper AT, Bassi R, Ellis LM, Waksal HW, Hicklin DJ. (2002): Enhanced antitumour activity of anti-epidermal growth factor receptor monoclonal antibody IMC-C225 in combination with irinotecan (CPT-11) against human colorectal tumour xenografts. *Clin Cancer Res*. **8**: 994-1003.
- Prinz C, Zanner R, Gratzl M. (2003): Physiology of gastric enterochromaffin-like cells. *Annual Review of Physiology*. **65**:371-382.
- Puri, C., Tosoni, D., Comai, R., Rabellino, A., Segat, D., Caneva, F., Luzzi, P., Di Fiore, P. P., and Tacchetti, C. (2005): Relationships between EGFR signaling-competent and endocytosis-competent membrane microdomains. *Mol Biol Cell* **16**, 2704-18.
- Qiu FH, Ray P, Brown K, Barker PE, Jhanwar S, Ruddle FH, Besmer P. (1988): Primary structure of c-kit: relationship with the CSF-1/PDGF receptor kinase family--oncogenic activation of v-kit involves deletion of extracellular domain and C terminus. *The EMBO Journal*. **7**(4):1003-11.
- Raderer M, Wrba F, Kornek G, Maca T, Koller DY, Weinlaender G, Hejna M, Scheithauer W. (1998): Association between Helicobacter pylori infection and pancreatic cancer. *Oncology*. **55**(1):16-9.
- Raderschall E, Stout K, Freier S, Suckow V, Schweiger S, Haaf T. (2002): Elevated levels of Rad51 recombination protein in tumor cells. *Cancer Res*. **62**: 219-25.
- Ravid, T., Sweeney, C., Gee, P., Carraway, K. L., 3rd, and Goldkorn, T. (2002): Epidermal growth factor receptor activation under oxidative stress fails to promote c-Cbl mediated down-regulation. *J Biol Chem*. **277**, 31214-9.
- Raymond E, Raoul JL, Niccoli P, Bang YJ, Borbath I, Lombard-Bohas C, Metrakos P, Lu DR, Blanckmeister C, Vinik A (2009) Phase III, Randomized, Double-Blind Trial of Sunitinib vs Placebo in Patients with Progressive, Well-Differentiated, Malignant Pancreatic Islet Cell Tumors 2009, 11th World Congress on Gastrointestinal Cancers: Abstract 0-0013.
- Reed, E. (1999): Cisplatin. *Cancer Chemother Biol Response Modif* **18**, 144-51.
- Reeves, P. M., Bommarius, B., Lebeis, S., McNulty, S., Christensen, J., Swimm, A., Chahroudi, A., Chavan, R., Feinberg, M. B., Veach, D., Bornmann, W., Sherman, M., and Kalman, D. (2005): Disabling poxvirus pathogenesis by inhibition of Abl-family tyrosine kinases. *Nat Med* **11**, 731-9.
- Reichlin, S. (1983): Somatostatin. *N Engl J Med* **309**, 1495-501.
- Reubi, J. C. (2004): Somatostatin and other Peptide receptors as tools for tumor diagnosis and treatment. *Neuroendocrinology* **80 Suppl 1**, 51-6.
- Reubi, J. C., and Waser, B. (2003): Concomitant expression of several peptide receptors in neuroendocrine tumours: molecular basis for in vivo multireceptor tumour targeting. *Eur J Nucl Med Mol Imaging* **30**, 781-93.
- Reubi, J. C., Krenning, E., Lamberts, S. W., and Kvols, L. (1992): In vitro detection of somatostatin receptors in human tumors. *Metabolism* **41**, 104-10.
- Reubi, J. C., Kvols, L., Krenning, E., and Lamberts, S. W. (1990): Distribution of somatostatin receptors in normal and tumor tissue. *Metabolism* **39**, 78-81.
- Richard, D. E., Vouret-Craviari, V., and Pouyssegur, J. (2001): Angiogenesis and G-protein-coupled receptors: signals that bridge the gap. *Oncogene* **20**, 1556-62.

- Riese DJ 2nd, Stern DF. (1998): Specificity within the EGF family/ErbB receptor family signaling network. *Bioessays*. **20**(1):41-8.
- Rindi G, Candusso ME, Solcia E. (1999): Molecular aspects of the endocrine tumours of the pancreas and the gastrointestinal tract. *Italian Journal of Gastroenterology and Hepatology*. **31** Suppl 2:S135-8.
- Rinke, A., Muller, H. H., Schade-Brittinger, C., Klose, K. J., Barth, P., Wied, M., Mayer, C., Aminossadati, B., Pape, U. F., Blaker, M., Harder, J., Arnold, C., Gress, T., and Arnold, R. (2009): Placebo-controlled, double-blind, prospective, randomized study on the effect of octreotide LAR in the control of tumor growth in patients with metastatic neuroendocrine midgut tumors: a report from the PROMID Study Group. *J Clin Oncol* **27**, 4656-63.
- Rocha-Lima, C. M., Soares, H. P., Raez, L. E., and Singal, R. (2007): EGFR targeting of solid tumors. *Cancer Control* **14**, 295-304.
- Rosenberg B. (1985): Fundamental studies with cisplatin. *Cancer*. **55**: 2303-2306.
- Rubenstein L and Lanzara, (1998): Activation of G-protein coupled receptors entails cysteine modulation of agonist binding, *J. Mol. Struc. (Theochem)* **430**, 57-71
- Rusch, V., Mendelsohn, J., and Dmitrovsky, E. (1996): The epidermal growth factor receptor and its ligands as therapeutic targets in human tumors. *Cytokine Growth Factor Rev* **7**, 133-41.
- Sabah, M., Leader, M., and Kay, E. (2003): The problem with KIT: clinical implications and practical difficulties with CD117 immunostaining. *Appl Immunohistochem Mol Morphol* **11**, 56-61.
- Sakurai S, Fukasawa T, Chong JM, Tanaka A, Fukayama M. (1999): C-kit gene abnormalities in gastrointestinal stromal tumors (tumors of interstitial cells of Cajal. *Japanese Journal of Cancer Research*. **90**(12):1321-8.
- Saleh MN, Raisch KP, Stackhouse MA, Grizzle WE, Bonner JA, Mayo MS, Kim HG, Meredith RF, Wheeler RH, Buchsbaum DJ. (1999): Combined modality therapy of A431 human epidermoid cancer using anti-EGFr antibody C225 and radiation. *Cancer Biother Radiopharm*. **14**: 451-63.
- Salomon, D. S., Brandt, R., Ciardiello, F., and Normanno, N. (1995): Epidermal growth factor-related peptides and their receptors in human malignancies. *Crit Rev Oncol Hematol* **19**, 183-232.
- Sambrook J., Fritsch E. F., Maniatis T. *Molecular Cloning: A Laboratory Manual*. Cold Spring Harbour Press, New York, Third Edition. 1989; Vol. 1,2,3.
- Sarkar, S., Davies, A. A., Ulrich, H. D., and McHugh, P. J. (2006): DNA interstrand crosslink repair during G1 involves nucleotide excision repair and DNA polymerase zeta. *Embo J* **25**, 1285-94.
- Sawyers CL. (2002): Rational therapeutic intervention in cancer: kinases as drug targets. *Current Opinion in Genetics and Development*. **12**(1):111-5.
- Schachtrup, C., Lu, P., Jones, L. L., Lee, J. K., Lu, J., Sachs, B. D., Zheng, B., and Akassoglou, K. (2007): Fibrinogen inhibits neurite outgrowth via beta 3 integrin-mediated phosphorylation of the EGF receptor. *Proc Natl Acad Sci U S A* **104**, 11814-9.

- Schiller JH. (2003): New directions for ZD1839 in the treatment of solid tumors. *Seminars in Oncology*. **30**(1 Suppl 1):49-55.
- Schindler, M., Kidd, E. J., Carruthers, A. M., Wyatt, M. A., Jarvie, E. M., Sellers, L. A., Feniuk, W., and Humphrey, P. P. (1998): Molecular cloning and functional characterization of a rat somatostatin sst2(b) receptor splice variant. *Br J Pharmacol* **125**, 209-17.
- Schlessinger, J. (2004): Common and distinct elements in cellular signaling via EGF and FGF receptors. *Science* **306**, 1506-7.
- Schubert, M. L. (2003): Gastric secretion. *Curr Opin Gastroenterol* **19**, 519-25.
- Scotlandi K, Manara MC, Strammiello R, Landuzzi L, Benini S, Perdichizzi S, Serra M, Astolfi A, Nicoletti G, Lollini PL, Bertoni F, Nanni P, Picci P. (2003): C-kit receptor expression in Ewing's sarcoma: lack of prognostic value but therapeutic targeting opportunities in appropriate conditions. *Journal of Clinical Oncology*. **21**(10):1952-60.
- Seidal T, Edvardsson H. (1999): Expression of c-kit (CD117) and Ki67 provides information about the possible cell of origin and clinical course of gastrointestinal stromal tumours. *Histopathology*. **34**(5):416-24.
- Shah, T., Hochhauser, D., Frow, R., Quaglia, A., Dhillon, A. P., and Caplin, M. E. (2006): Epidermal growth factor receptor expression and activation in neuroendocrine tumours. *J Neuroendocrinol* **18**, 355-60.
- She, Q. B., Solit, D., Basso, A., and Moasser, M. M. (2003): Resistance to gefitinib in PTEN-null HER-overexpressing tumor cells can be overcome through restoration of PTEN function or pharmacologic modulation of constitutive phosphatidylinositol 3'-kinase/Akt pathway signaling. *Clin Cancer Res* **9**, 4340-6.
- Shepherd FA, Rodrigues Pereira J, Ciuleanu T, Tan EH, Hirsh V, Thongprasert S, Campos D, Maoleekoonpiroj S, Smylie M, Martins R, van Kooten M, Dediu M, Findlay B, Tu D, Johnston D, Bezjak A, Clark G, Santabarbara P, Seymour L; National Cancer Institute of Canada Clinical Trials Group. (2005): Erlotinib in previously treated non-small-cell lung cancer. *N Engl J Med*. **353**: 123-32.
- Sirotnak, F. M., Zakowski, M. F., Miller, V. A., Scher, H. I., and Kris, M. G. (2000): Efficacy of cytotoxic agents against human tumor xenografts is markedly enhanced by coadministration of ZD1839 (Iressa), an inhibitor of EGFR tyrosine kinase. *Clin Cancer Res* **6**, 4885-92.
- Skehan P, Storeng R, Scudiero D, Monks A, McMahon J, Vistica D, Warren JT, Bokesch H, Kenney S, and Boyd MR. (1990): New colorimetric cytotoxicity assay for anticancer-drug screening. *J Natl. Cancer Inst.* **82**:1107-1112.
- Skorski T. (2002): Oncogenic tyrosine kinases and the DNA-damage response. *Nat Rev Can.* **2**: 1-10.
- Slupianek A, Hoser G, Majsterek I, Bronisz A, Malecki M, Blasiak J, Fishel R, Skorski T. (2002): Fusion tyrosine kinases induce drug resistance by stimulation of homology-dependent recombination repair, prolongation of G(2)/M phase, and protection from apoptosis. *Mol Cell Biol.* **22**: 4189-201.
- Slupianek A, Schmutte C, Tomblin G, Nieborowska-Skorska M, Hoser G, Nowicki MO, Pierce AJ, Fishel R, Skorski T. (2001): BCR/ABL regulates mammalian RecA homologs, resulting in drug resistance. *Mol Cell.* **8**: 795-806.

- Smith, J. (2005): Erlotinib: small-molecule targeted therapy in the treatment of non-small-cell lung cancer. *Clin Ther* **27**, 1513-34.
- Smith, J. P., Verderame, M. F., McLaughlin, P., Martenis, M., Ballard, E., and Zagon, I. S. (2002): Characterization of the CCK-C (cancer) receptor in human pancreatic cancer. *Int J Mol Med* **10**, 689-94.
- Sodhi, A., Montaner, S., and Gutkind, J. S. (2004): Viral hijacking of G-protein-coupled-receptor signalling networks. *Nat Rev Mol Cell Biol* **5**, 998-1012.
- Somogyi L, Mishra G. (2000): Diagnosis and staging of islet cell tumors of the pancreas. *Current Gastroenterology Reports*. **2**:159-64.
- Spanswick VJ, Hartley JM, Ward TH and Hartley JA. (1999): Measurement of drug-induced interstrand crosslinking using single-cell gel electrophoresis (Comet) assay. In Brown,R. and Boger-Brown,U. (eds), *Methods in Molecular Medicine*, Vol. 28, Cytotoxic Drug Resistance Mechanisms. Humana Press, Totowa, NJ.
- Srirajaskanthan, R., Toumpanakis, C., Meyer, T., and Caplin, M. E. (2009): Review article: future therapies for management of metastatic gastroenteropancreatic neuroendocrine tumours. *Aliment Pharmacol Ther* **29**, 1143-54.
- Stark, A., and Mentlein, R. (2002): Somatostatin inhibits glucagon-like peptide-1-induced insulin secretion and proliferation of RINm5F insulinoma cells. *Regul Pept* **108**, 97-102.
- Strano S, Rossi M, Fontemaggi G, Munarriz E, Soddu S, Sacchi A, Blandino G. (2001): From p63 to p53 across p73. *FEBS Lett*. **490**: 163-70.
- Szumiel, I. (2006): Epidermal growth factor receptor and DNA double strand break repair: the cell's self-defence. *Cell Signal* **18**, 1537-48.
- Taal, B. G., and Visser, O. (2004): Epidemiology of neuroendocrine tumours. *Neuroendocrinology* **80 Suppl 1**, 3-7.
- Tallarida RJ. (2001): Drug synergism: its detection and applications. *J Pharmacol Exp Ther*. **298**(3): 865-72.
- Tang, C., Liu, C., Zhou, X., and Wang, C. (2004): Enhanced inhibitive effects of combination of rofecoxib and octreotide on the growth of human gastric cancer. *Int J Cancer* **112**, 470-4.
- Tannenbaum, G. S., Ling, N., and Brazeau, P. (1982): Somatostatin-28 is longer acting and more selective than somatostatin-14 on pituitary and pancreatic hormone release. *Endocrinology* **111**, 101-7.
- Tewey, K. M., Rowe, T. C., Yang, L., Halligan, B. D. & Liu, L. F. (1984): Adriamycin-induced DNA damage mediate by mammalian DNA topoisomerase II. *Science*. **226**: 466-468.
- Tomassetti, P., Migliori, M., Lalli, S., Campana, D., Tomassetti, V., and Corinaldesi, R. (2001): Epidemiology, clinical features and diagnosis of gastroenteropancreatic endocrine tumours. *Ann Oncol* **12 Suppl 2**, S95-9.
- Torihashi S, Ward SM, Nishikawa S, Nishi K, Kobayashi S, Sanders KM. (1995): C-kit-dependent development of interstitial cells and electrical activity in the murine gastrointestinal tract. *Cell and Tissue Research*. **280**(1):97-111.

- Traxler P, Bold G, Buchdunger E, Caravatti G, Furet P, Manley P, O'Reilly T, Wood J, Zimmermann J. (2001): Tyrosine kinase inhibitors: from rational design to clinical trials. *Medicinal Research Reviews*. **21**(6):499-512.
- Trimmer, E. E., and Essigmann, J. M. (1999): Cisplatin. *Essays Biochem* **34**, 191-211.
- Tsujimura T. (1996): Role of c-kit receptor tyrosine kinase in the development, survival and neoplastic transformation of mast cells. *Pathology International*. **46**(12):933-8.
- Tsuura Y, Hiraki H, Watanabe K, Igarashi S, Shimamura K, Fukuda T, Suzuki T, Seito T. (1994): Preferential localization of c-kit product in tissue mast cells, basal cells of skin, epithelial cells of breast, small cell lung carcinoma and seminoma/dysgerminoma in human: immunohistochemical study on formalin-fixed, paraffin-embedded tissues. *Virchows Archive*. **424**(2):135-41.
- Turchi JJ, Henkels KM, Hermanson IL, Patrick SM. (1999): Interactions of mammalian proteins with cisplatin-damaged DNA. *J Inorg Biochem*. **77**: 83-7.
- Ugurel, S., Hildenbrand, R., Zimpfer, A., La Rosee, P., Paschka, P., Sucker, A., Keikavoussi, P., Becker, J. C., Rittgen, W., Hochhaus, A., and Schadendorf, D. (2005): Lack of clinical efficacy of imatinib in metastatic melanoma. *Br J Cancer* **92**, 1398-405.
- Van der Veeken J, Oliveira S, Schifflers RM, Storm G, van Bergen En Henegouwen PM, Roovers RC. (2009): Crosstalk between epidermal growth factor receptor- and insulin-like growth factor-1 receptor signaling: implications for cancer therapy. *Curr Cancer Drug Targets*. **9**(6):748-60.
- Verweij, J., Casali, P. G., Zalcberg, J., LeCesne, A., Reichardt, P., Blay, J. Y., Issels, R., van Oosterom, A., Hogendoorn, P. C., Van Glabbeke, M., Bertulli, R., and Judson, I. (2004): Progression-free survival in gastrointestinal stromal tumours with high-dose imatinib: randomised trial. *Lancet* **364**, 1127-34.
- Virgolini, I., Traub, T., Novotny, C., Leimer, M., Fuger, B., Li, S. R., Patri, P., Pangerl, T., Angelberger, P., Raderer, M., Burggasser, G., Andrae, F., Kurtaran, A., and Dudczak, R. (2002): Experience with indium-111 and yttrium-90-labeled somatostatin analogs. *Curr Pharm Des* **8**, 1781-807.
- Vispe, S., Cazaux, C., Lesca, C., and Defais, M. (1998): Overexpression of Rad51 protein stimulates homologous recombination and increases resistance of mammalian cells to ionizing radiation. *Nucleic Acids Res* **26**, 2859-64.
- Vitali, R., Cesi, V., Nicotra, M. R., McDowell, H. P., Donfrancesco, A., Mannarino, O., Natali, P. G., Raschella, G., and Dominici, C. (2003): c-Kit is preferentially expressed in MYCN-amplified neuroblastoma and its effect on cell proliferation is inhibited in vitro by STI-571. *Int J Cancer* **106**, 147-52.
- Vogelstein B, and Kinzler KW. (1993): The multi-step nature of cancer. *Trends Genet*. **9**: 138-141.
- Voigt W. (2005): Sulforhodamine B assay and Chemosensitivity. *Methods Mol Med*. **110**:39-48.
- Waldherr, C., Pless, M., Maecke, H. R., Schumacher, T., Crazzolara, A., Nitzsche, E. U., Haldemann, A., and Mueller-Brand, J. (2002): Tumor response and clinical benefit in neuroendocrine tumors after 7.4 GBq (90)Y-DOTATOC. *J Nucl Med* **43**, 610-6.
- Wang CH, Tang CW, Liu CL, Tang LP. (2003): Inhibitory effect of octreotide on gastric cancer growth via MAPK pathway. *World Journal of Gastroenterology*. **9**(9):1904-8.

- Wang D, Lippard SJ. (2005): Cellular processing of platinum anticancer drugs. *Nat Rev Drug Discov.* **4**: 307-20.
- Wang DG, Johnston CF, Buchanan KD. (1997): Oncogene expression in gastroenteropancreatic neuroendocrine tumors: implications for pathogenesis. *Cancer.* **80**(4):668-75.
- Wank SA. (1998): G protein-coupled receptors in gastrointestinal physiology. I. CCK receptors: an exemplary family. *American Journal of Physiology.* **274**(4 Pt 1):G607-13.
- Ward, C. W., Lawrence, M. C., Streltsov, V. A., Adams, T. E., and McKern, N. M. (2007): The insulin and EGF receptor structures: new insights into ligand-induced receptor activation. *Trends Biochem Sci* **32**, 129-37.
- Weckbecker G, Raulf F, Stolz B, Bruns C. (1993): Somatostatin analogs for diagnosis and treatment of cancer. *Pharmacology and Therapeutics.* **60**(2):245-64.
- Welin, S., Fjallskog, M. L., Saras, J., Eriksson, B., and Janson, E. T. (2006): Expression of tyrosine kinase receptors in malignant midgut carcinoid tumors. *Neuroendocrinology* **84**, 42-8.
- Wells, A. (1999): EGF receptor. *Int J Biochem Cell Biol* **31**, 637-43.
- Williams DE, Eisenman J, Baird A, Rauch C, Van Ness K, March CJ, Park LS, Martin U, Mochizuki DY, Boswell HS, Burgess GS, Cosman D, Lyman SD. (1990): Identification of a ligand for the c-kit proto-oncogene. *Cell.* **63**(1):167-74.
- Wiseman, G. A., and Kvols, L. K. (1995): Therapy of neuroendocrine tumors with radiolabeled MIBG and somatostatin analogues. *Semin Nucl Med* **25**, 272-8.
- Wosikowski, K., Schuurhuis, D., Kops, G. J., Saceda, M., and Bates, S. E. (1997): Altered gene expression in drug-resistant human breast cancer cells. *Clin Cancer Res* **3**, 2405-14.
- Wulbrand U, Wied M, Zofel P, Goke B, Arnold R, Fehmann H. (1998): Growth factor receptor expression in human gastroenteropancreatic neuroendocrine tumours. *European Journal of Clinical Investigation.* **28**(12):1038-49.
- Xu W, Liu L, Smith GC, Charles G. (2000): Nitric oxide upregulates expression of DNA-PKcs to protect cells from DNA-damaging anti-tumour agents. *Nat Cell Biol.* **2**: 339-45.
- Yao, J. C., Hassan, M., Phan, A., Dagohoy, C., Leary, C., Mares, J. E., Abdalla, E. K., Fleming, J. B., Vauthey, J. N., Rashid, A., and Evans, D. B. (2008): One hundred years after "carcinoid": epidemiology of and prognostic factors for neuroendocrine tumors in 35,825 cases in the United States. *J Clin Oncol* **26**, 3063-72.
- Yarden Y, Kuang WJ, Yang-Feng T, Coussens L, Munemitsu S, Dull TJ, Chen E, Schlessinger J, Francke U, Ullrich A. (1987): Human proto-oncogene c-kit: a new cell surface receptor tyrosine kinase for an unidentified ligand. *The EMBO Journal.* **6**(11):3341-51.
- Yarden Y, Sliwkowski MX. (2001): Untangling the ErbB signalling network. *Nat Rev Mol Cell Biol.* **2**: 127-37.
- Yarden Y. (2001): The EGFR family and its ligands in human cancer: signalling mechanisms and therapeutic opportunities. *Eur J Cancer.* **37**: S3-S8.
- Yeager TR, Reddel RR. (1999): Constructing immortalized human cell lines. *Curr Opin Biotechnol.* **10**(5):465-9.

- Yoneda, Y., Imamoto-Sonobe, N., Yamaizumi, M., and Uchida, T. (1987): Reversible inhibition of protein import into the nucleus by wheat germ agglutinin injected into cultured cells. *Exp Cell Res* **173**, 586-95.
- Yotsumoto F, Sanui A, Fukami T, Shiota K, Horiuchi S, Tsujioka H, Yoshizato T, Kuroki M, Miyamoto S. (2009): Efficacy of ligand-based targeting for the EGF system in cancer. *Anticancer Res.* **29**(11):4879-85
- Yu D, Hung MC. (2000): Role of erbB2 in breast cancer chemosensitivity. *Bioessays*. **22**: 673-80.
- Yu H, Jove R. (2004): The STATs of cancer - new molecular targets come of age. *Nat Rev Cancer*. **4**: 97-105.
- Zemke D, Yamini B, Yuzbasiyan-Gurkan V. (2002): Mutations in the juxtamembrane domain of c-KIT are associated with higher grade mast cell tumors in dogs. *Veterinary Pathology*. **39**(5):529-35.
- Zhao, B., Zhao, H., Zhao, N., and Zhu, X. G. (2002): Cholangiocarcinoma cells express somatostatin receptor subtype 2 and respond to octreotide treatment. *J Hepatobiliary Pancreat Surg* **9**, 497-502.
- Zhong, D., Pal, S. K., Wan, C. & Zewail, A. H. (2001): Femtosecond dynamics of a drug-protein complex: daunomycin with Aporiboflavin-binding protein. *Proc. Natl Acad. Sci USA*. **98**: 11873-11878.
- Zhou BP, Liao Y, Spohn B, Hung MC. (2001): HER-2/neu induces p53 ubiquitination via Akt-mediated MDM2 phosphorylation. *Nat Cell Biol*. **3**: 973-82.
- Zsebo KM, Williams DA, Geissler EN, Broudy VC, Martin FH, Atkins HL, Hsu RY, Birkett NC, Okino KH, Murdock DC, Jacobsen FW, Langley KE, Smith KA, Takeish T, Cattanch BM, Galli SJ, Suggs SV. (1990): Stem cell factor is encoded at the Sl locus of the mouse and is the ligand for the c-kit tyrosine kinase receptor. *Cell*. **63**(1):213-24.